

AD-A048 482

TEXAS INSTRUMENTS INC DALLAS CENTRAL RESEARCH LABS  
MICROBEAM ANALYSIS TECHNIQUES FOR ICS.(U)

F/G 20/12

OCT 77 G B LARRABEE, R D DOBROTT

F30602-76-C-0316

UNCLASSIFIED

TI-08-77-16

RADC-TR-77-339

NL

1 OF 3  
AD  
AO48482



ADA 048482

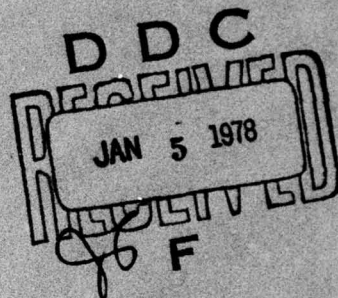
RADC-TR-77-339  
Final Technical Report  
October 1977

2



MICROBEAM ANALYSIS TECHNIQUES FOR ICs

Texas Instruments Incorporated



Approved for public release; distribution unlimited.

10 NO. \_\_\_\_\_  
DDC FILE COPY

ROME AIR DEVELOPMENT CENTER ✓  
Air Force Systems Command  
Griffiss Air Force Base, New York 13441

RADC-TR-77-339 has been reviewed by the Office of Information (OI), RADC, and approved for release to the National Technical Information Service (NTIS). At NTIS it will be available to the general public, including foreign nations.

This report has been reviewed and is approved for publication.

APPROVED: *John J. Bart*

JOHN J. BART  
Reliability Physics Section  
Reliability Branch

APPROVED: *Joseph J. Naresky*

JOSEPH J. NARESKY  
Chief, Reliability and Compatibility Division

FOR THE COMMANDER:

*John P. Huss*

JOHN P. HUSS  
Acting Chief, Plans Office

If your address has changed or if you wish to be removed from the RADC mailing list, or if the addressee is no longer employed by your organization, please notify RADC (RBRP) Griffiss AFB NY 13441. This will assist us in maintaining a current mailing list.

Do not return this copy. Retain or destroy.

## UNCLASSIFIED

SECURITY CLASSIFICATION OF THIS PAGE (When Data Entered)

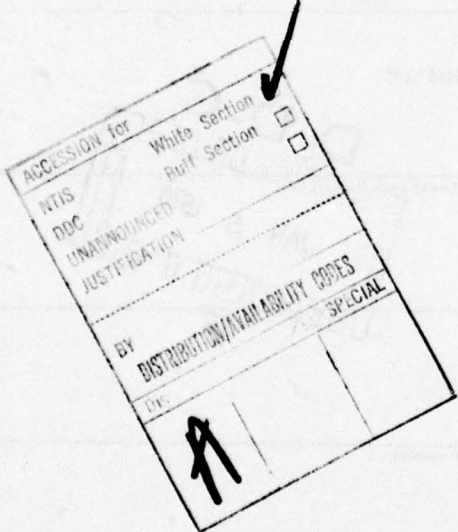
(19) REPORT DOCUMENTATION PAGE		READ INSTRUCTIONS BEFORE COMPLETING FORM
1. REPORT NUMBER <b>(18) RADCR-TR-77-339</b>	2. GOVT ACCESSION NO.	3. RECIPIENT'S CATALOG NUMBER
4. TITLE (and Subtitle) <b>(6) MICROBEAM ANALYSIS TECHNIQUES FOR ICs</b>	5. TYPE OF REPORT & PERIOD COVERED Final Technical Report, 9 June 1976 - 9 March 1977	6. PERFORMING ORG. REPORT NUMBER <b>(14) TI-08-77-16</b>
7. AUTHOR(s) <b>G. B. Larrabee R. D. Dobrott</b>	8. CONTRACT OR GRANT NUMBER(s) <b>(15) F30602-76-C-0316</b> <i>New</i>	9. PERFORMING ORGANIZATION NAME AND ADDRESS Texas Instruments Incorporated, Central Research Laboratories 13500 North Central Expressway, P. O. Box 5936 Dallas TX 75222
10. PROGRAM ELEMENT, PROJECT, TASK AREA & WORK UNIT NUMBERS <b>(16) P.E. 62702F J.O. 23380113</b>	11. REPORT DATE <b>(11) October 1977</b>	12. NUMBER OF PAGES <b>222</b>
13. SECURITY CLASS. (of this report) <b>UNCLASSIFIED</b>	14. MONITORING AGENCY NAME & ADDRESS (if different from Controlling Office) <b>Same</b>	15a. DECLASSIFICATION/DOWNGRADING SCHEDULE <b>N/A</b>
16. DISTRIBUTION STATEMENT (of this Report)  Approved for public release; distribution unlimited.		
17. DISTRIBUTION STATEMENT (of the abstract entered in Block 20, if different from Report)  Same		
18. SUPPLEMENTARY NOTES  Project Engineer: John J. Bart (RBRP)		
19. KEY WORDS (Continue on reverse side if necessary and identify by block number) Ion Microprobe Mass Analysis Microelectronic Devices Chemical Analysis Thin Films Failure Analysis Techniques		
20. ABSTRACT (Continue on reverse side if necessary and identify by block number) The ion microprobe mass analyzer was used for a general chemical characterization of actual integrated circuits. Simple operational amplifiers, general purpose amplifiers, inverters, emitter coupled flip-flops, and radiation hardened NAND gates were chosen as representative of the bipolar family. CMOS gates with both doped and undoped oxides and CMOS-SOS devices represented the field effect device family. All devices were randomly chosen without regard to actual operational characteristics. <i>next page</i>		

*403833**JB*

**UNCLASSIFIED**

SECURITY CLASSIFICATION OF THIS PAGE(When Data Entered)

The analysis technique was designed to determine impurities at the surface, in the deposited oxide, in the thermal oxide, in the metallization, and at the various interfaces between these layers. The identification of the intentional dopants in the silicon was performed where concentrations were above the detection limit. In-depth concentration profiles of intentional dopants such as phosphorus were obtained by monitoring the dopant ion signal as a function of sputter time. A quantitative estimate of some of the common dopants and/or impurities was accomplished using an empirical calibration. Depths were determined by empirically calibrating the sputter rates as a function of area, total primary ion current, and primary ion species. Interface regions were identified by sputter time analysis of layers where successive layers have an elemental matrix change. The interfaces between layers of similar matrix elements, such as deposited oxide - thermal oxide were assumed to have the same sputter time as dissimilar matrices, i.e., deposited oxide over metal has the same thickness and sputter characteristics as over thermal oxide. Negative or positive oxygen was used as the primary sputtering ion for data collection. Positive argon was used as the primary sputtering ion for data collection. Positive argon was used to rapidly sputter through layers for interfacial analysis. Dielectric films were observed to be contaminated with carbon, fluorine, tin, lead, barium and other impurities, while oxides over nichrome resistors were observed to contain lead and tin.



**UNCLASSIFIED**

SECURITY CLASSIFICATION OF THIS PAGE(When Data Entered)

TABLE OF CONTENTS

<u>SECTION</u>		<u>PAGE</u>
I	INTRODUCTION AND SUMMARY.	1
II	STATUS OF MICROBEAM TECHNIQUES.	3
III	ION MICROPROBE MASS ANALYZER.	10
IV	SAMPLE ANALYSIS PROCEDURE	14
V	CMOS TECHNOLOGY GROUP .	20
	A. CMOS-Undoped Silicon Dioxide Gate Circuit on Sapphire Substrate .	20
	B. CMOS-Undoped Silicon Dioxide Gate Insulator.	25
	C. CMOS Aluminum Implanted Silicon Dioxide Gate Structure.	29
	D. Aluminum Oxide Gate Dielectric .	29
	E. CMOS-Chromium Doped Silicon Dioxide Gate Circuit on Sapphire Substrate.	32
VI	GENERAL TECHNOLOGY GROUP.	34
	A. Radiation Hardened Gates with Ni-Cr Resistor Films .	34
	B. Aluminum Metalized and Glassivated Devices .	39
VII	SIMS PROCEDURE EVALUATION .	54
	A. Special Sample Preparation Procedures.	54
	1. Package Delidding .	54
	2. Chip Removal.	54
	3. Sample Mounting .	54
	4. Conductive Coating.	56
	5. Instrument Mounting .	56
	B. Spatial Resolution .	56
	C. In-Depth Resolution.	59
	D. SIMS Parameter Control .	60
	1. Primary Ions. .	60
	2. Secondary Ions.	61
	3. Dynamic Range .	62
	E. Detection Limits .	62
	F. Analysis Time.	66
	G. Quantitation .	68

TABLE OF CONTENTS

(Continued)

<u>SECTION</u>	<u>PAGE</u>
VIII CONCLUSIONS . . . . .	70
IX RECOMMENDATIONS . . . . .	72
A. Failure Analysis . . . . .	72
B. Device Process Evaluation. . . . .	72
C. Instrumentation. . . . .	73
D. Future Studies . . . . .	74

LIST OF APPENDICES

A. Ion Probe Characterization Data for CMOS Group . . . . .	75
B. Ion Probe Characterization Data for General Group. . . . .	132

LIST OF ILLUSTRATIONS

<u>FIGURE</u>		<u>PAGE</u>
1	Effect of Diameter of Analyzed Area on Detection Limit. . . . .	9
2	Schematic of the Applied Research Laboratories Ion Microprobe Mass Analyzer. . . . .	11
3	Illustration of Electronic Gating . . . . .	13
4	ASMD02 150-16 . . . . .	16
5	Sputter Rate Profile -- ASMD02 150-16 . . . . .	17
6	CMOS-SOS-Clean Oxide Unit #739. . . . .	22
7	CMOS-SOS-Clean Oxide Unit #739. . . . .	23
8	CMOS-SOS-Clean Oxide Unit #739. . . . .	24
9	CMOS-SOS-Clean Oxide Unit #739. . . . .	25
10	CMOS-SOS-Clean Oxide Unit #739. . . . .	26
11	CMOS-SOS-Clean Oxide Unit #739. . . . .	27
12	CMOS-SOS-Clean Oxide Unit #739. . . . .	28
13	CMOS NAND Gate Unit #86 . . . . .	30
14	CMOS Al Implant Unit #890 . . . . .	31
15	CMOS Cr Doped Unit #504 . . . . .	33
16	54L00 Double Glass Unit #120 Area 6 . . . . .	37
17	54L00 Double Glass Unit #120 Area 8 . . . . .	38
18	54L00 Old Unit #103 . . . . .	40
19	54L00 Old Unit #103 . . . . .	41
20	Op Amp #1 Unit #3 . . . . .	42
21	Dopant Analysis in Active Silicon Regions on Op Amp #1, Unit #3 . . . . .	44
22	Phosphorus Profile. . . . .	45
23	Op Amp #2 LM741 Unit #62. . . . .	46
24	Op Amp #3 Unit #13. . . . .	47
25	Op Amp #3 HA 2600-02 Unit #13 . . . . .	48
26	ECL D Flop MC1670L Unit #21 . . . . .	50
27	ECL D Flop MC1670L Unit #21 . . . . .	51
28	Hex Inverter 5404J Unit #94 Area 7. . . . .	52
29	Hex Inverter SN5404J Unit #94 . . . . .	53
30	Secondary Ion Mass Number . . . . .	57

LIST OF ILLUSTRATIONS

(Continued)

<u>FIGURE</u>		<u>PAGE</u>
31	Secondary Ion Mass Number . . . . .	58
32	Microbeam Analysis Techniques for IC's. . . . .	63

LIST OF TABLES

<u>TABLE</u>		<u>PAGE</u>
1	Electron and Ion Microbeam Techniques Used for Integrated Circuit and Silicon Analysis . . . . .	4
2	Diameter or Width of Analysis Area. . . . .	5
3	Minimum Sample Dimensions: Volume, Weight, Atoms, and Associated Detection Limits . . . . .	6
4	Maximum Sensitivity: Associated Analytical Volume and Probe Diameter . . . . .	7
5	Sputter Rate for 17.9° Primary Beam . . . . .	18
6	CMOS Technology Group . . . . .	21
7	Radiation Hardened Gates. . . . .	35
8	Aluminum Metalized Glassivated Devices. . . . .	36
9	Detection Limits Determined for the Ion Microprobe Mass Analyzer in Silicon and Silicon Dioxide. . . . .	65
10	Analysis Times Required for SIMS Analysis of an Integrated Circuit. . . . .	67

## EVALUATION

This technical report describes the chemical evaluation of a variety of microcircuits using the ion microprobe mass analyzer. The data are presented in sufficient detail to permit a critical evaluation of the strengths and limitations of this secondary ion mass spectrometry technique especially for small scale integrated circuit analysis.

The description of the role that the IMMA can have in conjunction with other more standard analytical techniques such as electron probe analysis, Auger electron spectroscopy and scanning electron microscopy is valuable to those individuals responsible for decisions on how to approach device chemical characterization and failure analysis.

The study has shown that many of today's questions can be answered with available instrumentation. The challenge remains to refine and apply these analytical techniques to the study of large scale integrated microcircuits. While costly and time-consuming these efforts are necessary and proper for the assurance of the reliable design and performance of future electronic devices.

*John J. Bart*  
JOHN J. BART  
Reliability Physics Section  
Reliability Branch

SECTION I  
INTRODUCTION AND SUMMARY

The objective of Contract No. F30602-76-C-0316 was to apply secondary ion mass spectroscopy (SIMS) using an ion microprobe mass analyzer (IMMA) to evaluate the chemical nature of the laminar structures found in integrated circuits. This application was effected through the analysis of specific devices supplied by RADC. These devices were in two classes: (1) CMOS group and (2) general technology group.

Some of the major accomplishments under this contract were:

- (1) Establishment of integrated circuit sample preparation and coating procedures to enable the successful use of the IMMA on such devices.
- (2) Identification and in-depth characterization of heretofore undetected impurities in integrated circuit structures, e.g., F and Li.
- (3) Development and application of an  $\text{Ar}_{40}^+$  ion sputtering technique for the localization and identification of interfaces.
- (4) Measurement of the in-depth concentration profiles of dopants in specific areas of integrated circuits, e.g., P in  $\text{SiO}_2$ .
- (5) Establishment of the spatial resolution capabilities of the IMMA technique for integrated circuit analysis.
- (6) Determination of the most probable detection limits for impurities in structures on devices.
- (7) Prognostication of the role of secondary ion mass spectroscopy and the ion microprobe mass analyzer in device failure analysis and materials characterization.

The remainder of this report is organized as follows. The status of various microbeam characterization techniques is discussed in Section II. The ion microprobe mass analyzer is described in Section III. Sample analysis procedures are detailed in Section IV. The analytical results for the CMOS

**technology group are given in Section V and those of the general technology group in Section VI. Conclusions are given in Section VII and Recommendations in Section VIII.**

## SECTION II STATUS OF MICROBEAM TECHNIQUES

Two types of microbeam techniques, electron and ion beam, are available for the characterization of integrated circuit structures and microdefects in silicon materials. The most widely used techniques with their associated acronyms are shown in Table 1. Initial examination might seem to indicate the duplication of techniques in this list. However, it is important to understand that while scanning Auger microscopy (SAM) is Auger spectroscopy (AES), the converse is not true. SAM has microbeam capability, while AES does not. Similarly, while ion microprobe mass analysis (IMMA) is secondary ion mass spectroscopy (SIMS), again, the converse is not true. This difference is best shown in Table 2 where the diameter of the analysis area is shown for each analytical technique. As can be seen, the electron beam techniques have significantly better resolution capabilities and can simultaneously perform microanalysis and high resolution imaging. The ion beam techniques generally cannot analyze areas as small as 10  $\mu\text{m}$  in diameter, nor do they have high resolution imaging capabilities. To achieve optimum resolution, all characterization techniques must use small beam diameters, and inherent with small beam diameters are small beam currents. As a result, at optimum resolution all techniques have the smallest beam currents and therefore substantially degraded elemental sensitivities. This is shown in Table 3, where both analysis area and depth of analysis are taken into consideration. It is readily apparent that detection limits for all techniques are in the percent range. The ion beam techniques have the better sensitivities.

To obtain maximum analytical sensitivity, it is necessary to maximize the analytical volume, as shown in Table 4. The diameters analyzed can become quite large, particularly for the analysis of integrated circuit structures. The IMMA and SIMS techniques have the best analytical sensitivities. IMMA covers one specific class of SIMS instruments because it is a microbeam technique. SIMS, on the other hand, covers many different instruments, from the ion microscope to inexpensive quadrupole mass spectrometers attached to broad beam ( $\sim 1 \text{ mm}$ ) ion sputtering techniques such as ISS, AES, and ESCA or XPS.

TABLE 1. ELECTRON AND ION MICROBEAM TECHNIQUES USED  
FOR INTEGRATED CIRCUIT AND SILICON ANALYSIS

<u>Electron Beam</u>	<u>Acronym</u>
Auger Electron Spectroscopy	AES
Electron Microprobe	EMP
Scanning Auger Microscopy	SAM
Scanning Electron Microscopy	SEM
SEM with Silicon Detector	SEM-Si (Li)

<u>Ion Beam</u>	<u>Acronym</u>
Rutherford Backscattering	BS
Ion Induced X-Ray Fluorescence	IIXF
Ion Microprobe Mass Analysis	IMMA
Ion Scattering Spectroscopy	ISS
Secondary Ion Mass Spectroscopy	SIMS

TABLE 4. MAXIMUM SENSITIVITY: ASSOCIATED ANALYTICAL VOLUME AND PROBE DIAMETER

<u>Technique</u>	<u>Detection Limit, ppm<sub>a</sub></u>	<u>Minimum Detection Limit</u>		<u>Volume cc Analyzed</u>	<u>Diameter Analyzed</u>
		<u>Atoms</u>	<u>Grams</u>		
<u>Electron Beam</u>					
AES	1000 - 10,000	$2 \times 10^9$	$1 \times 10^{-13}$	$1 \times 10^{-10}$	250 $\mu\text{m}$
EMP	100 - 10,000	$2 \times 10^{10}$	$8 \times 10^{-13}$	$8 \times 10^{-9}$	25 $\mu\text{m}$
SAM	1 - 50%	$3 \times 10^5$	$2 \times 10^{-17}$	$2 \times 10^{-15}$	1 $\mu\text{m}$
SEM-Si(Li)	100 - 10,000	$2 \times 10^{10}$	$8 \times 10^{-13}$	$8 \times 10^{-9}$	25 $\mu\text{m}$
<u>Ion Beam</u>					
BS	100 - 10,000	$2 \times 10^{11}$	$8 \times 10^{-12}$	$8 \times 10^{-8}$	0.1 cm
IIXF	1 - 100	$4 \times 10^{10}$	$2 \times 10^{-12}$	$2 \times 10^{-6}$	0.1 cm
IMMA	0.01 - 100	$1 \times 10^5$	$5 \times 10^{-18}$	$2 \times 10^{-10}$	150 $\mu\text{m}$
ISS	10,000	$2 \times 10^{13}$	$1 \times 10^{-9}$	$4 \times 10^{-9}$	0.1 cm
SIMS	0.1 - 1000	$2 \times 10^6$	$1 \times 10^{-16}$	$5 \times 10^{-10}$	250 $\mu\text{m}$

Assumptions used for calculating volume analyzed:

AES - 2 nm x 250  $\mu\text{m}$  diameter

EMP and SEM-Si(Li) - 25  $\mu\text{m}$  diameter sphere

SAM - 2 nm x 1  $\mu\text{m}$  diameter

BS - 100 nm x 1 cm diameter

IIXF - 2.5  $\mu\text{m}$  x 0.1 cm diameter

IMMA - 10 nm x (150  $\mu\text{m}$ )<sup>2</sup>

ISS - 5 nm x 0.1 cm diameter

SIMS - 10 nm x 250  $\mu\text{m}$  diameter

The effect of analysis area is best shown in Figure 1, which is a plot of "typical" detection limits versus the diameter of the analyzed area. Superimposed on this figure are shaded areas that show the detection limits and diameters of areas of interest in integrated circuits analysis. Notice that only IMMA and SIMS are applicable for the determination of impurities and dopants in silicon. The electron beam techniques, SEM-SI(Li), EMP, and SAM have excellent resolution, but detection limits that prevent measurement of chemical variations within integrated circuit dielectric films and diffused silicon areas. The importance of IMMA, an ion microbeam technique, as a potential technique for integrated circuit analysis can be seen in this figure. The work in this report was directed toward establishing the capabilities of IMMA for device failure analysis.

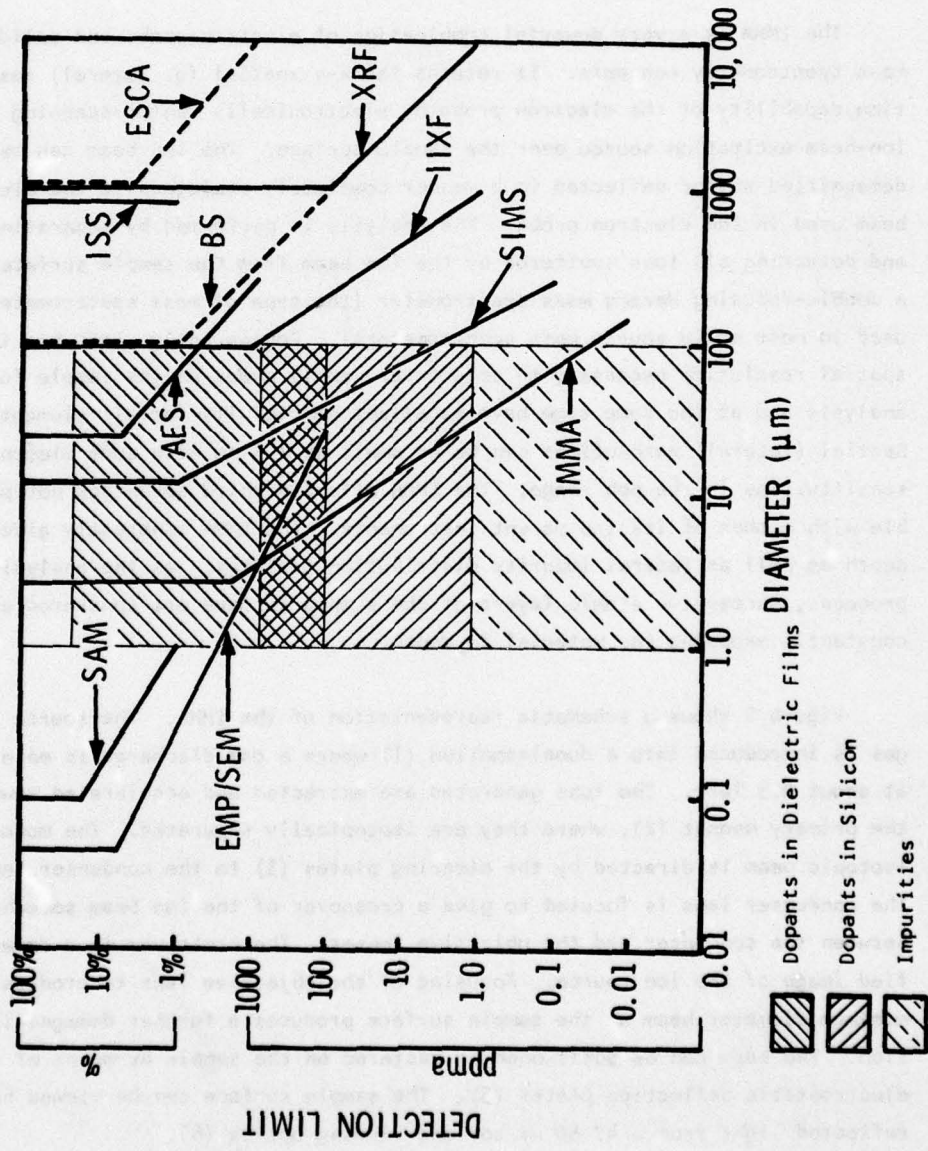
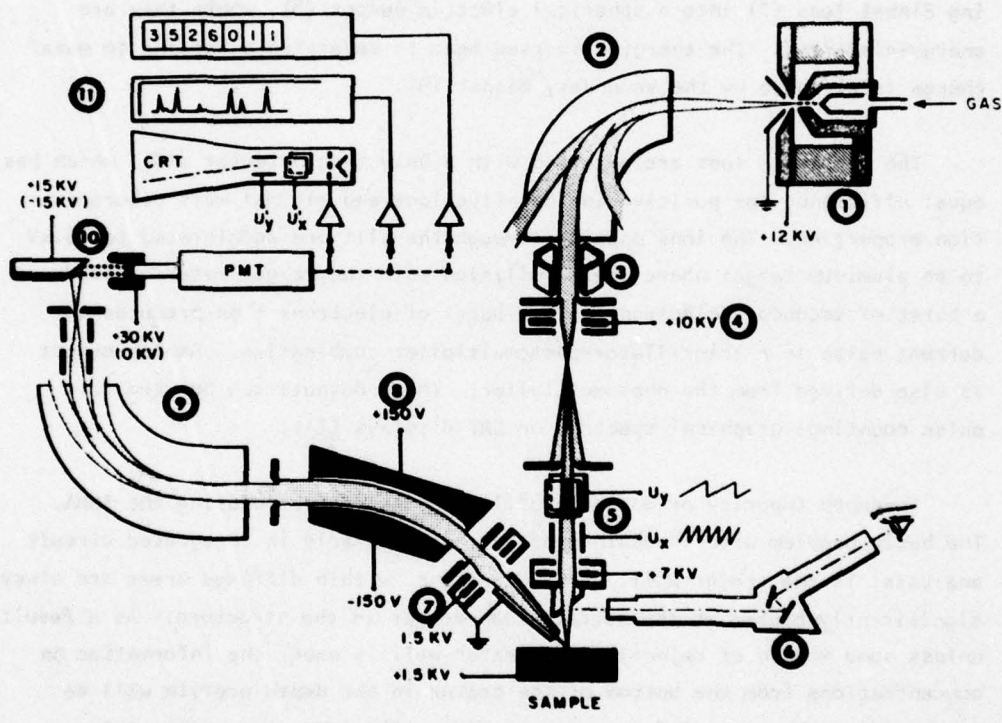


Figure 1 Effect of Diameter of Analyzed Area on Detection Limit

### SECTION III ION MICROPROBE MASS ANALYZER

The IMMA is a very powerful combination of electron-probe and solids mass spectrometry concepts. It retains the x-y spatial (or lateral) resolution capability of the electron probe by electronically raster-scanning an ion-beam excitation source over the sample surface. The ion beam can be demagnified and/or deflected in a manner completely analogous to the electron beam used in the electron probe. The analysis is performed by separating and detecting all ions sputtered by the ion beam from the sample surface with a double-focusing Herzog mass spectrometer (the type of mass spectrometer used in most solid source mass spectrometers). Consequently, IMMA has the spatial resolution necessary to select very small areas on the sample for analysis and at the same time have excellent sensitivity for all elements. Spatial (lateral) resolutions can be as small as 2.5  $\mu\text{m}$  with some elemental sensitivities in the ppb range. The IMMA offers a third advantage not possible with either of its two parent instruments. The IMMA inherently gives depth as well as lateral impurity distribution profiles: as the analysis proceeds, successive atomic layers of the sample surface are sputtered away, constantly exposing the material in depth.

Figure 2 shows a schematic representation of the IMMA. The source ion gas is introduced into a duoplasmatron (1) where a gas discharge is maintained at about 0.3 Torr. The ions generated are extracted and accelerated toward the primary magnet (2), where they are isotopically separated. The mono-isotopic beam is directed by the steering plates (3) to the condenser lens (4). The condenser lens is focused to give a crossover of the ion beam somewhere between the condenser and the objective lenses. The crossover is a demagnified image of the ion source. Focusing of the objective lens to produce a minimum diameter beam at the sample surface produces a further demagnification. The beam can be positioned or rastered on the sample by means of the electrostatic deflection plates (5). The sample surface can be viewed by reflected light from a 47.50 mirror and viewing optics (6).



**Figure 2 Schematic of the Applied Research Laboratories  
Ion Microprobe Mass Analyzer**

The impact of the primary beam on the sample results in both implantation of primary ions and sputtering of the sample surface. The sputtered, or secondary, ions are collected by a pickup electrode by a bias potential applied to the sample. The polarity of the ions collected is controlled by polarity of this potential bias. The collected ions pass through a focusing Einzel lens (7) into a spherical electric sector (8), where they are energy-dispersed. The energy-dispersed beam is separated according to mass/charge ( $m/e$ ) ratio by the secondary magnet (9).

The secondary ions are detected with a Daly type detector (10), which has equal efficiency for positive and negative ions and minimal mass discrimination properties. The ions passing through the slit are accelerated to 15 kV to an aluminum target where their collision with the target material produces a burst of secondary electrons. This burst of electrons then produces a current pulse in a scintillator-photomultiplier combination. Analog output is also derived from the photomultiplier. These outputs can be used for pulse counting, graphical spectra, or CRT displays (11).

In-depth impurity or dopant profiles can be performed using the IMMA. The basic problem with in-depth profiles, particularly in integrated circuit analysis, is the crater wall. Concentrations within diffused areas are always significantly higher at the surface than deeper in the structure. As a result, unless some method of rejecting the crater wall is used, the information on concentrations from the bottom of the crater in the depth profile will be dominated by the high surface concentration. The IMMA circumvents this problem by rastering the ion beam in the form of a rectangle as shown in Figure 3. The sputtered ions are accepted or rejected by electronic gating of the detector, depending on the position of the sputtering ion beam. In Figure 3, this is illustrated by the inner rectangle where the detector is gated on at point A of the raster and off at point B. This inner rectangle is commonly referred to as an electronic aperture of secondary ion acceptance.

The IMMA, as described in this section, has been used for all the analyses on the integrated circuits described in the remaining sections of this report.

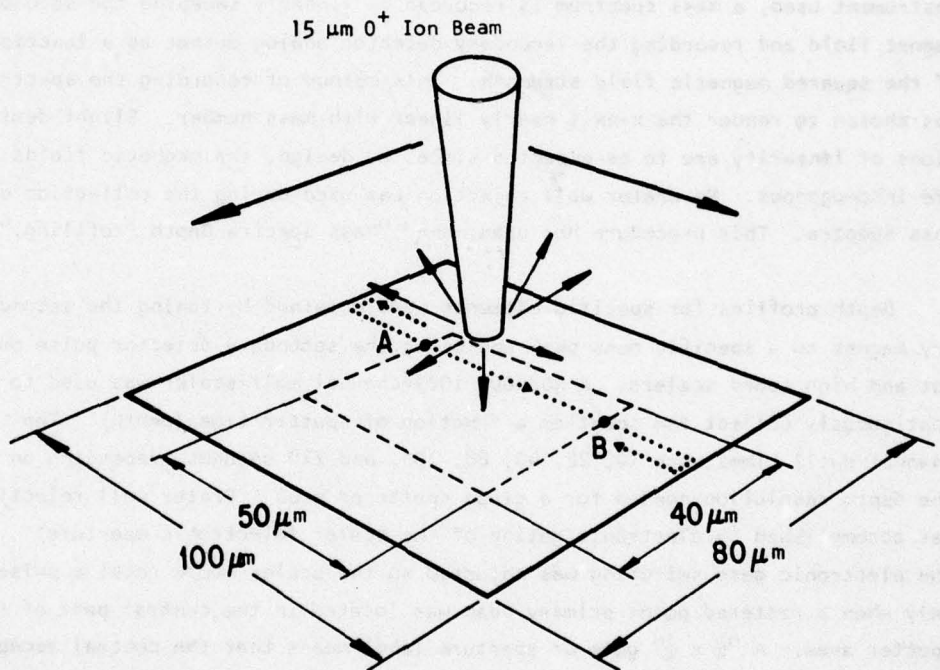


**Figure 3 Illustration of Electronic Gating**

SECTION IV  
SAMPLE ANALYSIS PROCEDURE\*

The analysis procedure most commonly used was to sputter the area of interest and collect complete mass spectra as a function of time. In the instrument used, a mass spectrum is recorded by linearly sweeping the secondary magnet field and recording the secondary detector analog output as a function of the squared magnetic field strength. This method of recording the spectrum was chosen to render the x-axis nearly linear with mass number. Slight deviations of linearity are to be expected since, by design, the magnetic fields are inhomogenous. No crater wall rejection was used during the collection of mass spectra. This procedure has been named "Mass Spectra Depth Profiling."

Depth profiles for specific elements were obtained by tuning the secondary magnet to a specific mass peak and using the secondary detector pulse output and high speed scalers. A ND2400, 1023-channel multiscaler was used to continuously collect the count as a function of sputter time (depth). The channel dwell times were 10, 22, 40, 88, 100, and 220 seconds, depending on the depth resolution needed for a given sputtered area. Crater wall rejection was accomplished by electronic gating of the scaler (electronic aperture). The electronic gate switching was adjusted so the scaler would receive pulses only when a rastered point primary beam was located in the central part of the sputter area. A " $\frac{1}{4} \times \frac{1}{4}$ " gate or aperture label means that the central acceptance area was one-fourth the X raster dimension and one-fourth the Y raster dimension. Two masses can be monitored nearly simultaneously by electrostatic peak switching just before the secondary detector entrance slit. The requirement is that both mass peaks must simultaneously pass through the analyzing magnet and be resolved. Normally, this is true for masses of  $M \pm 0.07M$ . The switching is done between the two masses every 100 ms with a 10 ms pause in a blank position. This feature allowed mass pairs such as Si-P, Cr-Ni,  $Si_2O$ -As, etc., to be collected from the same sputtered crater. This technique has been named "Point Count Depth Profiling."

---

\* Sample preparation procedures developed and employed are discussed in Section VII.A of this report.

The primary beam used for all data collection on devices where thick oxide remained intact was 17.8 kV O<sup>-</sup> (negative oxygen). Positive primary beams could not be used since the ejection of secondary electrons from the sample upon impact and simultaneous injection of positive particles render it impossible to reach an equilibrium surface charge state, which is mandatory to gain control of the sputtered secondary ion trajectory. The surface charge equilibrium is attained using negative sputter beams. The negative beam size and total current parameters were adjusted to obtain the maximum current with a beam diameter of less than 25  $\mu\text{m}$ . The beam was normally rastered over an area to cut a flat bottom crater. When electronic gating was employed, the minimum raster size was at least 3 X the beam diameter. All crater areas reported were measured with the high precision x-y stage since area is a very important parameter for depth calculation.

Positive secondary ions were monitored in these analyses. Negative secondary ions cannot be monitored from insulating layers for much the same reason positive primary beams cannot be used. To monitor negative secondaries, the surface of the sample must be highly negatively biased, a condition that does not allow any ejected secondary electron to reenter the sample; therefore, no surface charge equilibrium can be attained.

The sputter rate for 17.8 kV O<sup>-</sup> was experimentally determined by point count depth profiling an As implanted 120 nm SiO<sub>2</sub> film as a function of sputtered area and beam current. The actual As peak depth was determined by SiO<sub>2</sub>-As point count depth profiling the same SiO<sub>2</sub> film using an Ar<sup>+</sup> primary beam (120 nm SiO<sub>2</sub> on Si can be considered a noninsulator to high energy beams). The fall of the Si<sub>2</sub>O signal depicts the SiO<sub>2</sub>-Si interface, and since the SiO<sub>2</sub> thickness was known, this point gives an absolute calibration to the depth scale; hence, the As peak depth can be measured. The SiO<sub>2</sub>-As profiles used are shown in Figure 4. A series of As point count profiles using the 17.8 kV O<sup>-</sup> beam for this calibration is shown in Figure 5. A summary of the sputter rate determination is given in Table 5.

Ar<sup>+</sup> ion sputtering was used for rapid sputtering through the glassivation for an interface analysis. The preceding discussion on the inapplicability of

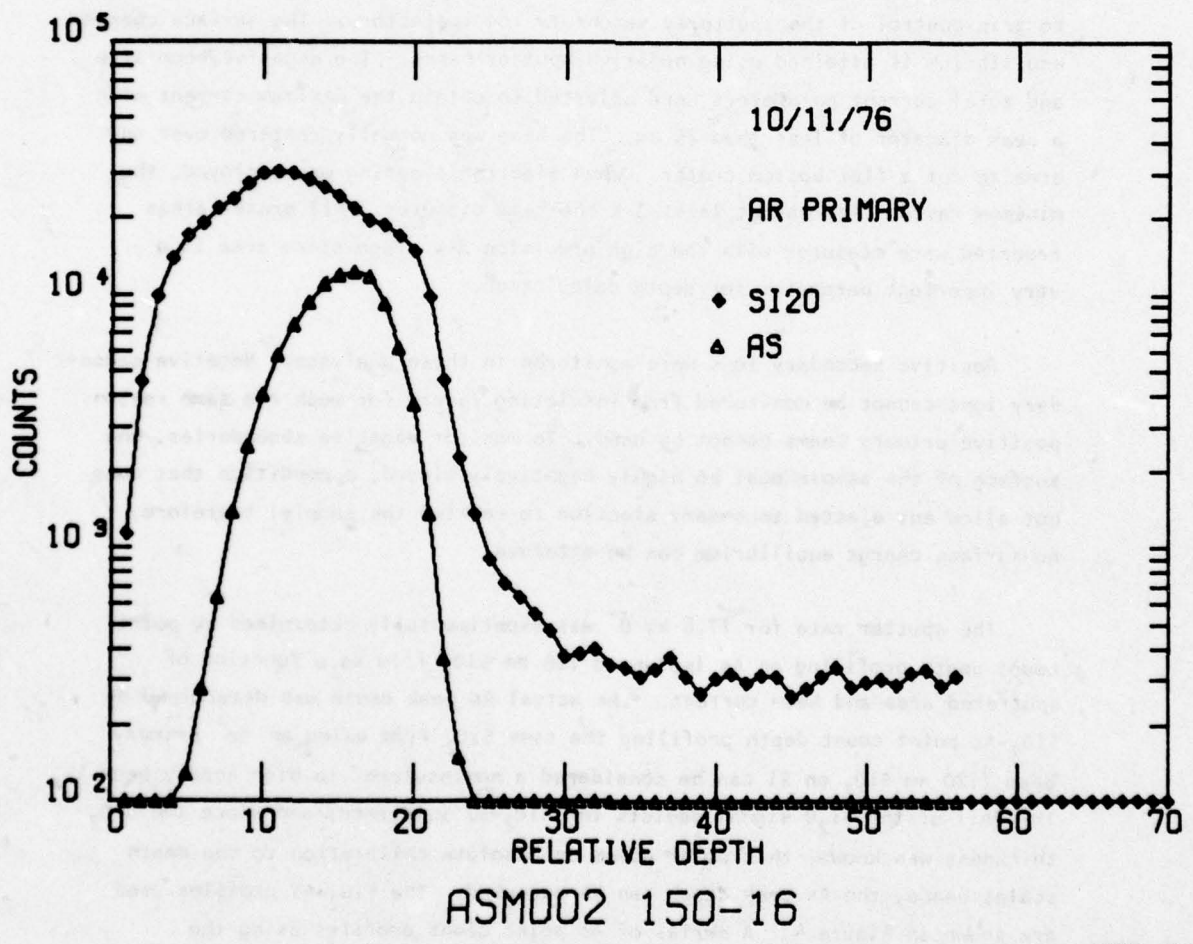


Figure 4

JMMA--MCL

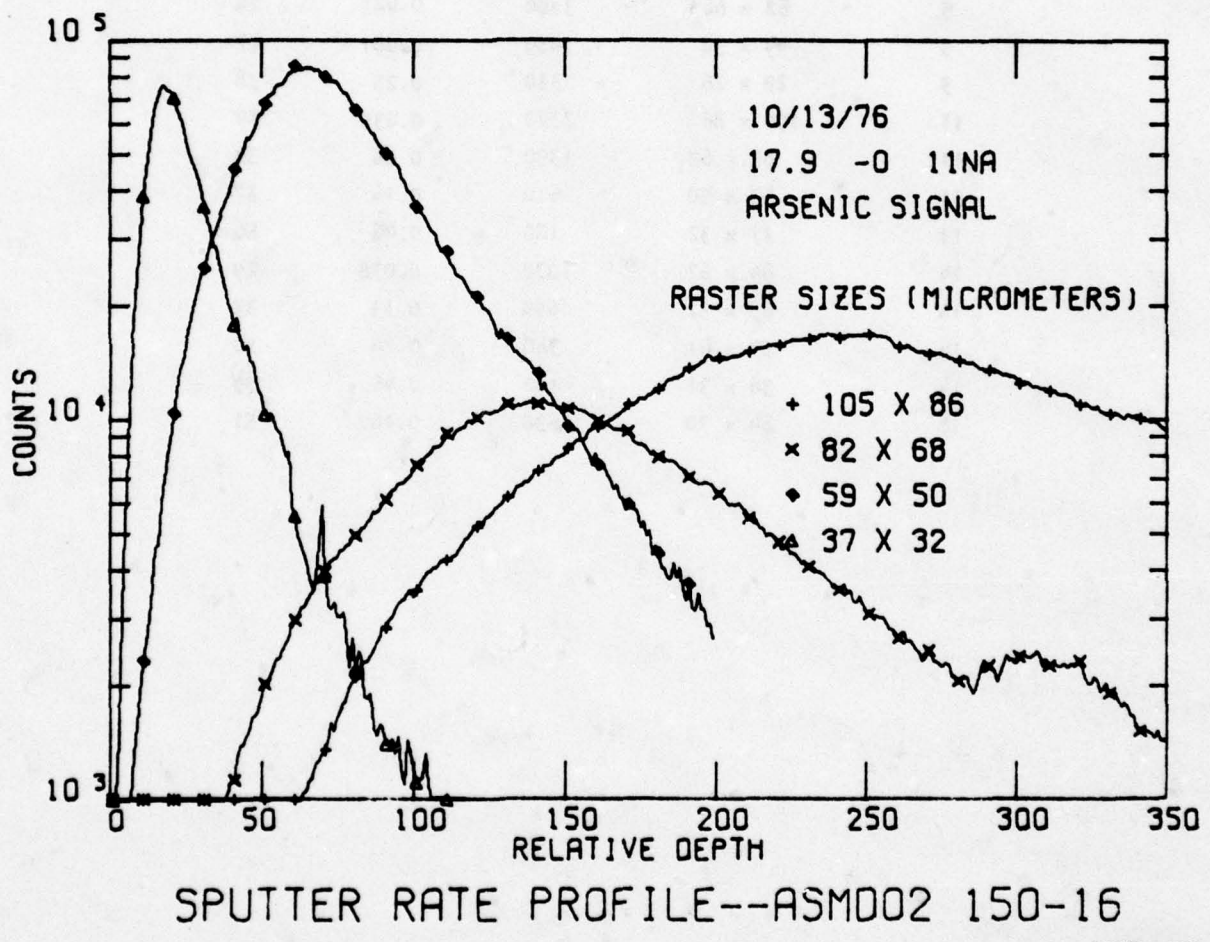


Figure 5

TABLE 5. SPUTTER RATE FOR 17.9° PRIMARY BEAM

Beam Current nA	Raster Size ( $\mu\text{m} \times \mu\text{m}$ )	Sec to 83.4 nm	nm/Sec	$\frac{\text{(nm)}}{\text{(Sec)}}$ $\frac{(\mu\text{m}^2)}{(\text{nA})}$
5	82 x 68	3880	0.021	24
5	44 x 38	1030	0.081	27
5	29 x 26	330	0.25	38
11	105 x 86	2370	0.035	29
11	85 x 69	1390	0.06	32
11	59 x 50	610	0.14	37
11	37 x 32	180	0.46	50
14	84 x 62	1070	0.078	29
14	68 x 52	650	0.13	32
14	53 x 41	340	0.24	38
14	38 x 31	180	0.46	39
18	84 x 70	530	0.16	51

positive primary beams applies only to secondary ion detection, not sample sputtering. The time necessary to sputter through the glassivation was determined by sputtering a small crater over aluminum metallization and monitoring the  $Al^+$  signal. At the aluminum layer, the sputtered surface becomes a conductor with a major matrix change which is apparent in the  $Al^+$  signal. Large craters were opened in selected interface analysis areas using the reciprocity relationship among depth, current, and area. The actual interface analysis used a 17.8 kV  $O^-$  beam that was rastered in only the central part of the area opened; this, in effect, gave surface and crater wall rejection.

All mass spectra were taken with a 4.8 mm entrance aperture ( $\alpha$ ) and a 12.7 mm exit aperture ( $\beta$ ) for the energy analyzer. A 0.25 mm resolving slit was used between the momentum analyzer and secondary ion detector. These parameters give a resolution number ( $M/\Delta M$  at 10% valley) of 320, which is sufficient to resolve the Pb isotopes. The point count depth profiles normally used the same  $\alpha$  and  $\beta$  apertures with a 0.5 mm resolving slit for a resolution number of 190.

The sample chamber vacuum attained before analysis with no oxygen leak to the duoplasmatron was 1 to  $5 \times 10^{-8}$  torr. The sample chamber pressure increased to about  $4 \times 10^{-7}$  torr during analysis when the duoplasmatron was pressurized at 200 to 300 torr. The vacuum was measured by the ion pump current.

SECTION V  
CMOS TECHNOLOGY GROUP

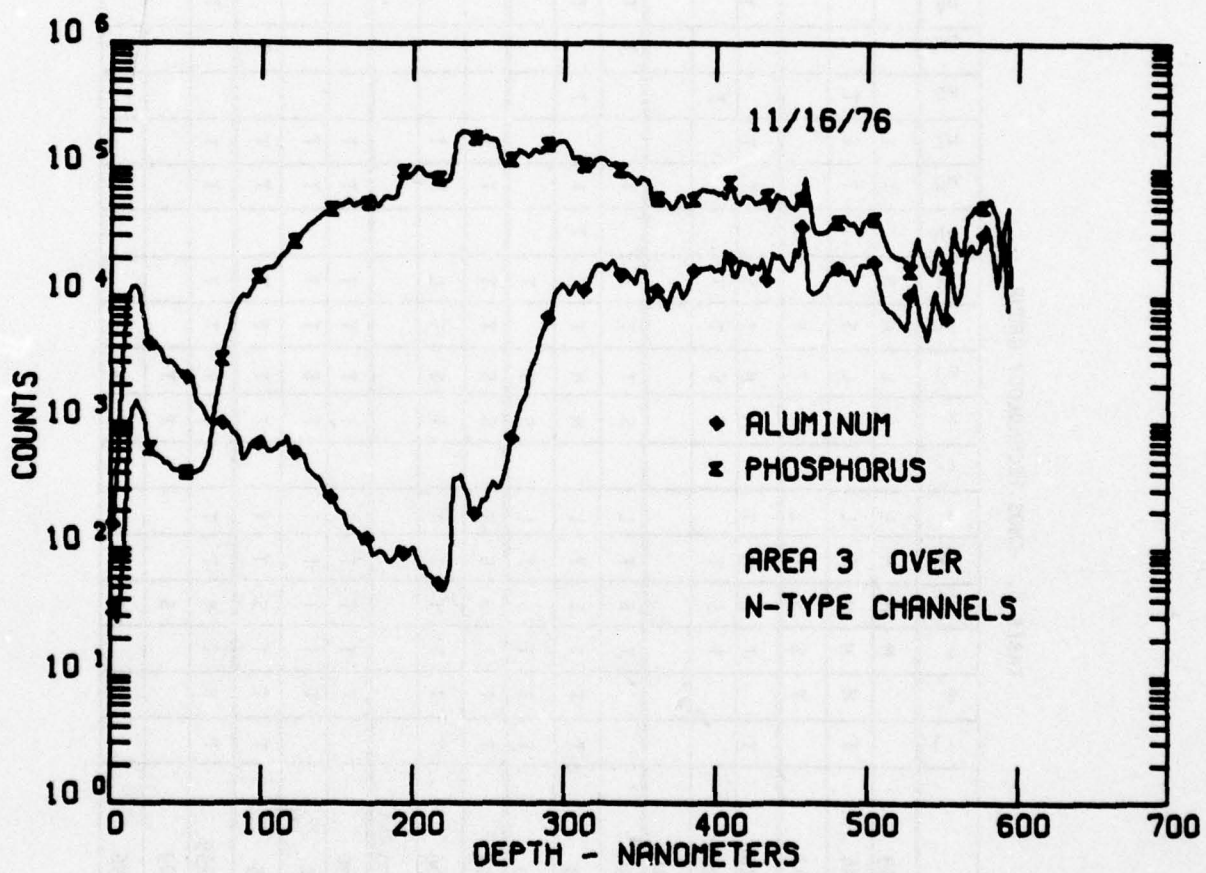
The general analyses of the entire CMOS technology group (about 300 mass spectra) are summarized qualitatively in Table 6. The symbols used in this table are T for trace (just detectable), S for small quantity, M for medium amounts, and L for large concentrations such as P in phosphosilicate glasses. The symbol was entered if the element was detected in any mass spectrum from any area on the device. Appendix A contains a more detailed analysis of Set #1 spectra, along with optical pictures identifying the exact areas sputtered. Scanning electron micrographs of each area analyzed, depicting oxide defects, metallization problems, and silicon quality, are included for one set of circuits.

A. CMOS-Undoped Silicon Dioxide Gate Circuit on Sapphire Substrate

CMOS-SOS-clean oxide, Unit #739: An Al-P peak count depth profile was prepared to show the variation in P concentration through the glassivation into the thermal oxide. The raster was cut over oxide as well as aluminum metal to sample the thermal oxide. The profile is shown in Figure 6. The phosphorus concentration increased until the glassivation-aluminum interface was reached at about 280 to 300 nm. At this point, the P decreases slightly due to the reduced oxide surface area. This suggests the thermal oxide is uniformly doped with P. Figure 7 shows the F-Ca ( $\text{Ca}^{+2}$ ) depth profile of an area over n-type channels. The profile indicates Ca is highly localized at the surface, in contrast to the F, which has concentration maxima and minima as a function of depth. Figure 8 shows a quantitative P profile of the oxide in the n-channel region. The P levels are at about  $1.5 \times 10^{21}$  atoms/cc. Attempts to strip the circuit stepwise using HF gas were unsuccessful because the first one-minute exposure removed all the oxide and metal over oxide. The surface mass spectra of the device after this chemical stripping were very complicated, showing strong impurity peaks (see Appendix A). Figures 9 and 10 show the relative B-P concentrations found in n-channel and p-channel regions. Figures 11 and 12 are attempts to determine the Al up-diffusion from the sapphire during

TABLE 6. CMOS TECHNOLOGY GROUP

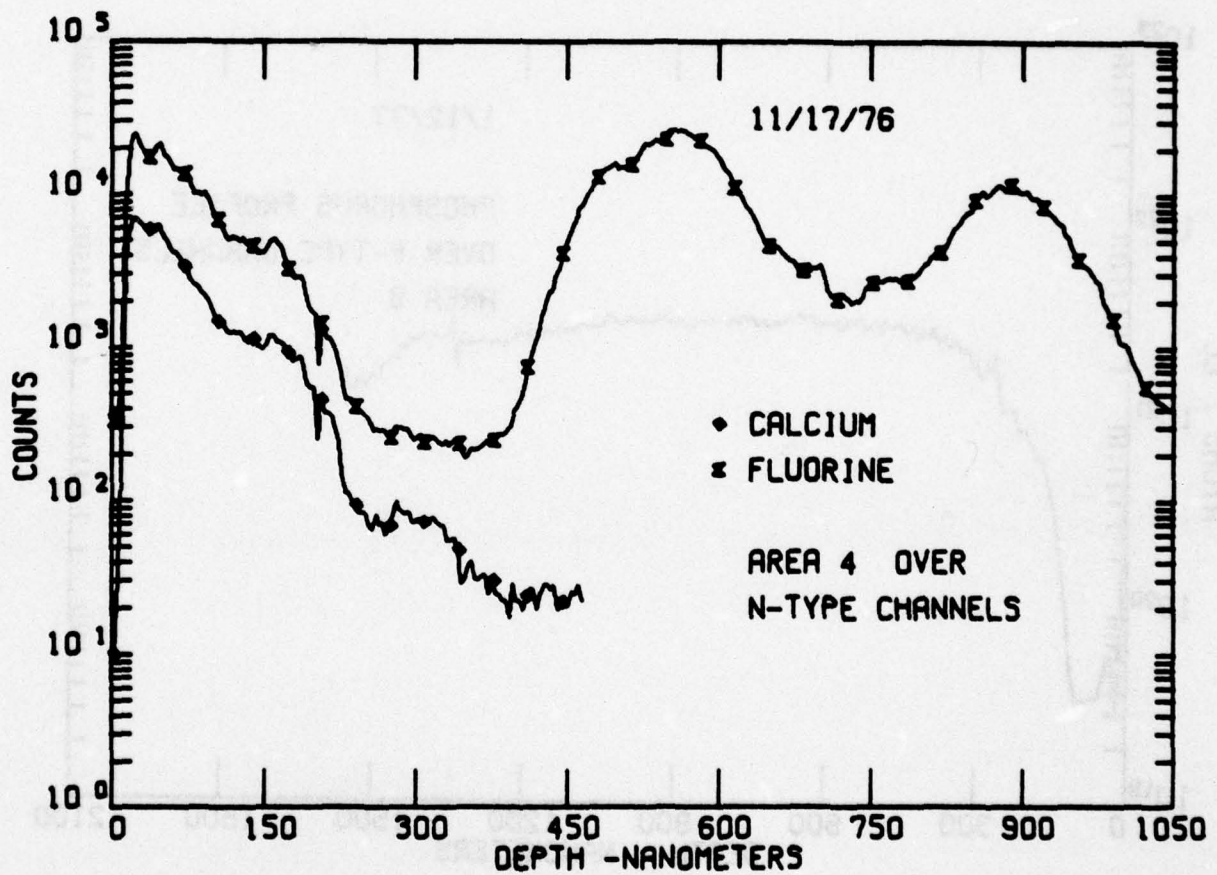
DEVICE	L	B	T	E	Mg	C	X	Ca	Ni	Cr	Ti	Zn	C	N	Cr	Pb
	-	-	-	-	-	-	-	-	-	-	-	-	-	-	-	-
SOS 739					M M M L	M L M S		T T T T								S
SOS 746	T	M	M	M	S L	S L S T		T T T T								
SOS 743	T	S	S	T	L	S T T										
BULK CLEAN R202	T	T	L	M	T	M M M S		T T T								
BULK CLEAN R203		T	S	T		T S T T		T T T T								
BULK CLEAN R198																
NAND GATE 86		T	S	T	L	S T T T		T T T T								
NAND GATE 63	T	T	S	T	L	M M T T		T T T T								
NAND GATE 50	T	T	S	T	L	S S T T		T T T T								
Cr DOPED 504	T	T	S	S	T	S S T T		T T T T								
Cr DOPED 506	T	T	T	T	T	T S T L		T T T T								
Cr DOPED 500																
A1 IMPLANT 890		T	T	T	T	T T T T		T T T T								T
A1 IMPLANT 92		T	T	T	T	T S T T		T T T T								
A1 IMPLANT 25		T	T	S	T	T T T T		T T T T								T
A1 <sub>2</sub> 0 <sub>3</sub> A259	T	T	T	S	T	T S T T		T T T T								T T
A1 <sub>2</sub> 0 <sub>3</sub> 309																
A1 <sub>2</sub> 0 <sub>3</sub> 356																



CMOS-SOS-CLEAN OXIDE UNIT #739

Figure 6

JWMA-MCL



CMOS-SOS-CLEAN OXIDE UNIT #739

Figure 7

JMMA--MCL

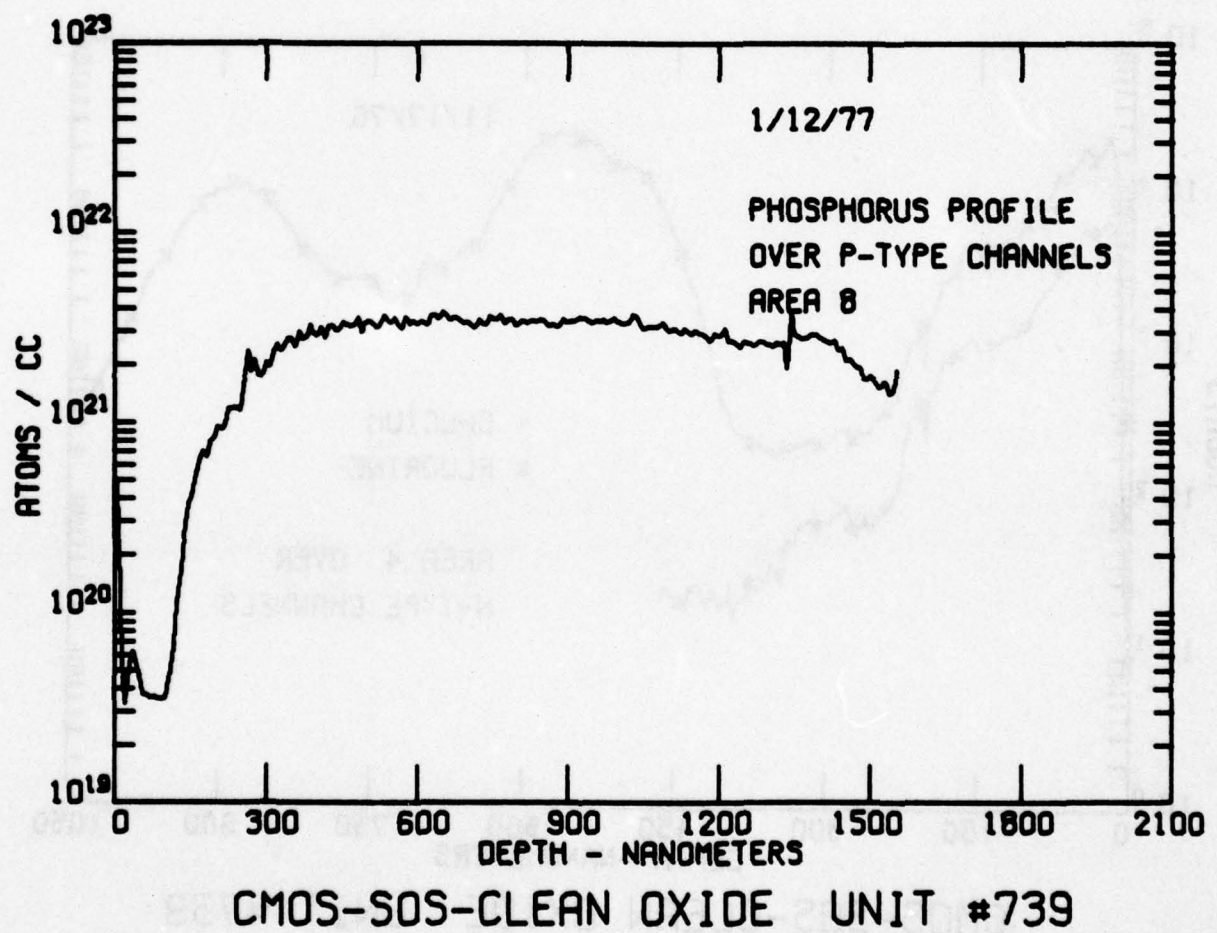


Figure 8

JMMR-MCL

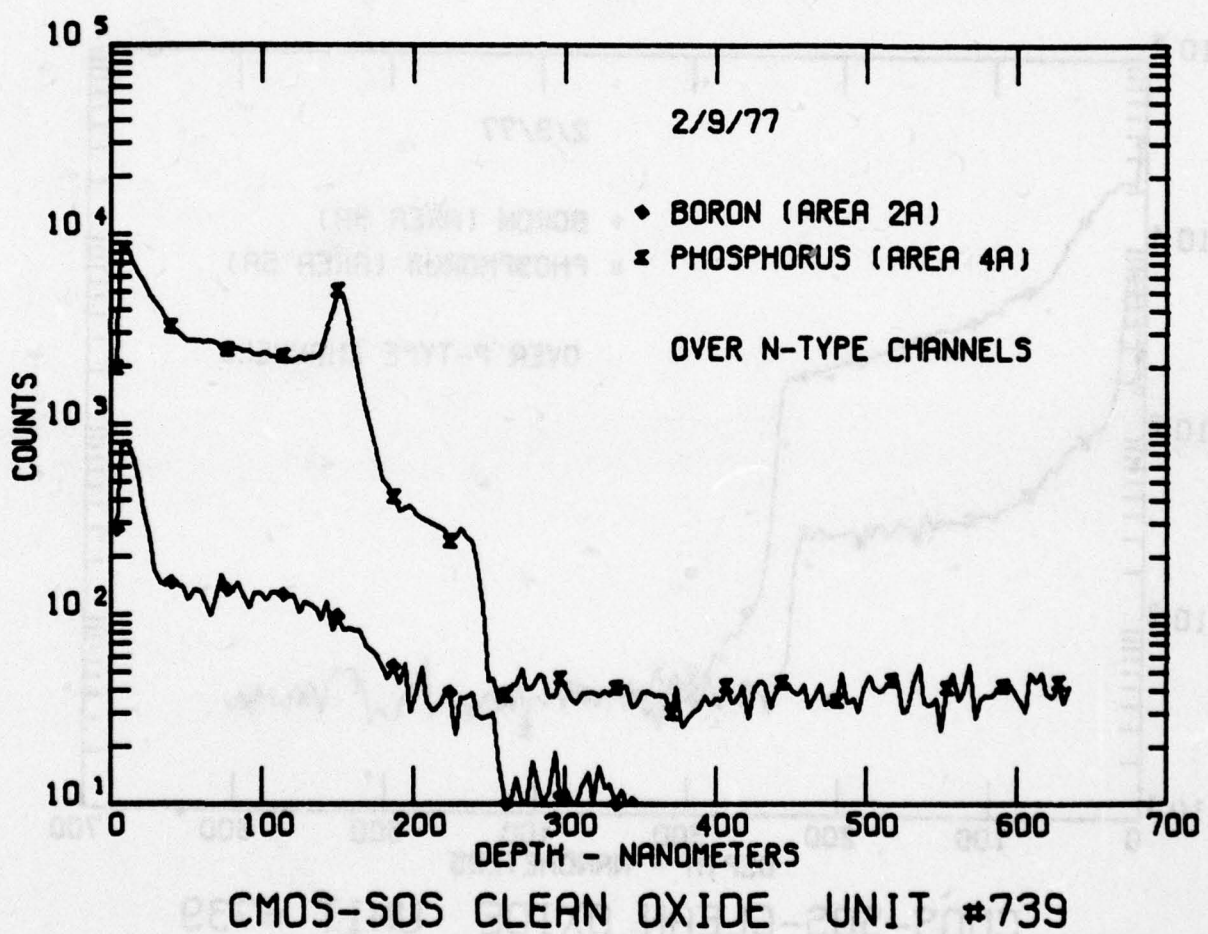


Figure 9

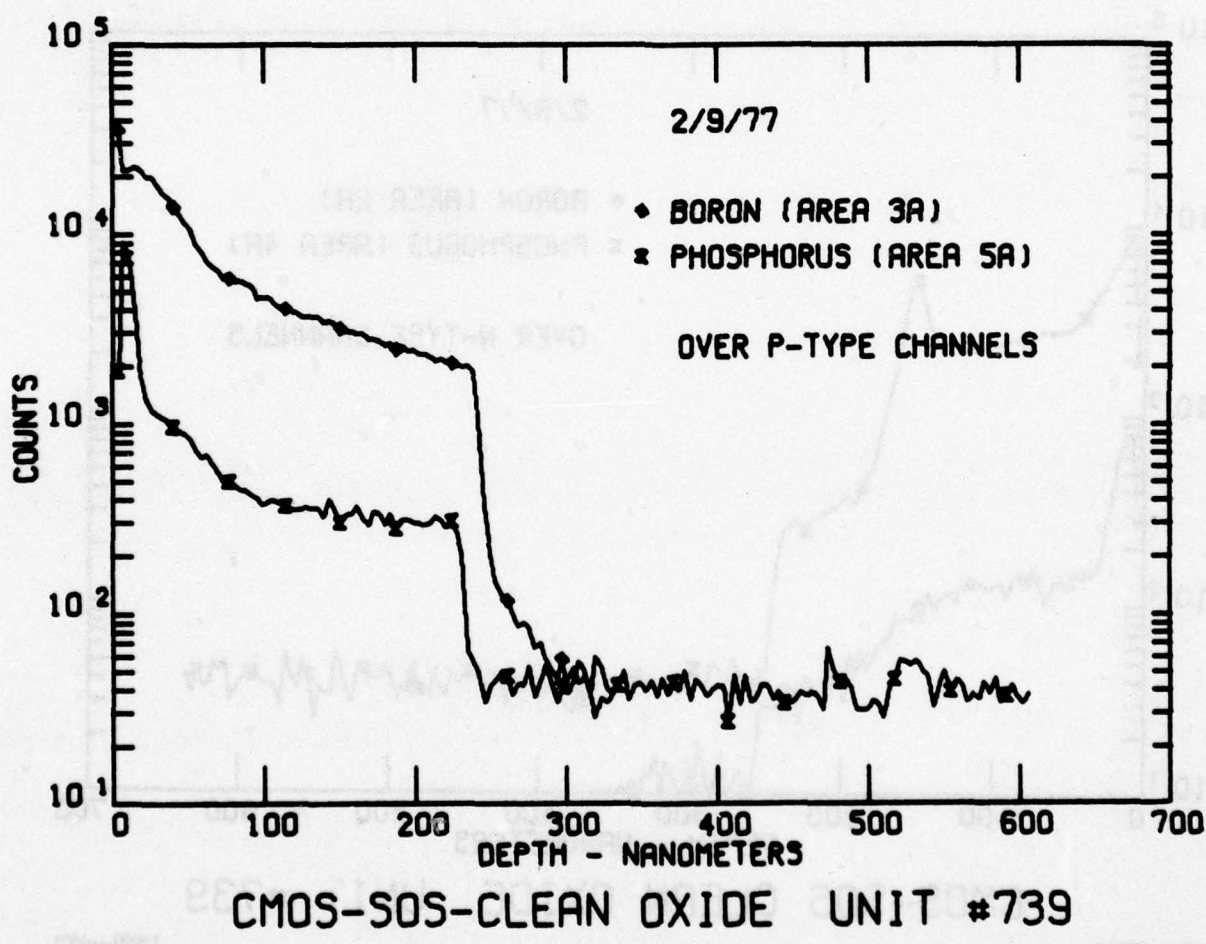
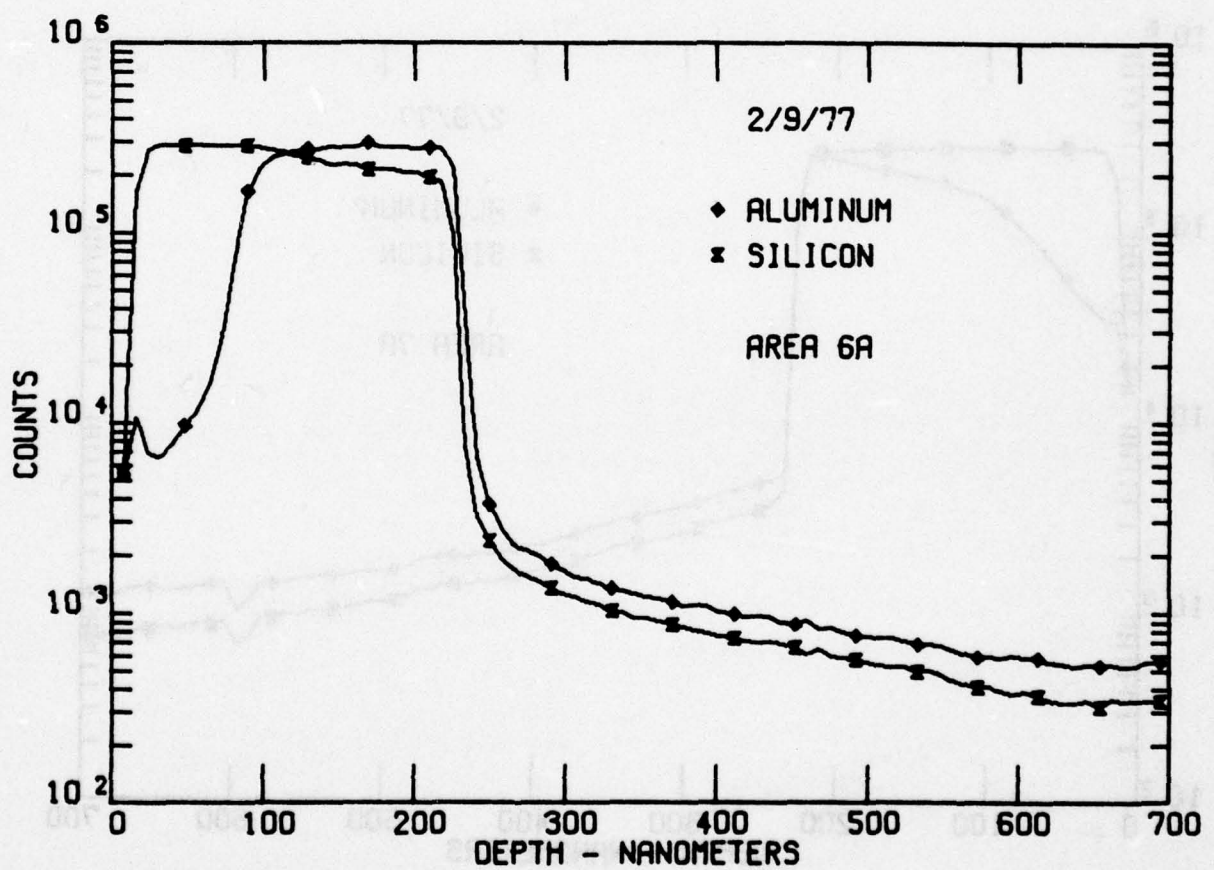


Figure 10



CMOS-SOS-CLEAN OXIDE UNIT #739

JMMR-MCL

Figure 11

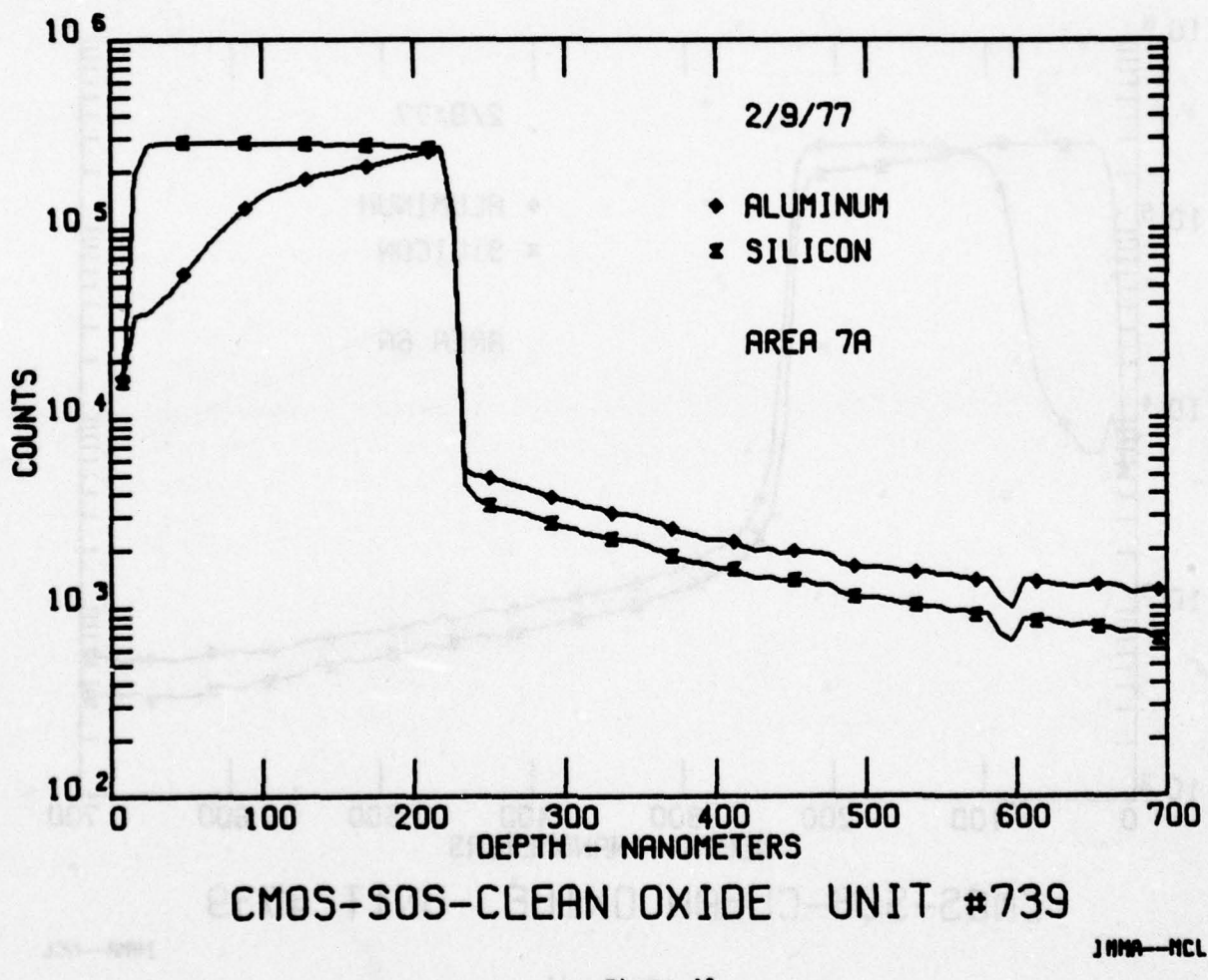


Figure 12

silicon growth by depth profiling the Al-Si signals. The silicon was so completely consumed by the upper metal layer that this analysis is inconclusive. The silicon dissolution by aluminum can occur in SOS structures during elevated temperature processing and/or testing. The SEM of the bond pad shown in Appendix A confirmed the porous silicon layer.

B. CMOS-Undoped Silicon Dioxide Gate Insulator

CMOS bulk clean oxide, Unit #R202: Only mass spectra depth profile data were gathered on this circuit. No P was detected in the oxide.

CMOS-Nand gate, Unit #86: The P profile taken over an oxide area is shown in Figure 13. The P starts at about 150 nm, stays level at about  $10^{21}$  atoms/cc until the 1.2  $\mu\text{m}$  depth is reached, then drops sharply. An interpretation is that the glassivation is P-free and about 150 nm thick and that the thermal oxide (not necessarily gate oxide) is about 1  $\mu\text{m}$  thick, uniformly doped with P. The sharp drop then represents either the thermal oxide-gate oxide interface or the thermal oxide-silicon interface. This shows the difficulty in interpreting this type of spectral information.

C. CMOS Aluminum Implanted Silicon Dioxide Gate Structure

CMOS-Al implant, Unit #890: The oxides were not doped with P. Figure 14 is the Al-Ti point count profile in this device to a depth of about 2.2  $\mu\text{m}$ . The Ti contaminant appears to track the Al through the oxide into the gate oxide, which suggests it could be related to the implant process.

D. Aluminum Oxide Gate Dielectric

Only mass spectra depth profiles were collected on this circuit. No phosphorus was found in the dielectric.

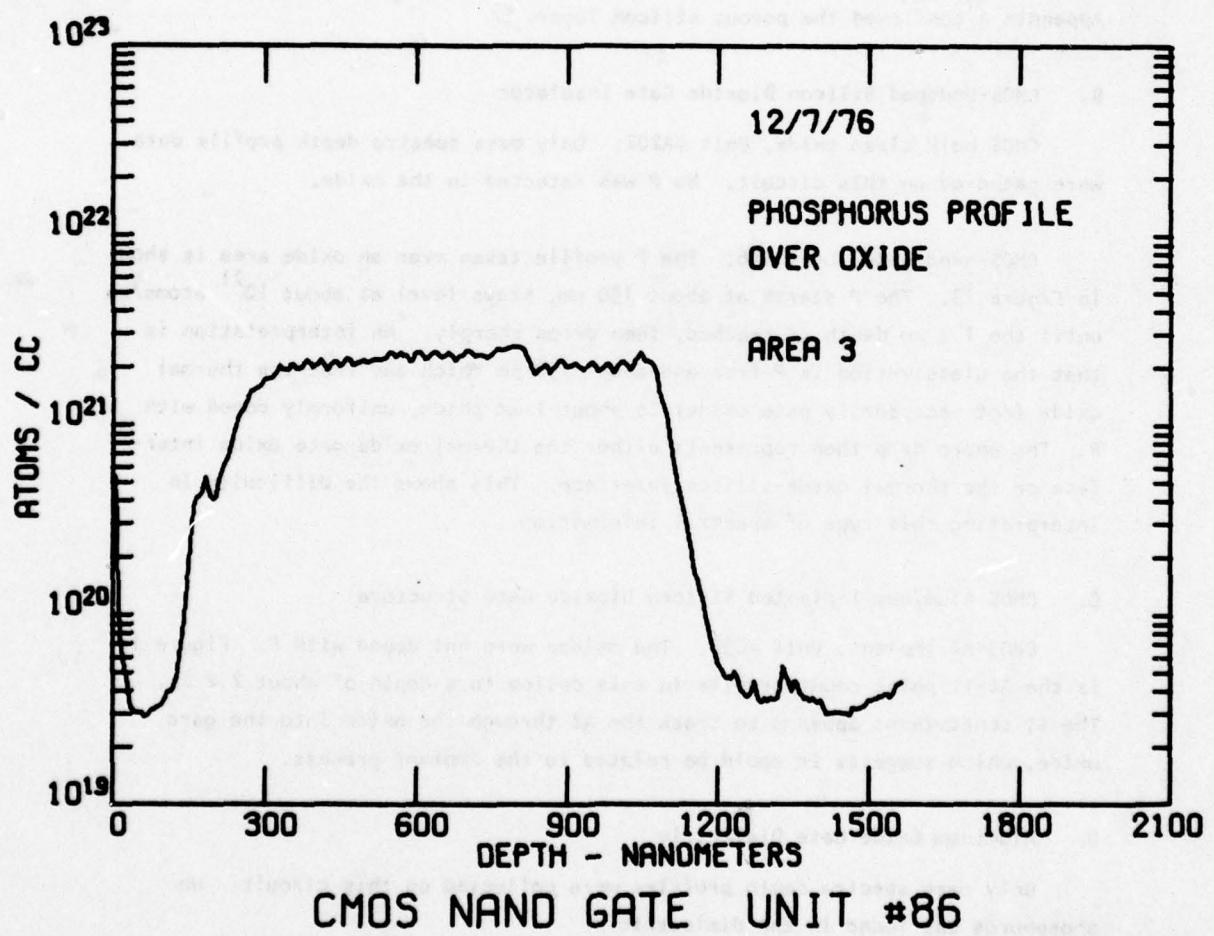


Figure 13

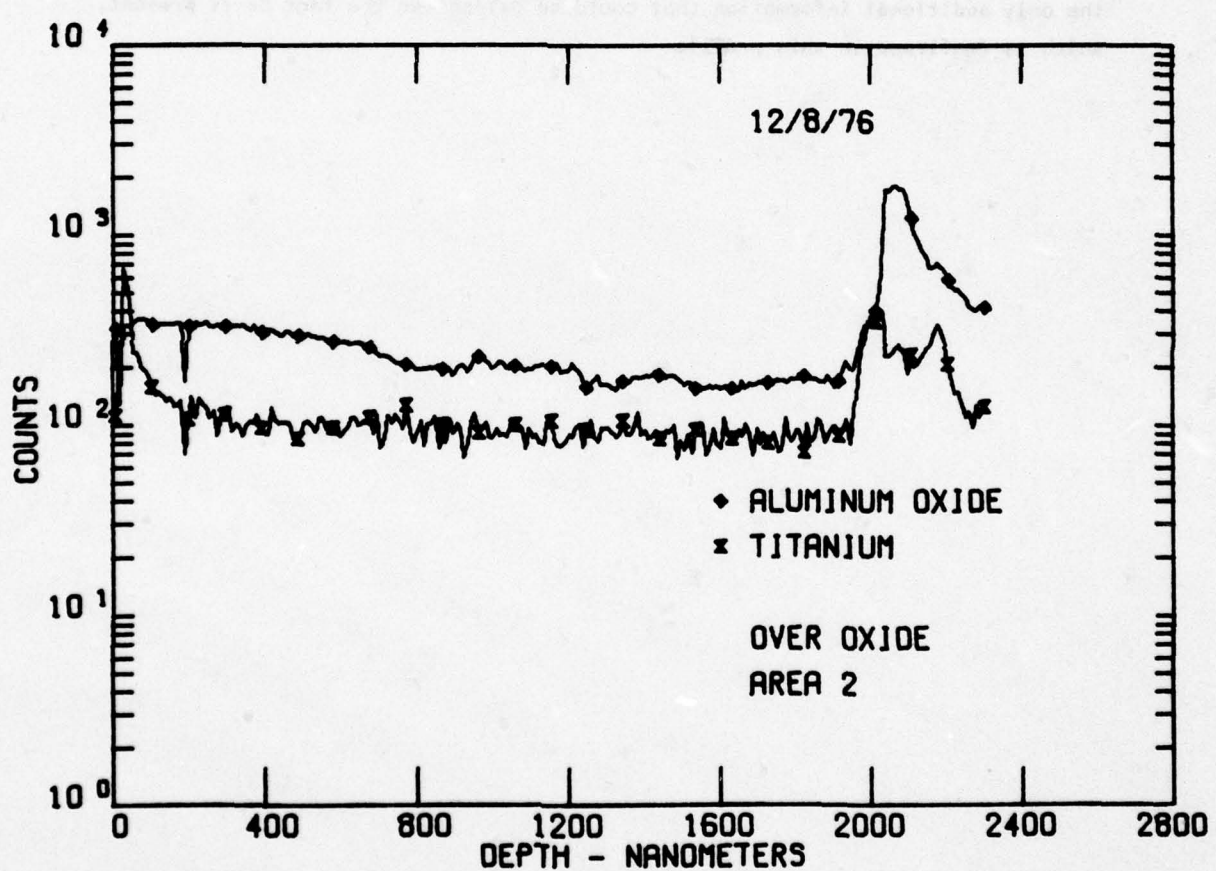


Figure 14

JHMA-MCL

E. CMOS-Chromium Doped Silicon Dioxide Gate Circuit on Sapphire Substrate

CMOS-Cr doped; Unit #504: The oxides were not P doped. Figure 15 gives a shallow Cr profile in this device. The Cr concentration does not appear to be uniform in this region. The gate oxide region was not profiled, since the only additional information that could be gained was the fact Cr is present, which is confirmed in this profile.

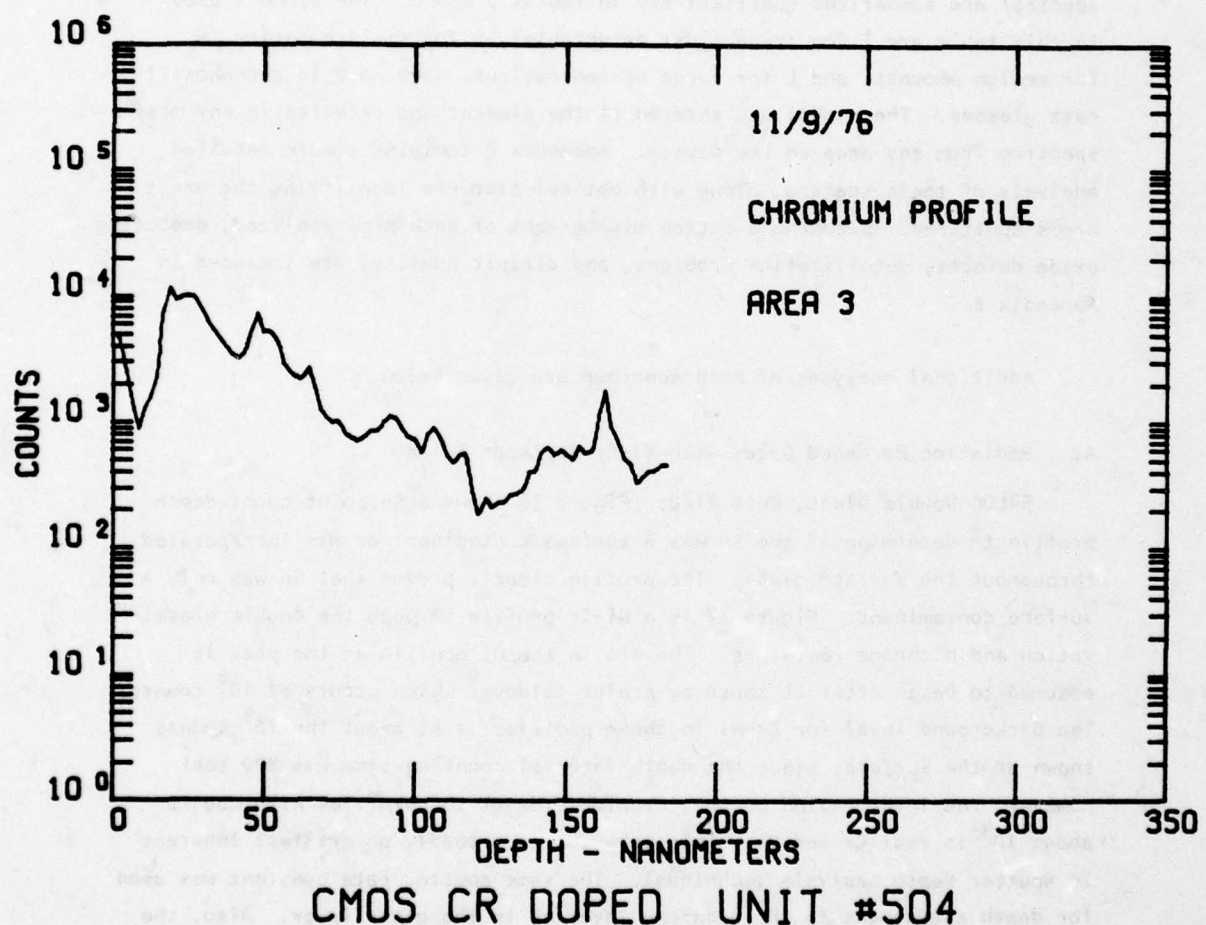


Figure 15

SECTION VI  
GENERAL TECHNOLOGY GROUP

The analyses of the entire general technology group (about 400 mass spectra) are summarized qualitatively in Tables 7 and 8. The symbols used in this table are T for trace (just detectable), S for small quantity, M for medium amounts, and L for large concentrations, such as P in phosphosilicate glasses. The symbol was entered if the element was detected in any mass spectrum from any area on the device. Appendix B contains a more detailed analysis of these spectra, along with optical pictures identifying the exact areas sputtered. Scanning electron micrographs of each area analyzed, depicting oxide defects, metallization problems, and circuit quality, are included in Appendix B.

Additional analyses of each subgroup are given below.

A. Radiation Hardened Gates with Ni-Cr Resistor Films

54L00 Double Glass, Unit #120: Figure 16 shows a Sn point count depth profile to determine if the Sn was a surface contaminant or was incorporated throughout the surface glass. The profile clearly proves that Sn was only a surface contaminant. Figure 17 is a Ni-Cr profile through the double glassivation and nichrome resistors. The dip in the Ni profile at the peak is assumed to be an artifact cause by scaler foldover which occurs at  $10^6$  counts. The background level for Cr-Ni in these profiles is at about the  $10^3$  counts shown at the surface, since the depth interval counting time was 200 sec. However, the level region on the interior side of the profiles with counts about  $10^4$  is real Cr and Ni. This behavior is probably an artifact inherent in sputter depth analysis techniques. The same sputter rate constant was used for depth assignment in the nichrome layer as in the glass layer. Also, the nichrome layer was assumed to be uniformly surface cleaned of the glass coating at the start of the Ni and Cr signal. Each of these assumptions, along with the normal sputtering broadening effect, would result in an apparent thicker nichrome layer than is actually present. The glass layers over the nichrome on this device were sputtered quartz and chemical vapor deposited oxide. The

TABLE 7  
RADIATION HARDENED GATES

TABLE 8  
ALUMINUM METALLIZED GLASSIVATED DEVICES

DEVICE	Li	B	T	Na	Mg	P	Cl	K	Ca	Cr	Ti	Ag	Mo	Ga	Zn	Cu	Ni	Cr	Ag	Sn	Ba	Pb
Op Amp 1	3	T	T	S	S	L		H	T	T	T									S	T	
Op Amp 1	48		T	T	L	L		L	L	S	S	L	L						T	S	S	T
Op Amp 1	50	T	T	S	T	L		M	S	T	T								T	T	T	T
Op Amp 2	62	H	M	T	M	T		L	S	T	T											H
Op Amp 2	64	T	T	L	M	T		L	M	T									S	T	T	
Op Amp 2	16	T	T	S	T	T		S	S	T	T								T	T	T	
Op Amp 3	13		T	M	T	L		H	H	T									T	T	T	
Op Amp 3	165	T	T	M	M	L		L	M	T									T	T	T	
Op Amp 3	33		S	L															T	T		
Gen Pur Amp	64	S	T	T	L	T																
Gen Pur Amp	2	S	S	T	M	S	L	H	H	H									H	T	T	
Gen Pur Amp	3	S	M	S	M	S	L	S	T										S		H	
ECL D	21	S		S	T	L		T	T	T									T			
ECL D	39	T	T	H	T	L		S	H	T	T								T			T
ECL D	92	T	T	T	S	L		T	S	T	T								T	T	T	T
Hex Inverter	94	T	T	T	T	L		T	T	T									T	T	S	
Hex Inverter	125	T	T	L	S	T		S	M	T	T								T	T	T	
Hex Inverter	29	T	T	T	T	T		T	S	T	T								T	T	T	

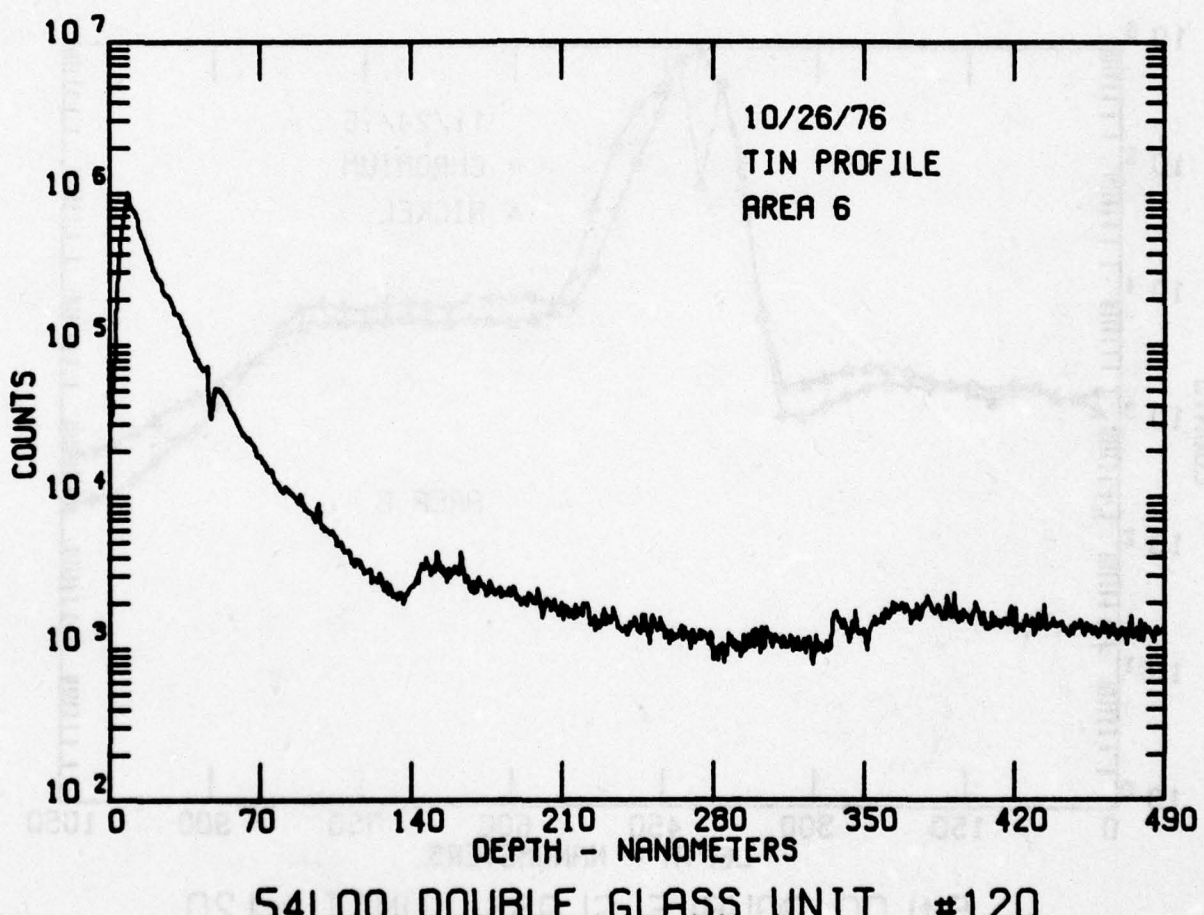
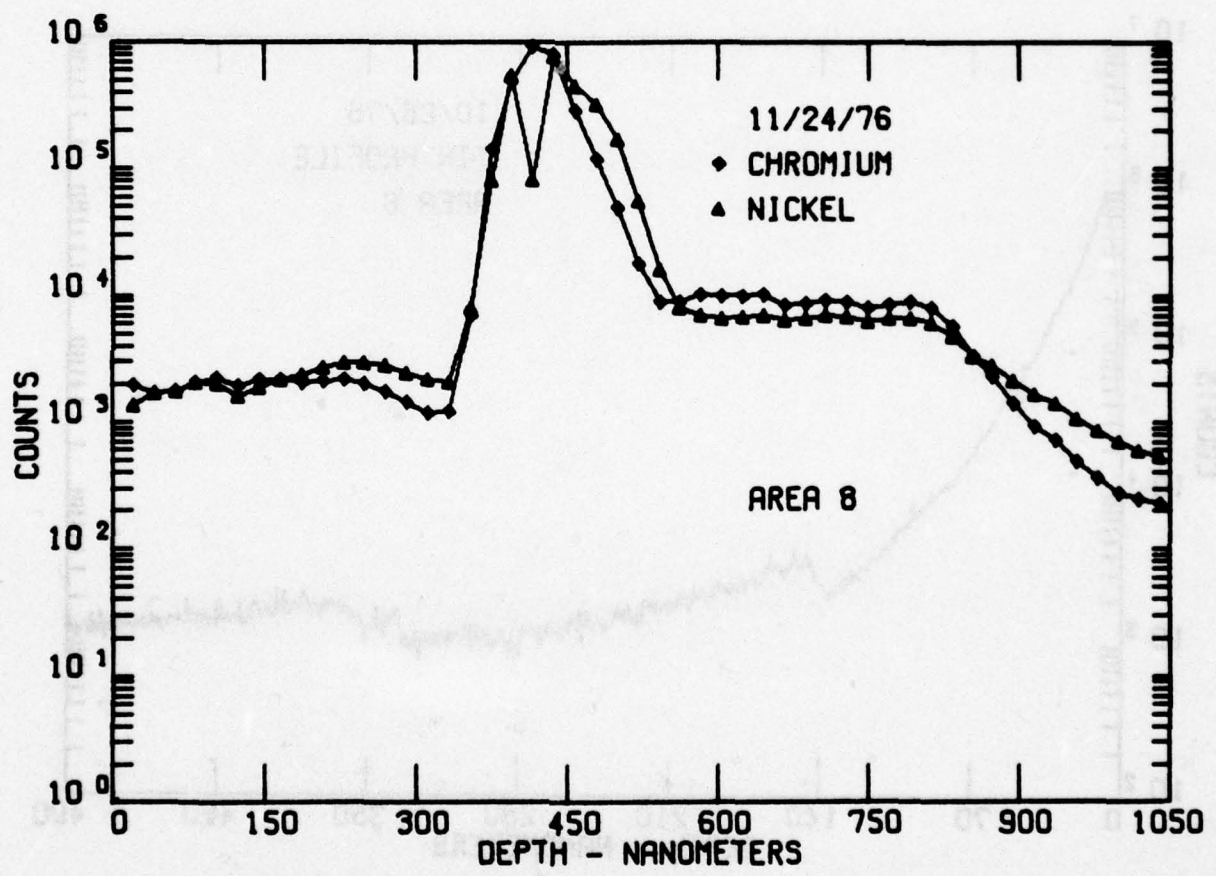


Figure 16

JWW-MCL



54L00 DOUBLE GLASS UNIT #120

JMMA-MCL

Figure 17

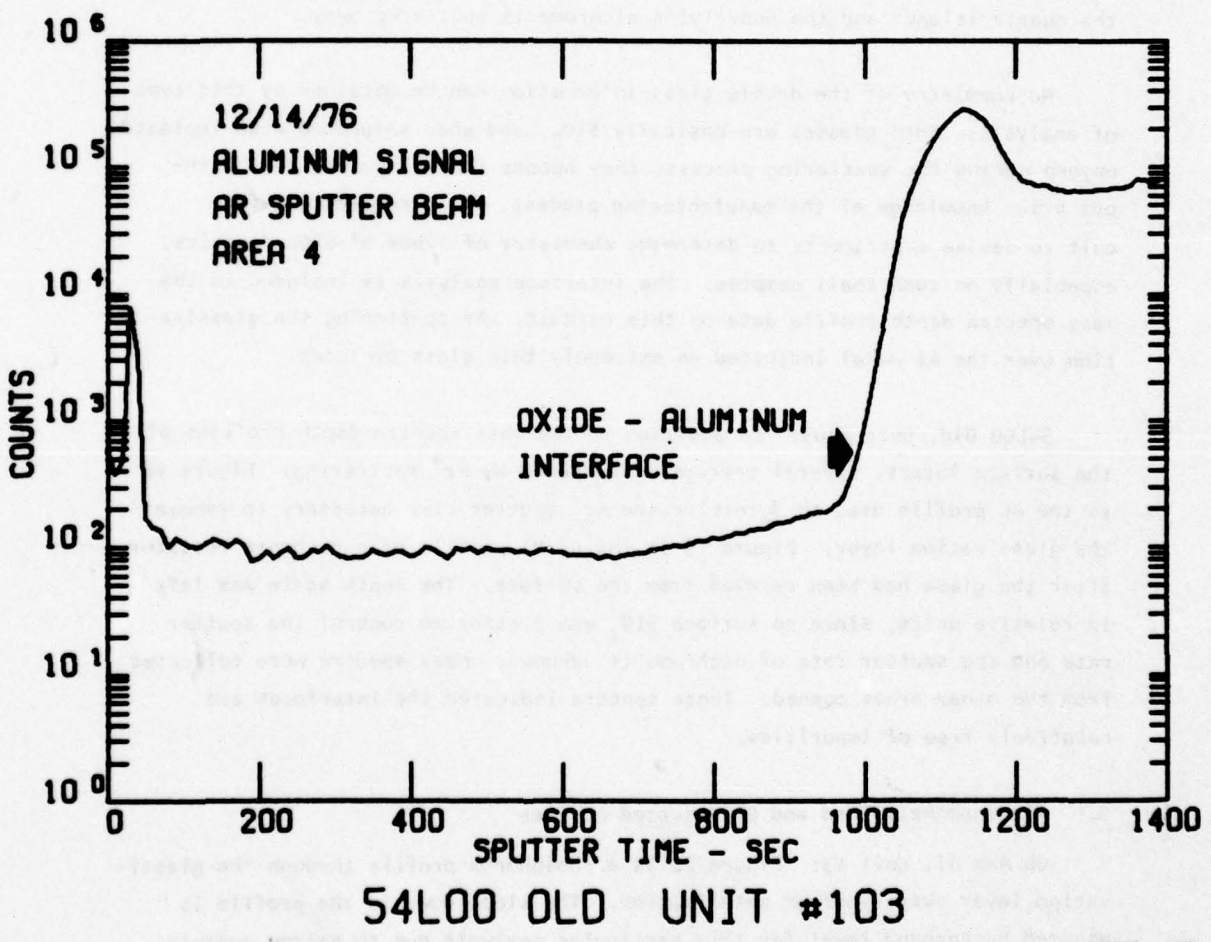
sputtered quartz is known to have a columnar-type structure that, when sputtered, would tend to leave small islands of quartz scattered over the nichrome. These islands would then slowly sputter away, resulting in a profile as shown in Figure 17, where the Ni-Cr signal sharply drops off the peak as the main portion of the nichrome is sputtered away, but levels out above background while the quartz islands and the underlying nichrome is sputtered away.

No chemistry of the double glass information can be obtained by this type of analysis. Both glasses are basically  $\text{SiO}_2$ , and when saturated with implanted oxygen during the sputtering process, they become indistinguishable. Without prior knowledge of the manufacturing process, it is extremely difficult to devise experiments to determine chemistry of types of  $\text{SiO}_2$  deposits, especially on such small samples. The interface analysis is included in the mass spectra depth profile data on this circuit. Ar sputtering the glassivation over the Al metal indicated an extremely thin glass overcoat.

54L00 Old, Unit #103: In addition to the mass spectra depth profiles of the surface layers, several craters were opened by  $\text{Ar}^+$  sputtering. Figure 18 is the Al profile used to determine the  $\text{Ar}^+$  sputter time necessary to remove the glassivation layer. Figure 19 is the Cr-Ni profile of a nichrome resistor after the glass had been removed from the surface. The depth scale was left in relative units, since no surface  $\text{SiO}_2$  was present to control the sputter rate and the sputter rate of nichrome is unknown. Mass spectra were collected from the other areas opened. These spectra indicated the interfaces are relatively free of impurities.

#### B. Aluminum Metalized and Glassivated Devices

Op Amp #1, Unit #3: Figure 20 is a phosphorus profile through the glassivation layer over aluminum metalization. The slope down in the profile is assumed background level for this particular analysis due to narrow dynamic range of the instrument when going high to low with a negative beam and small craters. The interface analysis using  $\text{Ar}^+$  sputtering to remove the glassivation showed the interfaces was relatively free of impurities. The attempt to



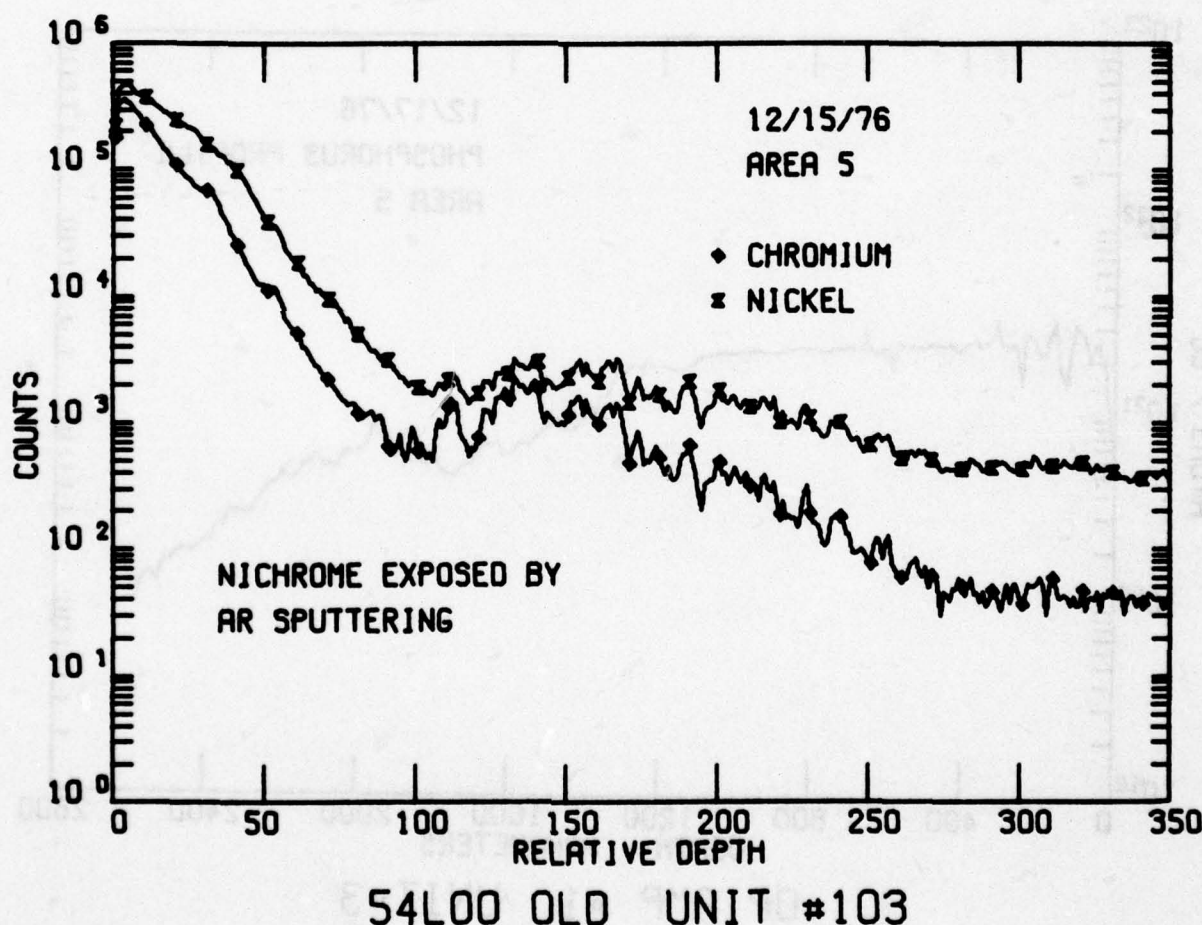
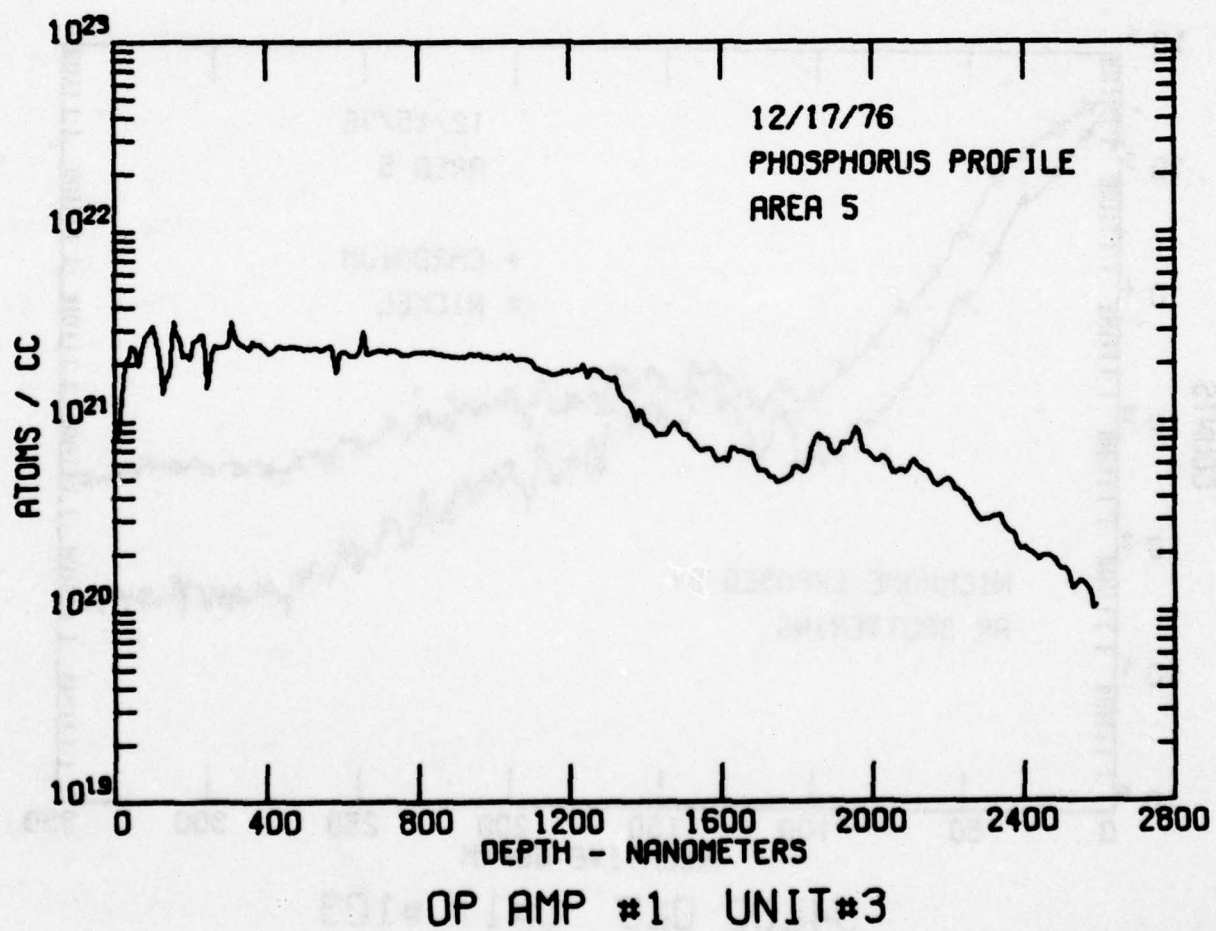


Figure 19



JMMR-NCL

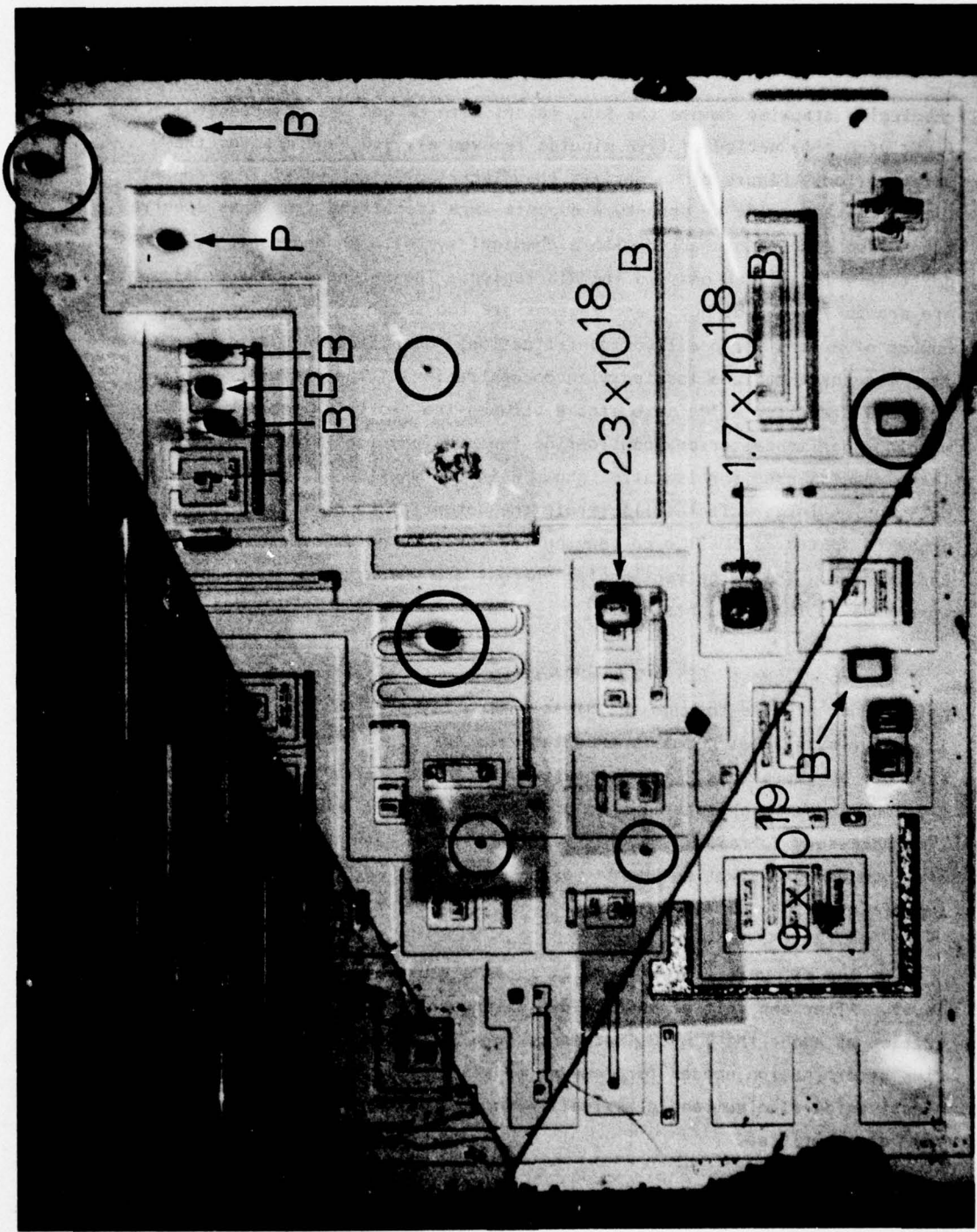
Figure 20

chemically stepwise remove the  $\text{SiO}_2$  layers with HF gas was unsuccessful. The first etch time period of five minutes removed all  $\text{SiO}_2$  and most of the metalization. Figure 21 summarizes the electrically active silicon dopant identification. The n- or p-type dopants were identified from mass spectra taken from each point marked with a chemical symbol. An n-dopant, P, was positively identified only in the MIS region. The n-type transistor elements are probably P doped, but these regions are too small to supply a sufficient number of P ions for positive identification. Quantitative B data were taken from the three regions labeled with concentrations. The difference between  $2.3 \times 10^{18}$  and  $1.7 \times 10^{18}$  atoms/cc B between the two transistors tanks is within experimental error, considering that the physical size is limited. The  $\text{P}^+$  region used for isolation shows B in the  $9 \times 10^{19}$  range. The small dots inside larger circles illustrate the potential capability of the ion probe to sputter a small area leaving the surrounding area essentially undisturbed. The large rectangular shadows are where unsuccessful attempts were made to image dopants.

Op Amp #2, Unit #62: Figure 22 shows a mass 31 (either  $\text{P}^+$  or  $\text{SiH}^+$ ) point count profile through the glassivation layer. The low count obtained is at the same level normally expected from the  $\text{SiH}^+$  molecular species, which strongly suggests that P is not present, at least, certainly not in the concentrations found in phosphosilicate glasses. Figure 23 shows the  $\text{Ar}^+$  sputter time necessary to remove the glassivation layer. Both the glassivation-aluminum and glassivation-thermal oxide interfaces were relatively free of impurities.

Op Amp #3, Unit #13: Figure 24 shows a P profile in the glassivation layer. After the initial surface depletion, the P reaches a constant concentration at about the  $2 \times 10^{21}$  atoms/cc level. Figure 25 is the  $\text{Ar}^+$  sputter time determination needed for removal of the glassivation layer. Both the glassivation-aluminum and glassivation-thermal oxide interfaces were relatively free of impurities.

Figure 21 Dopant Analysis in Active Silicon Regions on Op Amp #1, Unit #3



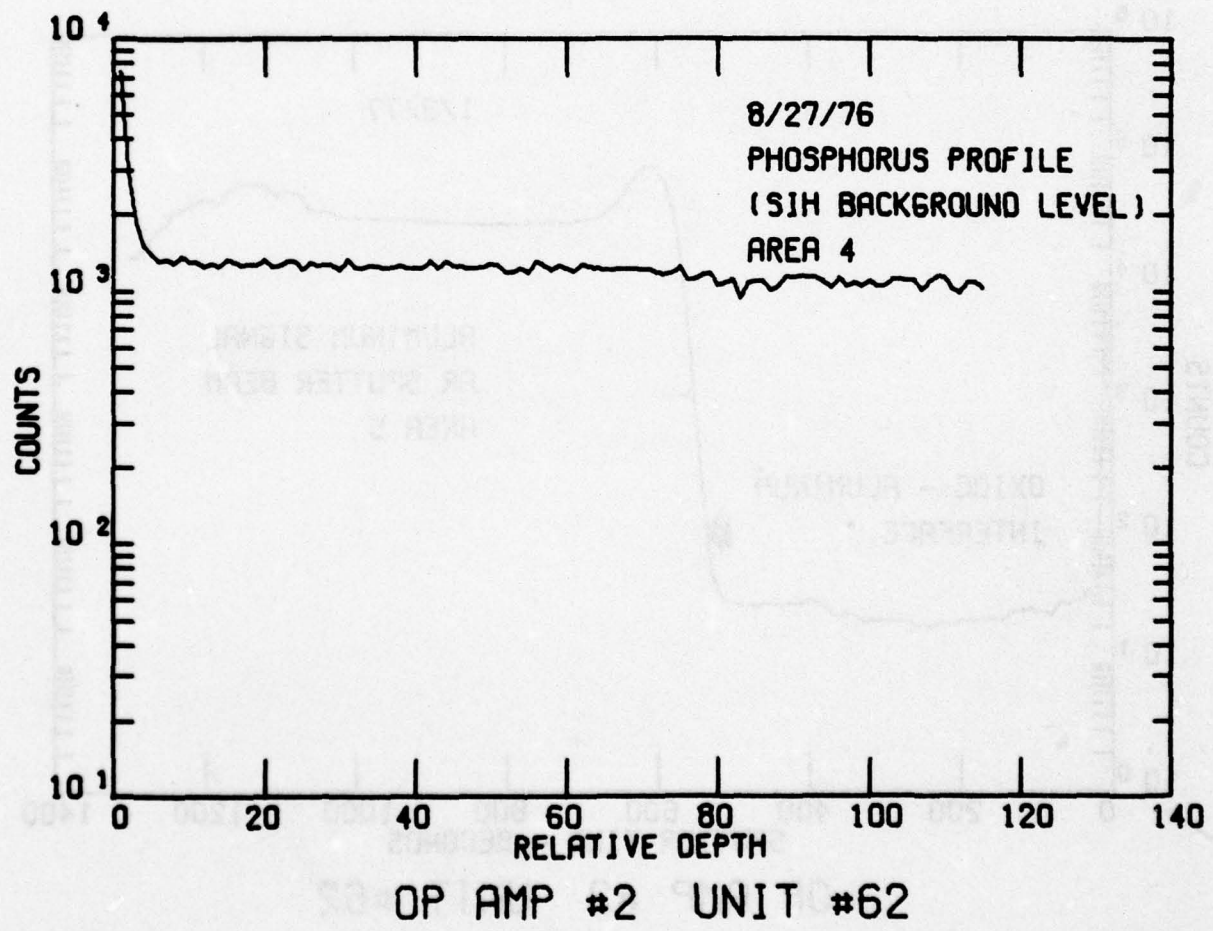
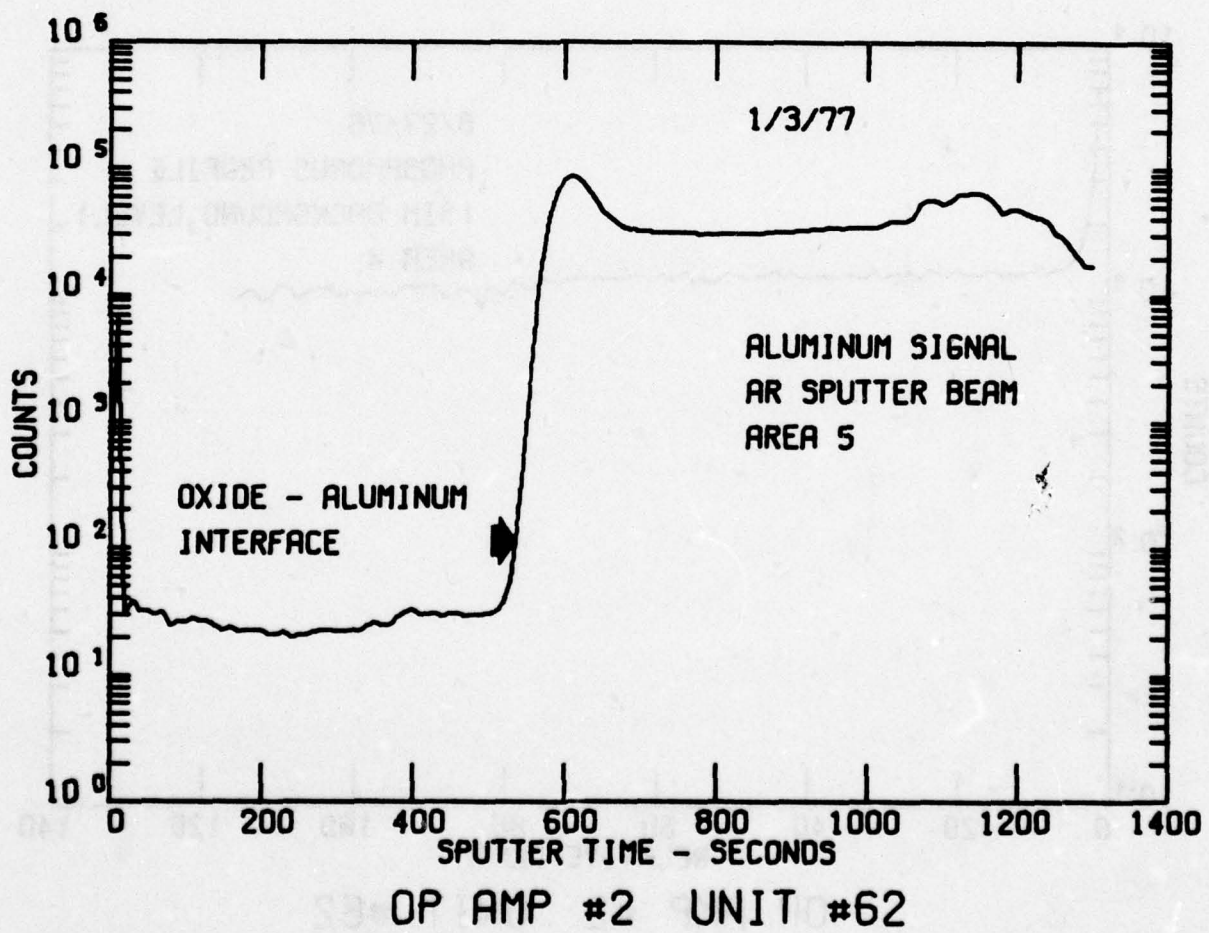


Figure 22

JMMR—MCL



JAN 20 MCL

Figure 23

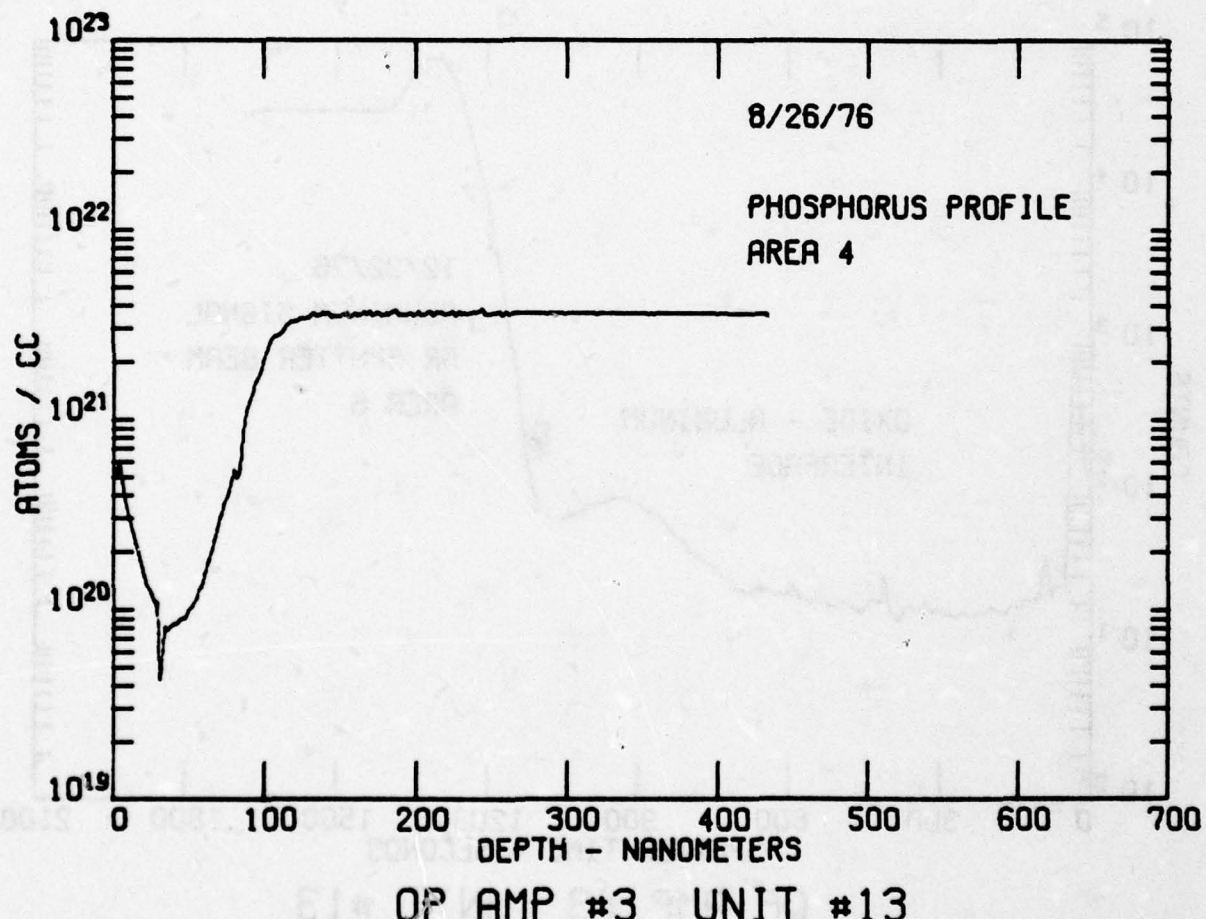


Figure 24

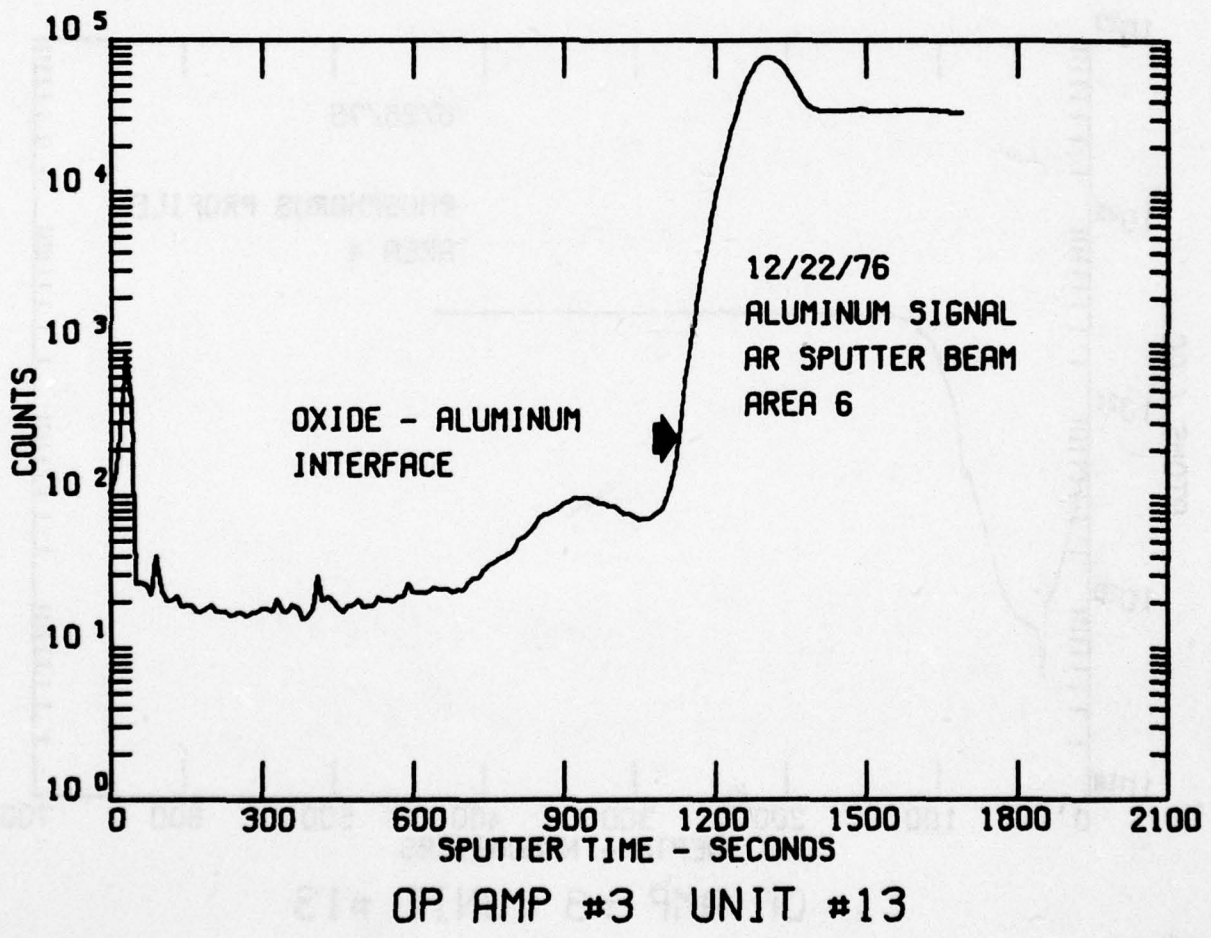


Figure 25

General Purpose Amplifier, Unit #64: Only mass spectra depth profiles were taken on this device. Phosphosilicate glass was used, but not profiled. No interface analysis was attempted.

ECL D Flip Flop, Unit #21: Figure 26 is the P profile through the glassivation and insulator oxide of the device. The P remained at the same concentration within experimental error throughout the entire depth. Figure 27 shows the Ar<sup>+</sup> sputter time determination for removal of the glassivation layer, second level metal, and insulator dielectric for interface analysis. Interface analysis at the glassivation-insulator oxide and glassivation-aluminum interfaces showed the interfaces were relatively free of impurities. No attempt was made to analyze deeper interfaces.

Hex Inverter, Unit #94: The glassivation and thermal oxides were P-free. Figure 28 is a Pb profile taken through the glassivation to determine if the Pb found by the mass spectra profiles was a surface contaminant or a component of the glassivation. The high surface peak (after gold coating sputtered away) shows the Pb was a surface contaminant. Figure 29 is the Ar<sup>+</sup> sputter time determination needed for interface analysis. The glassivation-aluminum and the glassivation-thermal oxide interfaces were relatively free of impurities. Neither of these interfaces opened by Ar sputtering showed the impurity types and/or amounts found on interfaces analyzed where the glassivation had delaminated from the thermal oxide. Experiments to determine if impurities concentrated in glassivation cracks gave only negative results.

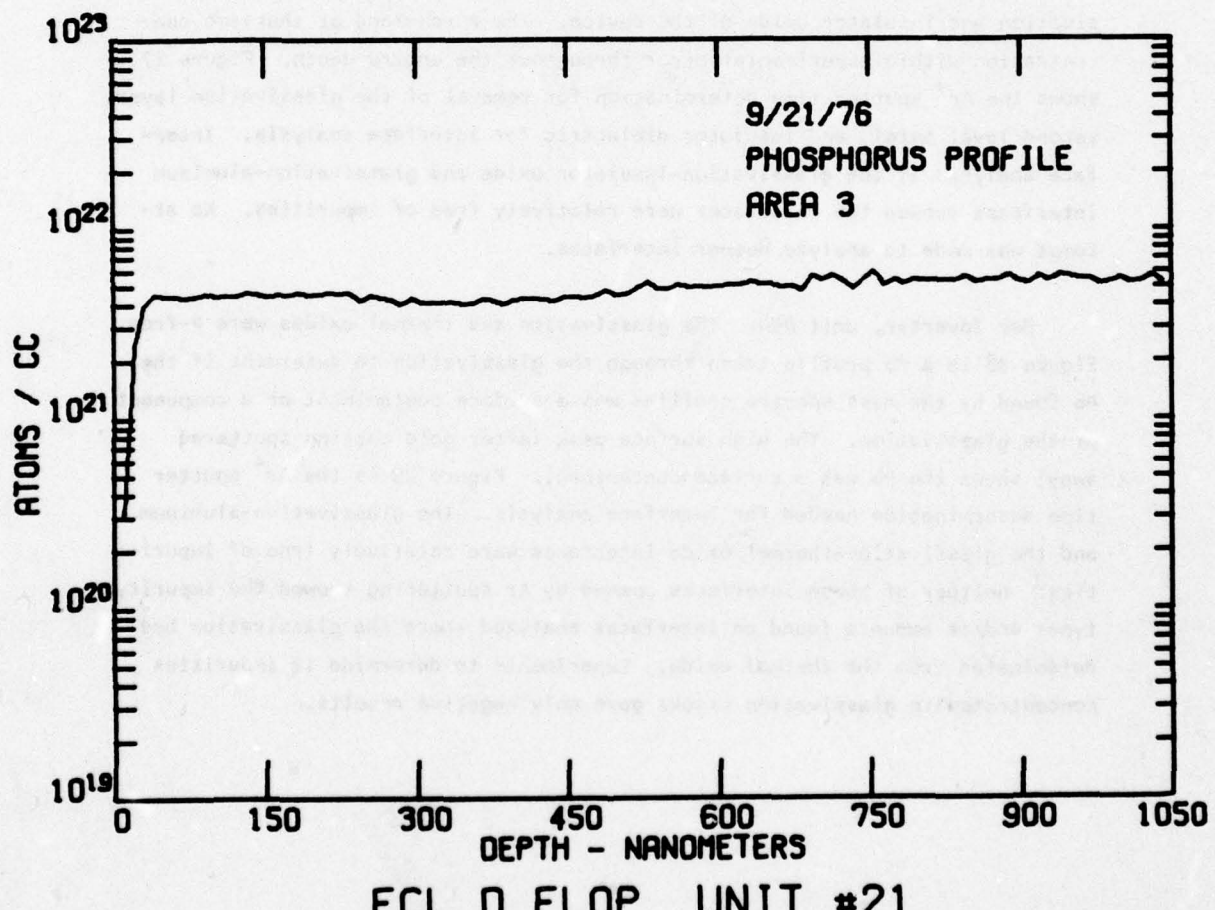
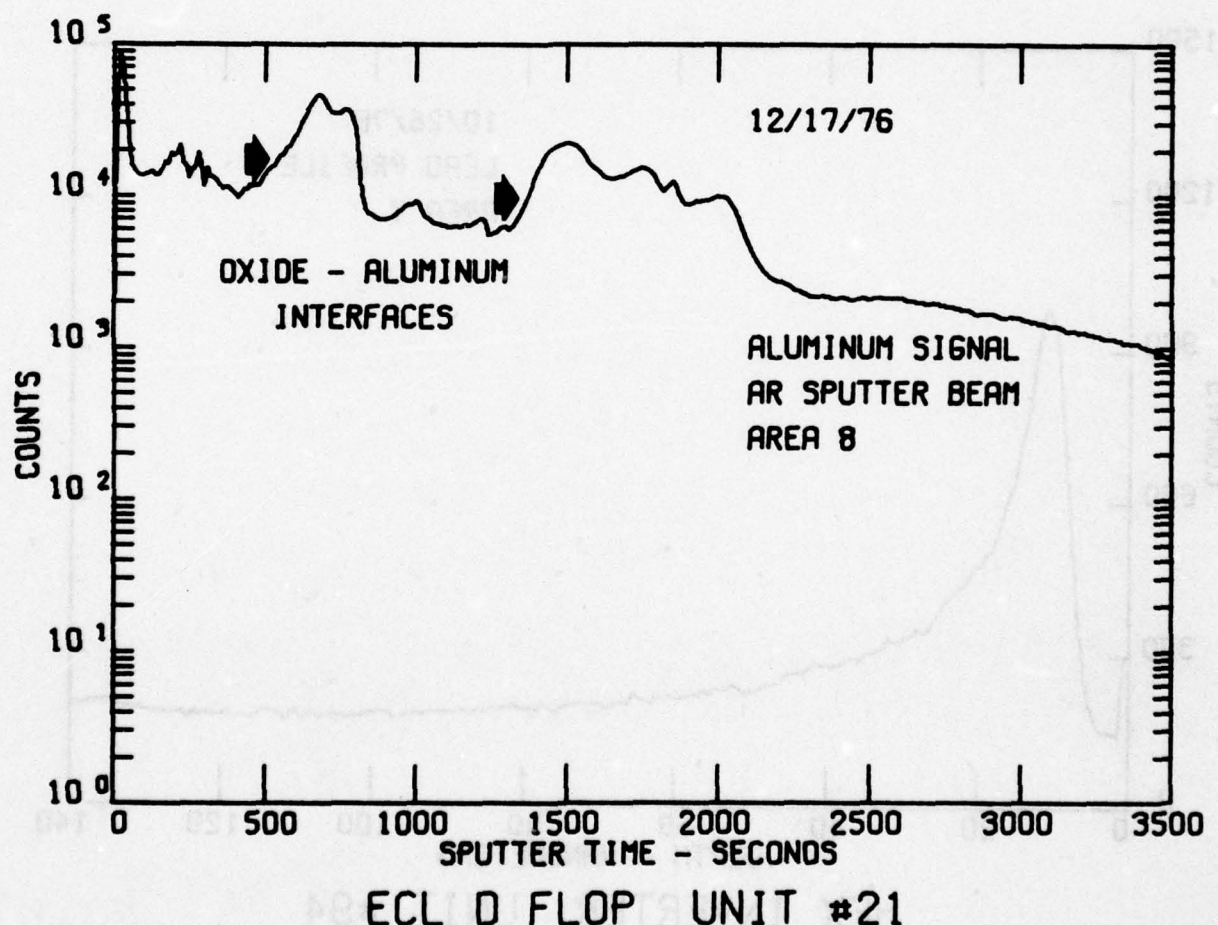


Figure 26

JWW-MCL



JMMR-MCL

Figure 27

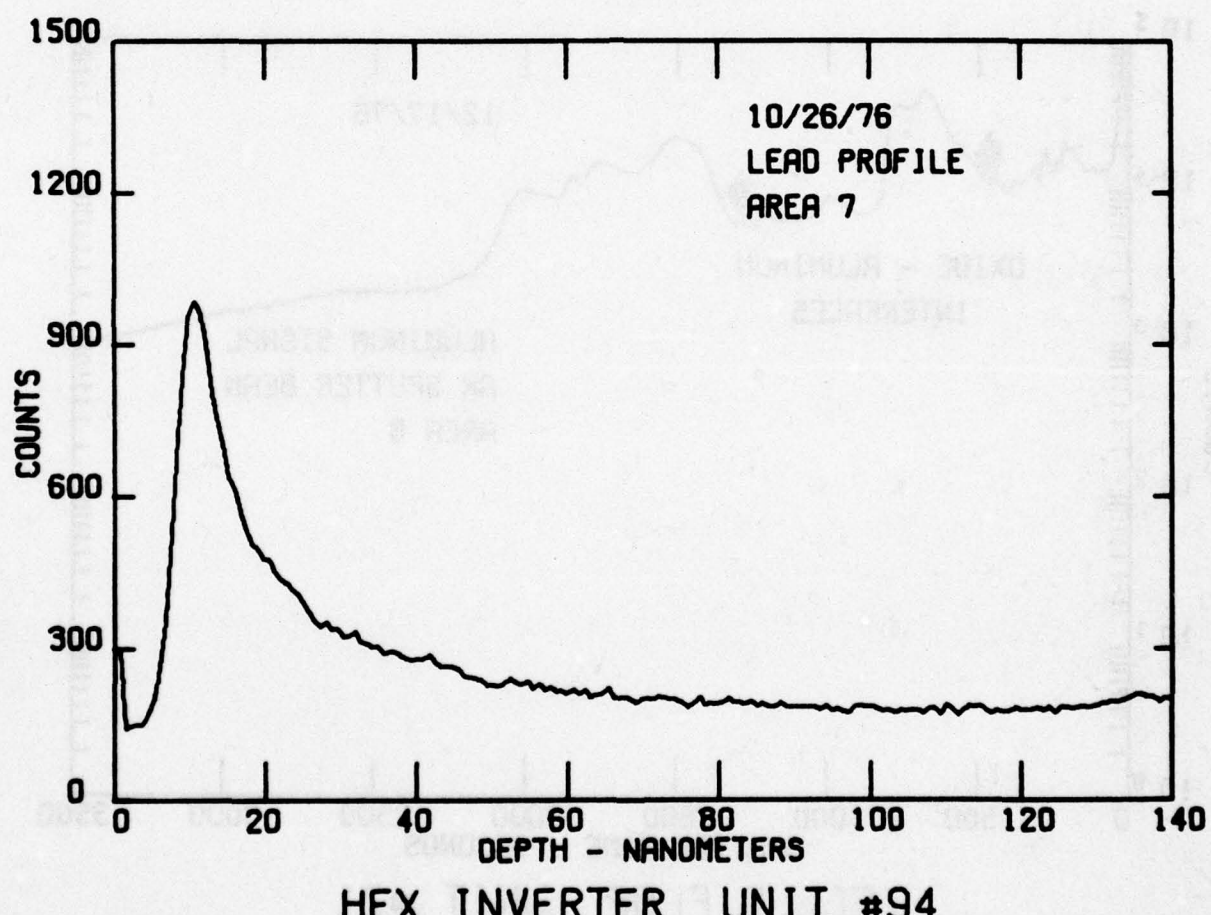


Figure 28

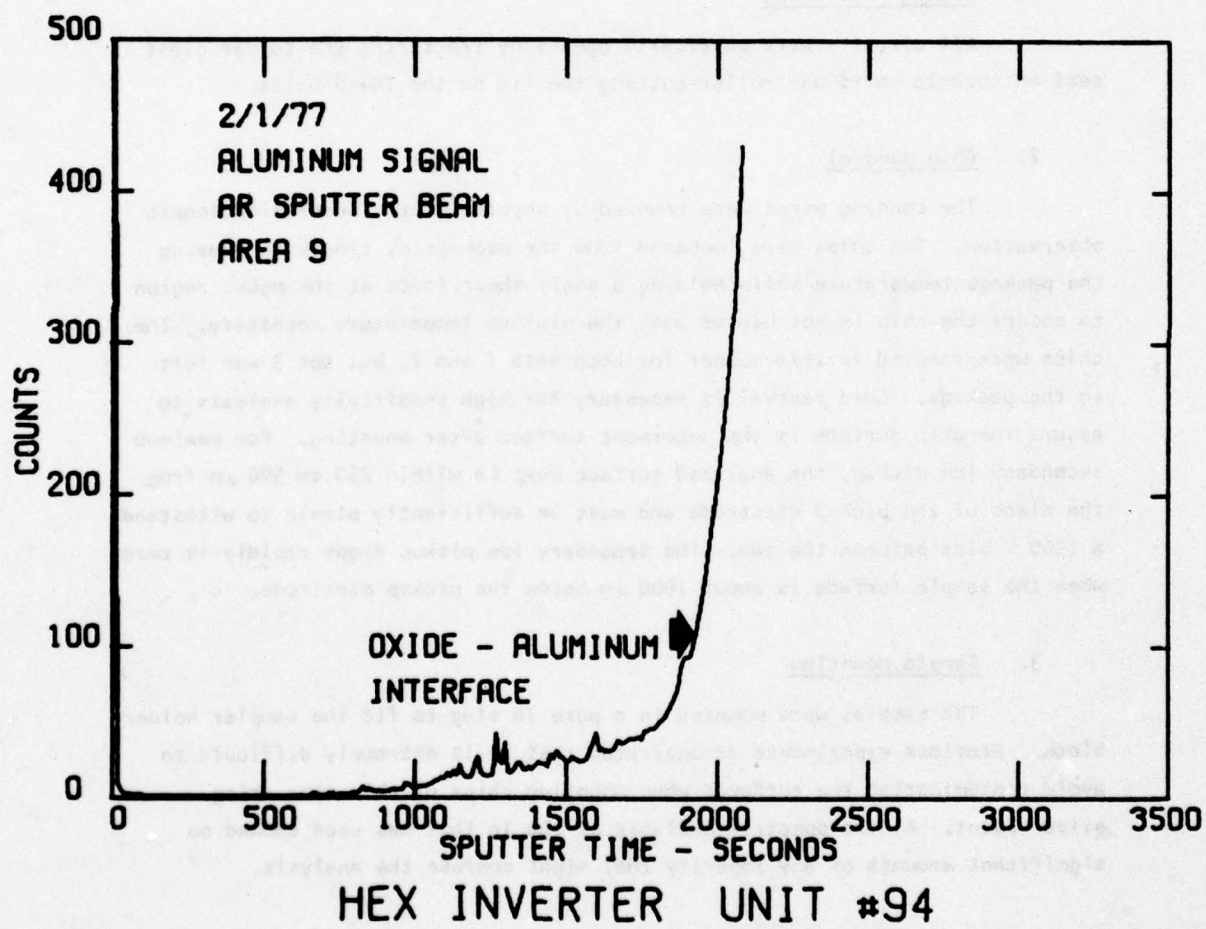


Figure 29

SECTION VII  
SIMS PROCEDURE EVALUATION

A. Special Sample Preparation Procedures

1. Package Delidding

All circuits were physically opened by fracturing the solder glass seal on ceramic units and roller-cutting the lid on the TO-18 units.

2. Chip Removal

The bonding wires were removed by physical force under microscopic observation. The chips were loosened from the package by slowly increasing the package temperature while holding a small shear force at the mount region to ensure the chip is not heated past the minimum temperature necessary. The chips were removed in this manner for both sets 1 and 2, but set 3 was left in the package. Chip removal is necessary for high sensitivity analysis to assure the chip surface is the uppermost surface after mounting. For maximum secondary ion pickup, the analyzed surface must be within 250 to 500  $\mu\text{m}$  from the plane of the pickup electrode and must be sufficiently planar to withstand a 1500 V bias between the two. The secondary ion pickup drops rapidly to zero when the sample surface is about 1000  $\mu\text{m}$  below the pickup electrode.

3. Sample Mounting

The samples were mounted in a pure In slug to fit the sampler holder block. Previous experiments demonstrated that it is extremely difficult to avoid contaminating the surfaces when mounting chips of this size using silver paint. A mass spectrum analysis of the In that was used showed no significant amounts of any impurity that might confuse the analysis.

Three methods of In mounting were developed and used for these analyses:

(1) The chips were placed face down on a cleaned stainless steel block. A cleaned, large copper ring was placed around the chips rested on the stainless block. Molten In was poured into the ring and solidified immediately upon contact with the stainless heat sink. The technique was successful because there was very little In migration onto the chip surface, as evidenced by the very small In peaks in the mass spectra. The problems with the method were that the chip had a tendency to move when the molten In was poured in and adhered poorly to the In; in addition, an excessive amount of In was required for each mount, which made it economically necessary to recycle the In slugs.

(2) The second method is similar to the first, except that the large copper ring is replaced with a small, 8.3 mm O.D. stainless steel tube. In this technique, only one chip per tube was mounted, whereas in method (1) an array of chips was mounted in each ring. A second difference is that the stainless tube had to be kept at the melting temperature of In to keep the In from solidifying before it surrounded the chip. The main problems with this method are that considerable In migrated over the surface of the chip, which resulted in strong In peaks in many of the mass spectra; and that unless the procedure was done quickly, the chip had a tendency to float in the molten In.

(3) The third method is a further refinement of method (2) and is the method recommended for future analysis. The end of the stainless steel tube is filled with molten pure In in any convenient manner, and the surface is mechanically scraped clean. The chip is placed face down on the cleaned stainless steel block and cold-pressed into the In end of the stainless steel tube. No samples were mounted by this method that had not been previously mounted by method (2) so the In migration is not known; however, since only cold flow takes place, no migration should occur. The only problem that might develop is physical fracture of the chip, but none occurred (due to mounting) on the few chips mounted by this method.

#### 4. Conductive Coating

To direct the secondary ions toward the pickup electrode, most of the sample surface must be biased + 1500 V with respect to the pickup electrode. High purity gold is sputtered over the surface after mounting to provide this conductive plane. The sputter apparatus used an aluminum target with all exposed surfaces wrapped with a high purity gold foil. A high purity quartz liner was used between the sample and target to shield the sample from line-of-sight impurities of other parts of the sputtering system. The gold was dc-sputtered, using an Ar ambient, to a thickness of 20 to 50 nm. Figure 30 is the mass spectrum obtained from a cleaned silicon slice before gold coating in this sputter apparatus. Figure 31 is the mass spectrum of a second portion of the silicon slice that had been gold coated. These spectra demonstrate that the only element added by coating was gold.

#### 5. Instrument Mounting

The array of chips mounted by method (1) was clamped into the standard sample holder and placed in one position of the carrousel. The tubes used in methods (2) and (3) were mounted in a specially designed sample holder that held six tubes on the circumference of a 25 mm diameter circle.

#### B. Spatial Resolution

The minimum beam diameter of the ion microprobe mass analyzer is  $2.5 \mu\text{m}$ . This beam diameter is achieved when all operating parameters of the instrument are optimized for this purpose. However, these parameters are not necessarily optimized for analysis of solids. In fact, the working ion beam diameters are typically in the  $10$  to  $25 \mu\text{m}$  range. Since ion sputtering and in-depth concentration profiles require crater wall rejection, it is necessary to raster the beam 4 to 6 beam diameters in the x-y plane. This means that the criterion of crater wall rejection dictates a minimum raster size of on the order of  $40 \times 40 \mu\text{m}$ .

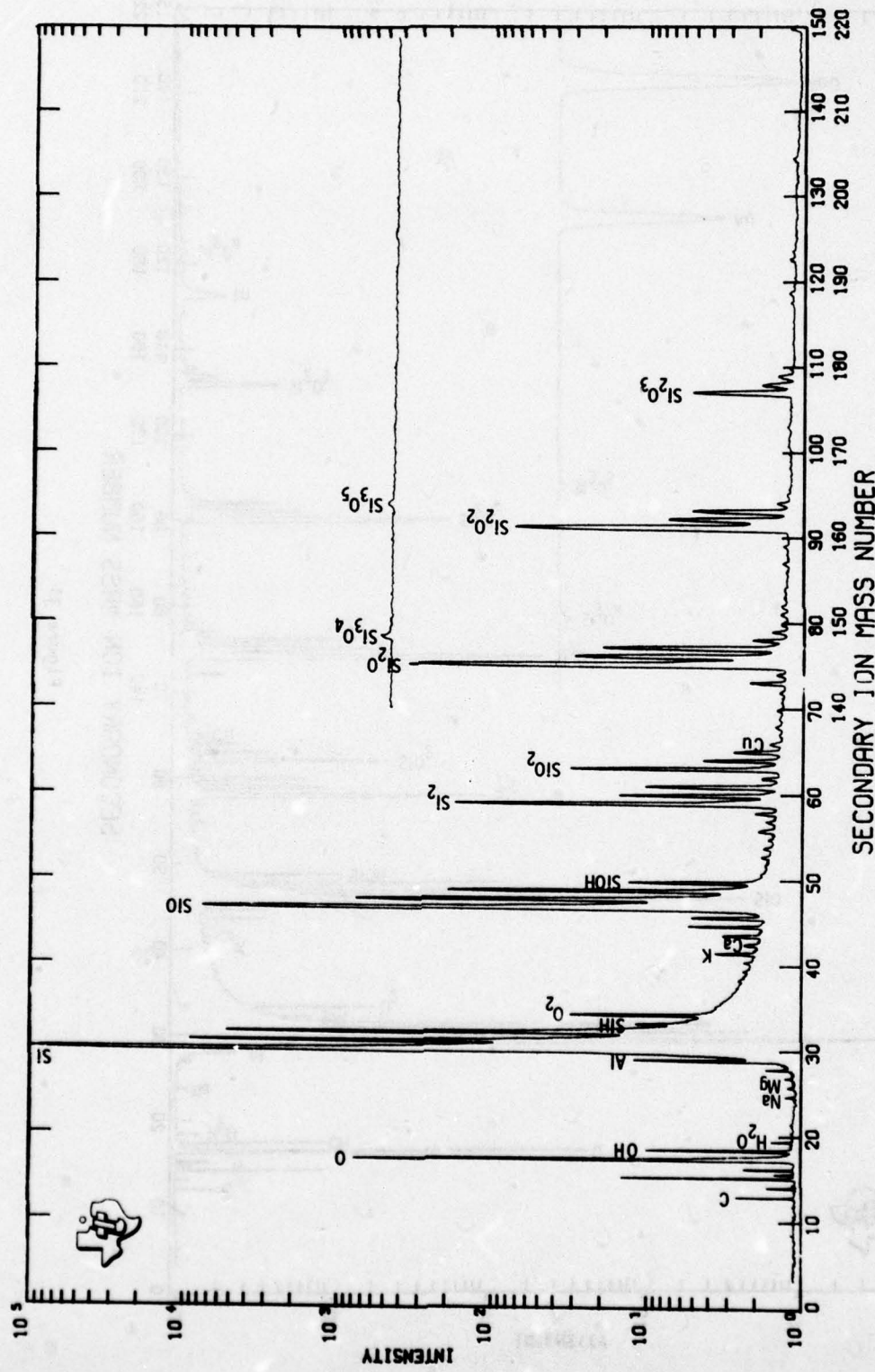


Figure 30

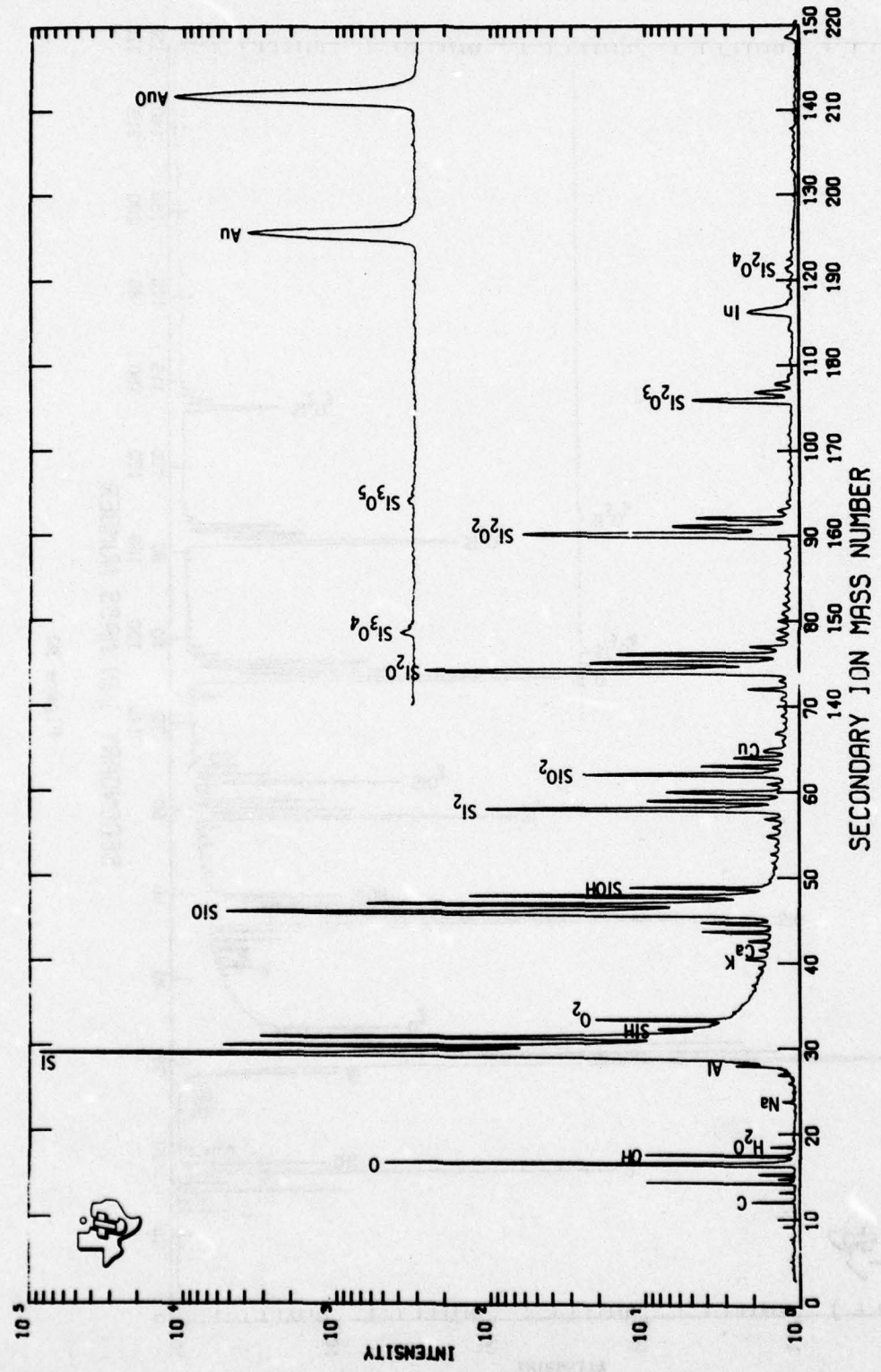


Figure 31

The second, and perhaps most stringent requirement on raster size, or analysis area, is detection limit optimization. Since the detection limit (see Sections II and VII-E) is a direct function of the analysis area, it is necessary to use the largest area possible for integrated circuit analysis. Maximum sensitivity is achieved during in-depth profiling with a  $150 \times 150 \mu\text{m}$  rastered analysis area. This area is obviously large when compared with today's integrated circuit devices. Design rules in 1977 are  $5 \mu\text{m}$ ; that is, the smallest opening in an oxide will be  $5 \mu\text{m}$ . Thus, a typical emitter will be  $10 \times 10 \mu\text{m}$  and a base  $20 \times 25 \mu\text{m}$  in a bipolar device. In CMOS or MOS devices the MOS gate will be  $10 \times 10 \mu\text{m}$  and the source/drain in the  $10 \times 15 \mu\text{m}$  range. Obviously, these design rules severely restrict the applicability of the microprobe in device failure analysis and for microdefect characterization. However, as was demonstrated in the work reported in Sections V and VI of this report, the ion microprobe can analyze many parts of a circuit and provide meaningful analytical data. The direct analysis of electrically active areas on MSI and LSI devices is very difficult. However, metalization, resistors, bond pads, capacitors, and dielectric film can be analyzed.

#### C. In-Depth Resolution

The ion sputtering technique is inherently capable of providing in-depth compositional analysis with a resolution of 2 to 3 nm. The sputter rate for an  $O_{32}^+$  ion beam in silicon is  $0.25 \text{ nm/sec}$ , and data are taken at 10 second intervals. It is generally believed that the mean escape depth of secondary ions from a sputtered surface is in the 2 nm range. These latter two factors confine the in-depth resolution to the 2 to 3 nm range.

Absolute or positional accuracy in a depth profile is more difficult to define. In the sputtering process, the oxygen ion beam implants oxygen about 20 nm ahead of the surface. This process continues as the in-depth sputtering continues with an oxygen saturated front continually moving about 20 nm ahead of the bottom of the sputtered crater. This is a violent process; it converts single crystal silicon to amorphous silicon saturated with oxygen. The process causes a continual mixing of atoms in the region of the implant. Sharp interfaces are mixed and turned into diffuse interfaces. As a result of these

processes, the assignment of an absolute position of an interface is difficult. It is generally accepted by workers in the field of ion sputtering that the range of error or standard deviation is  $\pm 10\%$  of the assigned depth. Therefore, typical uncertainties would be:

Metal films:  $2,000 \pm 200$  nm

Dielectric films:  $500 \pm 50$  nm

Ion implants:  $100 \pm 10$  nm

These uncertainties do not include possible changes in sputter rates due to matrix changes, structure and/or thickness variations. These latter uncertainties were all encountered in the nichrome resistor analysis of the radiation hardened devices.

This same implantation process severely limits the effectiveness of secondary ion mass spectroscopy for the analysis of the first 15 to 20 nm of depth into a sample. Equilibrium of the plasma is established only when the sputtered crater has reached the oxygen-saturated front ( $\sim 20$  nm). At that point, data in the depth profile will be in equilibrium with the matrix as well as all subsequent volumes of material consumed in the depth profile.

#### D. SIMS Parameter Control

##### 1. Primary Ions

All high sensitivity ion microprobe or secondary ion mass spectroscopy analysis on conductors is done with a positive oxygen ion ( $O^{+}_{32}$ ) primary ion beam. Significantly higher secondary ion yields, and therefore sensitivities, are obtained with  $O^{+}_{32}$  over the noble ion ( $Ar^{+}_{40}$ ) primary ion beams. However, positive primary ion beams cannot be used on insulators such as  $SiO_2$  and  $Si_3N_4$  films because of charging problems on the surface of the insulator. The charging results from secondary electrons being ejected from the sample surface by high energy ion impact. The positive surface created by this secondary electron emission is further aggravated by the implantation of positive ions. Since in insulators, electrons cannot flow from ground to neutralize this positive charge, the potential will build until there is sufficient field strength to jump some gap to ground, at which time the process starts over again. This surface charging has very little effect on the high

energy primary beam which allows the use of  $\text{Ar}^+$  sputtering for rapid removal of material. However, the charge has a major effect on the secondary ion trajectory, since these ions normally have very low energies. In fact, with the present instrumentation, very few secondary ions ever reach the detector. Dielectric films can be sputtered and analyzed using negative ( $\text{O}_{16}^-$  in this work) primary ion beams. The injection of negative ions tends to stabilize the charge at an equilibrium state where secondary ions can be controlled. Sputter rates are a factor of five slower with the  $\text{O}_{16}^-$  beam than with the  $\text{O}_{32}^+$  beam because of the lower total ion current generated, only half the number of sputtering particles, and an effective higher energy, which results in deeper implantation with a reduced sputter yield. This increases analysis time proportionately.

Since virtually all integrated circuit devices have dielectric films over the device, it is necessary to use the slower and less sensitive  $\text{O}_{16}^-$  primary ion beams. On metal films, thin dielectric films (< 150 nm), and on silicon, ( $\text{O}_{32}^+$ ) primary ion beams are employed.

## 2. Secondary Ions

SIMS instruments normally use unit or half-unit mass resolutions for secondary ion detection. Higher resolutions are possible, but are not generally employed because there is a strong inverse relationship between resolution and sensitivity. Since the actual sample volume that can be consumed per second is very small, most analysts prefer to use the lower resolution to gain sensitivity. This type of operation precludes the low level of detection of some elements because of matrix molecular ion interference. Examples of this type of interference on silicon integrated circuits include:

Mass 14 $\text{N}^+$ or $\text{Si}^{+2}$	Mass 55 $\text{Mn}$ or $\text{SiAl}^+$
Mass 31 $\text{P}^+$ or $\text{SiH}^+$	Mass 56 $\text{Fe}$ or $\text{Si}_2^+$
Mass 45 $\text{Sc}$ or $\text{SiO}^+$	Mass 75 $\text{As}$ or $\text{Si}_2\text{O}^+$ .
Mass 54 $\text{Fe}$ or $\text{Al}_2^+$	

Fortunately, very few molecular ions are formed in the ambient after sputtering, and the high energy sputter processes do not favor molecular particles being ejected. This minimizes the ambiguity.

### 3. Dynamic Range

The dynamic range of SIMS in depth profiles is 10 to 10,000 and is strongly dependent on the element, matrix, vacuum, and other experimental conditions. The primary dynamic range limitation is the crater wall effect, discussed in the preceding section. The secondary limitation is that a point primary beam cannot be obtained in practice, but it is actually made up of three components: a central hot spot, a small charged particle halo, and a much larger (300  $\mu\text{m}$  or objective aperture size) neutral particle halo. The charged particle halo arises from a slight energy spread of the ions emitted from the ion source and energy loss by glazing angle collisions with various aperture walls. The neutral particle halo results from ions that were directed toward the sample, but were neutralized before passing through the objective lens, thereby escaping focus. Both of these secondary effects can be minimized by hard vacuums and cutting large area craters. The latter is quite time consuming when using negative beams; hence, in many cases, the dynamic range was sacrificed in the interest of reasonable analysis time.

### E. Detection Limits

The question of detection limits in ion microprobe analysis is complex. Ultimately, detectability will be controlled by the number of impurity ions per second sputtered and detected. This comes down to the volume of the analytical region sputtered. In integrated circuit analysis, the areas available for analysis tend to be small, particularly when it is realized that maximum sensitivity is achieved with a raster size of 150 x 150  $\mu\text{m}$ . Therefore, in small areas the volume of sample must be maximized by sputtering deeply and integrating all signal over the sputter period. This mode of operation precluded in-depth concentration profiling. Alternatively, if in-depth concentration profiling is required, then large raster sizes or analysis areas are essential. This effect is illustrated in Figure 32. This figure

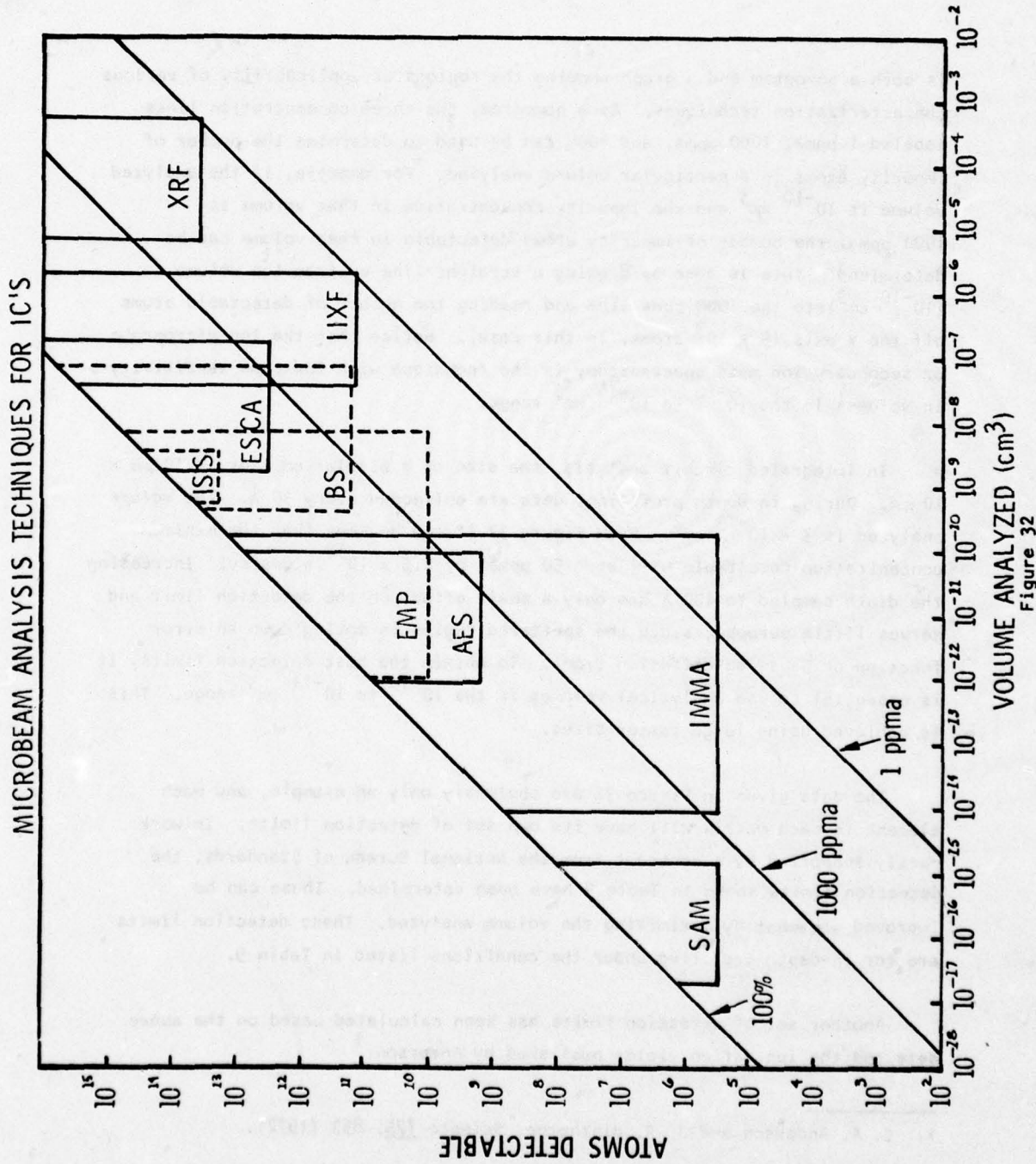


Figure 32

is both a nomogram and a graph showing the regions of applicability of various characterization techniques. As a nomogram, the three concentration lines labeled 1 ppma, 1000 ppma, and 100% can be used to determine the number of impurity atoms in a particular volume analyzed. For example, if the analyzed volume is  $10^{-10} \text{ cm}^3$  and the impurity concentration in that volume is 1000 ppma, the number of impurity atoms detectable in that volume can be determined. This is done by drawing a straight line up from the volume ( $10^{-10} \text{ cm}^3$ ) to the 1000 ppma line and reading the number of detectable atoms off the Y axis ( $5 \times 10^9$  atoms, in this case). Notice that the ion microprobe or secondary ion mass spectroscopy is the technique with low ppma sensitivity in volumes in the  $10^{-10}$  to  $10^{-14} \text{ cm}^3$  range.

In integrated circuit analysis, the size of a bipolar emitter is  $10 \mu\text{m} \times 10 \mu\text{m}$ . During in-depth profiling, data are collected every  $30 \text{ \AA}$ . The volume analyzed is  $3 \times 10^{-13} \text{ cm}^2$ . From Figure 32 it can be seen that the minimum concentration detectable will be  $\approx 50$  ppma, or  $2.5 \times 10^{18}$  atoms/cc. Increasing the depth sampled to  $100 \text{ \AA}$  has only a small effect on the detection limit and serves little purpose, since the sputtered region is moving down an error function or Gaussian diffusion front. To obtain the best detection limits, it is essential to use analytical volumes in the  $10^{-10}$  to  $10^{-11} \text{ cm}^3$  range. This is achieved using large raster sizes.

The data given in Figure 32 are obviously only an example, and each element in each matrix will have its own set of detection limits. In work partly supported by a contract from the National Bureau of Standards, the detection limits shown in Table 9 have been determined. These can be improved somewhat by maximizing the volume analyzed. These detection limits are for in-depth profiling under the conditions listed in Table 9.

Another set of detection limits has been calculated based on the above data and the ionization yields published by Anderson.<sup>1</sup>

1. C. A. Anderson and J. R. Hinckley, Science 175, 853 (1972).

TABLE 9. DETECTION LIMITS\* DETERMINED FOR THE ION  
MICROPROBE MASS ANALYZER IN SILICON AND SILICON DIOXIDE

<u>Element</u>	<u>ppma</u>	<u>Atoms/cm<sup>3</sup></u>	<u>Atoms</u>
Boron	0.1	$5 \times 10^{15}$	$1.5 \times 10^5$
Phosphorus	10	$5 \times 10^{17}$	$1.5 \times 10^7$
Arsenic	10	$5 \times 10^{17}$	$1.5 \times 10^7$
Antimony	0.2	$1 \times 10^{16}$	$3.0 \times 10^5$

\*Raster size 125  $\mu\text{m} \times 95 \mu\text{m}$  with 25  $\text{\AA}$  depth sampled ( $2.97 \times 10^{-11} \text{cm}^3$ )

10 to 100 ppba - Mg, Al, Ti, Cr, Mn, Ga, Zr, Mo, In, Na, Li, K and Ca

100 to 1000 ppba - Cu, Ta, and W

1 ppma to 1000 ppma - Fe, Ni, Ge, C, Zn, Se, Sn, Ag, Cd, Te, Pb, and Bi

> 1000 ppma - noble metals and rare gases.

In summary, and as shown in Figure 32, the only analytical microbeam technique with the detection limits required for integrated circuit analysis are the ion microprobe or some microbeam secondary ion mass spectroscopy technique.

#### F. Analysis Time

The analysis of an integrated circuit device covers the sequence of events and typical times shown in Table 10. The time elapsed between receiving the device and starting the SIMS analysis is usually from four to five hours. The major part of the time of the ion microprobe process is taken up by the sputtering process. The sputtering time for each area analyzed depends, as indicated below, on the primary ion used for analysis:

Silicon or metal films with  $O_{32}^+$   $\approx 2.5 \text{ \AA/sec}$

Dielectric films with  $O_{16}^-$   $\approx 0.5 \text{ \AA/sec}$

All films with  $Ar_{40}^+$   $\approx 6 \text{ \AA/sec}$

These sputter rates transpose into the analysis times for each area analyzed, as shown in Table 10. Thus, if two dielectric areas, two silicon areas, and one metal area are analyzed, the ion microprobe sputter time could be in the 12 to 24 hour range, depending on the thickness of the films. This represents a total analysis time of 16 to 29 hours per device without data reduction. Data reduction times vary depending on the analyst, but in this laboratory, using a 960A computer, one to four hours are required.

These analysis times assume that in each of the six areas, the data collected are mass spectra depth profile if a complete survey of all impurities is to be taken. For single element, high sensitivity depth profiles, or quantitative determinations, a six to twelve hour time period could apply to each element determined per area, depending on the depth and accuracy desired.

TABLE 10. ANALYSIS TIMES REQUIRED FOR SIMS ANALYSIS  
OF AN INTEGRATED CIRCUIT

<u>Process</u>	<u>Typical Time</u>
Open device and photograph	30-45 minutes
Remove bonds and dealloy chip	45-60 minutes
Mount chip and gold coat	45-60 minutes
SEM inspection, pictures and select areas for analyses	60-90 minutes
Introduce in IMMA and pump down	30-45 minutes
Locate areas in IMMA and start analysis	10-20 minutes
$^{+}_{32}$ ion sputter of silicon/metal area*	60-180 minutes
$^{+}_{16}$ ion sputter of dielectric area	300-900 minutes
$^{+}_{40}$ ion sputter of device area	10-60 minutes

\*Assumes silicon/metal area is exposed

#### G. Quantitation

Two methods are employed to obtain quantitative ion microprobe analysis. The first method is based on a model using the Saha-Eggert ionization equation which is based on the ion production process. Anderson and Hinshorne<sup>2</sup> have developed a computer program, CARISMA, for the ion microprobe and have reported success with their method on a variety of matrices. Efforts at Texas Instruments to apply this program to the quantitation of trace impurities in silicon have not demonstrated confidence in its accuracy.

The second method of quantitation is based on empirical calibration using standards. Work at Texas Instruments sponsored in part by a National Bureau of Standards contract<sup>3</sup> has been successful in establishing calibration curves for boron, arsenic, antimony, and phosphorus in silicon and silicon dioxide. These detection limits are discussed in Section VII.E. The standards used to obtain these calibration curves were infinite plane samples, that is, very large compared to the size of the raster used for the analysis.

Quantitation during integrated circuit analysis will be extremely difficult. Most of the problems result from the large areas or raster sizes required for ion microprobe analysis. Areas of the required size available for analysis on integrated circuits seldom have a single matrix, e.g., silicon or silicon dioxide. Since calibration curves are set up on a single matrix, any mixing of matrices, e.g., metalization, dielectric films, etc., will keep the results from being quantitative.

In summary, quantitation in ion microprobe analysis of integrated circuits is possible if there is available an area of sufficient size, i.e., 100 x 100  $\mu\text{m}$ , and of a single matrix of silicon or silicon dioxide. In reality, this will occur only with dielectric films, metalization, bond pads, resistor films, large area capacitors, and bulk or epitaxial silicon regions outside the bar.

2. C. A. Anderson and J. R. Hinshorne, Anal. Chem. 45, 1421 (1973).

3. National Bureau of Standards Contract No. 5-35917, "Development of Techniques for the Preparation and Analysis of Standard Silicon Semiconductor Specimens for the Ion Microprobe Mass Analyzer."

**The electrically active regions, e.g., emitters, bases in bipolar devices, and source-drain-bases in MOS devices, are very difficult to analyze, and much more to so quantitate.**

Difficulties in analyzing electrically active regions are due to the fact that they are often heavily doped with impurities which are present in high concentrations. These high concentrations of impurities can cause significant deviations from the simple theory of carrier transport. In addition, the presence of electrically active regions can affect the overall behavior of the device, such as the voltage-current characteristics, which may not be fully understood. Furthermore, the presence of electrically active regions can lead to non-uniformities in the device, such as variations in carrier density or potential across the device. These factors make it difficult to accurately model and analyze the behavior of electrically active regions in devices.

Another issue is that the electrically active regions in devices often contain different types of impurities, such as boron and phosphorus, which have different effects on carrier transport. For example, boron is a p-type dopant that increases carrier concentration and mobility, while phosphorus is an n-type dopant that decreases carrier concentration and mobility. This can lead to complex interactions between different types of impurities, making it difficult to predict the overall behavior of the device.

In addition, the presence of electrically active regions can affect the overall performance of the device. For example, if the electrically active regions are heavily doped, they can limit the current-voltage characteristics of the device, leading to lower current levels at higher voltages. This can be particularly problematic in high-current applications, such as power electronics or high-current sensors.

Overall, the analysis of electrically active regions in devices is a challenging task that requires a deep understanding of carrier transport and the effects of different types of impurities. While significant progress has been made in this field, there is still much work to be done to fully understand the behavior of electrically active regions in devices.

## SECTION VIII CONCLUSIONS

The ion microprobe mass analyzer analysis of these 42 integrated circuits has amply demonstrated the power of this technique to chemically characterize actual packaged commercial devices. The results reported here confirm the statement made in Section II of this report that IMMA (SIMS) is the only analytical technique that will even approach the analysis of integrated circuits with the geometrical resolution and sensitivity needed for 1977 timeframe devices. IMMA techniques must be extended even further by additional studies such as this one, coupled with more instrument research to meet the needs for the 1980 timeframe, large-scale integrated circuits.

The data presented here have successfully demonstrated the following analysis capabilities, many of which are not possible with any other analytical technique.

(1) Surface analysis: The surface analysis of small areas was obtained in the first and second mass spectra of any mass spectra depth profile series. The entire surface was not sputtered for any analysis, which allowed proof that some elements were found only on the surface, i.e., the Pb and Sn depth profile from the general technology group.

(2) Interface analysis: A technique was developed to open in-situ an interface for chemical analysis. The actual point of small area for this analysis could be readily chosen, again leaving the rest of the circuit intact for other types of analyses.

(3) Dopant identification: The ability to identify dopants and depth-profile the dopants in electrically active areas of the silicon was presented in Sections V and VI. Even though in some areas the dopant was not positively identified in this study, this does not detract from IMMA's potential.

(4) Depth profile: Many examples of the depth profiling capability have been presented. This type of analysis cannot be performed on actual circuits by any other technique presently known.

(5) Quantitation: Quantitation of dopants and/or impurities in the small total material volumes found in these circuits is extremely difficult. However, quantitation is possible, as evidenced by the many quantitative phosphorus profiles and the boron concentration in electrically active silicon areas. The Cr-Ni profiles of the nichrome resistors could have been quantitative had suitable standards been prepared to calibrate the observed signals.

These features and the many others discussed in this report prove conclusively that IMMA (SIMS) has a very important role in the analysis of all types of integrated circuits and other solid state devices.

## SECTION IX

### RECOMMENDATIONS

#### A. Failure Analysis

The ion probe can be an extremely valuable tool in the area of failure analysis if the failure mechanism is chemical in nature. However, because of the time involved in sample preparation and depth sputtering, the ion probe should be used only after exhaustive analysis has been done by electron probe techniques. For example, total phosphorus can be determined by the electron probe; however, it samples a depth of several micrometers, so if it is important to know the depth at which phosphorus is located, the ion probe must be used. In addition, only the ion probe has a real sensitivity for elements such as H, Li, B, and F, and it is several orders of magnitude more sensitive for the alkali elements.

The results presented in this report have shown that ion probe analysis does indeed yield copious amounts of chemical information from a single circuit chip. However, in terms of failure analysis, these results mean very little by themselves. A data base must be acquired which relates device performance, degradation, and/or failures to the chemical characterization by ion probe analysis. When such a data base is available, ion probe analysis will be one of the most powerful tools for failure analysis and determination of long-term reliability from actual integrated circuit chips.

#### B. Device Process Evaluation

Most of the reliability of any integrated circuit is built in during device processing. A major portion of the cost of integrated circuits is also determined by device processing, since yield is a critical cost factor. Most of the circuits built today use test subcomponents on each bar and/or replace one or more bars with test patterns on each slice. These testers are evaluated by electrical measurements, which are extrapolated back to the processing parameters. As circuits become more complex with higher densities and much

smaller geometries, these built-in test patterns are becoming infeasible, in that they no longer adequately represent the device processing and require too much usable real estate on the chip. In the near future, process evaluation and reliability will be determined by process evaluation slices where an entire slice is used for many types of test patterns designed for different types of testers. These testers include electrical, mechanical, and chemical types. The ion probe has a very real application here, since the necessary geometries can be included for maximum sensitivity. The ion probe can easily determine diffusion or ion implant profiles, junction depths, and/or impurities on these test patterns.

### C. Instrumentation

The instrument used in this study was as delivered from the manufacturer, without automation. A TI 960A computer was interfaced to handle the data for point-counting depth profiles of either one or two elements in a given run. If more elements need to be profiled, separate craters must be sputtered. This can be a severe problem in failure analysis, since separate areas may not be available. Therefore, if failure analysis is the primary goal, the instrument should be equipped with secondary magnet, computer-controlled peak switching so several elements can be profiled in narrow 1 to 3 nm layers from one crater hole.

An ideal instrument for failure analysis would have the characteristics listed below:

- (1) A basic ion probe capable of 1 to 2  $\mu\text{m}$  diameter beams
- (2) Computer-controlled secondary magnet system
- (3) Computer-controlled data collection system
- (4) Computer-controlled time clock for all beam rastering, electron gating, peak switching, beam blanking, and data collection
- (5) Computer monitoring of the primary ion beam current
- (6) Computer monitoring of the secondary ion non-mass analyzed ion current
- (7) Computer control of sample stage movements.

#### D. Future Studies

This study has demonstrated the potential of the ion probe to provide valuable information about a circuit. The analyses and techniques developed in the course of this work have merely scratched the surface in showing the potential usefulness of the instrument. It is recommended that future study should involve correlations between device performance and ion probe results, rather than a general survey of many types of devices. A correlation matrix involving electrical performance, SEM appearance, EBIC-voltage contrast images, electron microprobe analysis, and ion probe analysis, all concentrated to solve a particular problem, would prove invaluable.

## APPENDICES

These appendices are a more detailed summary of the ion probe characterization performed on each device. No data or profile are repeated in these appendices that appeared in the main text. For each device analyzed, the appendix includes the area identification optical photograph, typical mass spectra, and the mass spectra depth profile numerical summary.

The entries in the mass spectra depth are the measured peak heights from each spectrum and are normalized by the Si<sub>30</sub> peak height in order to obtain a common relative scale so meaningful comparisons can be made. The entry in the Si<sub>30</sub> row is the actual measured peak height without normalization. The type of common intensity base is good for most spectra, but on some it could lead to gross error. The normalization assumed the Si was the major matrix element in each area analyzed. If not, the normalization gives a gross error. Examination of the Si<sub>30</sub> row will reveal most of the error entries. Gross differences in the Si<sub>30</sub> peak height are the indicator of the error.

The key to mass spectra depth profile table is:

Unit:	Unit number assigned by RADC to the circuit.
Area:	Area analysis, identified in optical photograph.
Spectra:	Numbers assigned to spectra for internal identification.
Raster:	Measured crater size sputter by primary beam.
Spot:	Measured primary beam diameter.
BC:	Primary beam current measured on circuit at 1500 V bias.
SR:	Calculated sputter rate in Å/sec.
Start (column):	Time in seconds to reach peak in mass spectrum.
Plus (row):	Sputter time in seconds before mass spectrum started.

APPENDIX A

CMOS-SOS-CLEAN OXIDE, UNIT #739

Area 1: Single Mass Spectrum for Surface Analysis

Area 2: Depth Profile Mass Spectra

Area 3: Al-P Peak Count Depth Profile

Area 4: F-Ca Peak Count Depth Profile

Area 5: Al-P Peak Count Depth Profile (not used)

Area 6: Depth Profile Mass Spectra

Area 7: False Start

Area 8: P Concentration in Depth Profile

Area 9: Mass Spectra Depth Profile After Oxide and Metal Stripping

Area 1A: Mass Spectra Depth Profile After Oxide and Metallization  
Removed

Area 2A: B Depth Profile After Stripping

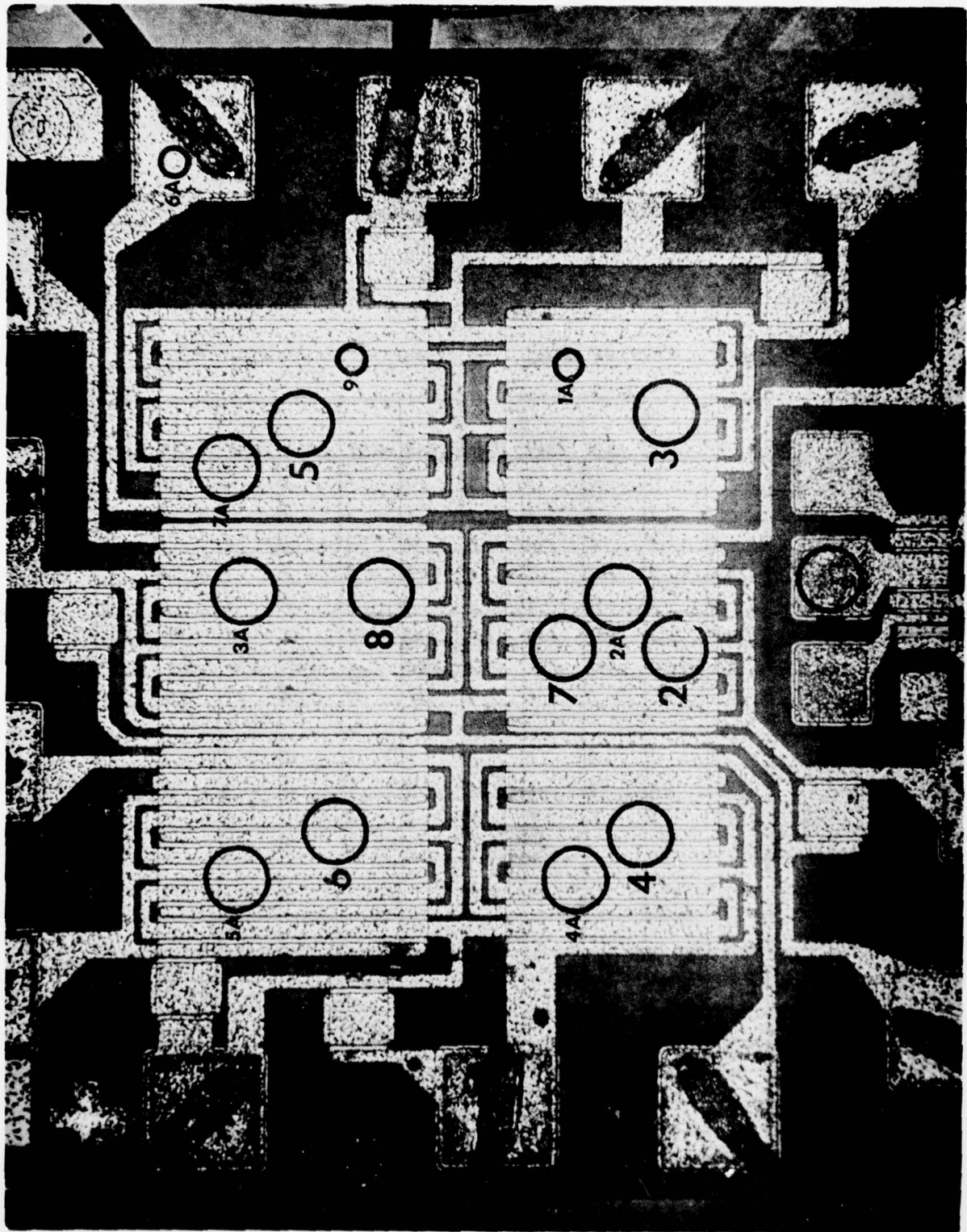
Area 3A: P Depth Profile After Stripping

Area 4A: B Depth Profile After Stripping

Area 5A: P Depth Profile After Stripping

Area 6A: Al-Si Depth Profiles After Stripping

Area 7A: Al-Si Depth Profiles After Stripping



CMOS-SOS-Clean Oxide Unit #739

CMOS SOS CLEAN OXIDE

UNIT #739 . AREA 2 . SPECTRA 145 - 155 .

RASTER 71 X 58  $\mu\text{m}$  . SPOT 19  $\mu\text{m}$  BC 11 NA SR ( $\text{\AA}/\text{SEC}$ ) .95 .

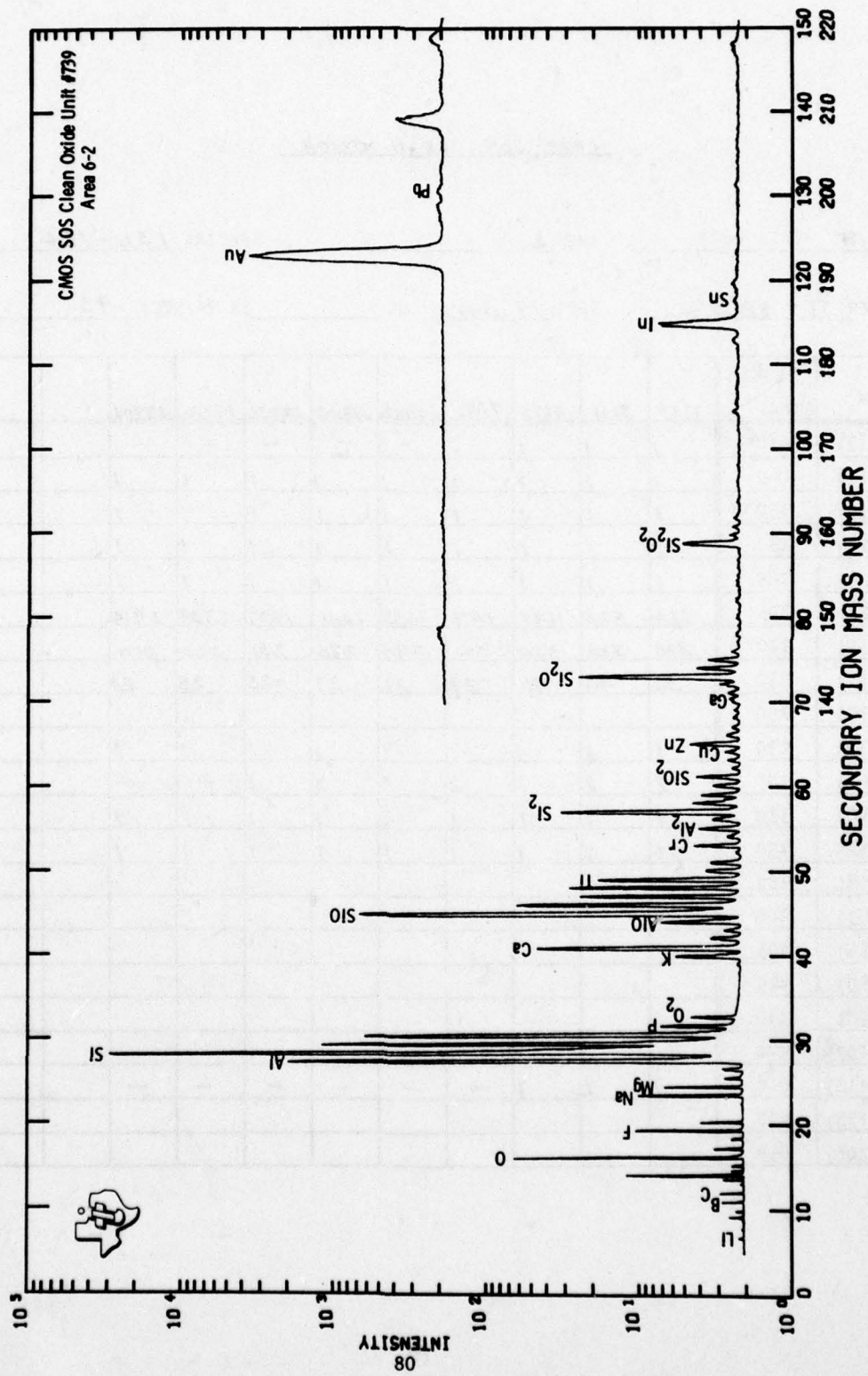
ELEM	PLUS START	0	689	1379	2069	2758	3447	4135	4822	5510	6353	7038
Li (7)	30	-	1	1	1	1	1	1	1	1	1	1
B (11)	60	-	1	1	1	1	1	1	1	1	1	1
F (19)	150	2	3	2	1	1	2	1	1	1	1	1
Na (23)	180	23	2	1	1	1	2	2	1	1	1	1
Mg (24)	185	4	2	1	1	1	2	1	1	1	1	1
Al (27)	205	1663	335	239	109	100	243	81	60	83	81	206
Si (30)	220	25	180	210	350	240	280	260	330	290	320	330
P (31)	230	-	-	1	4	9	11	17	24	27	28	30
Cl (35)	250											
K (39)	290	15	1	1	1	1	1	1	1	1	1	1
Ca (40)	295	171	22	10	11	5	17	9	6	7	5	3
Ti (48)	330	17	3	2	2	2	2	2	1	2	2	2
Cr (52)	350	-	1	-	-	-	1	1	1	1	1	-
Ni (58)	380											
Cu (63)	400											
Zn (64)	403											
Ga (69)	425											
Mo (98)	540											
Ag (107)	570											
Sn (118)	610	1	1	1	1	1	1	1	1	1	1	1
Ba (138)	670											
Pb (208)	858											

CMOS SOS CLEAN OXIDE

UNIT # 2 . AREA 2 . SPECTRA 156-164 .

RASTER 71 X 58 μm . SPOT 19 μm BC \_\_\_\_\_ SR (Å/SEC) .95 .

ELEM	PLUS START	7733	8511	9195	9891	10582	11265	12031	12716	13905	
Li (7)	30	1	1	1	1	-	-	-	-	-	
B (11)	60	1	1	1	1	1	1	1	1	1	
F (19)	150	1	1	1	1	1	1	1	1	1	
Na (23)	180	1	1	1	1	1	1	1	1	1	
Mg (24)	185	1	1	1	1	1	1	1	1	1	
Al (27)	205	324	820	1191	1471	1453	1635	1807	2739	2914	
Si (30)	220	340	330	320	300	290	270	250	220	200	
P (31)	230	32	33	31	28	26	27	25	25	24	
C1 (35)	250										
K (39)	290	1	1	1	1	1	1	1	1	1	
Ca (40)	295	2	2	2	2	3	3	2	-	-	
Ti (48)	330	1	1	1	1	1	1	1	1	1	
Cr (52)	350	1	1	1	1	1	1	1	1	1	
Ni (58)	380										
Cu (63)	400										
Zn (64)	403										
Ga (69)	425										
Mo (98)	540										
Ag (107)	570										
Sn (118)	610	1	1	1	-	-	-	-	-	-	
Ba (138)	670										
Pb (208)	858										



CMOS SOS CLEAN OXIDE

UNIT #739 . AREA 6 . SPECTRA 349 - 359 .

RASTER 69 X 56 μm . SPOT 12 μm BC 10 NA SR (1/SEC) . 92 .

ELEM	PLUS START	0	910	1831	2753	3735	4637	5549	6458	7386	8079	8808
Li (7)	30	1	1	1	-	-	-	-	-	-	-	-
B (11)	60	-	1	1	1	1	1	1	1	1	1	-
F (19)	150	1	2	1	1	1	1	1	1	1	1	1
Na (23)	180	3	2	1	1	1	1	1	1	1	1	1
Mg (24)	185	1	1	1	1	1	1	1	1	1	1	1
Al (27)	205	191	283	124	105	51	61	352	843	2061	2464	2401
Si (30)	220	220	170	170	190	160	180	160	110	98	74	96
P (31)	230	1	1	11	22	28	28	28	30	34	29	27
C1 (35)	250											
K (39)	290	1	1	1	1	1	1	1	1	1	1	1
Ca (40)	295	11	9	5	3	2	3	1	2	1	1	1
Ti (48)	330	2	4	1	1	1	1	1	1	1	1	1
Cr (52)	350	1	1	1	1	1	1	1	1	1	1	1
Ni (58)	380											
Cu (63)	400	1	1	1	1	1	1	1	1	1	1	1
Zn (64)	403	1	1	1	1	1	1	1	1	1	1	1
Ga (69)	425											
Mo (98)	540											
Ag (107)	570											
Sn (118)	610	1	1	1	-	-	-	-	-	-	-	-
Ba (138)	670											
Pb (208)	858											

## CMOS SOS CLEAN OXIDE

UNIT #739. AREA 6. SPECTRA 360.

RASTER 69 x 56 μm. SPOT 12 μm BC 10 NA SR ( $\text{\AA}/\text{SEC}$ ) .92.

ELEM	PLUS				
	START	9370			
Li (7)	30	-			
B (11)	60	/			
F (19)	150	/			
Na (23)	180	/			
Mg (24)	185	/			
Al (27)	205	2197			
Si (30)	220	92			
P (31)	230	25			
Cl (35)	250				
K (39)	290	/			
Ca (40)	295	/			
Ti (48)	330	/			
Cr (52)	350	/			
Ni (58)	380				
Cu (63)	400	/			
Zn (64)	403	/			
Ga (69)	425				
Mo (98)	540				
Ag (107)	570				
Sn (118)	610	-			
Ba (138)	670				
Pb (208)	858				

CMOS SOS CLEAN OXIDE

UNIT # 739 . AREA 9 . SPECTRA 781 - 782 .

RASTER 62 X 53 μm . SPOT 17 μm BC 16 NA SR (1/SEC) .

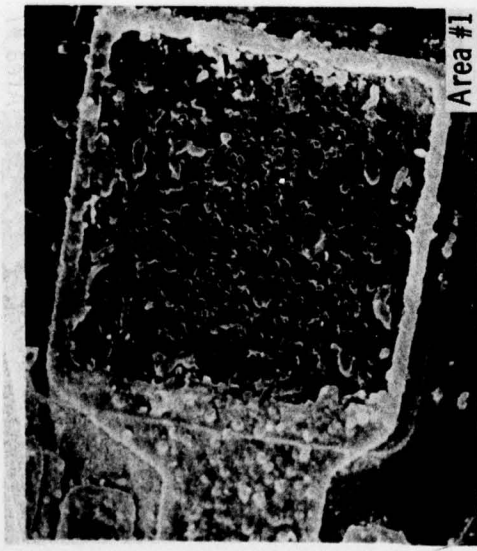
ELEM	PLUS START	0	1082								
Li (7)	30	1	-								
B (11)	60	1	-								
F (19)	150	2	2								
Na (23)	180	11	10								
Mg (24)	185	6	5								
Al (27)	205	489	4787								
Si (30)	220	1800	72								
P (31)	230	-									
Cl (35)	250										
K (39)	290	1	6								
Ca (40)	295	40	37								
Ti (48)	330	1	1								
Cr (52)	350	1	1								
Ni (58)	380										
Cu (63)	400	1	6								
Zn (64)	403	1	1								
Ga (69)	425										
Mo (98)	540										
Ag (107)	570	1	1								
Sn (118)	610										
Ba (138)	670										
Pb (208)	858										

## CMOS SOS CLEAN OXIDE

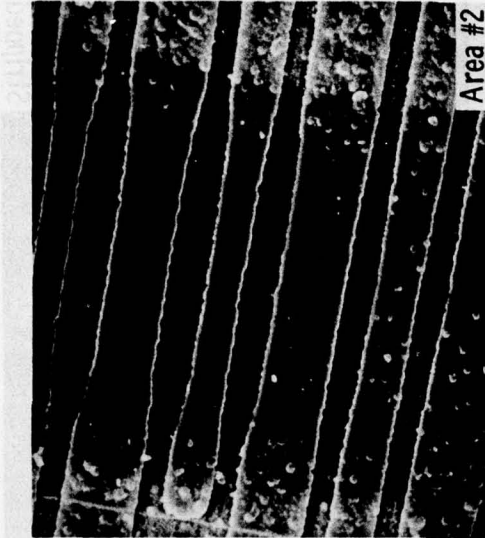
UNIT #739 . AREA 1A . SPECTRA 783-784

RASTER 62 X 53 μm. SPOT 17 μm BC 16 NA SR ( $\text{A}/\text{SEC}$ ) 100

CMOS SOS Clean Oxide Unit #739



Area #1



Area #2

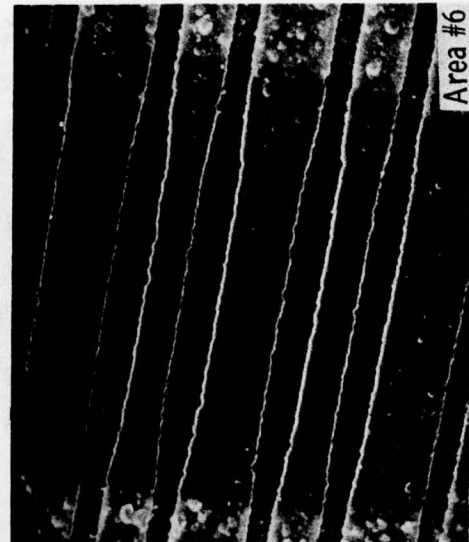
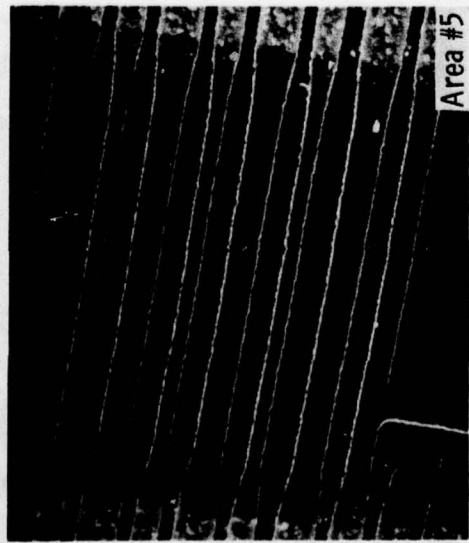


Area #3



Area #4

CMOS SOS Clean Oxide Unit #739



**CMOS BULK CLEAN OXIDE, UNIT #R202**

**Area 1: Mass Spectra Depth Profiles**

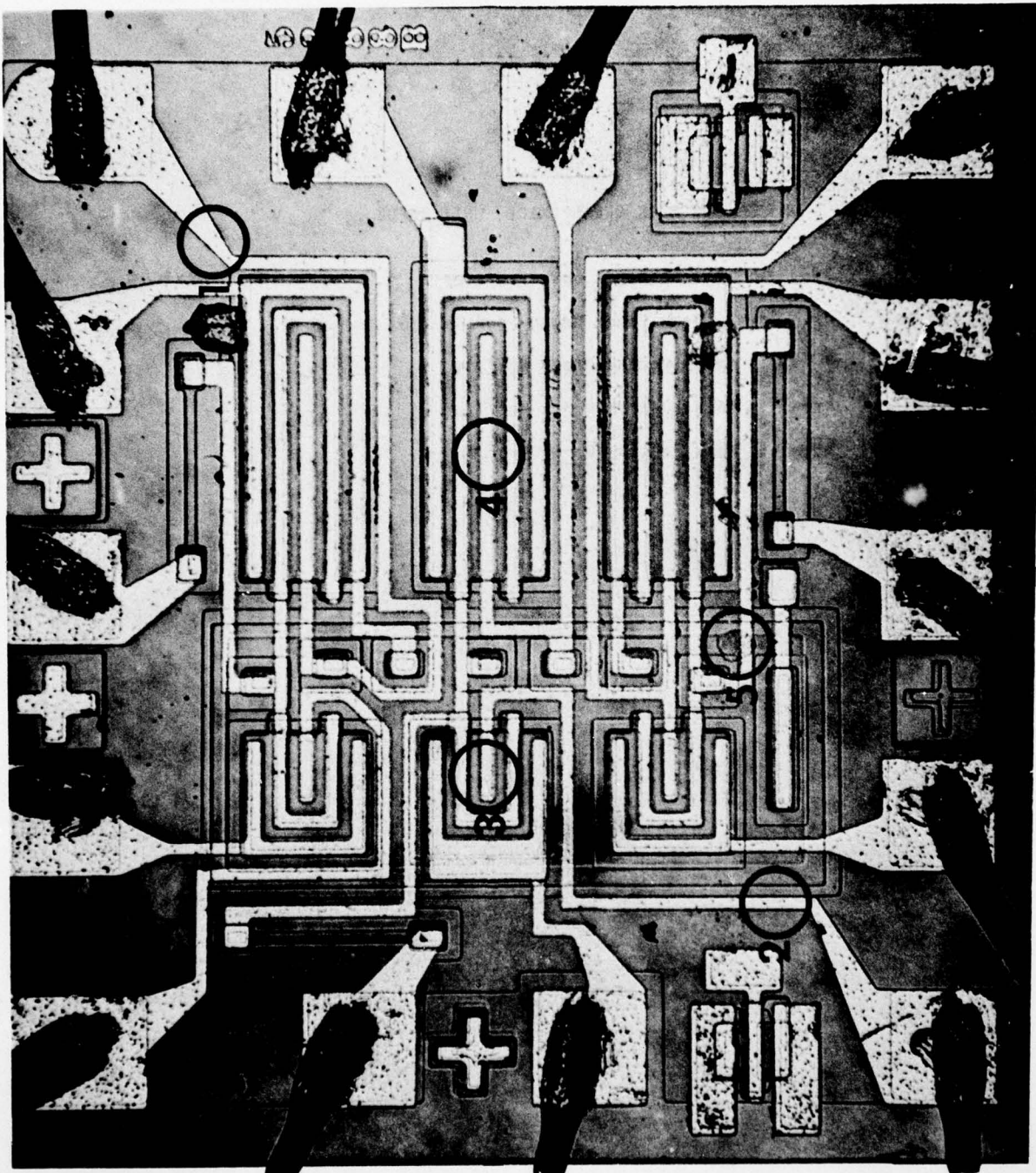
**Area 2: Cr Peak Count Depth Profile (not included)**

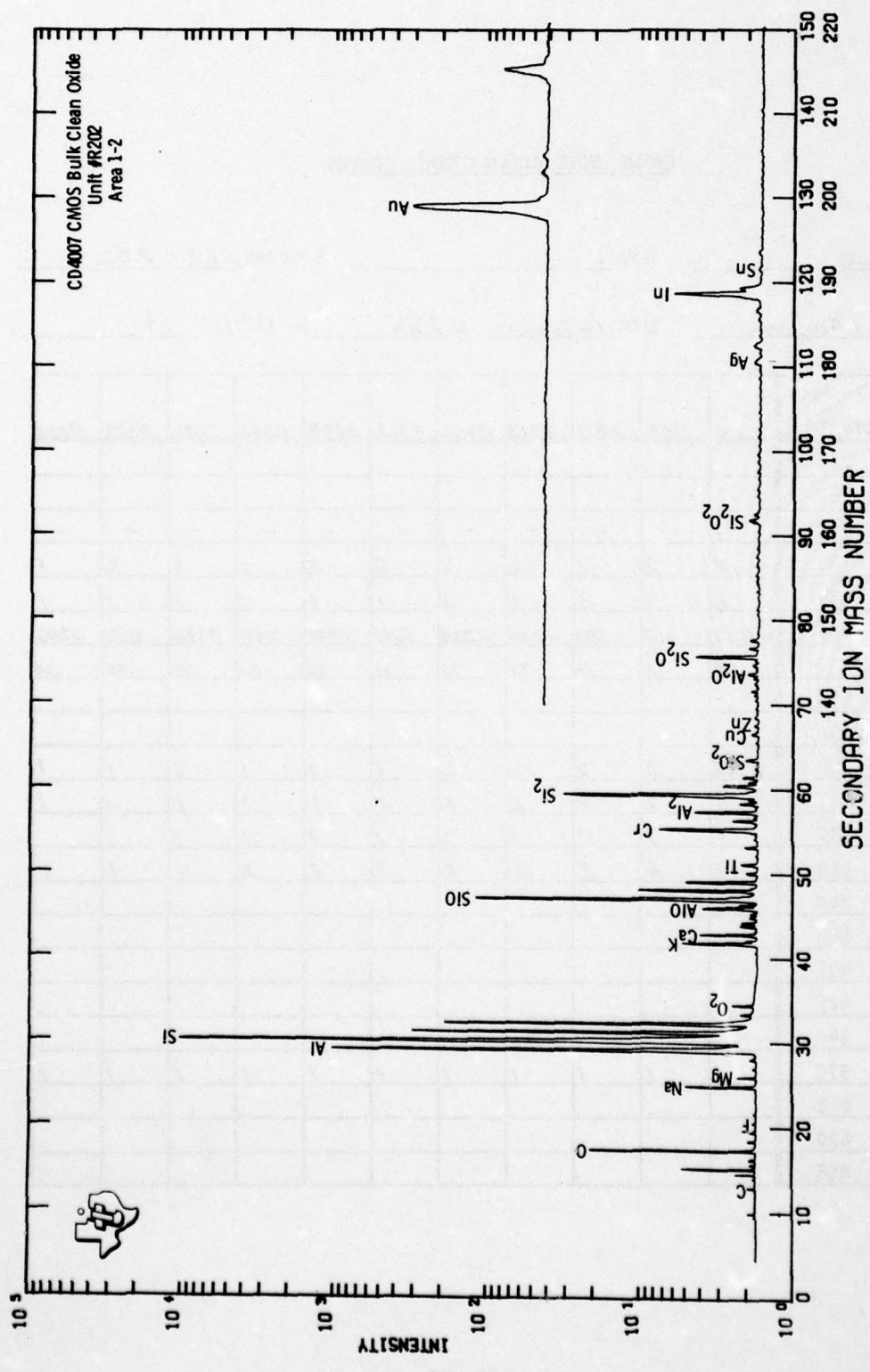
**Area 3: Mass Spectra Depth Profile**

**Area 4: Mass Spectra Depth Profile**

**Area 5: Mass Spectra Depth Profile**

Set 1 CMOS Bulk Clean Oxide Unit #R202





AD-A048 482

TEXAS INSTRUMENTS INC DALLAS CENTRAL RESEARCH LABS  
MICROBEAM ANALYSIS TECHNIQUES FOR ICS.(U)

OCT 77 G B LARRABEE, R D DOBROTT

F/G 20/12

F30602-76-C-0316

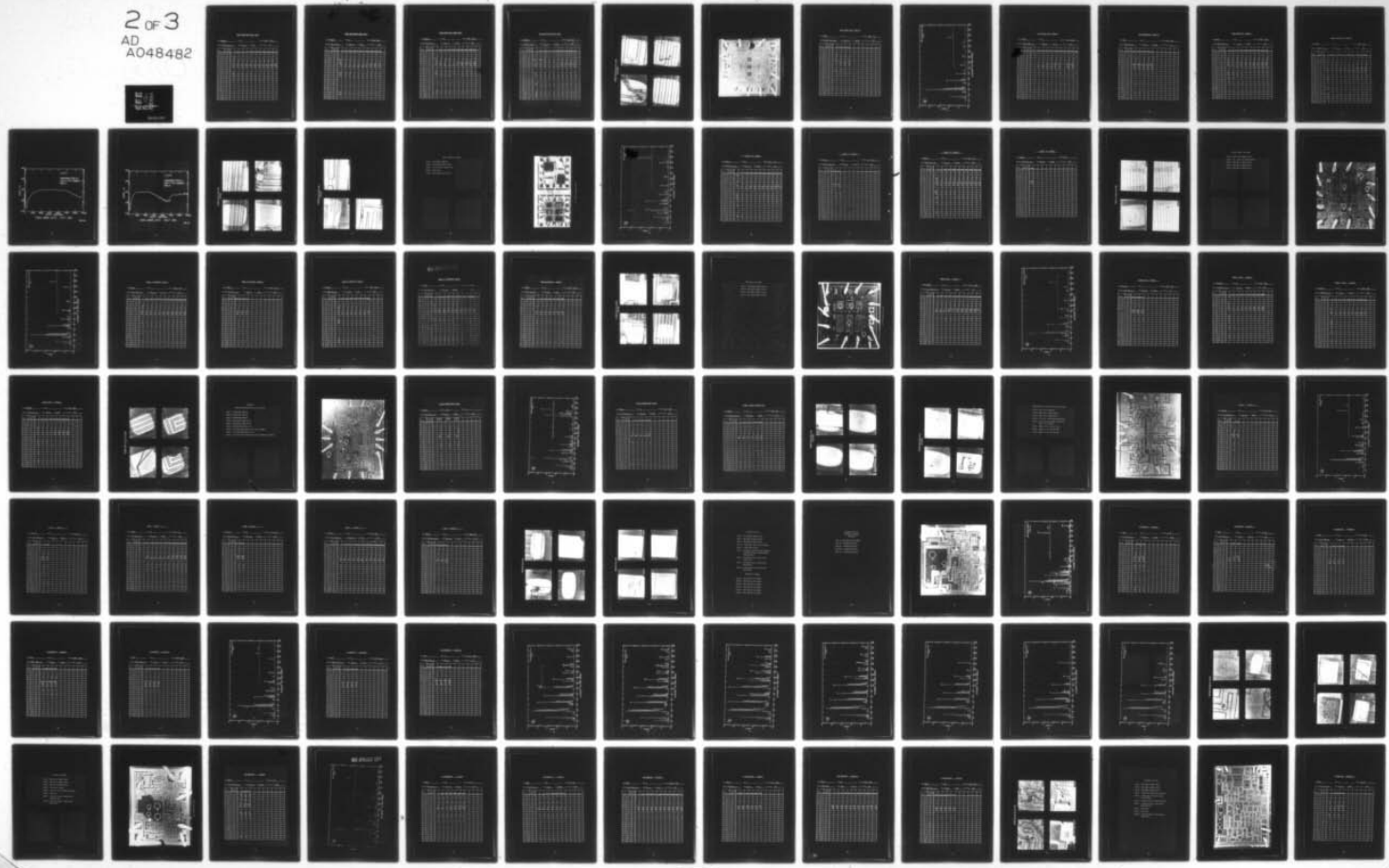
UNCLASSIFIED

TI-08-77-16

RADC-TR-77-339

NL

2 of 3  
AD  
A048482



CMOS BULK CLEAN OXIDE CD4007

UNIT #R202 . AREA 1 . SPECTRA 222 - 232 .

RASTER 69 X 90 μm . SPOT 16 μm BC 7 NA SR (Å/SEC) .4 .

ELEM	PLUS START	0	904	1611	2713	3612	4513	5423	6326	7231	8133	9030
Li (7)	30											
B (11)	60											
F (19)	150	1	-	-	-	-	-	-	-	-	-	-
Na (23)	180	19	2	2	2	2	2	2	2	2	2	1
Mg (24)	185	2	1	1	1	1	1	1	1	1	1	1
Al (27)	205	1177	462	399	1069	1332	1640	1998	2371	3156	3583	3206
Si (30)	220	23	70	76	72	70	68	66	60	58	54	54
P (31)	230											
Cl (35)	250											
K (39)	290	22	3	2	2	2	1	1	1	1	1	1
Ca (40)	295	9	2	2	2	2	2	1	1	1	1	1
Ti (48)	330	1	1	1	1	1	1	1	1	1	1	1
Cr (52)	350	17	4	3	6	4	3	2	2	1	1	1
Ni (58)	380											
Cu (63)	400											
Zn (64)	403											
Ga (69)	425											
Mo (98)	540											
Ag (107)	570	1	1	1	1	1	1	1	1	1	1	1
Sn (118)	610											
Ba (138)	670											
Pb (208)	858											

CMOS BULK CLEAN OXIDE CD4007

UNIT #R202 . AREA 3 . SPECTRA 444 - 453 .

RASTER 72 x 61 μm . SPOT 19 μm BC 6 NO SR (Å/SEC) . 48 .

ELEM	START	PLUS										
		0	907	1595	2284	2971	3661	4342	5036	5727	6415	
Li (7)	30											
B (11)	60											
F (19)	150											
Na (23)	180	3000	3	2	2	1	1	1	1	1	1	
Mg (24)	185	100	1	1	1	1	1	1	1	1	1	
Al (27)	205	700	11	11	11	10	10	39	203	254	379	
Si (30)	220	1.1	36	37	38	36	38	42	40	36	35	
P (31)	230											
C1 (35)	250											
K (39)	290	1000	2	2	1	1	1	1	1	1	1	
Ca (40)	295	300	1	1	1	1	1	1	1	1	1	
Ti (48)	330	-	1	1	1	1	1	1	1	1	1	
Cr (52)	350											
Ni (58)	380											
Cu (63)	400											
Zn (64)	403	-	1	1	1	1	1	1	-	-	-	
Ga (69)	425											
Mo (98)	540											
Ag (107)	570	100	1	-	-	-	-	-	-	-	-	
Sn (118)	610	100	1	1	-	-	-	-	-	-	-	
Ba (138)	670											
Pb (208)	858											

CMOS BULK CLEAN OXIDE CD4007

UNIT # R202 . AREA 4 . SPECTRA 454 - 465 .

RASTER 72 x 61 μm . SPOT 19 μm BC 64A SR (A/SEC) .48 .

ELEM	PLUS START	0	896	1573	2254	2930	3608	4286	4965	5645	6326
Li (7)	30										
B (11)	60										
F (19)	150										
Na (23)	180	200	5	3	3	2	1	1	1	1	1
Mg (24)	185	8	4	3	2	1	1	1	1	1	1
Al (27)	205	60	26	11	7	7	35	135	222	351	487
Si (30)	220	3.5	40	48	52	52	52	52	50	46	46
P (31)	230	1	1	1	1	1	1	1	-	1	1
C1 (35)	250										
K (39)	290	64	4	3	2	2	1	1	1	1	1
Ca (40)	295	20	2	1	1	1	1	1	1	1	1
Ti (48)	330	1	2	2	2	1	1	1	1	1	1
Cr (52)	350										
Ni (58)	380										
Cu (63)	400	-	-	-	-	-	-	-	-	-	1
Zn (64)	403	-	1	1	1	1	1	1	1	1	1
Ga (69)	425										
Mo (98)	540										
Ag (107)	570	4	1	1	1	1	1	1	1	-	-
Sn (118)	610	4	1	1	1	-	-	-	-	-	-
Ba (138)	670.										
Pb (208)	858										

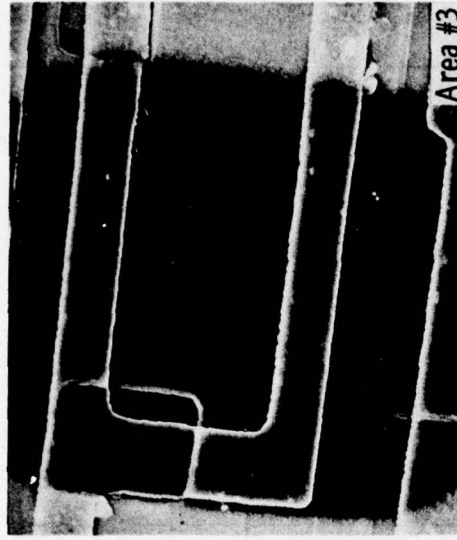
CMOS BULK CLEAN OXIDE CD4002

UNIT #R202 . AREA 5 . SPECTRA 464-473 .

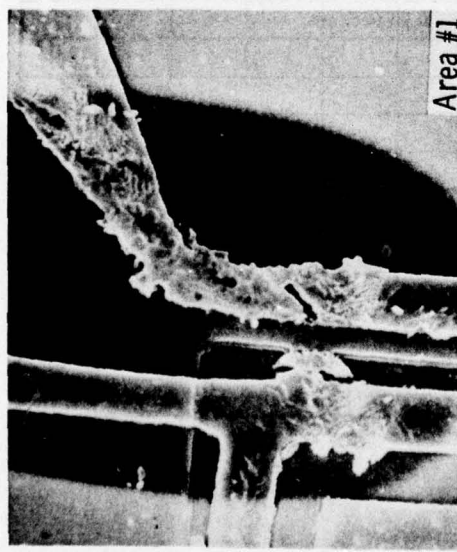
RASTER 72 X 61 μm . SPOT 19 μm BC 6NA SR (Å/SEC) .48 .

ELEM	PLUS START	0	694	1379	2060	2740	3420	4099	4780	5464	6174
Li (7)	30	1	1	1	-	-	-	-	-	-	-
B (11)	60	-	1	1	-	-	-	-	-	-	-
F (19)	150	-	1	1	-	-	-	-	-	-	-
Na (23)	180	3250	88	81	12	7	5	4	5	4	4
Mg (24)	185	50	13	12	8	8	6	6	7	6	6
Al (27)	205	300	44	17	11	9	9	33	135	235	319
Si (30)	220	1.4	53	54	60	60	52	56	52	56	54
P (31)	230	-	2	1	1	1	1	1	1	1	1
C (35)	250										
K (39)	290	1100	53	21	7	5	4	4	4	3	3
Ca (40)	295	125	16	8	5	4	3	3	3	2	2
Ti (48)	330	-	2	2	2	2	1	1	1	1	1
Cr (52)	350	-	1	1	1	1	1	1	1	1	1
Ni (58)	380										
Cu (63)	400	25	1	1	1	1	1	1	1	1	1
Zn (64)	403	-	1	1	1	1	1	1	1	1	1
Ga (69)	425										
Mo (98)	540										
Ag (107)	570	75	1	1	1	1	1	1	1	1	1
Sn (118)	610	25	1	1	1	1	1	1	-	-	-
Ba (138)	670	25	1	-	-	-	-	-	-	-	-
Pb (208)	858										

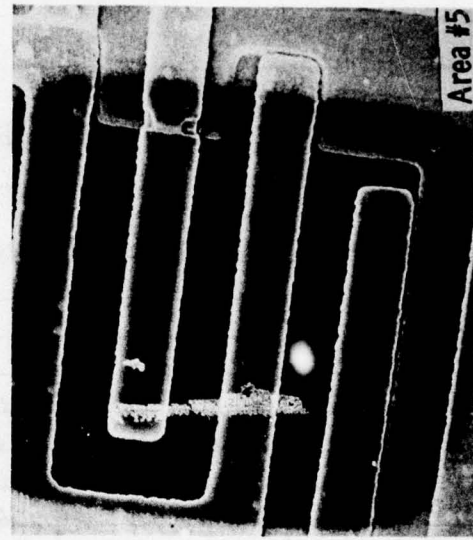
CD4007 CMOS Bulk Clean Oxide  
Unit #R202



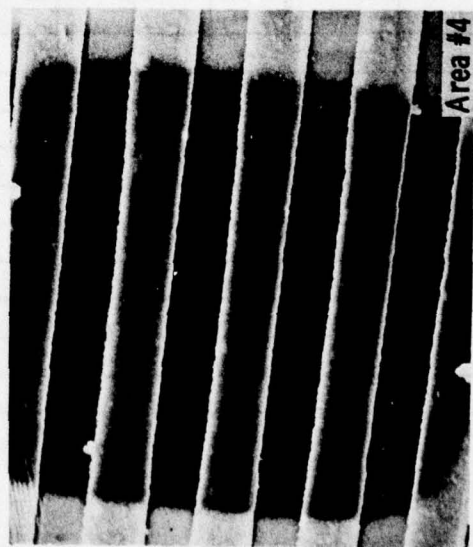
Area #3



Area #1

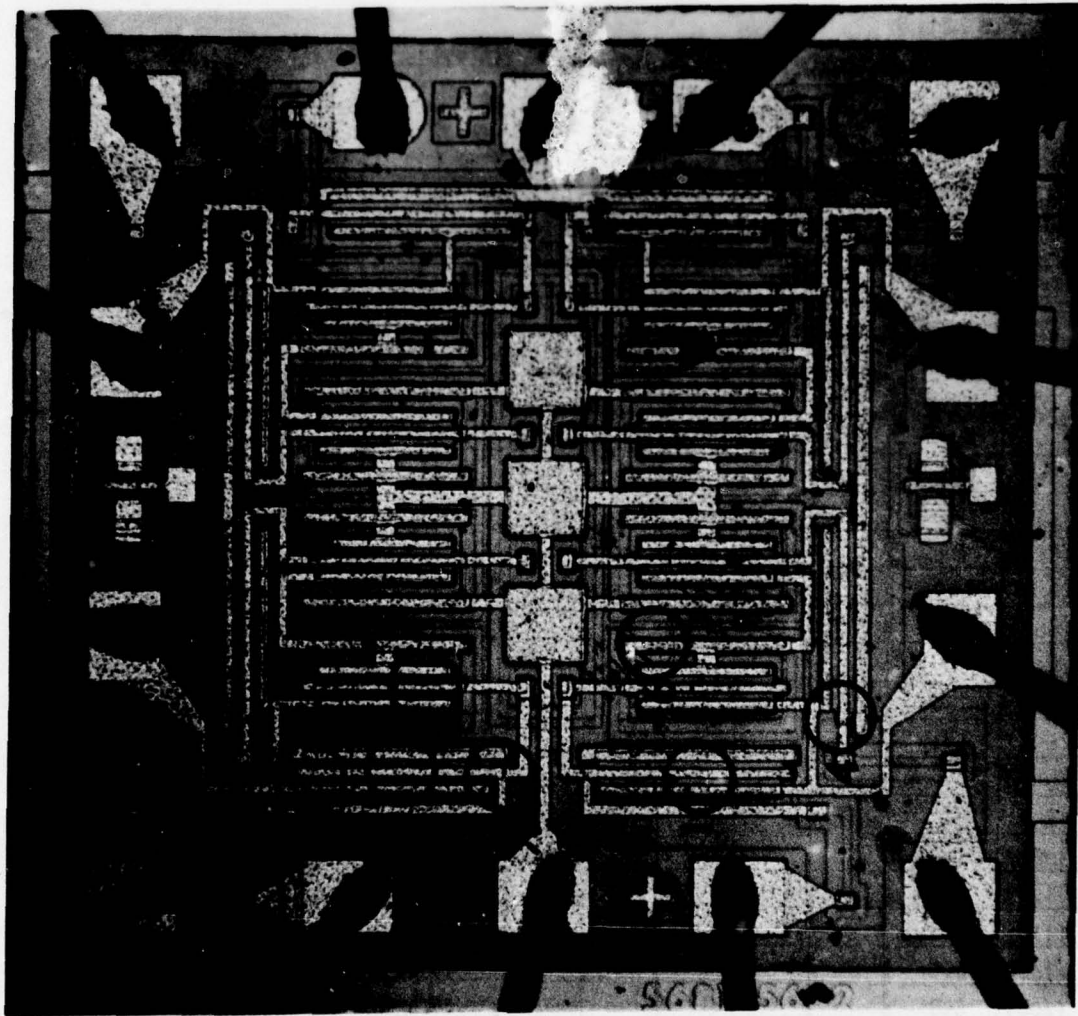


Area #5



Area #4

Set 1 CMOS NAND Gate Unit #86

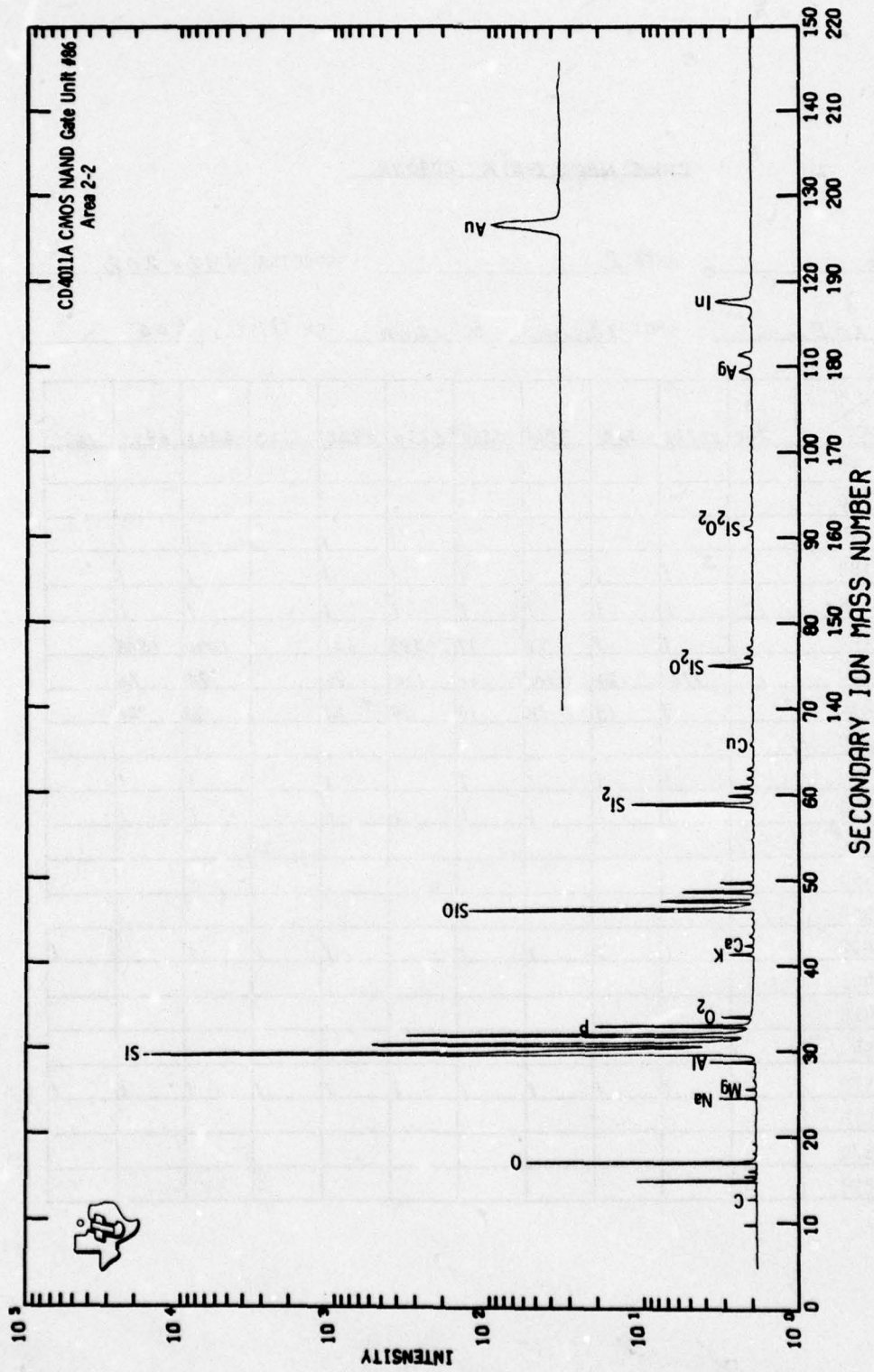


## CMOS NAND GATE CD4011A

UNIT #86 . AREA 1 . SPECTRA 188-191 .

RASTER 122 x 95 mm. SPOT 32 μm BC IBNA SR (Å/SEC) .55.

ELEM	START	PLUS			
		0	1052	1979	2666
Li (7)	30				
B (11)	60				
F (19)	150				
Na (23)	180	13	2	2	1
Mg (24)	185	2	1	1	1
Al (27)	205	30	9	10	10
Si (30)	220	15	23	21	19
P (31)	230	1	4	12	14
Cl (35)	250				
K (39)	290	6	2	1	1
Ca (40)	295	4	1	1	1
Ti (48)	330	1	-	-	-
Cr (52)	350	1	-	-	-
Ni (58)	380				
Cu (63)	400				
Zn (64)	403				
Ga (69)	425				
Mo (98)	540				
Ag (107)	570				
Sn (118)	610				
Ba (138)	670				
Pb (208)	858				



CMOS NAND GATE CD4011A

UNIT # 86. AREA 2. SPECTRA 192 - 202.

RASTER 69 X 58 um. SPOT 13 um BC 12 NA SR ( $\text{\AA}/\text{SEC}$ ) 1.06.

ELEM	PLUS START	360	1266	2181	2864	3550	4236	4922	5623	6307	6993	7681
Li (7)	30											
B (11)	60											
F (19)	150											
Na (23)	180		1	1	1	1	1	1	1	1	1	
Mg (24)	185		1	1	1	1	1	1	1	1	1	
Al (27)	205		1	1	16	17	383	651		1098	1548	
Si (30)	220		110	120	100	100	100	90		92	72	
P (31)	230		7	13	18	19	19	21		22	21	
C1 (35)	250											
K (39)	290		1	1	1	1	1	1		1	1	
Ca (40)	295		1	1	1	1	1	1		1	1	
Ti (48)	330											
Cr (52)	350											
Ni (58)	380											
Cu (63)	400			1	1	1	1	1	1	1	1	
Zn (64)	403											
Ga (69)	425											
Mo (98)	540	1										
Ag (107)	570	1	1	1	1	1	1	1	1	1	1	
Sn (118)	610											
Ba (138)	670											
Pb (208)	858											

CMOS NAND GATE CD4011A

UNIT #86 . AREA 2 . SPECTRA 203 - 207 .

RASTER 69 X 58 μm . SPOT 13 μm BC 12 NA SR (Å/SEC) 1.06 .

ELEM	PLUS START	8391	9076	9764	10450	11135						
Li (7)	30											
B (11)	60											
F (19)	150	/	-	/	/	/						
Na (23)	180	/	/	/	-/	/						
Mg (24)	185	/	/	/	/	/						
Al (27)	205	1684	1684	3034	4466	4876						
Si (30)	220	90	90	57	48	42						
P (31)	230	20	18	20	185	163						
Cl (35)	250											
K (39)	290	/	/	/	/	/						
Ca (40)	295	/	/	/	/	/						
Ti (48)	330											
Cr (52)	350											
Ni (58)	380											
Cu (63)	400	/	-	--	--	/						
Zn (64)	403											
Ga (69)	425											
Mo (98)	540											
Ag (107)	570	/	/	/	/	/						
Sn (118)	610											
Ba (138)	670											
Pb (208)	858											

CMOS NAND GATE CD4011A

UNIT #86 . AREA 4 . SPECTRA 399 - 408 .

RASTER 68 X 55 mm . SPOT 13 μm BC 9 NA SR (Å/SEC) .85 .

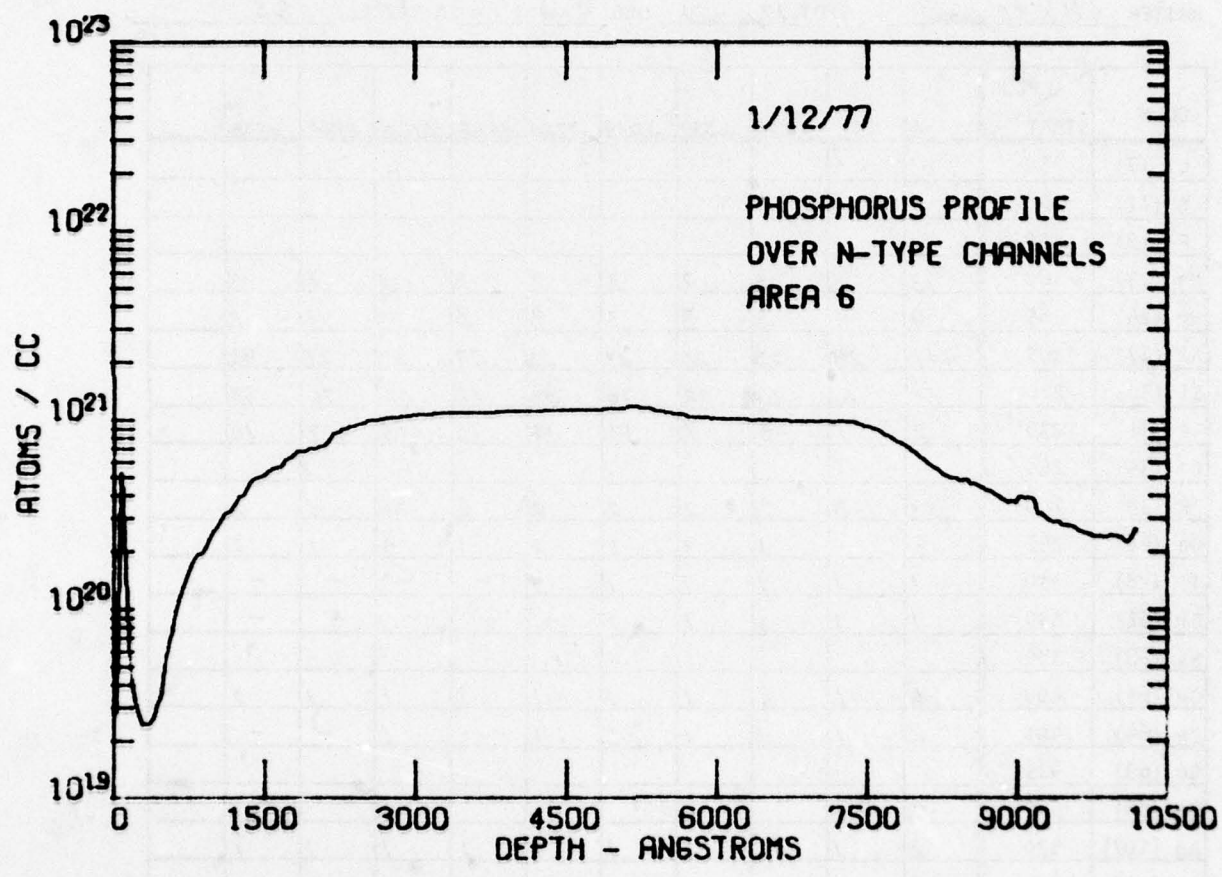
ELEM	PLUS START	0	914	1600	2291	2981	3667	4355	5045	5732	6419
Li (7)	30										
B (11)	60										
F (19)	150	1	1	1	1	1	1	1	1	1	1
Na (23)	180	95	10	8	7	5	4	4	3	3	3
Mg (24)	185	62	10	6	4	3	3	3	2	2	2
Al (27)	205	176	111	73	80	82	74	252	471	599	859
Si (30)	220	8.4	54	100	100	100	110	92	90	96	80
P (31)	230	1	1	3	7	11	14	16	19	18	19
Cl (35)	250										
K (39)	290	59	6	3	3	2	2	2	2	2	2
Ca (40)	295	36	3	2	2	1	1	1	1	1	1
Ti (48)	330	1	1	1	1	1	1	1	1	1	1
Cr (52)	350	30	9	-	-	-	-	-	-	-	-
Ni (58)	380										
Cu (63)	400	3	1	1	1	1	1	1	1	1	1
Zn (64)	403	-	1	1	1	1	1	1	1	1	1
Ga (69)	425										
Mo (98)	540										
Ag (107)	570	7	1	1	1	1	1	1	1	1	1
Sn (118)	610	1	-	-	-	-	-	-	-	-	-
Ba (138)	670										
Pb (208)	858										

CMOS NAND GATE CD4011A

UNIT #86 . AREA 5 . SPECTRA 409-418 .

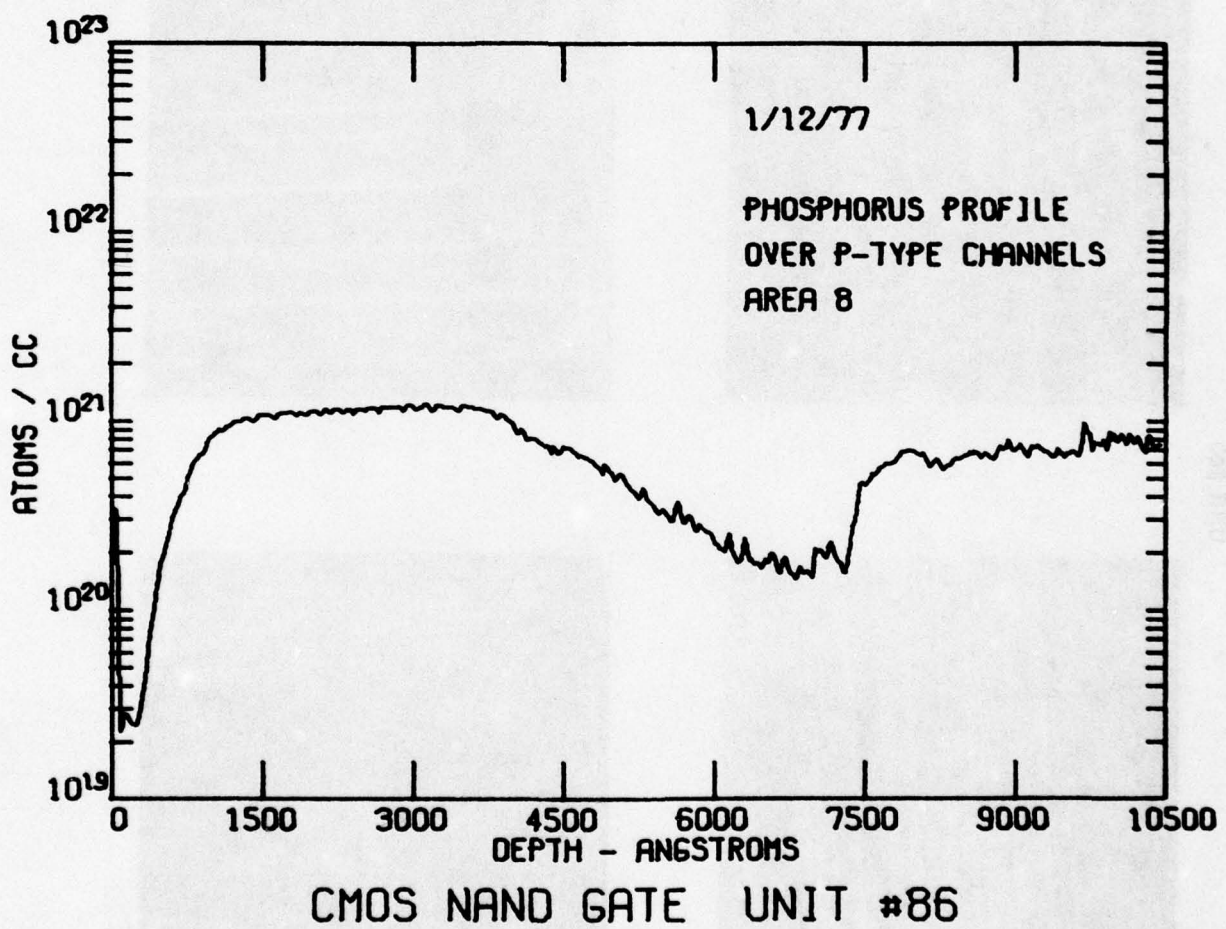
RASTER 68 X 55  $\mu\text{m}$  . SPOT 17  $\mu\text{m}$  BC 9 NA SR (Å/SEC) .85 .

ELEM	PLUS START										
		0	961	1651	2339	3029	3724	4426	5120	5864	6532
Li (7)	30										
B (11)	60										
F (19)	150										
Na (23)	180	75	3	3	2	3	2	2	24	5	3
Mg (24)	185	9	4	3	3	3	3	3	3	1	2
Al (27)	205	141	29	25	25	23	26	57	53	28	92
Si (30)	220	7.4	70	76	72	70	58	52	35	76	63
P (31)	230	2	1	3	7	13	14	16	13	7	16
C1 (35)	250										
K (39)	290	53	3	2	2	2	2	2	26	5	2
Ca (40)	295	8	1	1	1	1	1	1	4	1	1
Ti (48)	330	1	1	1	1	1	1	-	-	-	-
Cr (52)	350	1	1	1	1	1	-	-	-	-	-
Ni (58)	380										
Cu (63)	400	6	1	1	1	1	1	1	1	1	1
Zn (64)	403	2	1	1	1	1	1	1	1	-	-
Ga (69)	425										
Mo (98)	540	2									
Ag (107)	570	2	1	1	1	1	1	1	1	1	1
Sn (118)	610	2	1	1	1	1	1	1	1	-	-
Ba (138)	670										
Pb (208)	858										



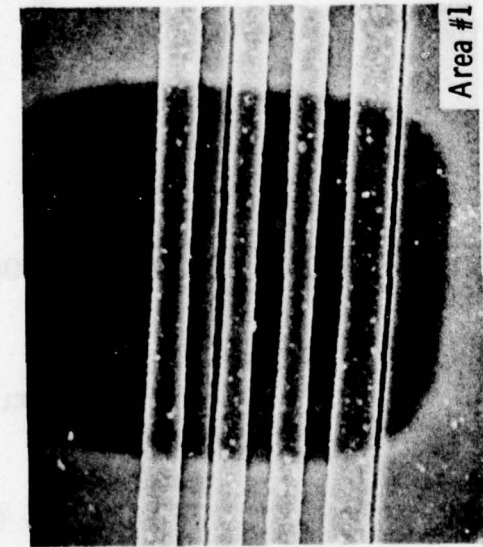
CMOS NAND GATE UNIT #86

JANNA-HCL

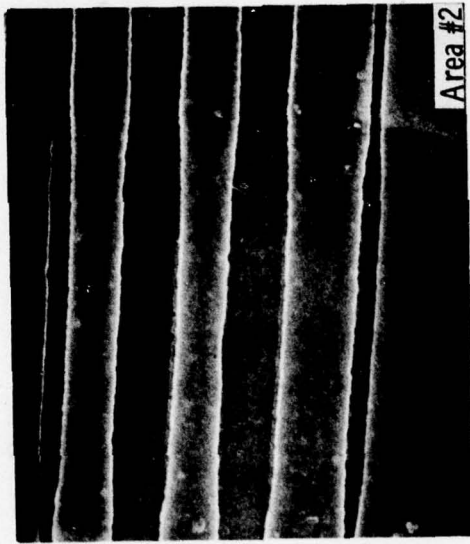


JANIA-MCL

CD4011A CMOS Nand Gate  
Unit #86



Area #1



Area #2

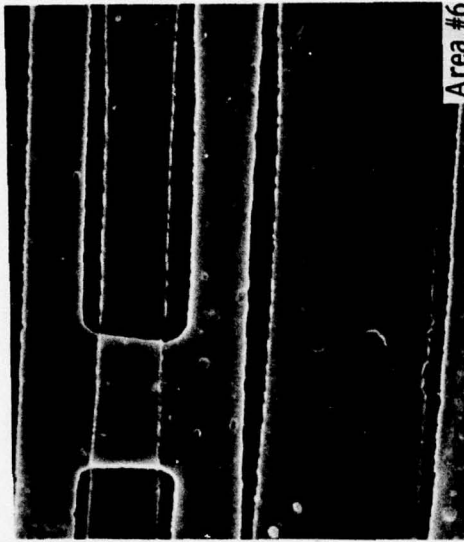


Area #3

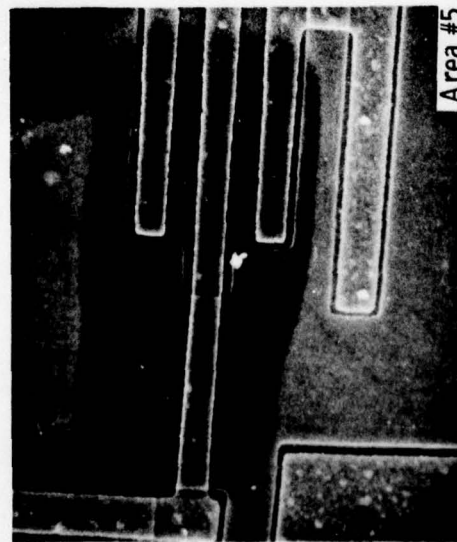


Area #4

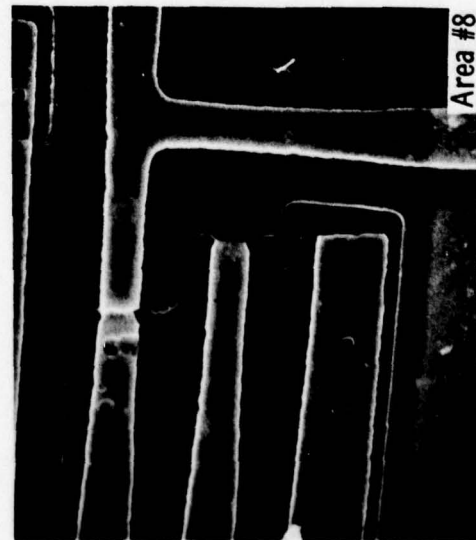
CD4011A CMOS Nand Gate  
Unit #86



Area #6



Area #5

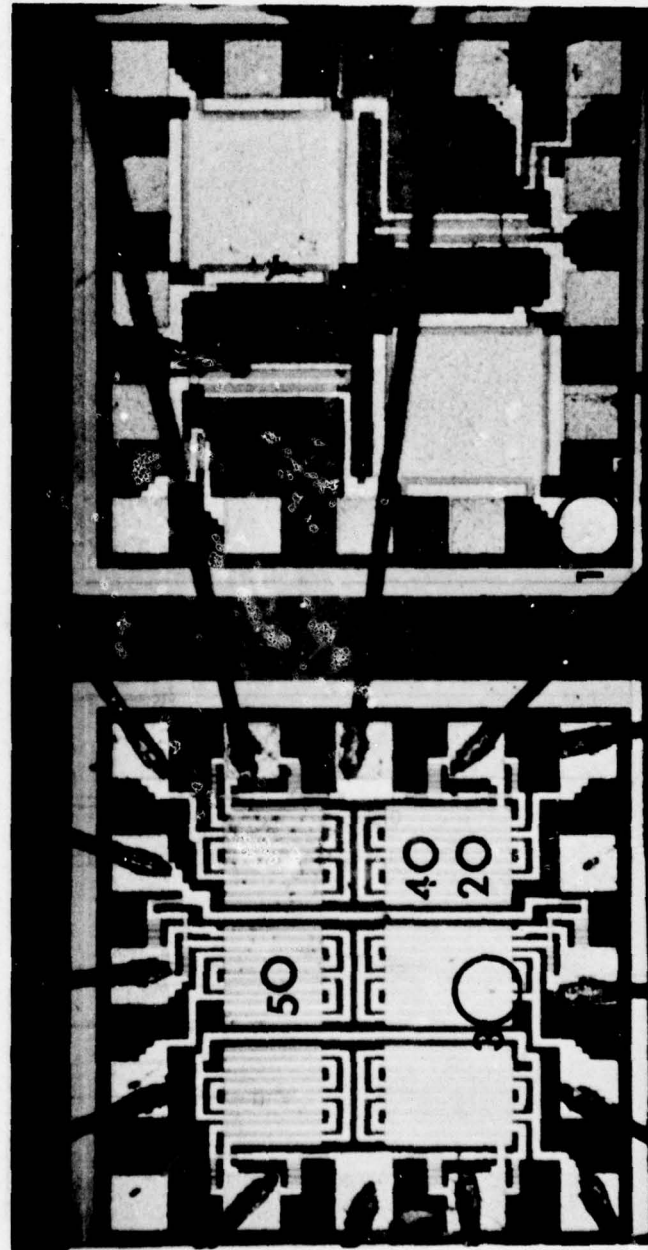


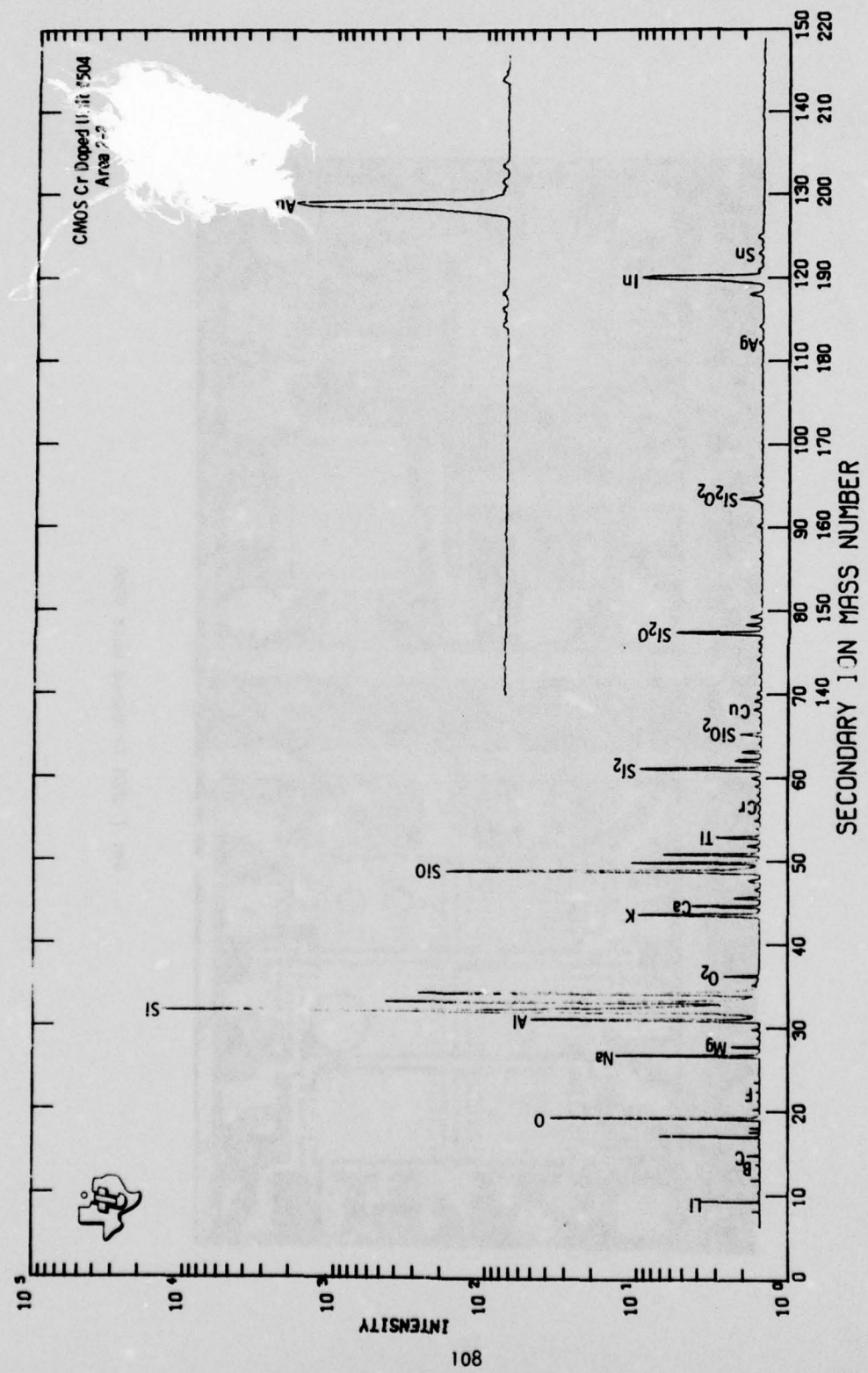
Area #8

**CMOS Cr Doped, Unit #504**

- Area 1: Surface Mass Spectrum**
- Area 2: Mass Spectra Depth Profile**
- Area 3: Cr Point Count Depth Profile**
- Area 4: False Start**
- Area 5: Mass Spectra Depth Profile**

Set 1 CMOS Cr Doped Unit #504





CMOS CR DOPED

UNIT #504 . AREA 2 . SPECTRA 161 - 171 .

RASTER 85 X 66 μm . SPOT 19 μm BC 10NA SR (Å/SEC) .63 .

ELEM	PLUS START	0	901	1793	2695	3567	4450	5363	6241	6920	7597	8274
Li (7)	30	260	1	1	1	1	1	1	1	1	1	1
B (11)	60	-	1	1	-	-	-	-	1	1	1	1
F (19)	150	1	1	1	1	1	1	1	1	1	1	1
Na (23)	180	640	6	4	3	3	4	5	4	3	4	4
Mg (24)	185	-	1	1	1	1	1	1	1	1	1	1
Al (27)	205	220	21	13	224	458	719	1079	1627	1705	2520	3210
Si (30)	220	2	110	150	130	140	140	140	130	130	120	110
P (31)	230											
Cl (35)	250											
K (39)	290	460	4	3	2	2	2	2	2	2	2	2
Ca (40)	295	80	1	1	1	1	1	2	2	2	1	1
Ti (48)	330	20	1	1	1	1	1	1	1	1	1	1
Cr (52)	350	10	1	1	-	1	1	1	5	6	5	4
Ni (58)	380											
Cu (63)	400	20	1	1	1	1	1	1	-	1	1	1
Zn (64)	403											
Ga (69)	425											
Mo (98)	540											
Ag (107)	570											
Sn (118)	610	20	1	1	1	1	1	-	-	-	-	-
Ba (138)	670											
Pb (208)	858											

## Cmos Cr Doped

UNIT 504. AREA 2. SPECTRA 172-173.

RASTER 85 X 66 μm . SPOT 19 μm BC 10 NA SR (Å/SEC) .63

ELEM	START	PLUS				
		8952	10303			
Li (7)	30	1	1			
B (11)	60	1	1			
F (19)	150	1	1			
Na (23)	180	4	4			
Mg (24)	185	1	1			
Al (27)	205	4210	4718			
Si (30)	220	110	90			
P (31)	230					
Cl (35)	250					
K (39)	290	2	2			
Ca (40)	295	1	1			
Ti (48)	330	1	1			
Cr (52)	350	4	4			
Ni (58)	380					
Cu (63)	400	1	-			
Zn (64)	403					
Ga (69)	425					
Mo (98)	540					
Ag (107)	570					
Sn (118)	610	-	-			
Ba (138)	670					
Pb (208)	858					

CMOS Cr DOPED

UNIT #504 . AREA 5 . SPECTRA 361 - 371 .

RASTER 69 X 56  $\mu m$  . SPOT 12  $\mu m$  BC 10 NA SR (Å/SEC) .92 .

ELEM	PLUS START	0	877	1479	2174	2872	3577	4290	5024	5783	6470	7242
Li (7)	30	-	2	1	1	1	1	1	1	1	1	1
B (11)	60	-	1	-	1	1	1	1	-	-	-	-
F (19)	150	-	1	-	1	1	1	1	1	1	1	1
Na (23)	180	1800	7	5	4	3	2	2	2	2	5	2
Mg (24)	185	20	3	4	5	4	2	1	1	1	1	1
Al (27)	205	1200	93	106	417	839	1344	3296	5537	6348	5973	7760
Si (30)	220	1.5	62	70	140	120	120	92	66	64	78	68
P (31)	230	-	1	1	1	1	1	1	1	1	1	1
Cl (35)	250											
K (39)	290	800	6	3	2	2	2	1	1	1	1	1
Ca (40)	295	800	7	3	2	2	1	1	1	1	1	1
Ti (48)	330	1	1	1	1	1	1	1	1	1	2	3
Cr (52)	350	100	1	1	1	2	4	5	6	6	5	5
Ni (58)	380											
Cu (63)	400	40	1	1	1	1	1	1	1	1	1	1
Zn (64)	403	1	1	1	1	1	1	1	1	1	1	1
Ga (69)	425											
Mo (98)	540											
Ag (107)	570											
Sn (118)	610	20	-	1	-	-	-	-	-	-	-	-
Ba (138)	670											
Pb (208)	858											

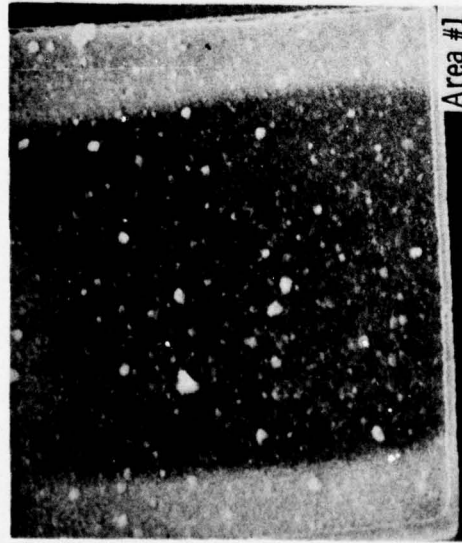
## CMOS CR DOPED

UNIT #504. AREA 5. SPECTRA 372.

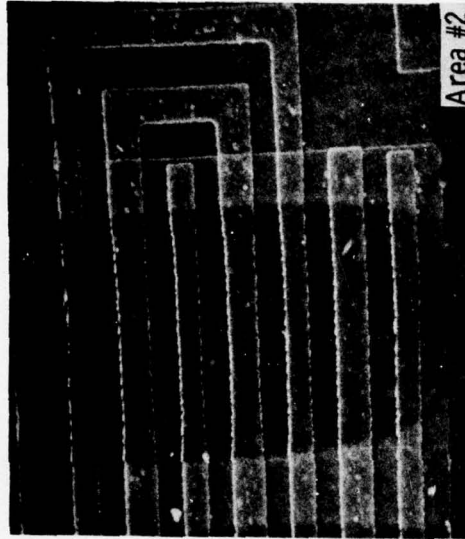
RASTER 69 x 56 um. SPOT 12 um BC 10mA SR ( $\text{\AA}/\text{SEC}$ ) .92.

ELEM	PLUS				
	START	7936			
Li (7)	30	1			
B (11)	60	-			
F (19)	150	1			
Na (23)	180	2			
Mg (24)	185	1			
Al (27)	205	8195			
Si (30)	220	62			
P (31)	230	1			
Cl (35)	250				
K (39)	290	1			
Ca (40)	295	1			
Ti (48)	330	1			
Cr (52)	350	6			
Ni (58)	380				
Cu (63)	400	1			
Zn (64)	403	1			
Ga (69)	425				
Mo (98)	540				
Ag (107)	570				
Sn (118)	610	-			
Ba (138)	670				
Pb (208)	858				

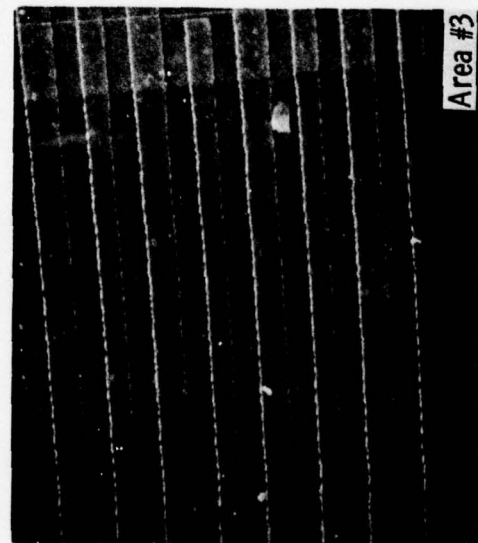
CMOS Cr Doped Unit #504



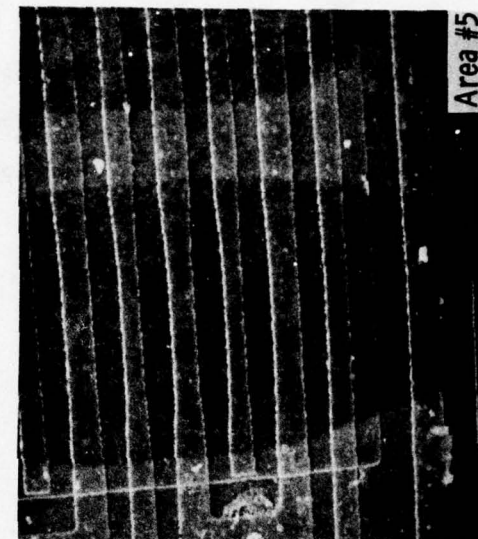
Area #1



Area #2



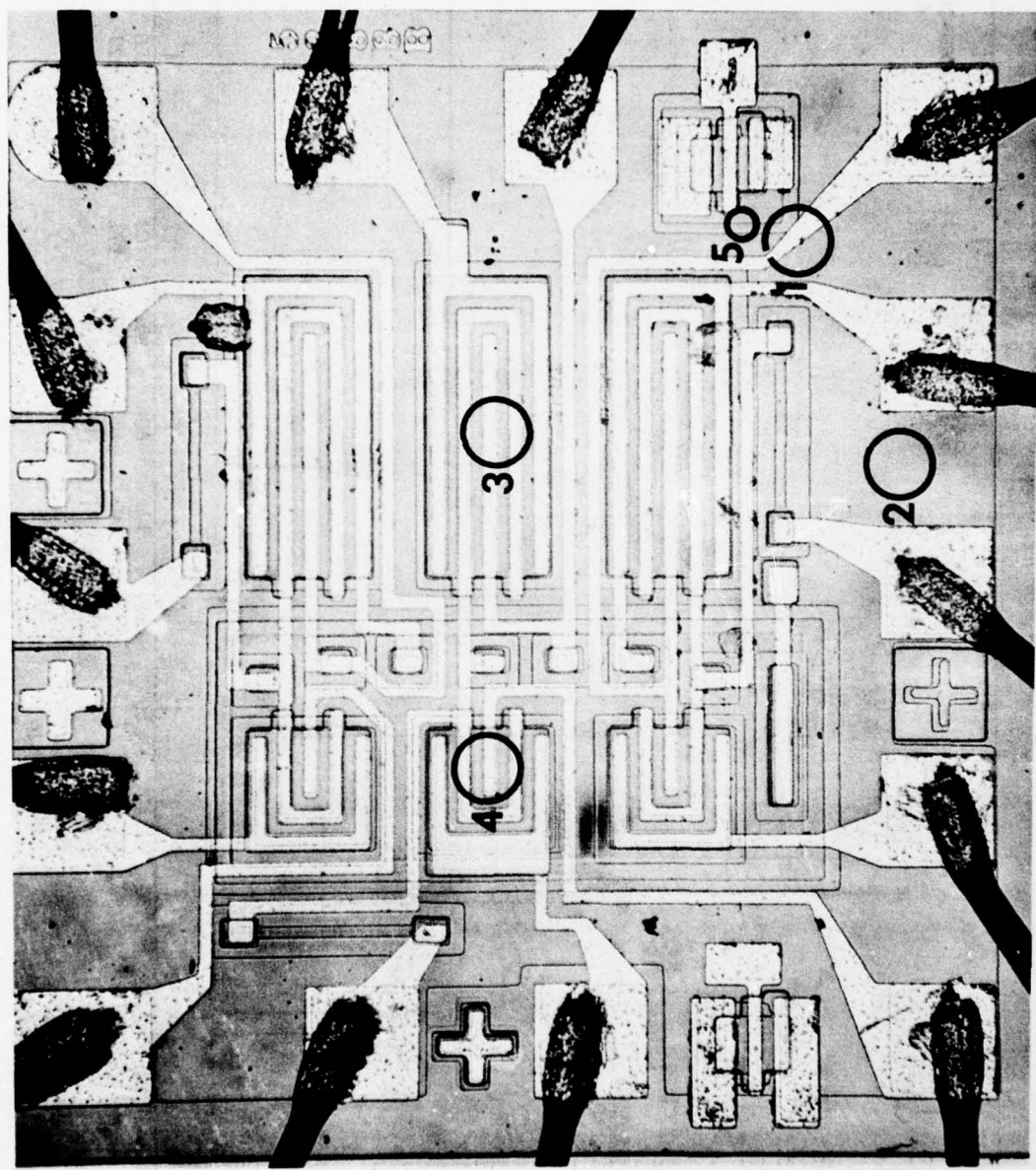
Area #3



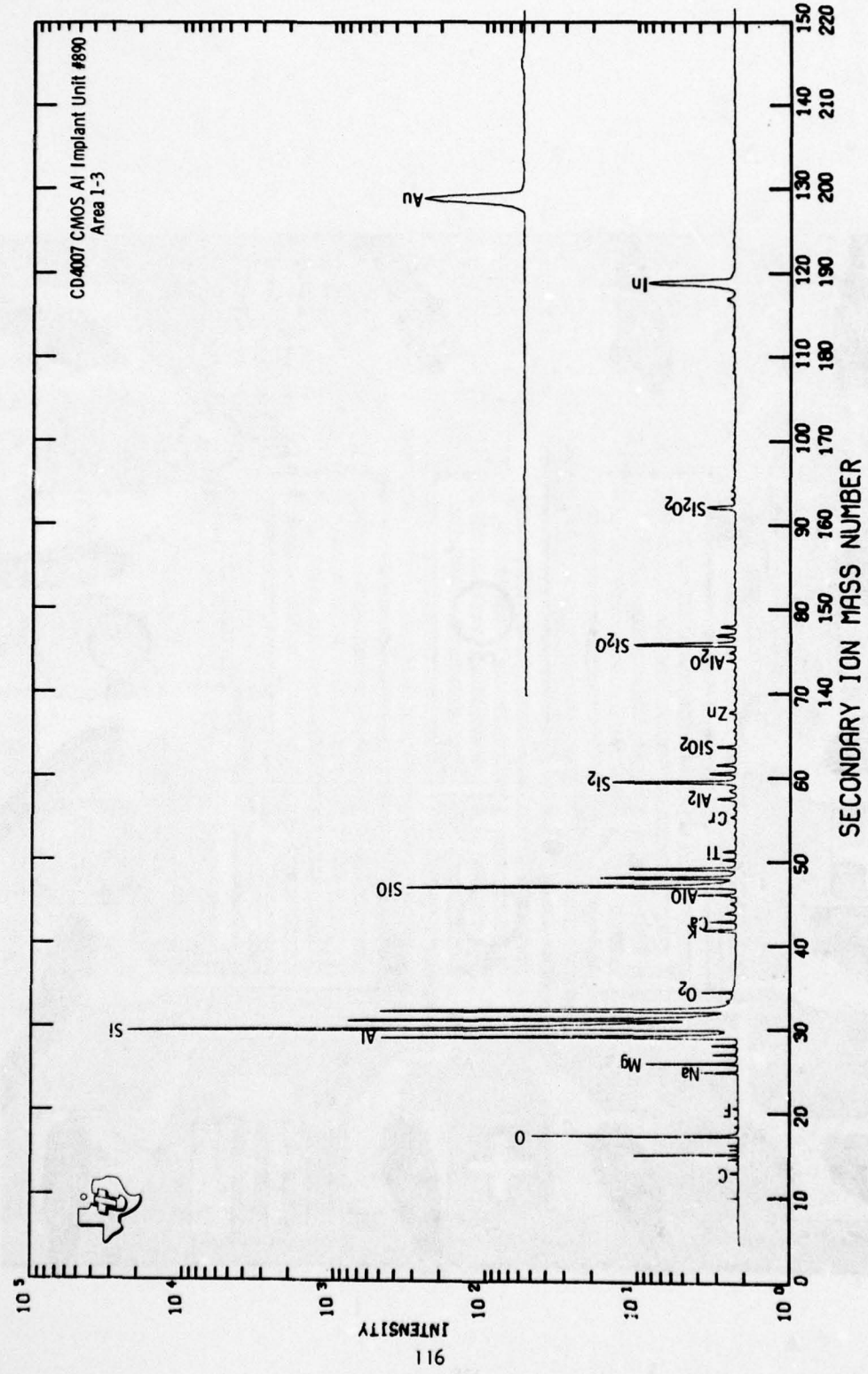
Area #5

**CMOS Al Implant, Unit #890**

- Area 1: Mass Spectra Depth Profile**
- Area 2: Al, Ti Peak Count Depth Profile**
- Area 3: Mass Spectra Depth Profile**
- Area 4: Mass Spectra Depth Profile**
- Area 5: Mass Spectra Depth Profile**



Set 1 CMOS Al Implant (Representative) CD 4007 Unit #890



CMOS AI IMPLANT CD4007

UNIT #890 . AREA 1 . SPECTRA 200 - 218 .

RASTER 96 X 144  $\mu m$  . SPOT 18  $\mu m$  BC 10NA SR ( $\text{\AA}/\text{SEC}$ ) . 257 .

ELEM	PLUS START	0	929	1834	2752	3453	4146	4837	5521	6185	6866	7526
Li (7)	30											
B (11)	60											
F (19)	150	2	1	1	1	1	-	-	-	1	1	-
Na (23)	180	12	1	1	1	1	1	1	1	1	1	1
Mg (24)	185	5	2	2	1	1	1	1	1	1	1	1
Al (27)	205	1998	178	108	93	167	260	340	402	503	509	666
Si (30)	220	46	130	130	140	120	120	130	130	120	150	130
P (31)	230											
C1 (35)	250											
K (39)	290	7	1	1	1	1	1	1	1	1	1	1
Ca (40)	295	3	1	1	1	1	1	1	1	1	1	1
Ti (48)	330	1	1	1	1	1	1	1	1	1	1	1
Cr (52)	350	1	1	1	1	1	1	1	1	1	1	1
Ni (58)	380											
Cu (63)	400	1	-	-	-	-	-	-	-	-	-	-
Zn (64)	403	1	1	1	1	1	1	1	1	1	1	1
Ga (69)	425											
Mo (98)	540											
Aq (107)	570											
Sn (118)	610	1	-	-	-	-	-	-	-	-	-	-
Ba (138)	670											
Pb (208)	858											

CMOS AI IMPLANT CD4007

UNIT #890. AREA 1. SPECTRA 219-221.

RASTER 96 x 44 μm. SPOT 18 μm BC 10NA SR ( $\text{Å}/\text{SEC}$ ) 257.

ELEM	START	PLUS						
		8215	8905	9599				
Li (7)	30							
B (11)	60							
F (19)	150	-	-	-				
Na (23)	180	/	/	/				
Mg (24)	185	/	/	/				
Al (27)	205	697	759	678				
Si (30)	220	130	130	110				
P (31)	230							
Cl (35)	250							
K (39)	290	/	/	/				
Ca (40)	295	/	/	/				
Ti (48)	330	/	/	/				
Cr (52)	350	/	/	/				
Ni (58)	380							
Cu (63)	400	-	-	-				
Zn (64)	403	/	/	/				
Ga (69)	425							
Mo (98)	540							
Ag (107)	570							
Sn (118)	610	-	-	-				
Ba (138)	670							
Pb (208)	858							

CMOS AI IMPLANT CD4007

UNIT #890 . AREA 3 . SPECTRA 419 - 426 .

RASTER 68X55 μm . SPOT 17 μm BC 9 NA SR (Å/SEC) . 85 .

ELEM	START	PLUS							
		0	690	1370	2050	2730	3410	4140	4820
Li (7)	30								
B (11)	60	-	1	1	1	-	-	-	-
F (19)	150	6	1	-	-	-	-	-	-
Na (23)	180	188	3	2	2	2	1	1	1
Mg (24)	185	6	1	1	1	1	1	1	1
Al (27)	205	94	11	5	5	2	3	14	158
Si (30)	220	2.6	80	82	80	80	78	72	70
P (31)	230	1	1	1	1	1	1	1	1
Cl (35)	250								
K (39)	290	69	1	1	1	1	1	1	1
Ca (40)	295	88	1	1	1	1	1	1	1
Ti (48)	330	-	1	1	1	1	1	1	-
Cr (52)	350								
Ni (58)	380								
Cu (63)	400								
Zn (64)	403								
Ga (69)	425								
Mo (98)	540								
Ag (107)	570	19	1	1	1	-	-	-	-
Sn (118)	610	13	1	1	1	1	1	1	1
Ba (138)	670								
Pb (208)	858								

BEST AVAILABLE COPY

CMOS AI IMPLANT CD4007

UNIT #890 . AREA 4 . SPECTRA 427-436 .

RASTER 61x50 μm . SPOT 11 μm BC BNA SR (A/SPEC) .93 .

ELEM	START	PLUS									
		0	914	1612	2309	3002	3703	4406	5087	5785	6476
Li (7)	30	1	-	-	-	-	-	-	-	-	-
B (11)	60	-	1	1	1	1	1	-	-	-	-
F (19)	150	-	1	1	1	1	1	1	-	-	-
Na (23)	180	52	1	1	1	1	1	1	1	1	1
Mg (24)	185	17	1	1	1	1	1	1	1	1	1
Al (27)	205	1119	154	119	72	76	107	316	537	719	E44
Si (30)	220	5.2	88	84	105	100	84	64	66	76	72
P (31)	230										
Cl (35)	250										
K (39)	290	21	1	1	1	1	1	1	1	1	1
Ca (40)	295	119	4	3	2	1	1	1	1	1	1
Ti (48)	330										
Cr (52)	350	2	-	-	-	-	-	-	-	-	-
Ni (58)	380										
Cu (63)	400	1	-	-	-	-	-	-	-	-	-
Zn (64)	403	1	-	-	-	-	-	-	-	-	-
Ga (69)	425										
Mo (98)	540										
Ag (107)	570	1	1	1	1	1	1	1	1	1	1
Sn (118)	610	5	1	1	1	1	1	1	1	1	1
Ba (138)	670										
Pb (208)	858										

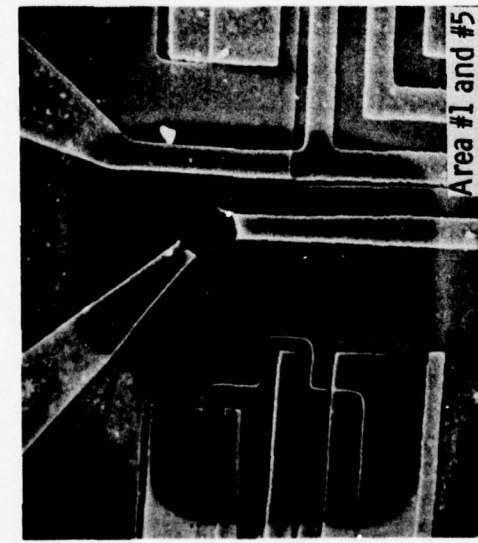
CMOS AL IMPLANT CD4007

UNIT #890. AREA 5. SPECTRA 437 - 445.

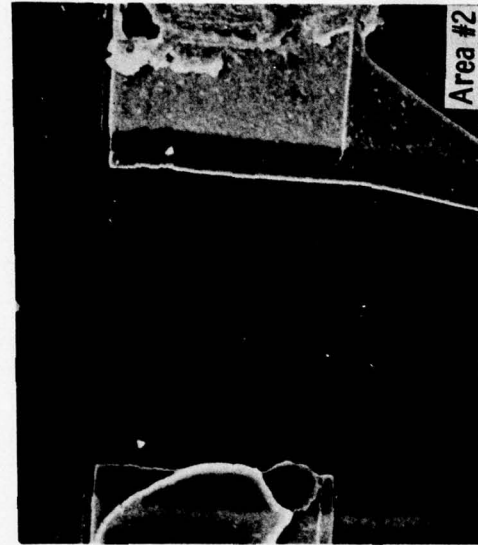
RASTER 61 X 50 μm. SPOT 11 μm BC 8 mA SR (A/SEC) .93.

ELEM	PLUS START	0	706	1403	2100	2801	3464	4296
Li (7)	30							
B (11)	60							
F (19)	150	1	1	1	1	1	1	1
Na (23)	180	7	1	1	1	1	1	1
Mg (24)	185	1	1	1	1	-	-	-
Al (27)	205	1217	1567	1525	1864	1719	1812	2497
Si (30)	220	19	52	56	46	44	44	35
P (31)	230							
Cl (35)	250							
K (39)	290	5	1	1	1	1	1	1
Ca (40)	295	2	1	1	1	1	1	1
Ti (48)	330							
Cr (52)	350							
Ni (58)	380							
Cu (63)	400	1	1	1	1	1	-	-
Zn (64)	403							
Ga (69)	425							
Mo (98)	540							
Ag (107)	570							
Sn (118)	610	1	1	1	1	1	-	-
Ba (138)	670							
Pb (208)	858							

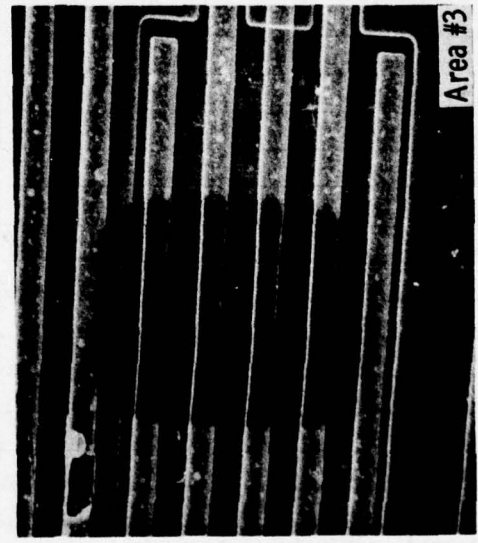
CD4007 CMOS AI Implant  
Unit #890



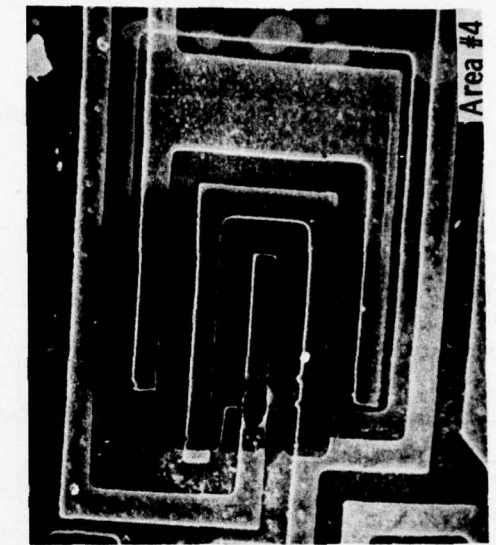
Area #1 and #5



Area #2



Area #3

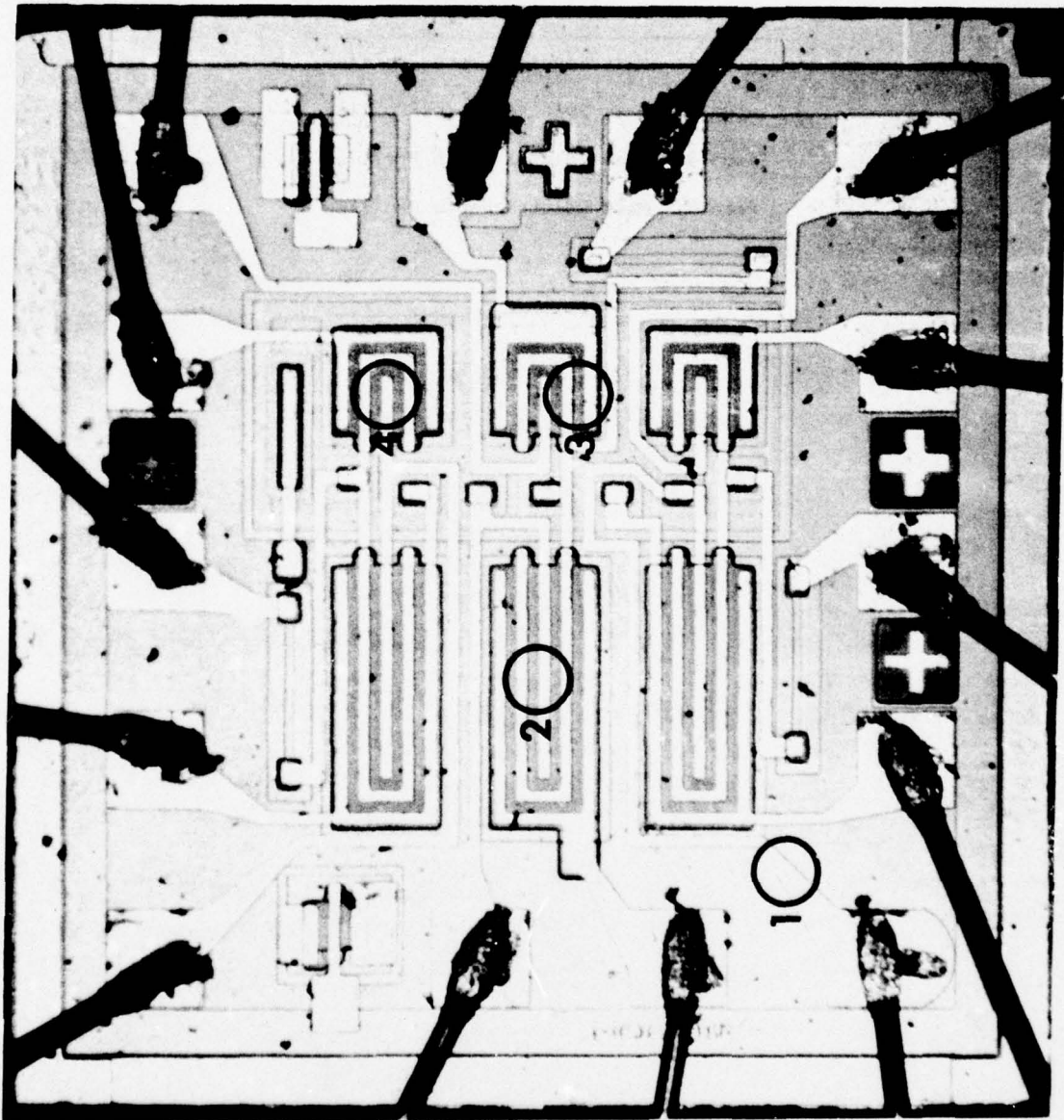


Area #4

CMOS  $\text{Al}_2\text{O}_3$ , Unit #A259

- Area 1: Mass Spectra Depth Profile**
- Area 2: Mass Spectra Depth Profile**
- Area 3: Mass Spectra Depth Profile**
- Area 4: Mass Spectra Depth Profile**

Set 1 CMOS Al<sub>2</sub>O<sub>3</sub> Unit #A259

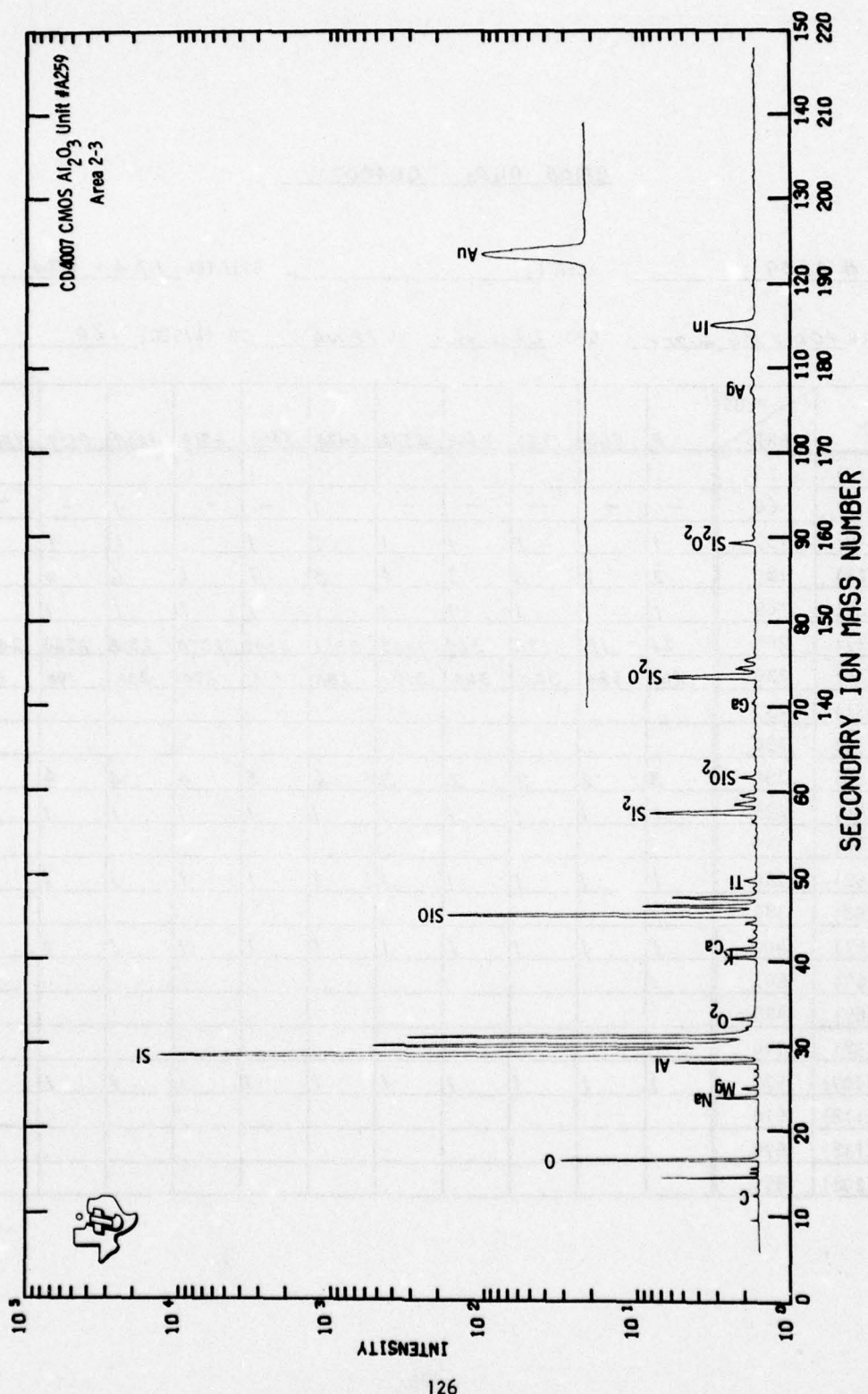


CMOS Al<sub>2</sub>O<sub>3</sub> CD4007

UNIT # A259 . AREA 1 . SPECTRA 174 - 184 .

RASTER 106 x 86 μm . SPOT 22 μm BC 1BNA SR ( $\text{\AA}/\text{SEC}$ ) .70 .

ELEM	PLUS START	0	863	1766	2669	3572	4475	5400	6319	7229	8139	9066
Li (7)	30											
B (11)	60	-	-	-	-	-	1	-	-	1	-	-
F (19)	150	1	1	1	1	1	1	1	-	1	1	1
Na (23)	180	2	2	3	3	4	8	7	6	6	6	7
Mg (24)	185	1	1	1	1	1	1	1	1	1	1	1
Al (27)	205	27	18	175	529	1003	3351	3092	2270	2358	2329	2011
Si (30)	220	260	380	320	360	310	180	195	230	230	190	170
P (31)	230											
C1 (35)	250											
K (39)	290	3	2	3	2	3	6	5	4	4	4	4
Ca (40)	295	1	1	1	1	1	1	1	1	1	1	1
Ti (48)	330											
Cr (52)	350	1	1	1	1	1	1	1	1	1	1	1
Ni (58)	380											
Cu (63)	400	1	1	1	1	1	1	1	1	1	1	1
Zn (64)	403											
Ga (69)	425											
Mo (98)	540											
Ag (107)	570	1	1	1	1	1	1	1	1	1	1	1
Sn (118)	610											
Ba (138)	670											
Pb (208)	858											



CMOS Al<sub>2</sub>O<sub>3</sub> CD4007

UNIT #259 . AREA / . SPECTRA 185-187 .

RASTER 106 x 86 μm . SPOT 22 μm BC 10NA SR (Å/SEC) .70 .

ELEM	PLUS START	9761	10488	11200								
Li (7)	30											
B (11)	60	-	-	-								
F (19)	150	-	-	-								
Na (23)	180	6	5	5								
Mg (24)	185	1	1	1								
Al (27)	205	2290	1643	1673								
Si (30)	220	180	220	240								
P (31)	230		1	1								
Cl (35)	250											
K (39)	290	4	3	3								
Ca (40)	295	1	1	1								
Ti (48)	330											
Cr (52)	350	1	1	1								
Ni (58)	380											
Cu (63)	400	1	1	1								
Zn (64)	403											
Ga (69)	425											
Mo (98)	540											
Ag (107)	570	1	1	1								
Sn (118)	610											
Ba (138)	670											
Pb (208)	858											

CMOS Al<sub>2</sub>O<sub>3</sub> CD4007

UNIT # A259 . AREA 2 . SPECTRA 373 - 381 .

RASTER 68X55 μm . SPOT 17 μm BC 9 NA SR (Å/SEC) 85 .

ELEM	START	PLUS	0	877	1571	2436	3120	3816	4518	5208	5888
			-	-	-	-	-	-	-	-	-
Li (7)	30	6	-	-	-	-	-	-	-	-	-
B (11)	60										
F (19)	150										
Na (23)	180	333	1	1	1	1	1	1	1	1	1
Mg (24)	185	31	1	1	1	1	1	1	1	1	1
Al (27)	205	130	4	2	31	231	312	493	631	838	
Si (30)	220	4.6	100	120	120	100	100	86	96	82	
P (31)	230										
C (35)	250										
K (39)	290	69	1	1	1	1	1	1	1	1	1
Ca (40)	295	53	1	1	1	1	1	1	1	1	1
Ti (48)	330	8	1	1	1	-	-	-	-	-	-
Cr (52)	350	6	1	1	-	-	-	-	-	-	-
Ni (58)	380										
Cu (63)	400	3	1	1	1	1	1	1	1	1	1
Zn (64)	403	3	-	-	-	-	-	-	-	-	-
Ga (69)	425										
Mo (98)	540										
Ag (107)	570	3	1	1	1	1	1	1	1	1	1
Sn (118)	610	3	1	-	-	-	-	-	-	-	-
Ba (138)	670										
Pb (208)	858										

CMOS Al<sub>2</sub>O<sub>3</sub> CD4007

UNIT #A259 . AREA 3 . SPECTRA 302 - 390 .

RASTER 68x55 μm . SPOT 17 μm BC 9 NA SR (Å/SEC) .85 .

ELEM	START	PLUS	0	692	1411	2106	2803	3490	4177	4860	5571
Li (7)	30	1	-	-	-	-	-	-	-	-	-
B (11)	60										
F (19)	150										
Na (23)	180	115	1	1	1	1	1	1	1	1	1
Mg (24)	185	10	1	1	1	1	1	1	1	1	1
Al (27)	205	185	21	18	22	23	421	586	768	1010	
Si (30)	220	5	110	120	130	120	110	110	105	90	
P (31)	230										
C1 (35)	250										
K (39)	290	58	1	1	1	1	1	1	1	1	1
Ca (40)	295	33	1	1	1	1	1	1	1	1	1
Ti (48)	330	5	1	1	1	1	-	-	-	-	-
Cr (52)	350	3	1	1	1	1	1	1	1	1	1
Ni (58)	380										
Cu (63)	400	3	1	1	1	1	1	1	1	1	1
Zn (64)	403	3	-	-	-	-	-	-	-	-	-
Ga (69)	425										
Mo (98)	540										
Ag (107)	570	5	1	1	1	1	1	1	1	1	1
Sn (118)	610	3	1	1	1	-	-	-	-	-	-
Ba (138)	670										
Pb (208)	858										

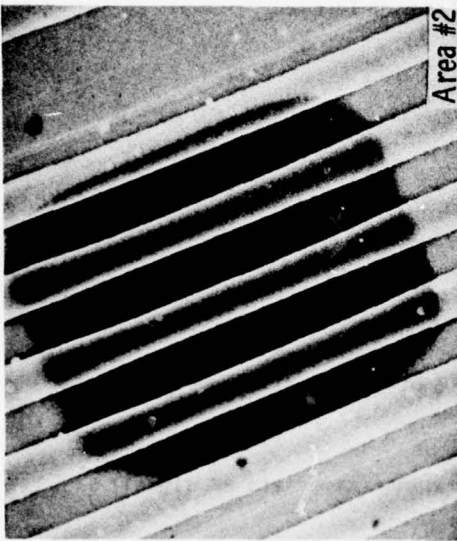
CMOS Al<sub>2</sub>O<sub>3</sub> CD4007

UNIT #A259. AREA 4. SPECTRA 391 - 398.

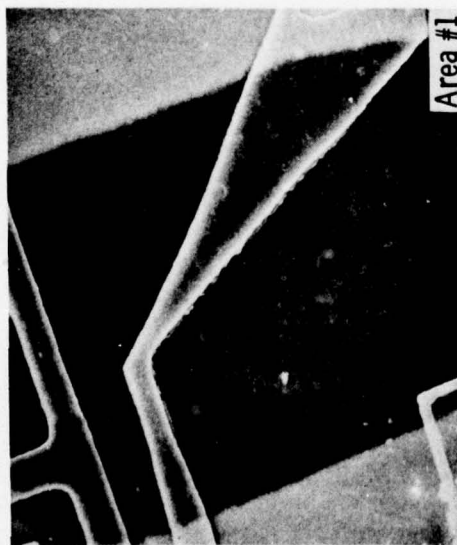
RASTER 68X55 μm. SPOT 17 μm BC 9NA SR (Å/SEC) .85.

ELEM	PLUS START	0	704	1400	2095	2787	3476	4169	4855		
Li (7)	30	1	-	-	-	-	-	-	-		
B (11)	60										
F (19)	150										
Na (23)	180	84	2	1	1	1	1	1	1		
Mg (24)	185	5	1	1	1	1	1	1	1		
Al (27)	205	113	10	6	4	146	373	538	698		
Si (30)	220	7.4	110	110	110	110	92	90	84		
P (31)	230										
Cl (35)	250										
K (39)	290	59	2	2	1	-	-	-	-		
Ca (40)	295	16	1	1	1	1	1	1	1		
Ti (48)	330	8	1	1	1	-	-	-	-		
Cr (52)	350	3	1	-	-	-	-	-	-		
Ni (58)	380										
Cu (63)	400	2	1	1	-	1	1	1	1		
Zn (64)	403	3	-	-	-	-	-	-	-		
Ga (69)	425										
Mo (98)	540										
Ag (107)	570	2	1	1	1	1	1	1	1		
Sn (118)	610	2	1	-	-	-	-	-	-		
Ba (138)	670										
Pb (208)	858										

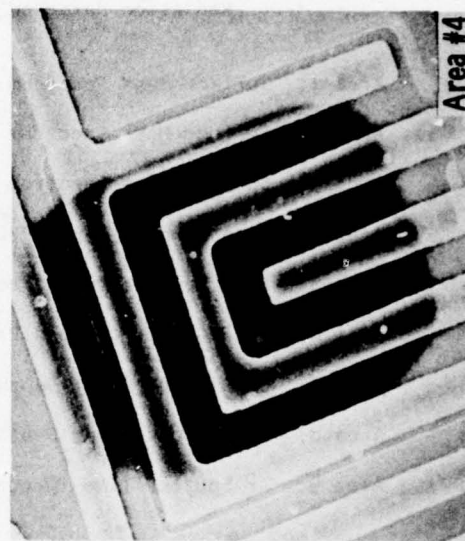
CD4007 CMOS Al<sub>2</sub>O<sub>3</sub> Unit #A259



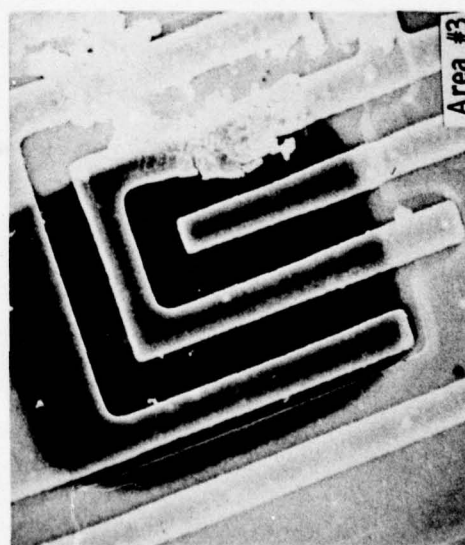
Area #2



Area #1



Area #4



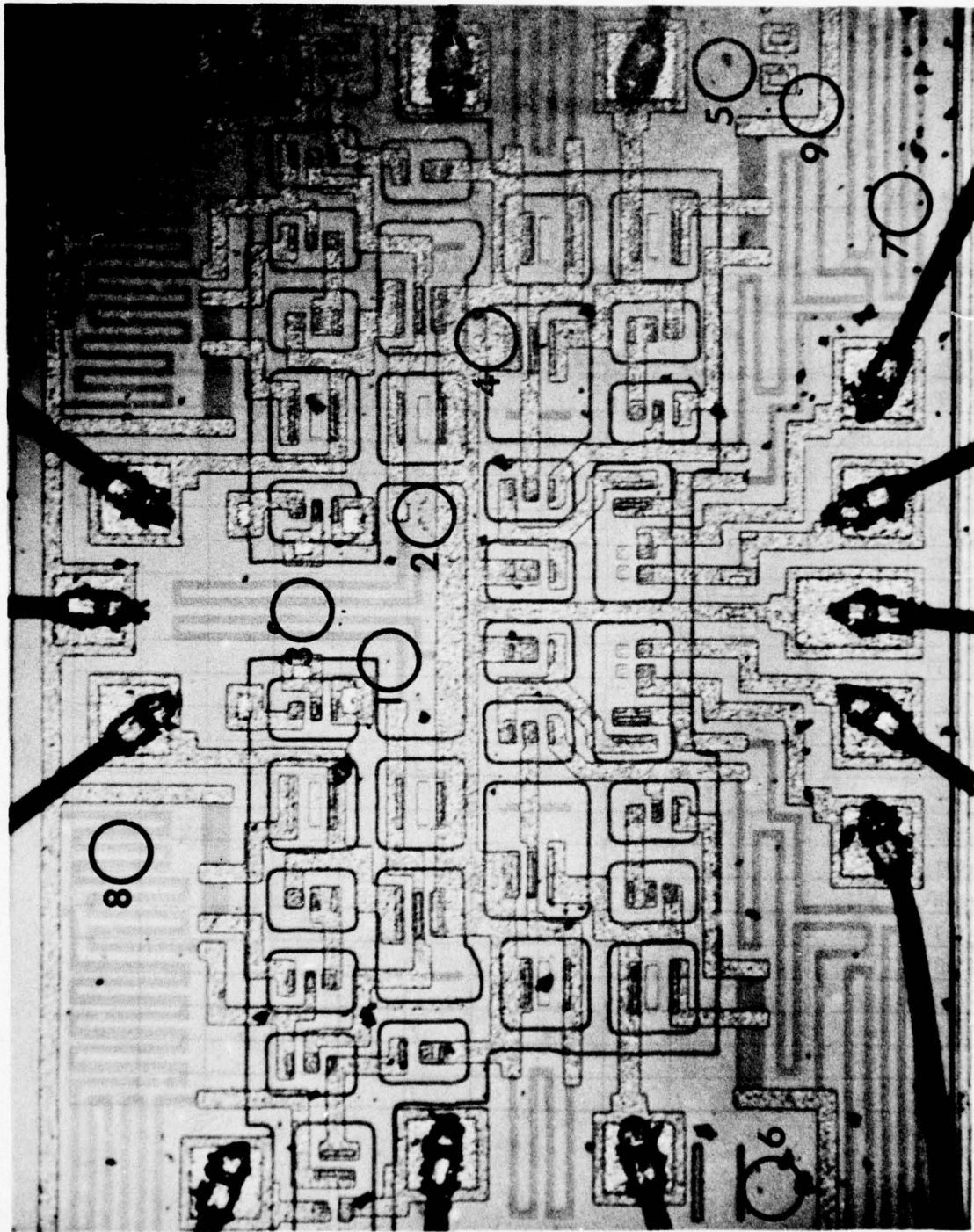
Area #3

APPENDIX B

Radiation Hardened Double Glass, Unit #120

- Area 1: Surface Mass Spectrum
- Area 2: Surface Mass Spectrum
- Area 3: Surface Mass Spectrum
- Area 4: Mass Spectra Depth Profile
- Area 5: Mass Spectra Depth Profile
- Area 6: Sn Peak Count Depth Profile
- Area 7: Cr-Ni Peak Count Depth Profile (not included)
- Area 8: Cr-Ni Peak Count Depth Profile
- Area 9: Ar Sputter Time Through Glassivation (immediate A& signal)

Set 1 54L00 Radiation Hardened Double Glass Unit #120

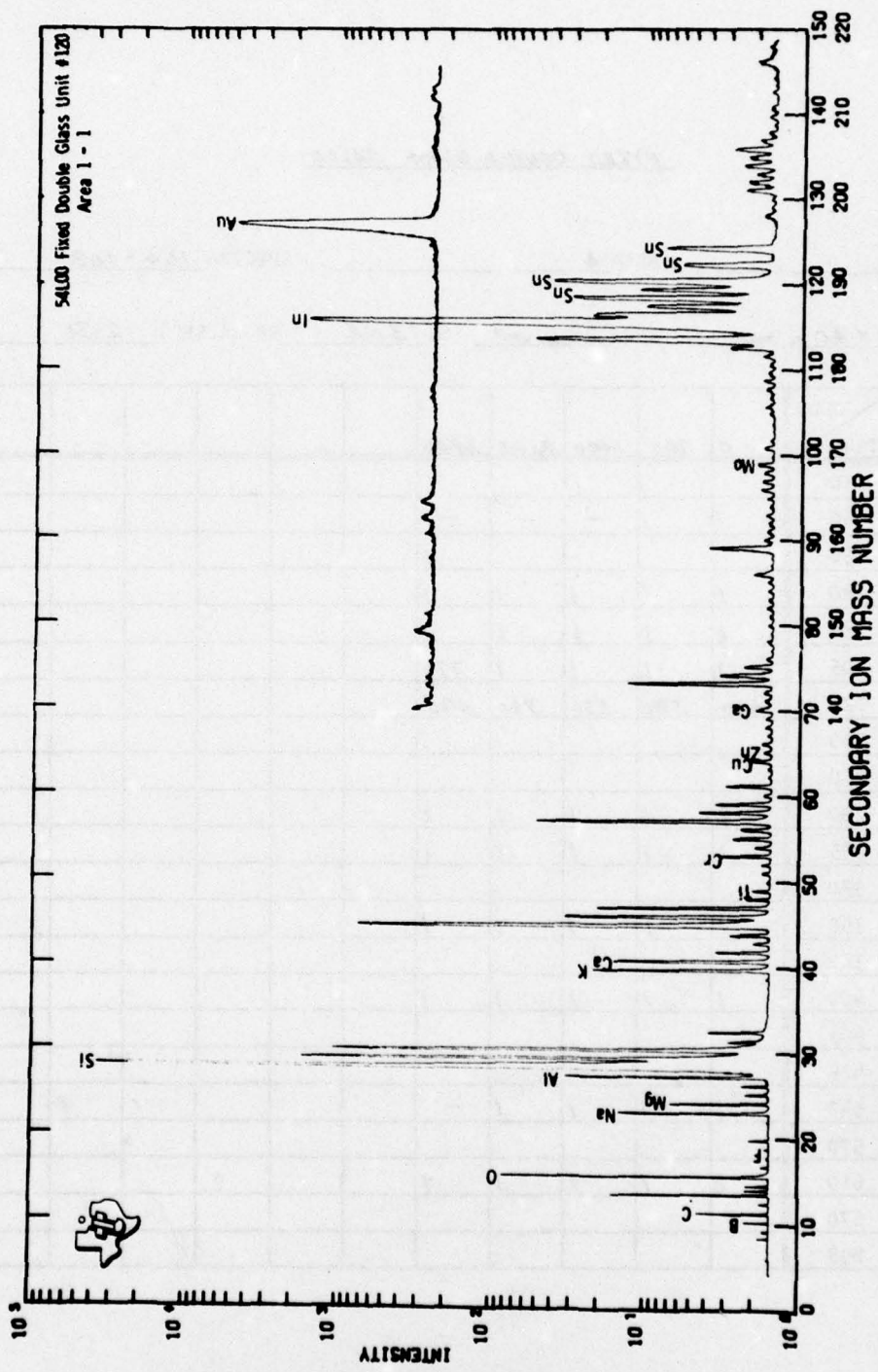


FIXED DOUBLE GLASS 5400

UNIT #120 . AREA 1-2-3 . SPECTRA \_\_\_\_\_.

RASTER 50 X 40 mm . SPOT 24 μm BC 13 NA SR (Å/SEC) 2.31 .

ELEM	PLUS START	AREA 1	AREA 2	AREA 3			
Li (7)	30						
B (11)	60	1	1	1			
F (19)	150	1	1	1			
Na (23)	180	2	3	6			
Mg (24)	185	1	1	3			
Al (27)	205	4	3	6			
Si (30)	220	350	550	270			
P (31)	230	1	1	1			
Cl (35)	250						
K (39)	290	3	2	9			
Ca (40)	295	2	3	6			
Ti (48)	330	1	1	1			
Cr (52)	350	1	1	1			
Ni (58)	380						
Cu (63)	400	1	1	1			
Zn (64)	403	1	1	1			
Ga (69)	425	1	1	1			
Mo (98)	540	1	1	1			
Aq (107)	570						
Sn (118)	610	5	4	7			
Ba (138)	670						
Pb (208)	858	1	1	1			



FIXED DOUBLE GLASS 54L00

UNIT #120 . AREA 4 . SPECTRA 104 - 108 .

RASTER 50 x 40 μm . SPOT 22 μm BC 13NA SR ( $\text{\AA}/\text{SEC}$ ) 2.31 .

ELEM	PLUS START	0	700	1400	2100	2800						
Li (7)	30											
B (11)	60	1	1	-	-	-						
F (19)	150						1					
Na (23)	180	1	1	1	1	1						
Mg (24)	185	1	1	1	1	1						
Al (27)	205	2	1	1	1	777						
Si (30)	220	610	580	550	520	490						
P (31)	230											
Cl (35)	250											
K (39)	290	2	1	1	1	1						
Ca (40)	295	1	1	1	1	1						
Ti (48)	330											
Cr (52)	350	1	1	1	1	1						
Ni (58)	380											
Cu (63)	400	1	1	1	1	1						
Zn (64)	403											
Ga (69)	425											
Mo (98)	540	1	1	1	1	-						
Ag (107)	570											
Sn (118)	610	2	1	1	1	1						
Ba (138)	670											
Pb (208)	858											

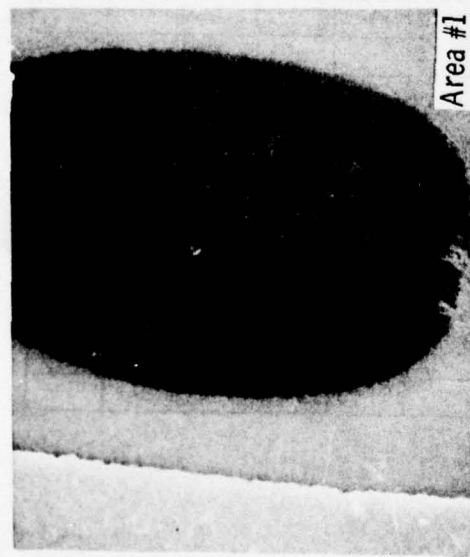
FIXED DOUBLE GLASS 54L00

UNIT #120. AREA 5. SPECTRA 109-114.

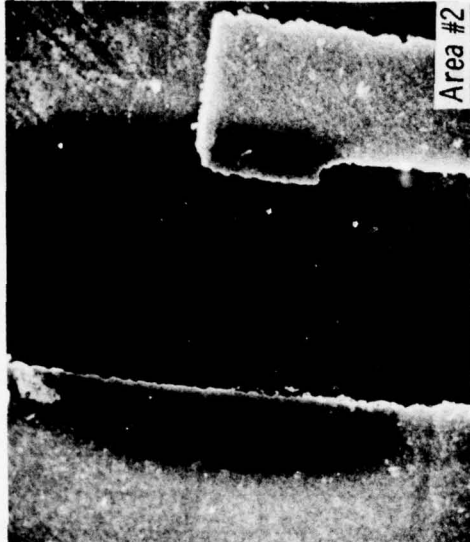
RASTER 50x40 μm. SPOT 22 μm BC 13 NA SR (1/SEC) 2.31.

ELEM	PLUS START						
		0	700	1400	2100	2800	3500
Li (7)	30						
B (11)	60	1	-	-	-	-	1
F (19)	150					1	
Na (23)	180	1	1	1	1	1	1
Mg (24)	185	1	1	1	1	1	1
Al (27)	205	1	1	1	1	8	6
Si (30)	220	550	580	600	600	580	600
P (31)	230	-	-	-	-	6	12
Cl (35)	250						
K (39)	290	1	1	1	1	1	1
Ca (40)	295	1	1	1	1	1	1
Ti (48)	330						
Cr (52)	350	1	1	1	1	6	4
Ni (58)	380	-	-	-	-	1	1
Cu (63)	400	1	1	1	1	1	1
Zn (64)	403						
Ga (69)	425						
Mo (98)	540	1	1	1	1	1	-
Ag (107)	570						
Sn (118)	610	1	1	1	1	1	1
Ba (138)	670						
Pb (208)	858						

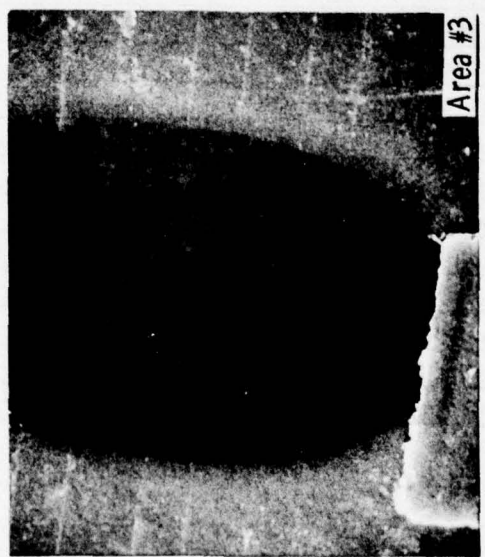
54L00 Fixed Double Glass  
Unit #120



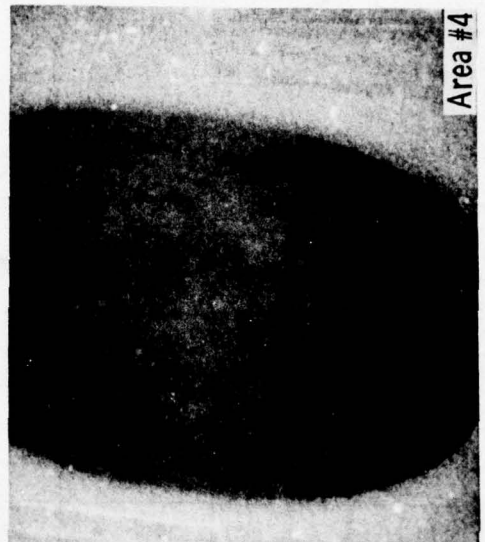
Area #1



Area #2



Area #3



Area #4

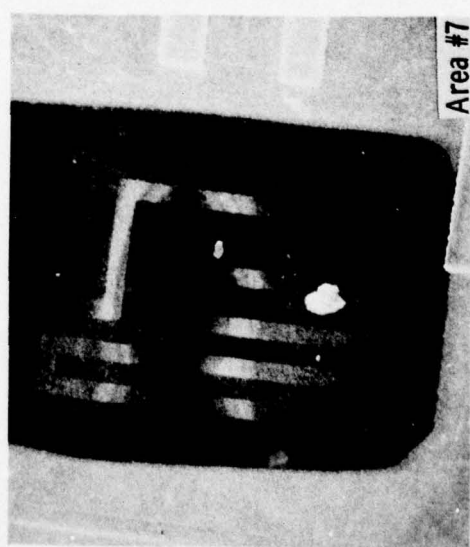
54L00 Fixed Double Glass  
Unit #120



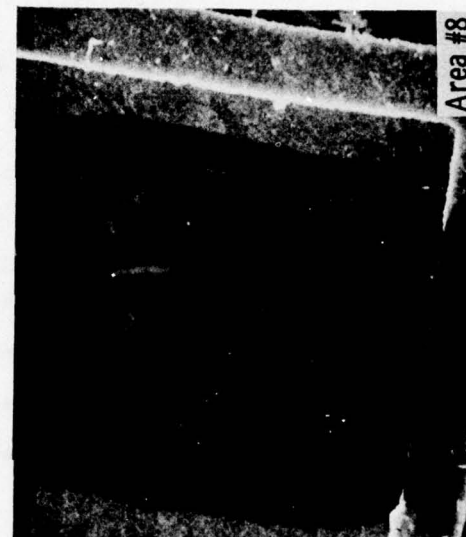
Area #5



Area #6



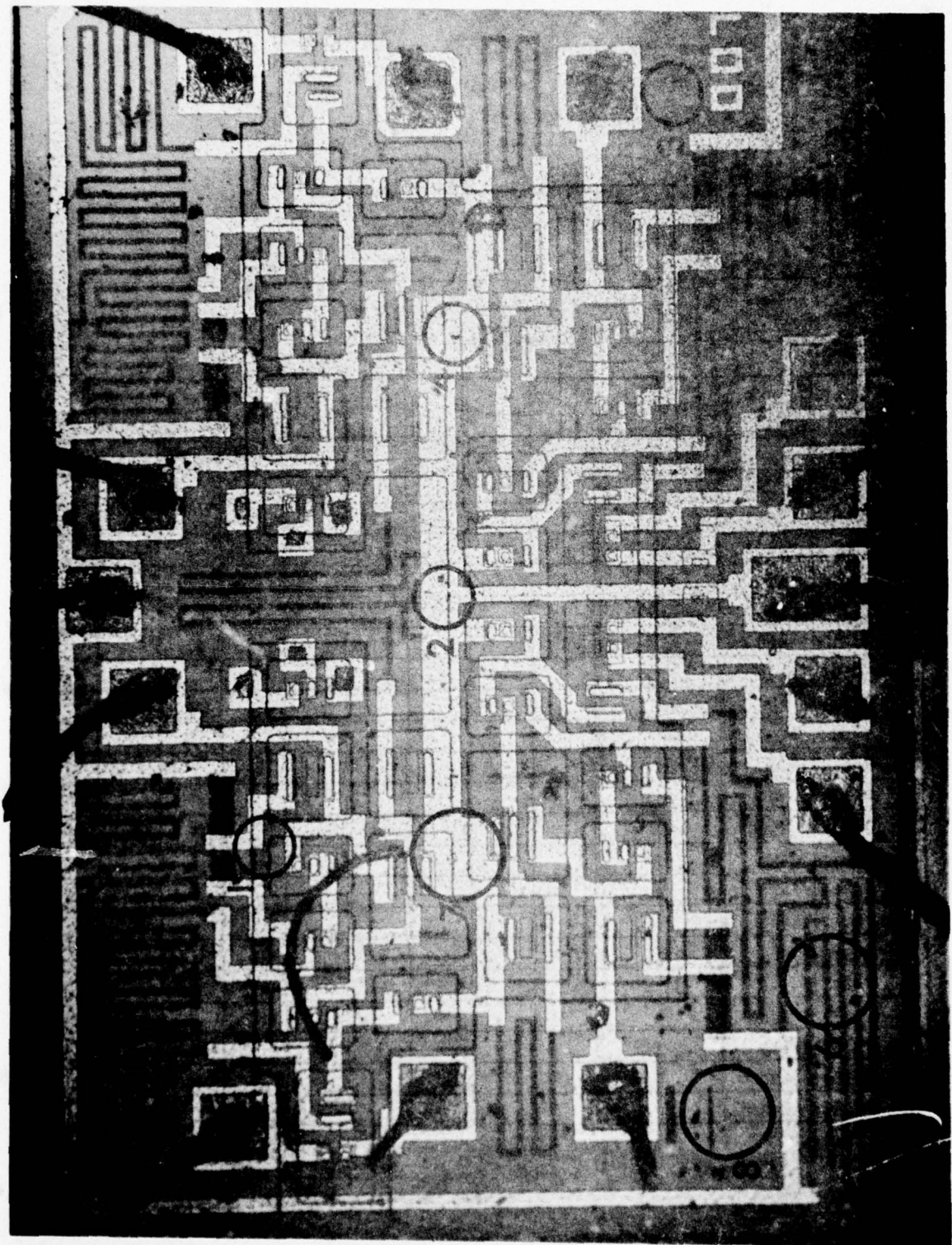
Area #7



Area #8

**54L00 Radiation Hardened, Old Style, Unit #103**

- Area 1: Surface Mass Spectrum**
- Area 2: Mass Spectra Depth Profile**
- Area 3: Mass Spectra Depth Profile**
- Area 4: Ar Sputter Time through Glassivation**
- Area 5: Cr-Ni Peak Count Depth Profile after  
Glassivation Removal**
- Area 6: Opened with Ar, But Not Used**
- Area 7: Opened with Ar, But not Used**
- Area 8: Opened with Ar, But not Used**



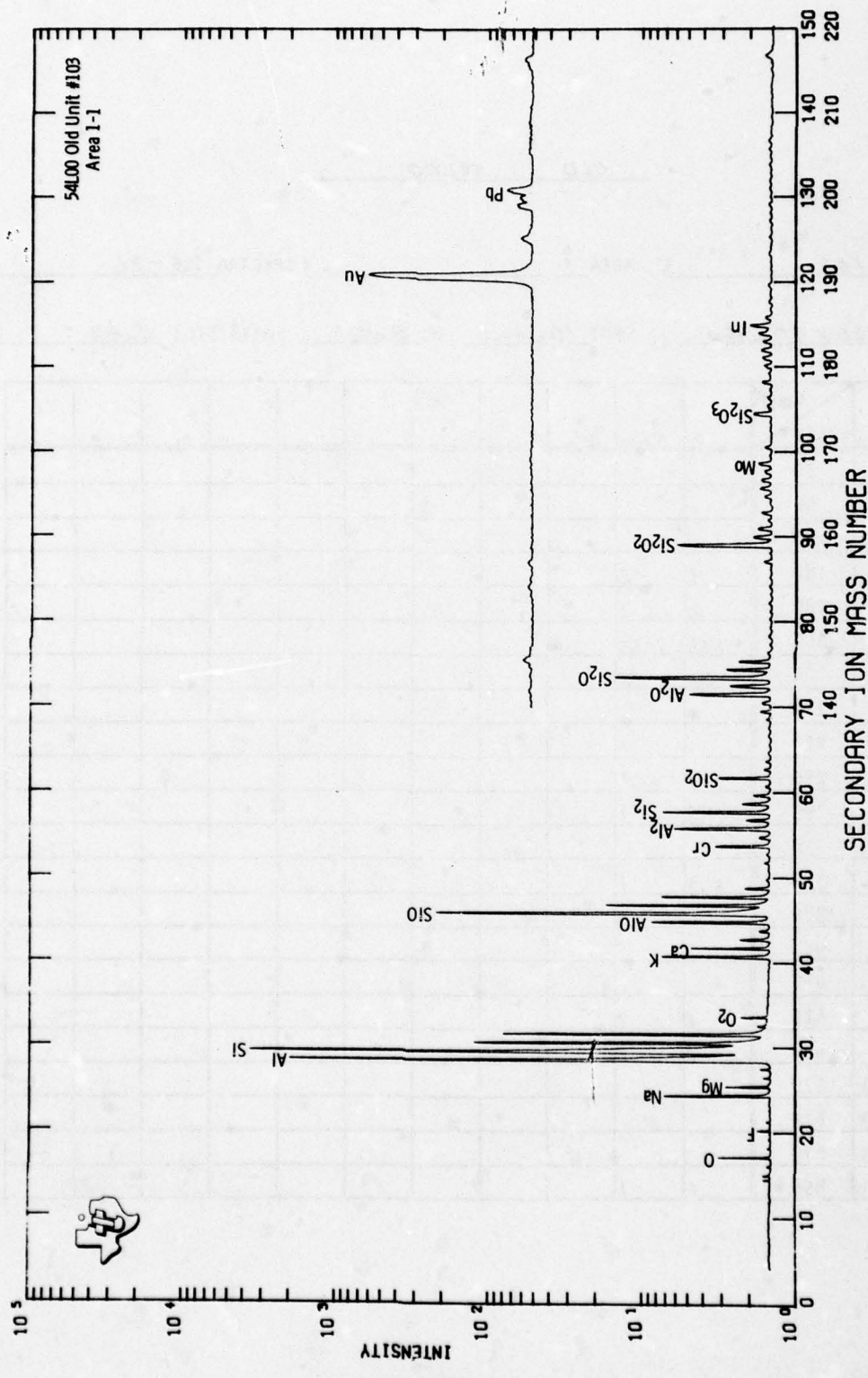
Set 1 54L00 Radiation Hardened Old Unit #103

OLD 54L00

UNIT #103. AREA 1. SPECTRA 75-76.

RASTER 50x40 μm. SPOT 16 μm BC BNA SR (Å/SEC) 1.42.

ELEM	PLUS START	0 926				
Li (7)	30					
B (11)	60					
F (19)	150					
Na (23)	180	9	2			
Mg (24)	185	2	1			
Al (27)	205	1835	1053			
Si (30)	220	38	56			
P (31)	230					
Cl (35)	250					
K (39)	290	9	3			
Ca (40)	295	5	1			
Ti (48)	330					
Cr (52)	350	3	1			
Ni (58)	380					
Cu (63)	400					
Zn (64)	403					
Ga (69)	425	1	1			
Mo (98)	540	1	1			
Ag (107)	570					
Sn (118)	610					
Ba (138)	670					
Pb (208)	858	1	1			



OLD      54L00

UNIT #103. AREA 1. SPECTRA 75 - 76.

RASTER 50x40 μm. SPOT 16 μm BC 8NA SR (Å/SEC) 1.42.

ELEM	PLUS START	0	926						
Li (7)	30								
B (11)	60								
F (19)	150								
Na (23)	180	9	2						
Mg (24)	185	2	1						
Al (27)	205	1835	1053						
Si (30)	220	38	56						
P (31)	230								
Cl (35)	250								
K (39)	290	9	3						
Ca (40)	295	5	1						
Ti (48)	330								
Cr (52)	350	3	1						
Ni (58)	380								
Cu (63)	400								
Zn (64)	403								
Ga (69)	425	1	1						
Mo (98)	540	1	1						
Ag (107)	570								
Sn (118)	610								
Ba (138)	670								
Pb (208)	858	1	1						

OLD 54L00

UNIT #103. AREA 2. SPECTRA 91-101.

RASTER 75x60 mm. SPOT 22 μm BC 17NA SR (A/SEC) 1.34.

ELEM	PLUS START	0	915	1615	2315	3015	3715	4415	5115	5815	6515	7215
Li (7)	30											
B (11)	60		1	1	1	1	1	1	1	1	1	1
F (19)	150											
Na (23)	180		2	1	1	1	1	1	1	1	2	1
Mg (24)	185		1	1	1	-	-	-	1	1	-	-
Al (27)	205		13	7	6	6	7	22	49	82	144	224
Si (30)	220		370	250	250	260	250	230	200	220	160	200
P (31)	230											
Cl (35)	250											
K (39)	290		3	2	2	3	3	3	3	3	4	3
Ca (40)	295		1	1	1	1	1	1	1	1	1	1
Ti (48)	330		1	1	1	1	1	1	1	-	1	1
Cr (52)	350		1	1	1	1	1	1	1	1	1	1
Ni (58)	380											
Cu (63)	400											
Zn (64)	403											
Ga (69)	425											
Mo (98)	540		1	1	1	1	1	1	1	-	-	-
Ag (107)	570											
Sn (118)	610		1	1	1	1	1	1	1	1	1	1
Ba (138)	670											
Pb (208)	858											

OLD 54L00

UNIT #103 . AREA 2 . SPECTRA 102-103 .

RASTER 75 x 60 mm . SPOT 22 mm BC 17NA SR (Å/SEC) 1.34 .

ELEM	PLUS START	7915	8615								
Li (7)	30										
B (11)	60	/	/								
F (19)	150	/	/								
Na (23)	180	/	/								
Mg (24)	185	-	-								
Al (27)	205	1798	1899								
Si (30)	220	190	180								
P (31)	230										
Cl (35)	250										
K (39)	290	3	3								
Ca (40)	295	/	/								
Ti (48)	330	/	-								
Cr (52)	350	/	/								
Ni (58)	380										
Cu (63)	400										
Zn (64)	403										
Ga (69)	425										
Mo (98)	540	-	-								
Ag (107)	570										
Sn (118)	610	/	/								
Ba (138)	670										
Pb (208)	858										

OLD      54L00

UNIT #103 . AREA 3 . SPECTRA 77 - 87 .

RASTER 75 X 60 μm . SPOT 22 μm BC 17 NA SR ( $\text{\AA}/\text{SEC}$ ) 1.34 .

ELEM	PLUS START											
		0	700	1400	2100	2800	3500	4200	4900	5600	6300	7000
Li (7)	30											
B (11)	60	-	1	1	1	1	1	1	1	1	1	1
F (19)	150											
Na (23)	180	7	1	1	1	1	1	1	1	1	1	1
Mg (24)	185	-	1	1	-	-	-	1	1	1	1	1
Al (27)	205	9	2	1	1	2	1	1	2	1	1	1
Si (30)	220	42	220	215	210	175	180	240	220	280	280	250
P (31)	230											
Cl (35)	250											
K (39)	290	9	1	1	1	1	1	1	1	1	1	1
Ca (40)	295	2	1	1	1	1	1	1	1	1	1	1
Ti (48)	330											
Cr (52)	350	6	1	1	1	1	1	1	1	1	1	1
Ni (58)	380											
Cu (63)	400											
Zn (64)	403											
Ga (69)	425											
Mo (98)	540											
Ag (107)	570											
Sn (118)	610	1	1	1	1	1	1	1	1	1	1	1
Ba (138)	670	-	-	-	-	1	1	1	-	1	1	1
Pb (208)	858											

OLD 54200

UNIT #103. AREA 3. SPECTRA 88-90.

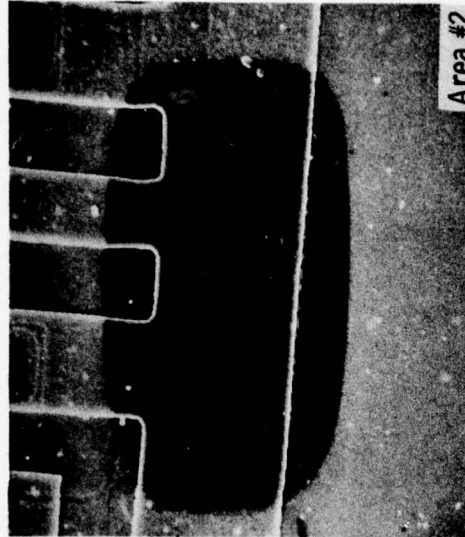
RASTER 75 X 60 mm. SPOT 22 mm BC 17 NA SR ( $\lambda$ /SEC) 1.34

ELEM	START	PLUS		
		7700	8400	9100
Li (7)	30			
B (11)	60	1	-	1
F (19)	150			
Na (23)	180	2	1	2
Mg (24)	185	-	-	-
Al (27)	205	3	5	3
Si (30)	220	240	250	230
P (31)	230	-	1	8
Cl (35)	250			
K (39)	290	1	-	1
Ca (40)	295	1	-	1
Ti (48)	330			
Cr (52)	350	1	-	1
Ni (58)	380			
Cu (63)	400			
Zn (64)	403			
Ga (69)	425			
Mo (98)	540			
Ag (107)	570			
Sn (118)	610	1	-	-
Ba (138)	670	1	1	1
Pb (208)	858			

54L00 Old Unit #103



Area #1



Area #2

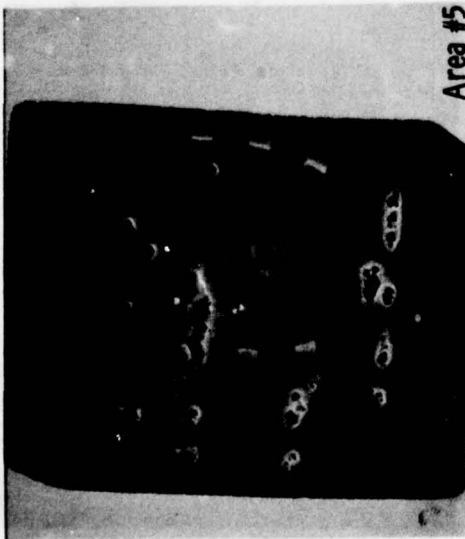


Area #3

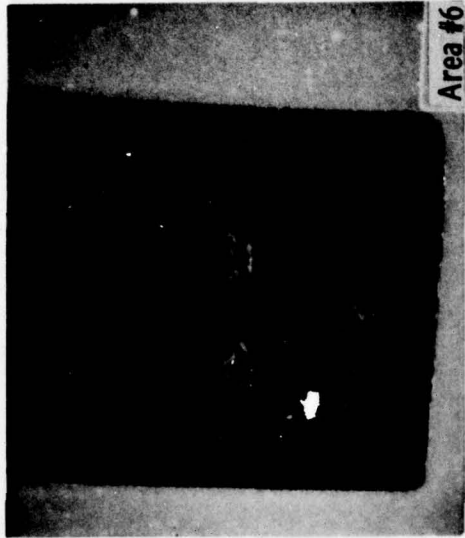


Area #4

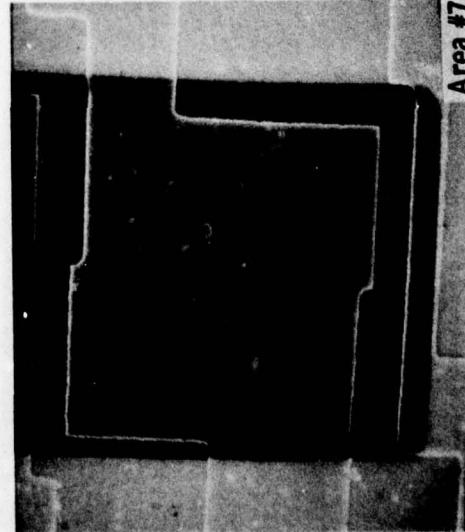
54L00 Old Unit #103



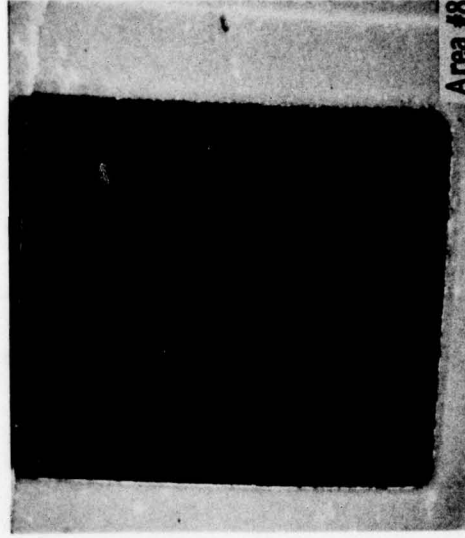
Area #5



Area #6



Area #7



Area #8

Op Amp #1, Unit #3

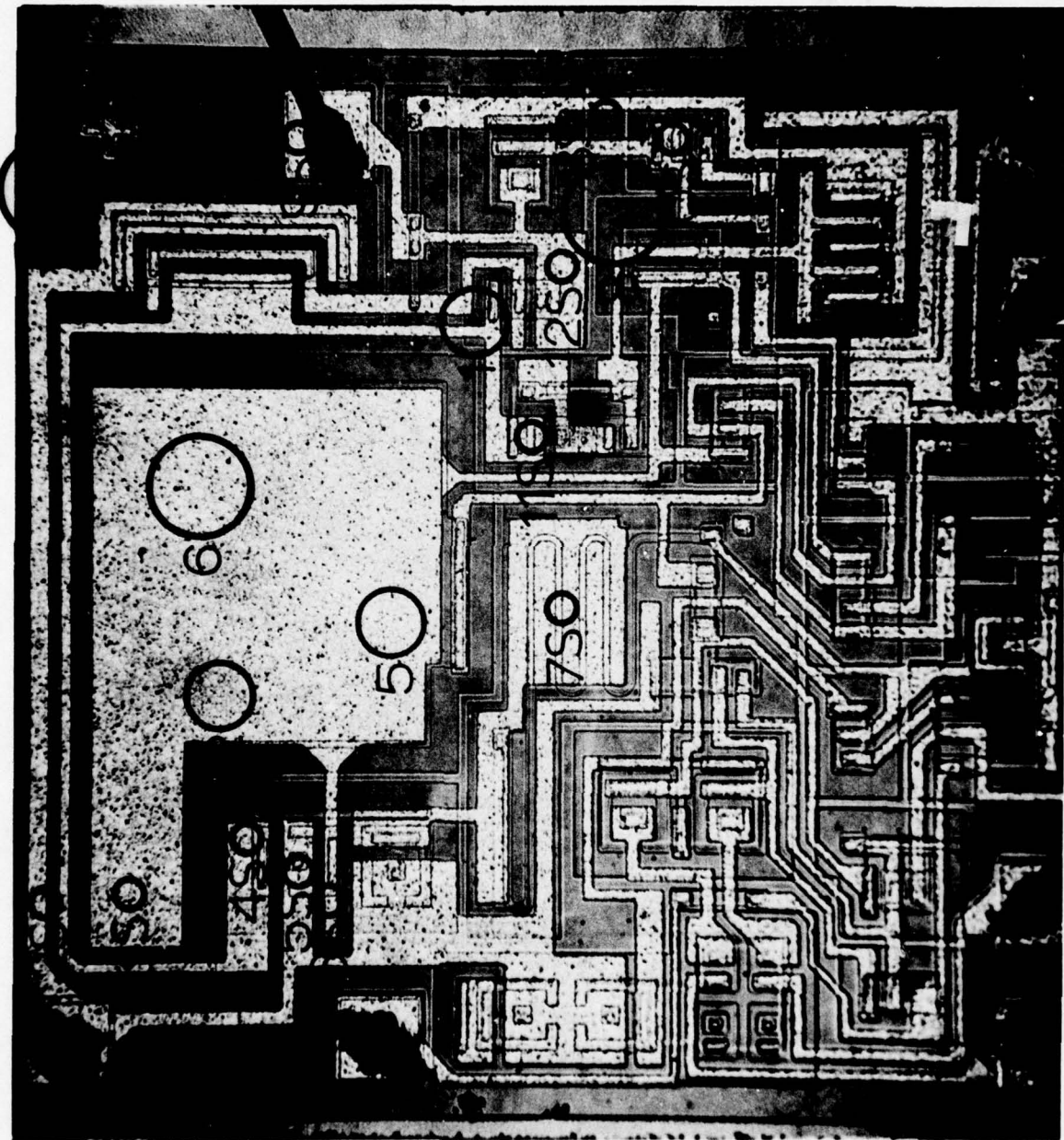
- Area 1: Mass Spectra Depth Profile
- Area 2: Mass Spectra Depth Profile
- Area 3: Mass Spectra Depth Profile
- Area 4: P Peak Count Profile (not included)
- Area 5: P Peak Count Profile
- Area 6: Ar Sputter for Glassivation Thickness -  
Interface Analysis at Glassivation-  
Aluminum Layers
- Area 7: Interface Analysis; Glassivation-  
Oxide Layers
- Area 8: Interface Analysis; Glassivation-  
Oxide Layers
- Area 9: Interface Analysis; Glassivation-  
Oxide Layers

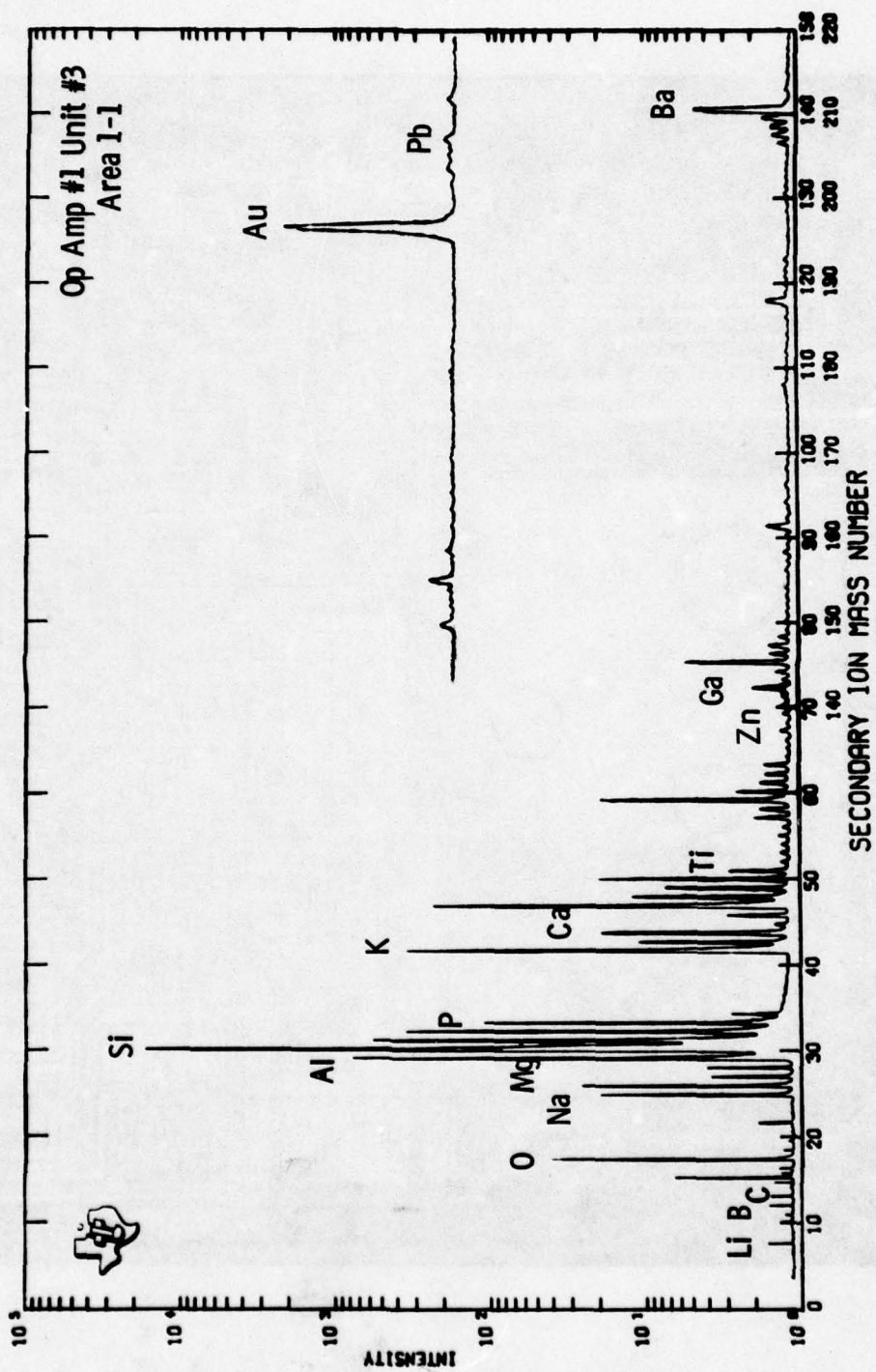
Oxide-Metal Stripped

- Area 1S: Mass Spectrum for Dopants
- Area 2S: Mass Spectrum for Dopants
- Area 3S: Mass Spectrum for Dopants
- Area 4S: Mass Spectrum for Dopants
- Area 5S: Mass Spectrum for Dopants
- Area 6S: Mass Spectrum for Dopants

**Op Amp #1, Unit #3  
Oxide-Metal Stripped  
(Continued)**

**Area 7S: Mass Spectrum for Dopants**  
**Area 8S: B Concentration Data**  
**Area 9S: B Concentration Data**  
**Area 10S: B Concentration Data**  
**Area 11S: B Concentration Data**





OP AMP #1 MC1471L

UNIT #3 . AREA 1 . SPECTRA 11-13

RASTER 50 x 40  $\mu$ m. SPOT 26  $\mu$ m BC 15 NA SR ( $\text{\AA}/\text{SEC}$ ) 2.66.

ELEM	START	PLUS			
		0	3260	5060	
Li (7)	30	1	1	-	
B (11)	60	1	1	1	
F (19)	150				
Na (23)	180	9	3	2	
Mg (24)	185	12	5	2	
Al (27)	205	271	670	5431	
Si (30)	220	130	180	82	
P (31)	230	47	32	26	
C1 (35)	250				
K (39)	290	139	61	30	
Ca (40)	295	5	1	1	
Ti (48)	330	1	1	1	
Cr (52)	350	1	-	-	
Ni (58)	380				
Cu (63)	400				
Zn (64)	403	1	-	-	
Ga (69)	425	1	1	1	
Mo (98)	540				
Ag (107)	570				
Sn (118)	610	1	-	-	
Ba (138)	670	2	1	1	
Pb (208)	858	1	1	1	

## OP AMP #1 MC1471L

UNIT 3. AREA 2. SPECTRA 14-16.

RASTER 50 x 40 μm . SPOT 17 μm BC 20 NA SR (Å/SEC) 3.55

ELEM	START	PLUS			
		0	706	1412	
Li (7)	30	1	-	-	
B (11)	60	1	1	-	
F (19)	150				
Na (23)	180	4	1	1	
Mg (24)	185	1	1	-	
Al (27)	205	1	31	5955	
Si (30)	220	120	120	18	
P (31)	230	33	31	32	
Cl (35)	250				
K (39)	290	1	1	1	
Ca (40)	295	1	1	1	
Ti (48)	330				
Cr (52)	350	1	-	-	
Ni (58)	380				
Cu (63)	400				
Zn (64)	403				
Ga (69)	425	1	1	1	
Mo (98)	540				
Ag (107)	570				
Sn (118)	610				
Ba (138)	670				
Pb (208)	858				

OP AMP #1      mc1471L

UNIT #3 AREA 3 SPECTRA 17-20

RASTER 50 x 40 μm SPOT 17 μm BC 20 NA SR ( $\text{\AA}/\text{SEC}$ ) 3.55

ELEM	START	PLUS			
		0	687	1375	2066
Li (7)	30	5	1	1	1
B (11)	60	1	1	1	2
F (19)	150				
Na (23)	180	9	2	1	1
Mg (24)	185	1	1	-	-
Al (27)	205	8	6	5	2
Si (30)	220	130	140	150	150
P (31)	230	32	29	15	9
Cl (35)	250				
K (39)	290	2	1	1	1
Ca (40)	295	1	1	1	1
Ti (48)	330				
Cr (52)	350				
Ni (58)	380				
Cu (63)	400				
Zn (64)	403				
Ga (69)	425	1	1	1	1
Mo (98)	540				
Ag (107)	570				
Sn (118)	610				
Ba (138)	670				
Pb (208)	858				

OP AMP #1 MC1741L

UNIT #3 AREA 6 SPECTRA 239 - 242

RASTER 86 x 59 μm. SPOT 14 μm BC 17NA SR ( $\text{Å/sec}$ ) 1.19.

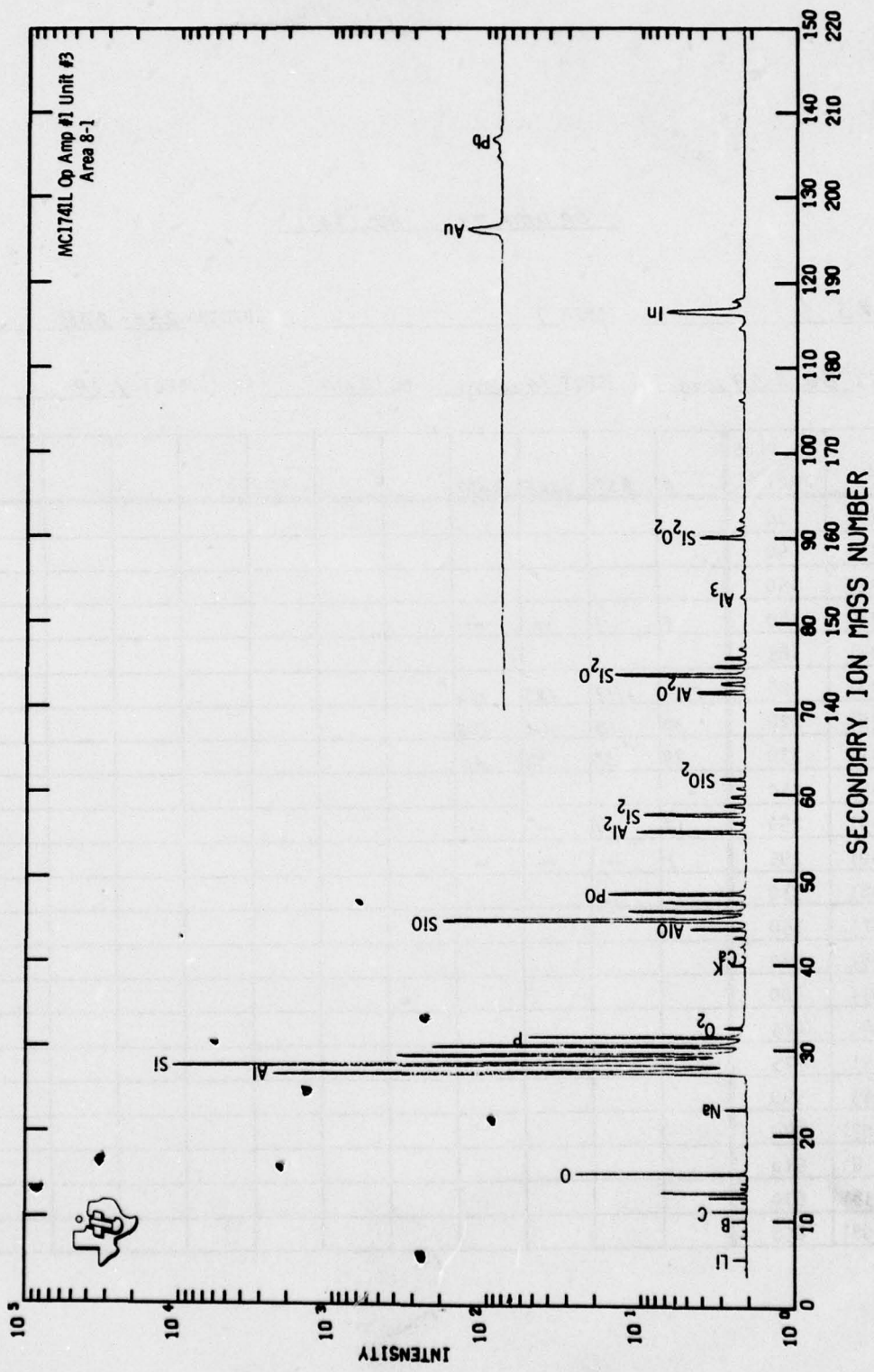
ELEM	START	PLUS						
		0	884	1825	2497			
Li (7)	30							
B (11)	60							
F (19)	150							
Na (23)	180	3	2	4	2			
Mg (24)	185							
Al (27)	205	6534	3460	3325	3564			
Si (30)	220	6.8	16	13	15			
P (31)	230	16	12	18	17			
Cl (35)	250							
K (39)	290	2	1	2	1			
Ca (40)	295							
Ti (48)	330	-	1	2	1			
Cr (52)	350							
Ni (58)	380							
Cu (63)	400							
Zn (64)	403							
Ga (69)	425							
Mo (98)	540							
Ag (107)	570							
Sn (118)	610							
Ba (138)	670							
Pb (208)	858							

OP AMP #1 MC1741L

UNIT #3 . AREA 7 . SPECTRA 235-238

RASTER 86 x 59 μm . SPOT 14 μm BC 17NA SR (Å/SEC) 1.19

ELEM	PLUS START	0	857	1564	2237							
Li (7)	30											
B (11)	60											
F (19)	150											
Na (23)	180	1	1	-	-							
Mg (24)	185											
Al (27)	205	113	117	125	116							
Si (30)	220	32	13	6.6	3.5							
P (31)	230	29	33	38	40							
C1 (35)	250											
K (39)	290	1	1	-	-							
Ca (40)	295	1	-	-	-							
Ti (48)	330											
Cr (52)	350											
Ni (58)	380											
Cu (63)	400											
Zn (64)	403											
Ga (69)	425											
Mo (98)	540											
Ag (107)	570											
Sn (118)	610											
Ba (138)	670											
Pb (208)	858											



OP AMP #1 MC1741L

UNIT #3 AREA 8 SPECTRA 243-246

RASTER 86 x 59  $\mu m$ . SPOT 14  $\mu m$  BC 17 NA SR ( $\text{\AA}/\text{SEC}$ ) 1.19.

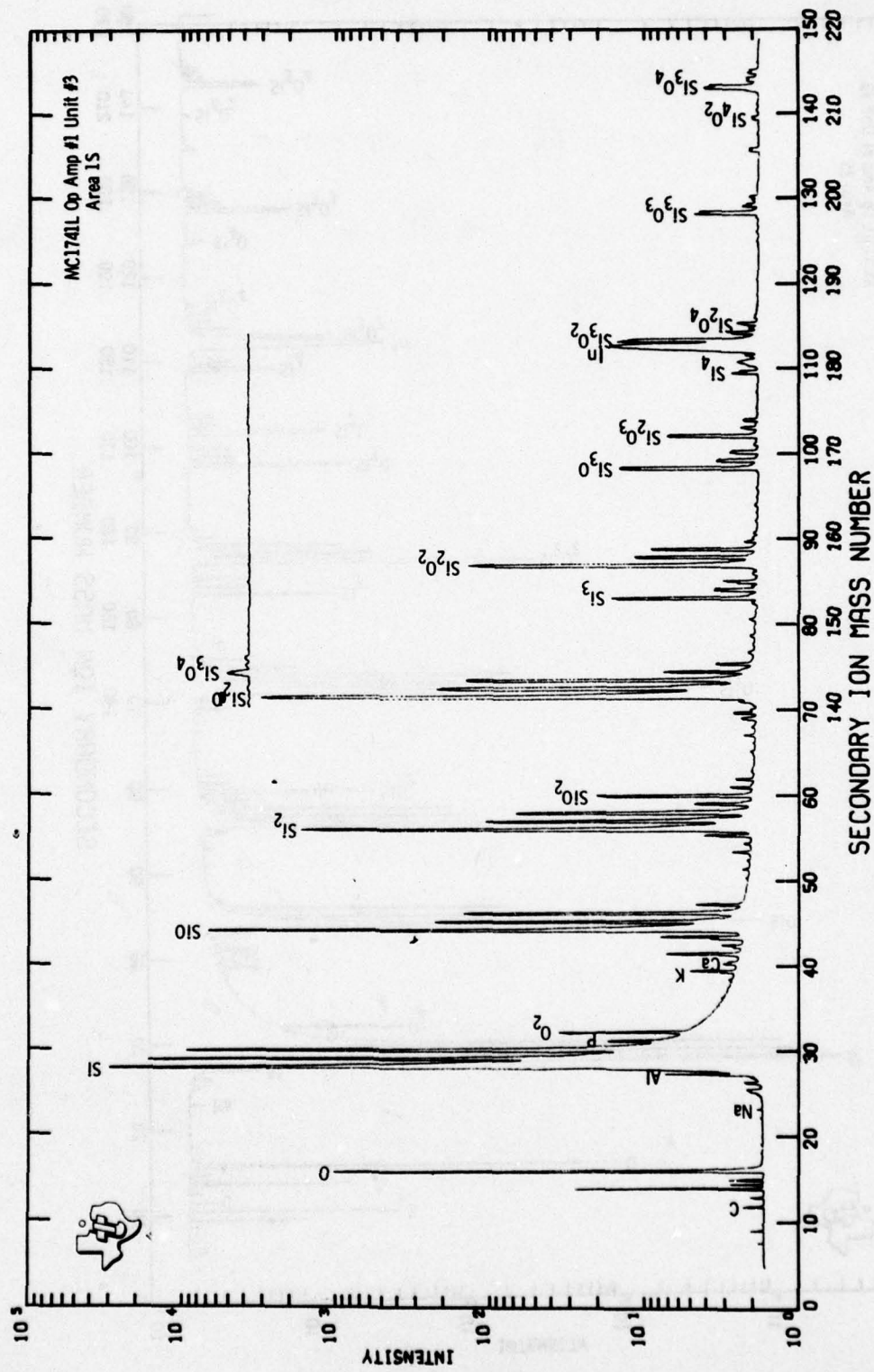
ELEM	PLUS START					
		0	859	1578	2220	
Li (7)	30					
B (11)	60					
F (19)	150	1	-	-	-	
Na (23)	180	1	1	1	1	
Mg (24)	185					
Al (27)	205	107	43	53	35	
Si (30)	220	56	54	52	52	
P (31)	230	27	28	24	31	
C1 (35)	250					
K (39)	290	1	1	1	-	
Ca (40)	295					
Ti (48)	330					
Cr (52)	350					
Ni (58)	380					
Cu (63)	400					
Zn (64)	403					
Ga (69)	425					
Mo (98)	540					
Ag (107)	570					
Sn (118)	610					
Ba (138)	670					
Pb (208)	858					

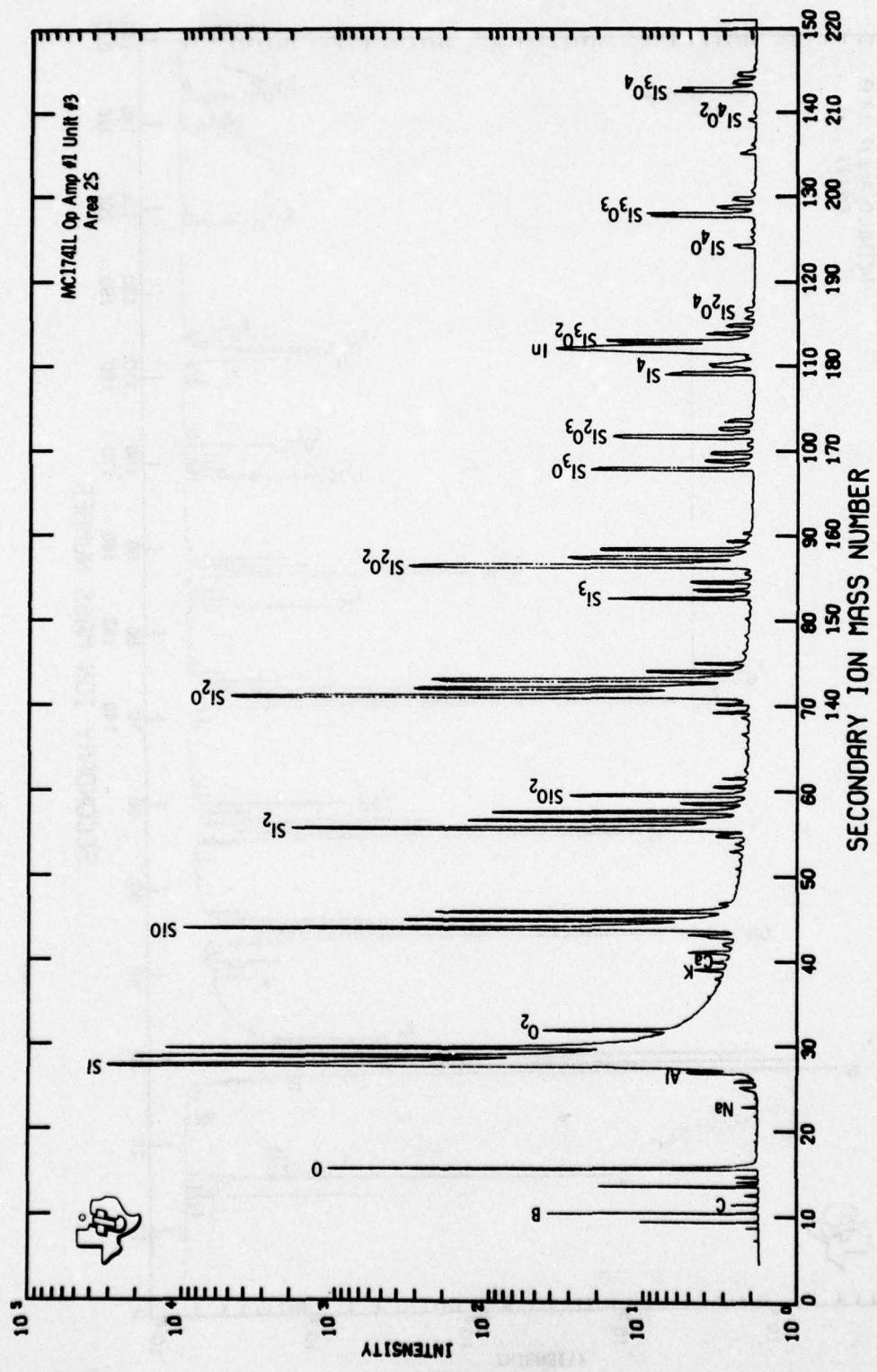
OP AMP #1 MC1741L

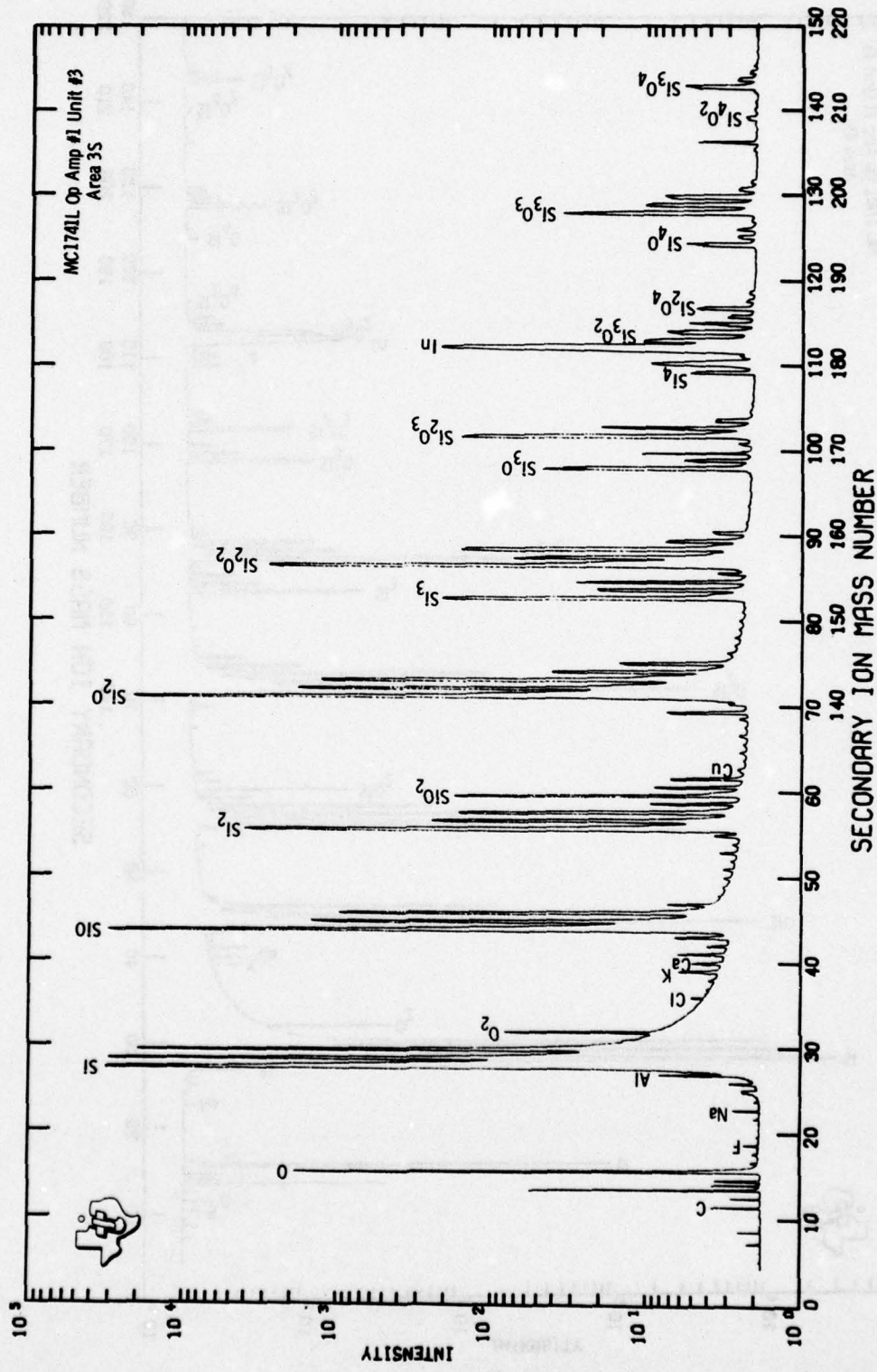
UNIT #3. AREA 9. SPECTRA 247 - 250.

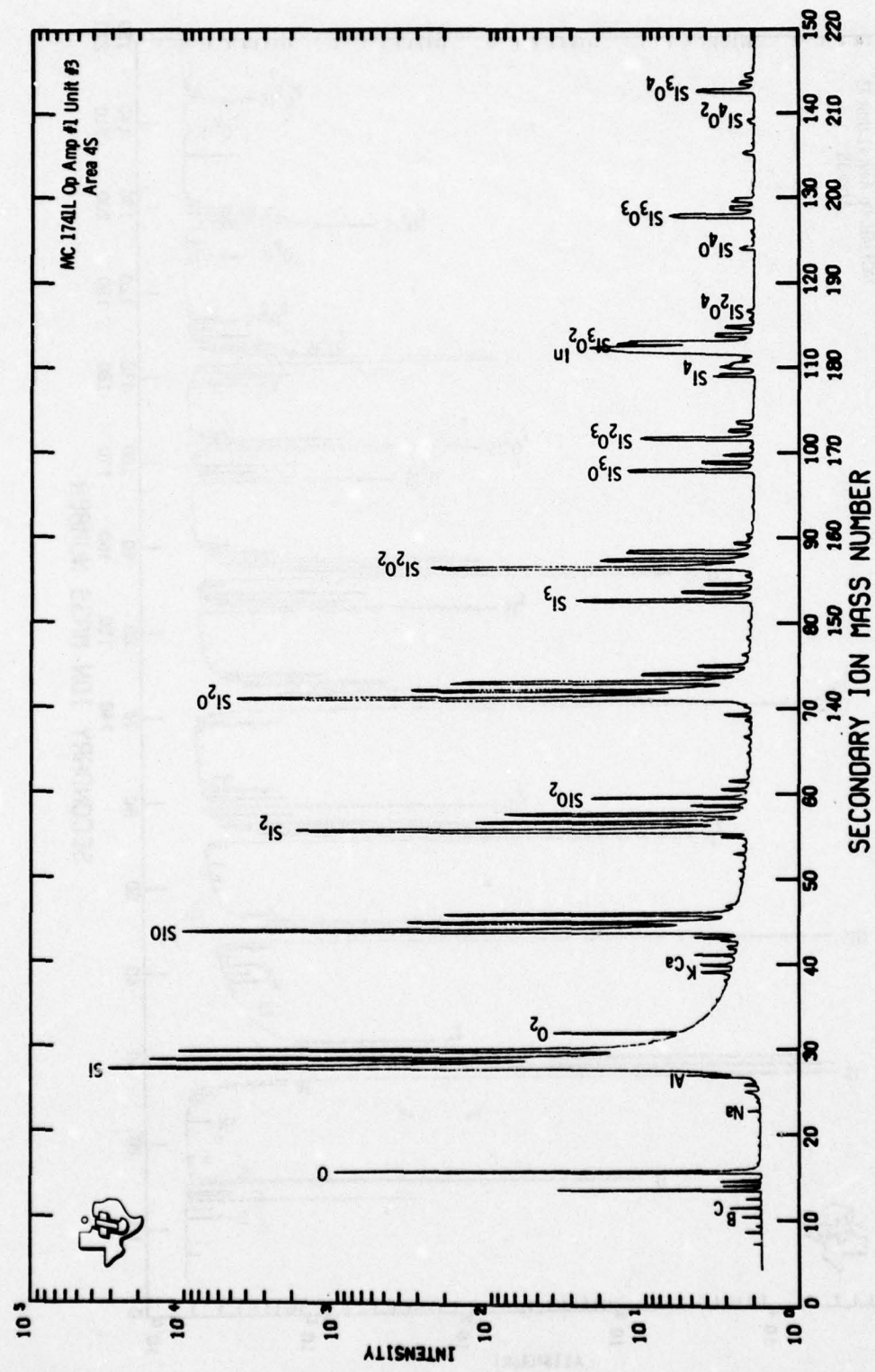
RASTER 86 X 59 μm. SPOT 14 μm BC 17 NA SR (Å/SEC) 1.19.

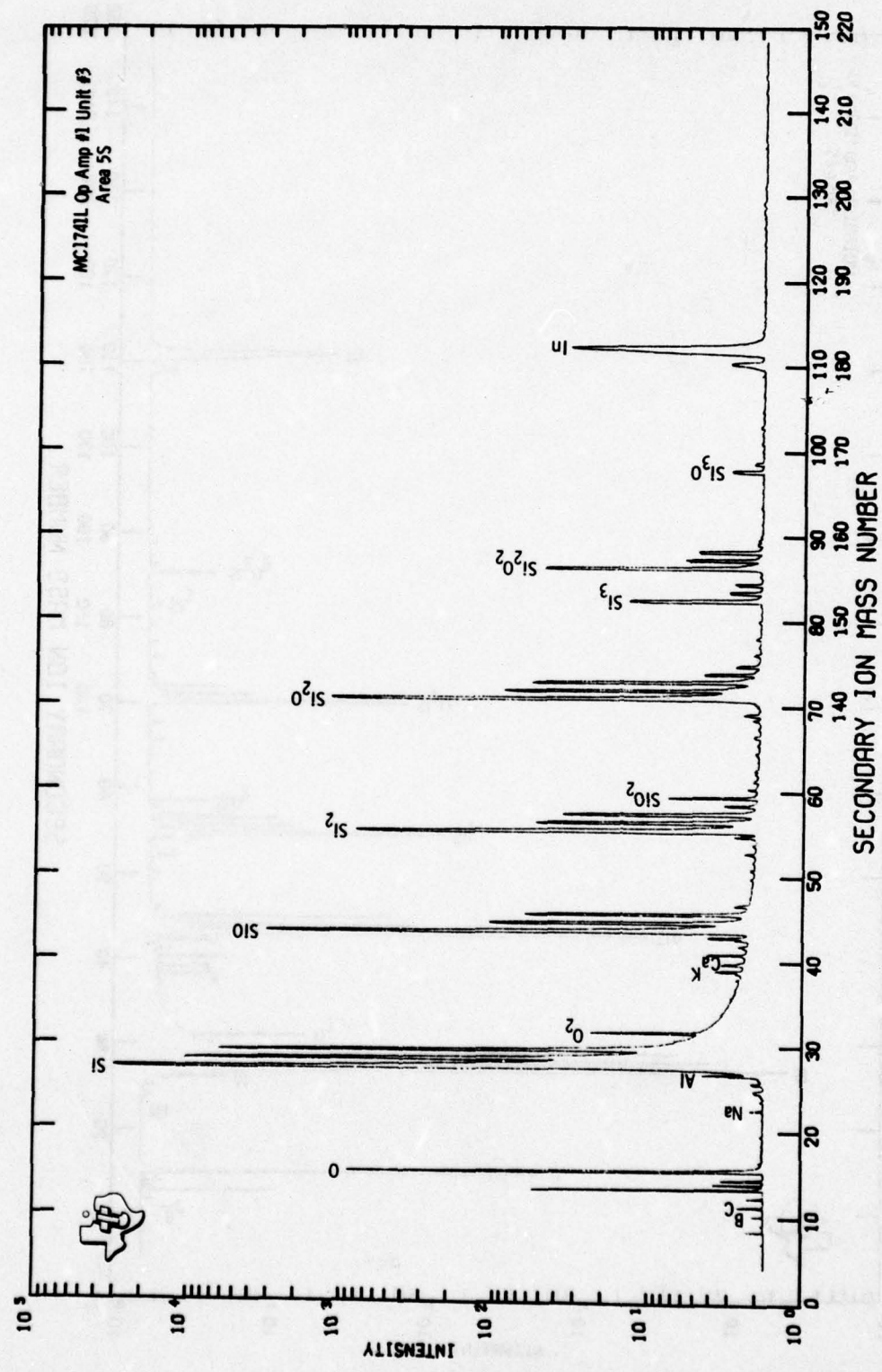
ELEM	PLUS START	0	882	1562	2287						
Li (7)	30										
B (11)	60										
F (19)	150										
Na (23)	180	/	/	/	/						
Mg (24)	185										
Al (27)	205	926	201	355	348						
Si (30)	220	70	70	74	64						
P (31)	230	26	28	26	22						
Cl (35)	250										
K (39)	290	/	/	/	/						
Ca (40)	295	/	/	/	/						
Ti (48)	330										
Cr (52)	350										
Ni (58)	380										
Cu (63)	400										
Zn (64)	403										
Ga (69)	425										
Mo (98)	540										
Ag (107)	570										
Sn (118)	610										
Ba (138)	670										
Pb (208)	858										

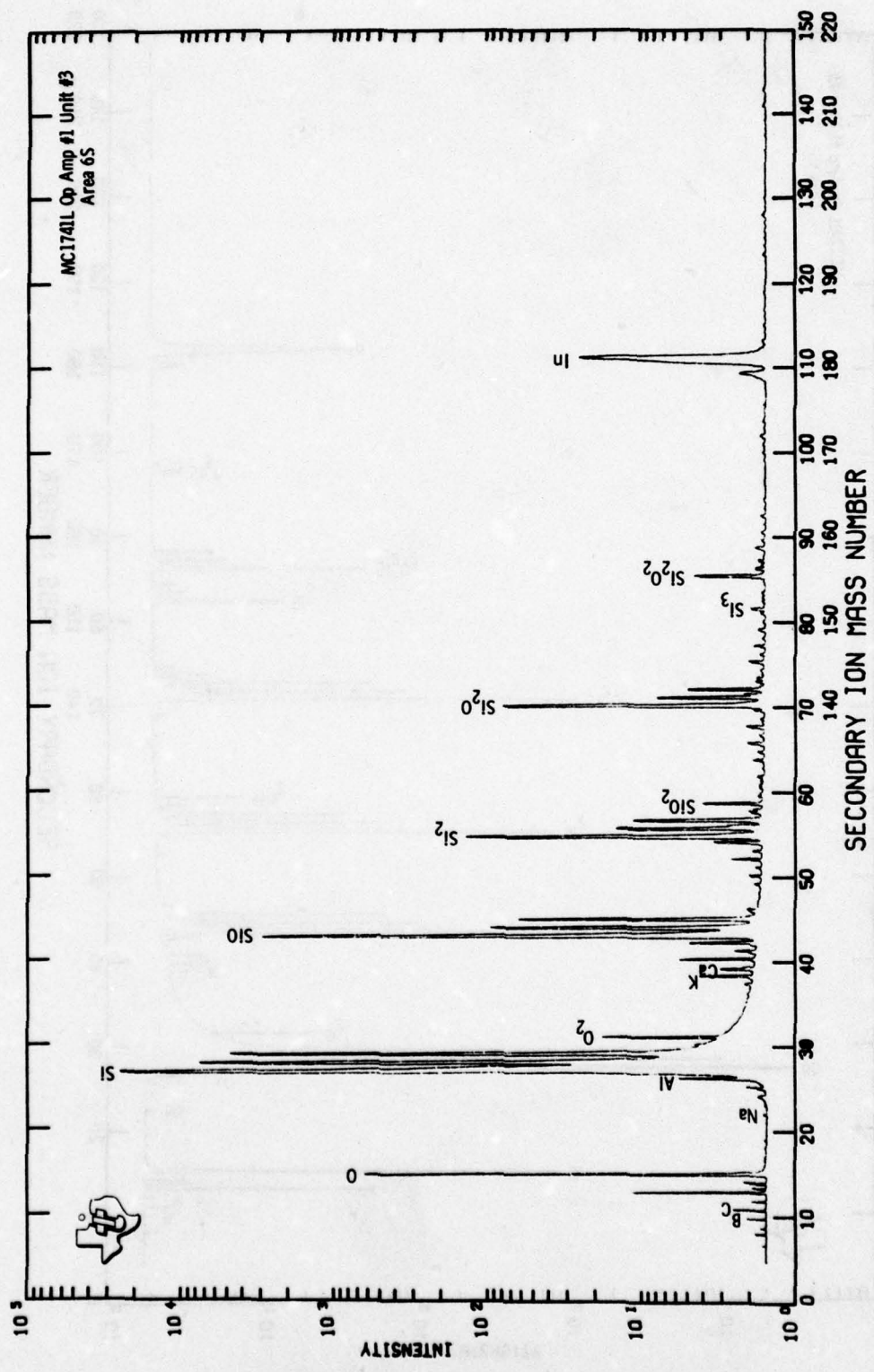


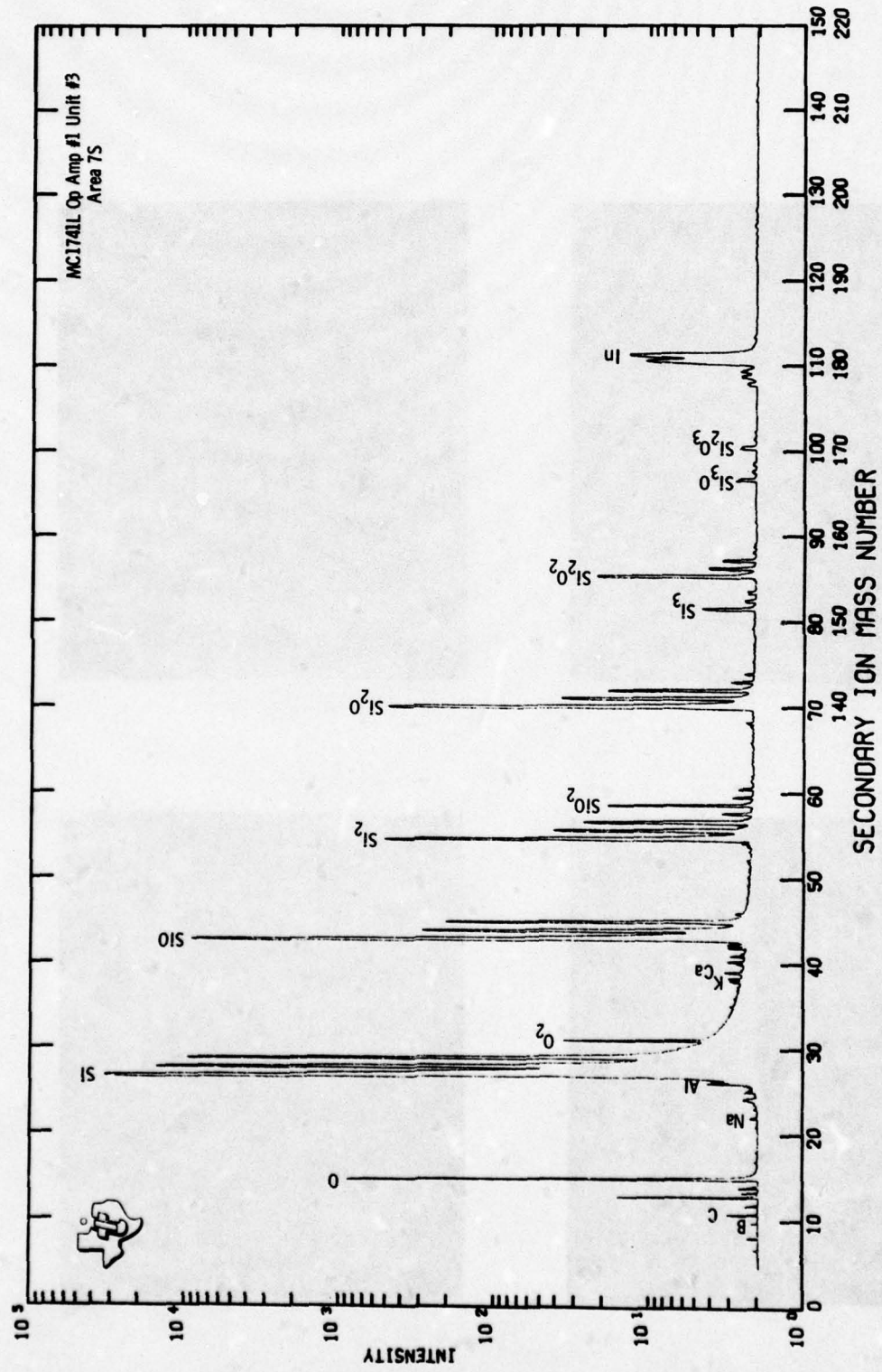




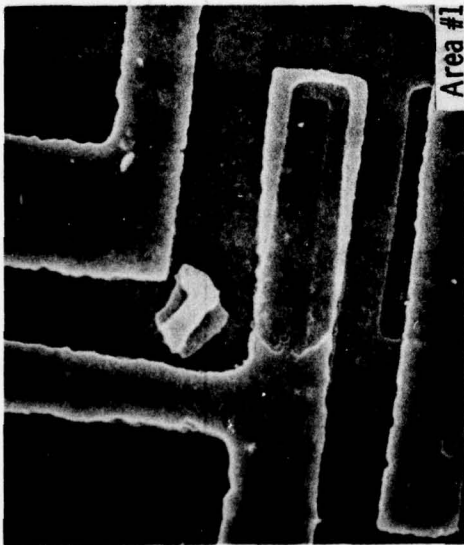








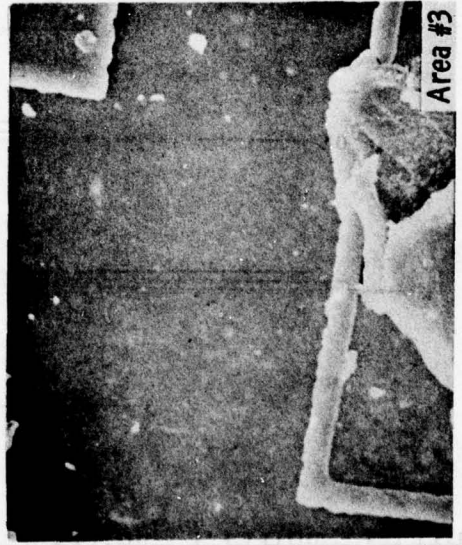
MC1741L Op Amp #1 Unit #3



Area #1



Area #2

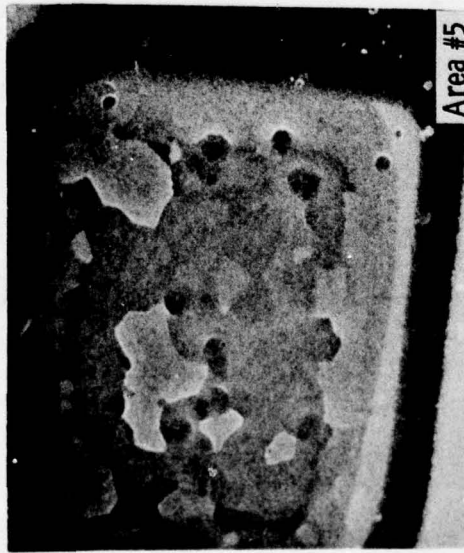


Area #3

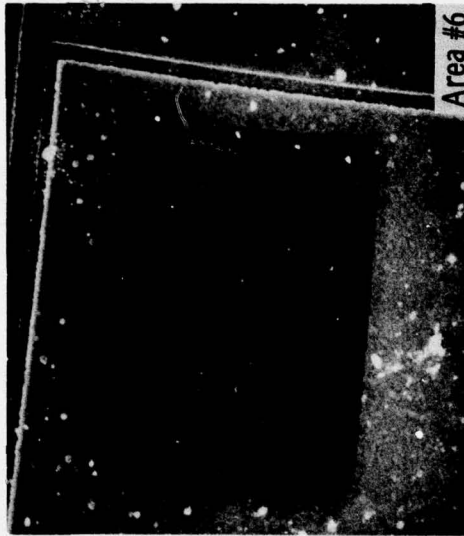


Area #4

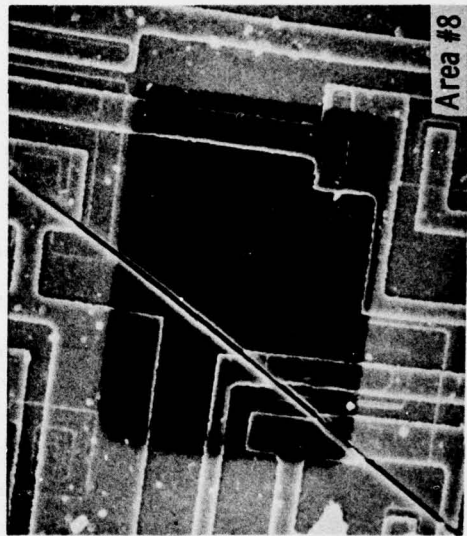
MC1741L Op Amp #1 Unit #3



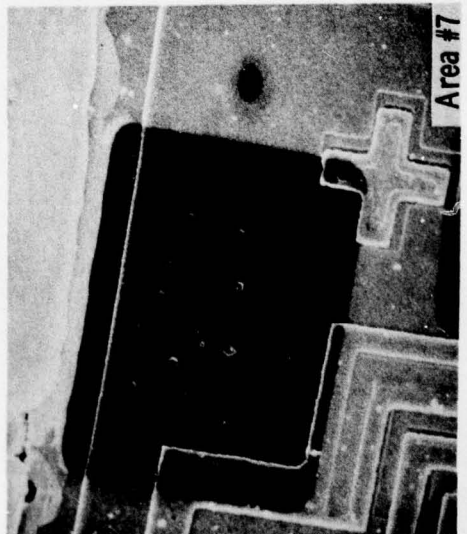
Area #6



Area #8



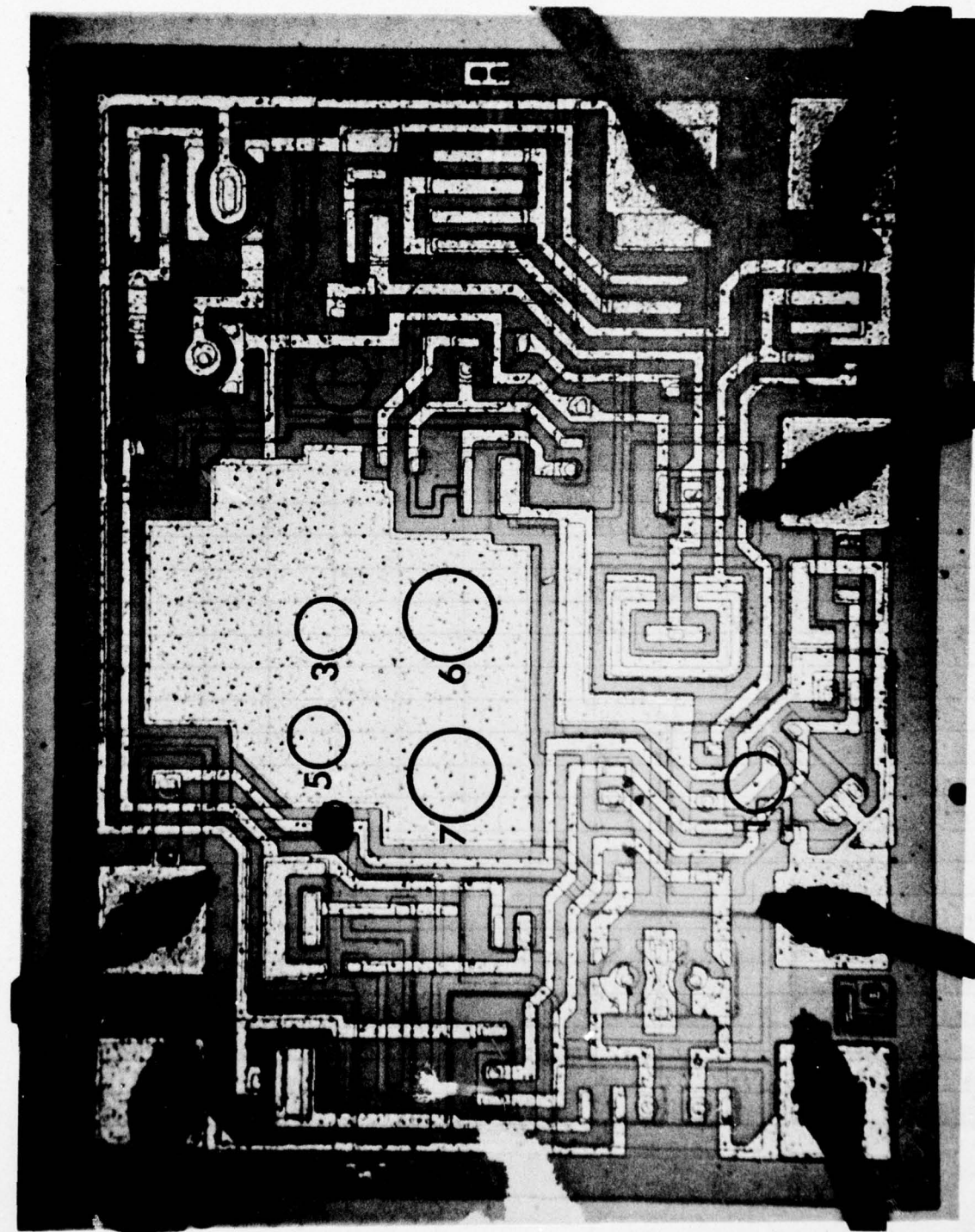
Area #7



Op Amp #2, Unit #62

- Area 1: Mass Spectra Depth Profile
- Area 2: Mass Spectra Depth Profile
- Area 3: Mass Spectra Depth Profile
- Area 4: P Peak Count Profile
- Area 5: Ar Sputter Time Through Glassivation
- Area 6: False Start
- Area 7: Interface Analysis, Glassivation-  
Aluminum Layers
- Area 8: Interface Analysis, Glassivation-  
Oxide Layers

Set 1 Op Amp #2 Unit #62

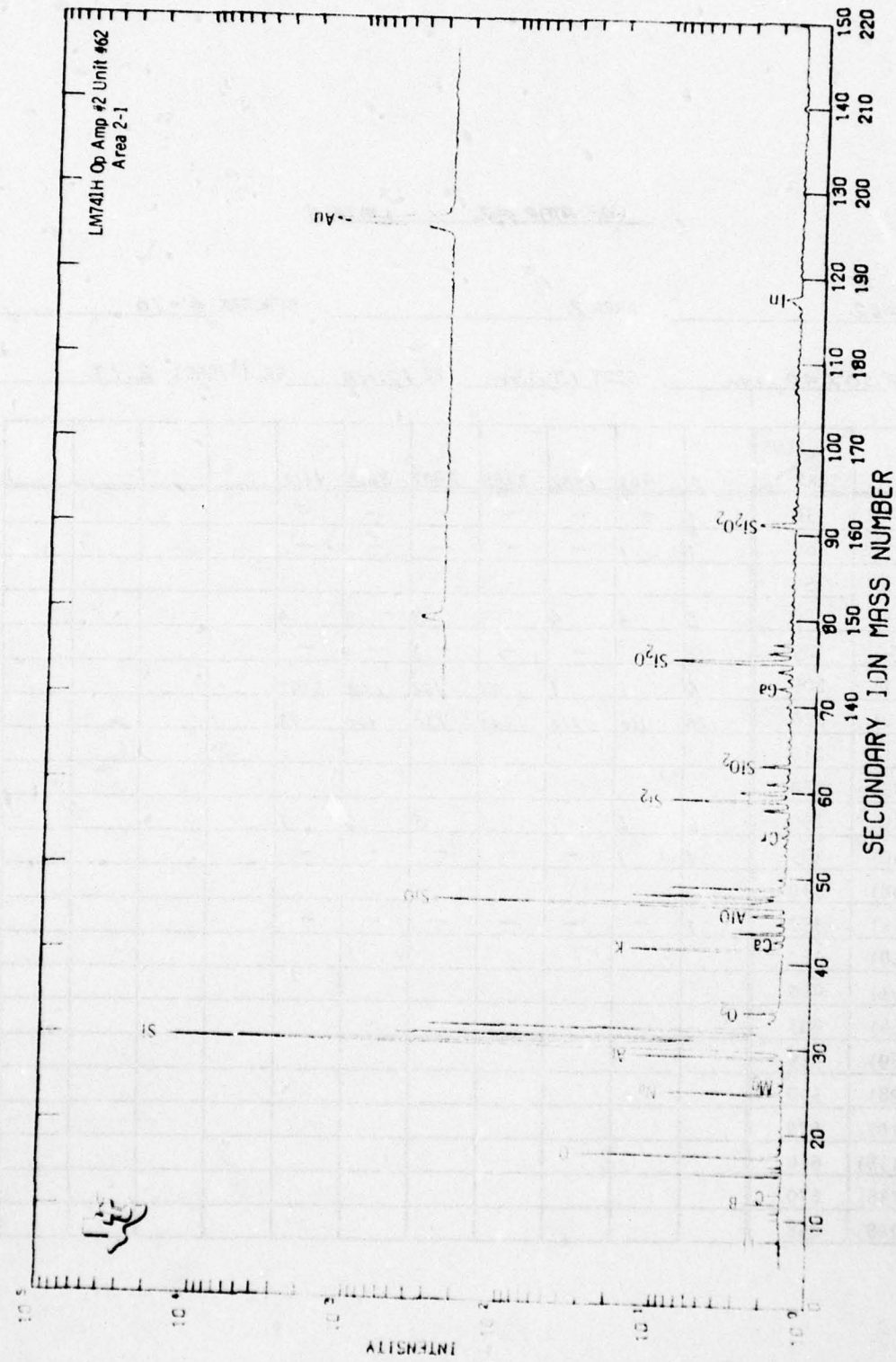


OP AMP #2 LM741H

**UNIT #62** \_\_\_\_\_ . AREA **1** \_\_\_\_\_ . SPECTRA **1-3** \_\_\_\_\_ .

RASTER 50 x 40 μm. SPOT 26 μm BC 16 NA SR ( $\frac{1}{sec}$ ) 2.84

**BEST AVAILABLE COPY**



OP AMP #2      LMT41H

UNIT #62. AREA 2. SPECTRA 4-10.

RASTER 50 x 40 μm. SPOT 13 μm BC 12 NA SR ( $\text{\AA}/\text{SEC}$ ) 2.13.

ELEM	PLUS START							
		0	906	1582	2295	2997	3663	4412
Li (7)	30	1	-	-	-	-	-	-
B (11)	60	1	1	-	-	-	-	-
F (19)	150							
Na (23)	180	3	4	4	3	3	3	4
Mg (24)	185	1	-	-	-	-	-	-
Al (27)	205	6	1	1	21	162	1312	2197
Si (30)	220	120	110	110	140	130	100	92
P (31)	230							
C1 (35)	250							
K (39)	290	6	6	7	5	5	6	7
Ca (40)	295	1	1	-	-	-	-	-
Ti (48)	330							
Cr (52)	350	1	-	-	-	-	-	-
Ni (58)	380							
Cu (63)	400							
Zn (64)	403							
Ga (69)	425							
Mo (98)	540							
Ag (107)	570							
Sn (118)	610							
Ba (138)	670							
Pb (208)	858							

OP AMP # 2 LM741H

UNIT #62 . AREA 3 . SPECTRA 21-27 .

RASTER 50 X 10 μm . SPOT 17 μm BC 28NA SR (Å/SEC) 4.97 .

ELEM	PLUS START	0	716	1421	2124	2822	3592	4303				
Li (7)	30	1	1	1	1	1	1	1				
B (11)	60	1	1	1	1	1	1	1				
F (19)	150											
Na (23)	180	3	3	3	3	3	3	3				
Mg (24)	185	1	-	-	-	-	-	-				
Al (27)	205	6	3	3	19	19	2	1				
Si (30)	220	240	230	220	180	160	150	140				
P (31)	230											
Cl (35)	250											
K (39)	290	6	6	5	6	5	7	6				
Ca (40)	295	1	1	1	1	1	-	-				
Ti (48)	330											
Cr (52)	350	1	-	-	-	-	-	-				
Ni (58)	380											
Cu (63)	400											
Zn (64)	403											
Ga (69)	425											
Mo (98)	540											
Ag (107)	570											
Sn (118)	610											
Ba (138)	670	1	1	1	1	-	1	1				
Pb (208)	858											

OP AMP #2 LM741H

UNIT #62 . AREA 7 . SPECTRA 308 - 318 .

RASTER 92 X 68 μm . SPOT 14 μm BC 6 NA SR (Å/SEC) .34 .

ELEM	PLUS START	0	907	1594	2285	2976	3668	4359	5045	5738	6424	7112
Li (7)	30											
B (11)	60											
F (19)	150											
Na (23)	180	1	1	1	1	1	1	1	1	1	1	1
Mg (24)	185											
Al (27)	205	42	94	63	65	85	96	104	137	122	164	209
Si (30)	220	94	96	92	92	92	92	90	88	90	86	82
P (31)	230	1	1	1	-	-	-	-	-	-	-	-
Cl (35)	250											
K (39)	290	1	1	1	1	1	1	1	1	1	1	1
Ca (40)	295	1	-	-	-	-	-	-	-	-	-	-
Ti (48)	330											
Cr (52)	350											
Ni (58)	380											
Cu (63)	400											
Zn (64)	403											
Ga (69)	425											
Mo (98)	540											
Ag (107)	570											
Sn (118)	610											
Ba (138)	670											
Pb (208)	858											

OP AMP #2 LM741H

UNIT #62. AREA 7. SPECTRA 319 - 324.

RASTER 92 X 68 μm. SPOT 14 μm BC 6 NA SR ( $\text{\AA}/\text{SEC}$ ) .34.

ELEM	START	PLUS										
		7799	8517	9218	9906	10595	11286					
Li (7)	30											
B (11)	60											
F (19)	150											
Na (23)	180	1	1	1	1	1	1					
Mg (24)	185											
Al (27)	205	212	252	258	308	556	880					
Si (30)	220	90	84	78	72	62	60					
P (31)	230	-	-	-	-	-	-					
Cl (35)	250											
K (39)	290	1	1	1	1	1	1					
Ca (40)	295	-	-	-	-	-	-					
Ti (48)	330											
Cr (52)	350											
Ni (58)	380											
Cu (63)	400											
Zn (64)	403											
Ga (69)	425											
Mo (98)	540											
Ag (107)	570											
Sn (118)	610											
Ba (138)	670											
Pb (208)	858											

OP AMP #2 LM741 H

UNIT #62 . AREA B . SPECTRA 292 - 302 .

RASTER 92 X 68 . SPOT 14 $\mu$  BC 6 NA SR ( $\text{\AA}/\text{SEC}$ ) .34 .

ELEM	START	PLUS	0	901	1591	2245	2935	3626	4315	5005	5698	6496	7187
Li (7)	30												
B (11)	60												
F (19)	150												
Na (23)	180		1	1	1	1	1	1	1	1	1	1	1
Mg (24)	185												
Al (27)	205		286	408	454	596	570	556	467	596	612	825	752
Si (30)	220		88	84	80	78	76	80	80	78	76	76	76
P (31)	230		1	1	1	1	1	1	1	1	1	-	-
Cl (35)	250												
K (39)	290		1	1	1	1	1	1	1	1	1	1	1
Ca (40)	295		1	-	-	-	-	-	-	-	-	-	-
Ti (48)	330												
Cr (52)	350												
Ni (58)	380												
Cu (63)	400												
Zn (64)	403												
Ga (69)	425												
Mo (98)	540												
Ag (107)	570		1	1	1	1	1	1	1	1	1	1	1
Sn (118)	610												
Ba (138)	670												
Pb (208)	858												

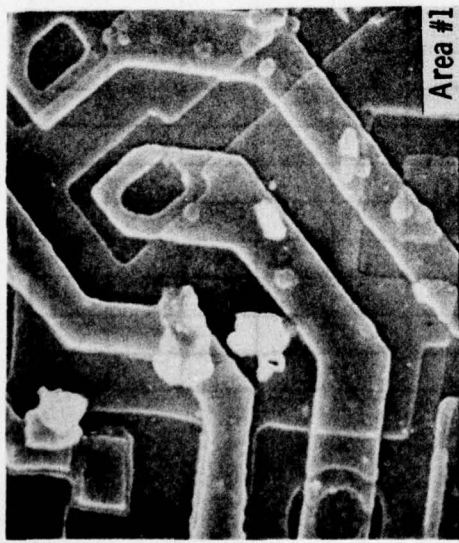
OP AMP #2      LM741H

UNIT #62 . AREA 8 . SPECTRA 303 - 307 .

RASTER 92 X 68  $\mu\text{m}$  . SPOT 14  $\mu\text{m}$  BC 6 NA SR ( $\text{\AA}/\text{SEC}$ ) .34 .

ELEM	PLUS START	7003	8579	9272	9974	10673							
Li (7)	30												
B (11)	60												
F (19)	150												
Na (23)	180	1	1	1	1	1							
Mg (24)	185												
Al (27)	205	682	852	799	852	821							
Si (30)	220	80	76	76	76	74							
P (31)	230	-	-	-	-	-							
Cl (35)	250												
K (39)	290	1	1	1	1	1							
Ca (40)	295	-	-	-	-	-							
Ti (48)	330												
Cr (52)	350												
Ni (58)	380												
Cu (63)	400												
Zn (64)	403												
Ga (69)	425												
Mo (98)	540												
Ag (107)	570	1	1	1	1	1							
Sn (118)	610												
Ba (138)	670												
Pb (208)	858												

LM741H Op Ann #2 Unit #62



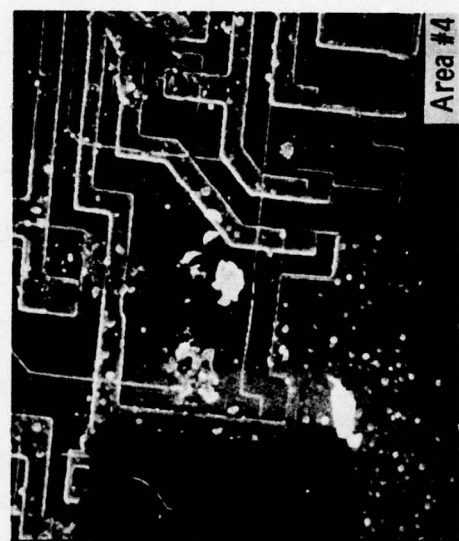
Area #1



Area #2



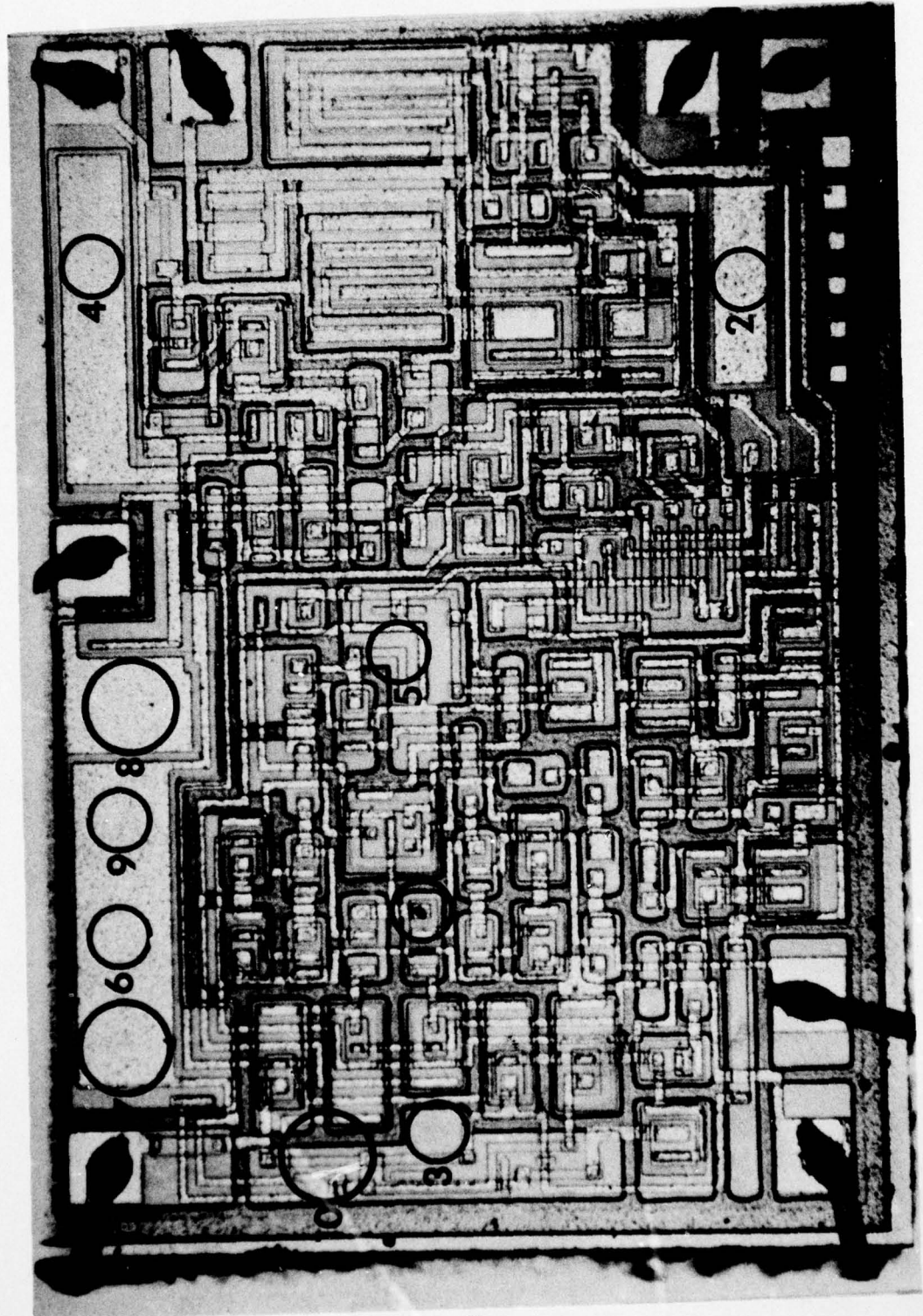
Area #3, #5, #6, and #7



Area #4

Op Amp #3, Unit #13

- Area 1: Mass Spectra Depth Profile
- Area 2: Mass Spectra Depth Profile
- Area 3: Mass Spectra Depth Profile
- Area 4: P Peak Count Profile Over Aluminum
- Area 5: P Peak Count Profile Over Oxide  
(not included)
- Area 6: Ar Sputter Time Through Glassivation
- Area 7: Interface Analysis, Glassivation-  
Aluminum Layers
- Area 8: False Start
- Area 9: False Start
- Area 10: Interface Analysis, Glassivation-  
Oxide Layers



Set 1 Op Amp #3 Unit #13

OP AMP #3 HA2600-02

UNIT #13 . AREA 1 . SPECTRA 28-31 .

RASTER 50 x 40 μm . SPOT 10 μm BC 10NA SR (A/SEC) 1.78 .

ELEM	START	PLUS			
		0	2660	4460	6260
Li (7)	30				
B (11)	60	1	1	1	1
F (19)	150				
Na (23)	180	461	14	27	2
Mg (24)	185	19	1	1	1
Al (27)	205	17	2	504	1926
Si (30)	220	29	130	100	110
P (31)	230	5	19	27	27
C1 (35)	250				
K (39)	290	211	9	12	1
Ca (40)	295	46	9	4	1
Ti (48)	330	1	1	1	-
Cr (52)	350				
Ni (58)	380				
Cu (63)	400	1	1	1	-
Zn (64)	403	1	1	1	-
Ga (69)	425	1	1	1	-
Mo (98)	540				
Ag (107)	570				
Sn (118)	610				
Ba (138)	670				
Pb (208)	858				

AD-A048 482

TEXAS INSTRUMENTS INC DALLAS CENTRAL RESEARCH LABS  
MICROBEAM ANALYSIS TECHNIQUES FOR ICS.(U)

F/G 20/12

OCT 77 G B LARRABEE, R D DOBROTT

F30602-76-C-0316

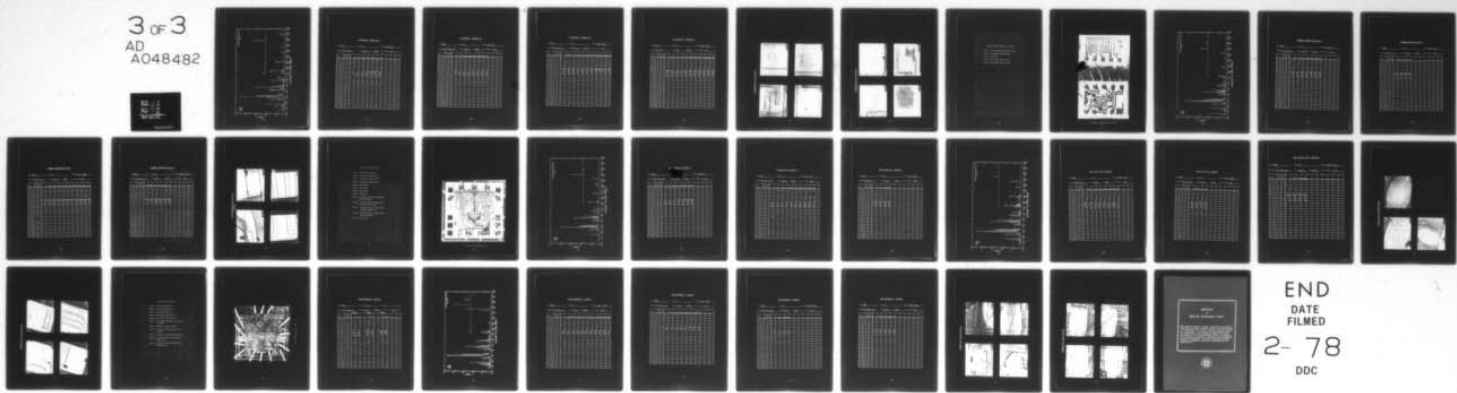
UNCLASSIFIED

TI-08-77-16

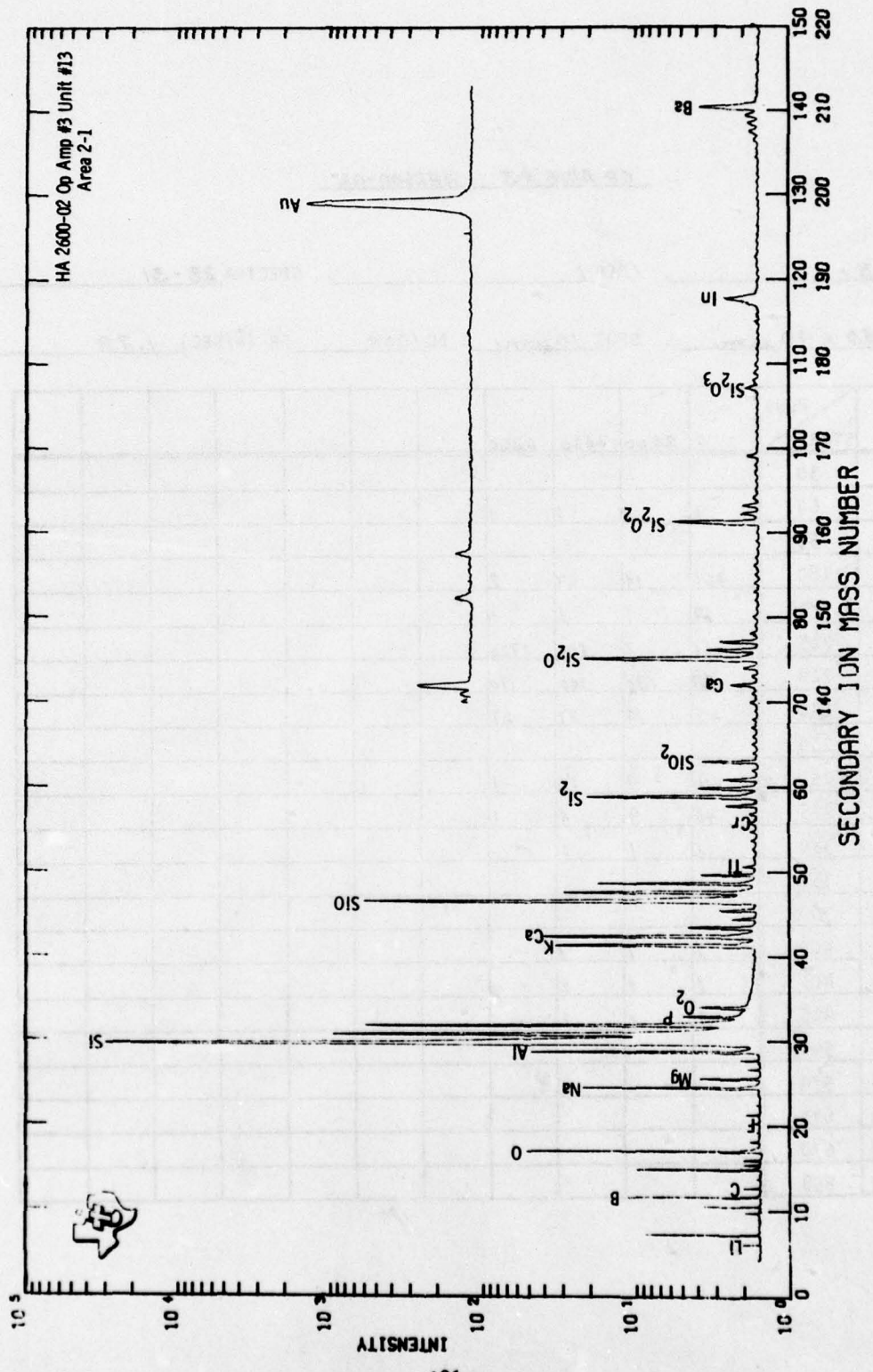
RADC-TR-77-339

NL

3 of 3  
AD  
A048482



END  
DATE  
FILED  
2- 78  
DDC



OP AMP#3 HA2600-02

UNIT #15 . AREA 2 . SPECTRA 38 - 32 .

RASTER 50 X 40 mm . SPOT 12 μm BC 10NA SR (Å/SEC) 3.20 .

ELEM	START	PLUS						
		0	907	1829	2752	3668	4591	5462
Li (7)	30	2	1	1	1	1	1	1
B (11)	60	2	1	1	1	1	1	1
F (19)	150							
Na (23)	180	5	2	1	2	1	2	2
Mg (24)	185	1	1	1	1	1	1	1
Al (27)	205	11	4	4	64	1608	3489	5426
Si (30)	220	210	280	260	250	200	150	130
P (31)	230	1	20	27	24	25	25	23
Cl (35)	250							
K (39)	290	7	4	2	2	3	4	4
Ca (40)	295	9	13	10	9	9	9	7
Ti (48)	330	1	1	-	-	-	-	-
Cr (52)	350	1	1	-	-	-	-	-
Ni (58)	380							
Cu (63)	400							
Zn (64)	403							
Ga (69)	425	1	1	1	1	1	1	1
Mo (98)	540							
Aq (107)	570							
Sn (118)	610							
Ba (138)	670	1	1	1	1	1	1	1
Pb (208)	858							

OP AMP #3 HA2600-02

UNIT #13. AREA 3. SPECTRA 39-46.

RASTER 50 x 40 mm. SPOT 10 μm BC IBNA SR (Å/SEC) 3.20.

ELEM	PLUS START	0	920	1037	2752	3670	4582	5493	6198		
Li (7)	30										
B (11)	60	1	-	-	-	1	1	-	1		
F (19)	150										
Na (23)	180	1	1	1	1	1	1	1	1		
Mg (24)	185	1	1	1	-	-	-	-	-		
Al (27)	205	2	1	1	1	2	7	4	19		
Si (30)	220	100	170	180	160	140	130	260	160		
P (31)	230	1	22	29	28	32	30	25	23		
Cl (35)	250										
K (39)	290	1	1	1	1	1	1	1	1		
Ca (40)	295	1	1	1	1	1	-	-	-		
Ti (48)	330	1	-	-	-	-	-	-	-		
Cr (52)	350										
Ni (58)	380										
Cu (63)	400										
Zn (64)	403										
Ga (69)	425										
Mo (98)	540										
Ag (107)	570										
Sn (118)	610										
Ba (138)	670										
Pb (208)	858										

OP AMP #3 HA2600-02

UNIT #13 . AREA 7 . SPECTRA 325 - 335 .

RASTER 83 x 69  $\mu\text{m}$  . SPOT 24  $\mu\text{m}$  BC 10NA SR (A/SEC) .62 .

ELEM	PLUS START												
		0	883	1570	2254	2951	3639	4324	5006	5690	6370	7054	
Li (7)	30												
B (11)	60												
F (19)	150	/	-	-	-	-	-	-	-	-	-	-	
Na (23)	180	/	/	/	/	/	/	/	/	/	/	/	
Mg (24)	185	/	-	-	-	-	-	-	-	-	-	-	
Al (27)	205	254	369	386	497	700	764	996	1829	3661	5707	7492	
Si (30)	220	40	56	57	31	28	29	28	25	19	15	15	
P (31)	230	28	29	21	17	12	9	7	7	7	9	8	
Cl (35)	250												
K (39)	290	/	/	/	/	/	/	/	/	/	/	/	
Ca (40)	295	/	/	/	/	/	/	-	-	-	-	-	
Ti (48)	330												
Cr (52)	350	/	/	/	/	/	/	/	/	/	/	/	
Ni (58)	380												
Cu (63)	400												
Zn (64)	403												
Ga (69)	425												
Mo (98)	540												
Ag (107)	570												
Sn (118)	610												
Ba (138)	670												
Pb (208)	858												

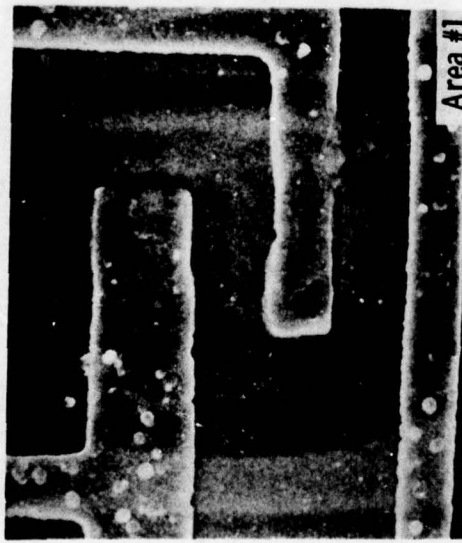
OP AMP #3 HA2600-02

UNIT #17. AREA 10. SPECTRA 337 - 547.

RASTER 72 X 49. SPOT 19. BC 5 NA SR ( $\text{\AA}/\text{SEC}$ ) .50.

ELEM	START	PLUS											
		0	893	1577	2261	2966	3724	4414	5103	5797	6489	7205	
Li (7)	30												
B (11)	60	/	/	/	/	/	/	/	/	/	/	/	
F (19)	150												
Na (23)	180	/	/	/	/	/	/	/	/	/	/	/	
Mg (24)	185						/	/	/	/	-	-	
Al (27)	205	858	973	1067	1315	1382	1457	1492	1642	1426	1085	930	
Si (30)	220	44	42	44	42	40	38	37	37	36	35	35	
P (31)	230	53	61	60	61	62	62	58	56	49	56	47	
Cl (35)	250												
K (39)	290	/	/	/	/	/	/	/	/	-	-	-	
Ca (40)	295												
Ti (48)	330												
Cr (52)	350												
Ni (58)	380												
Cu (63)	400												
Zn (64)	403												
Ga (69)	425												
Mo (98)	540												
Ag (107)	570												
Sn (118)	610												
Ba (138)	670												
Pb (208)	858												

HA2600-02 Op Amp #3 Unit #13



Area #1



Area #2



Area #3



Area #4

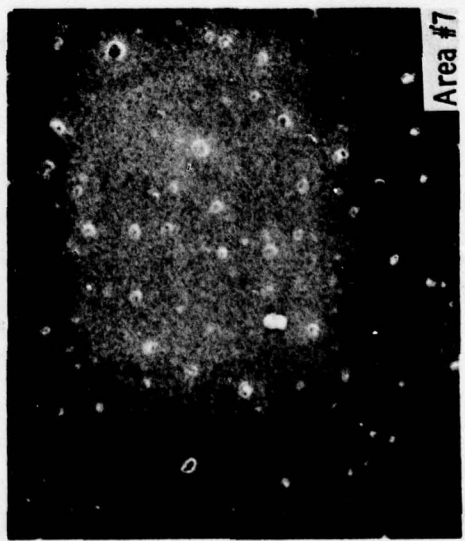
HA2600-02 Op Amp #3 Unit #13



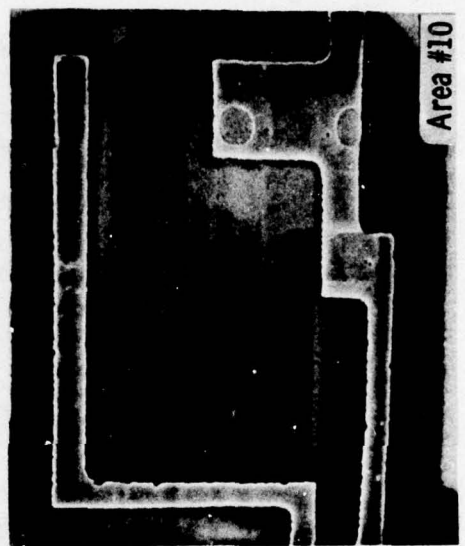
Area #5



Area #6



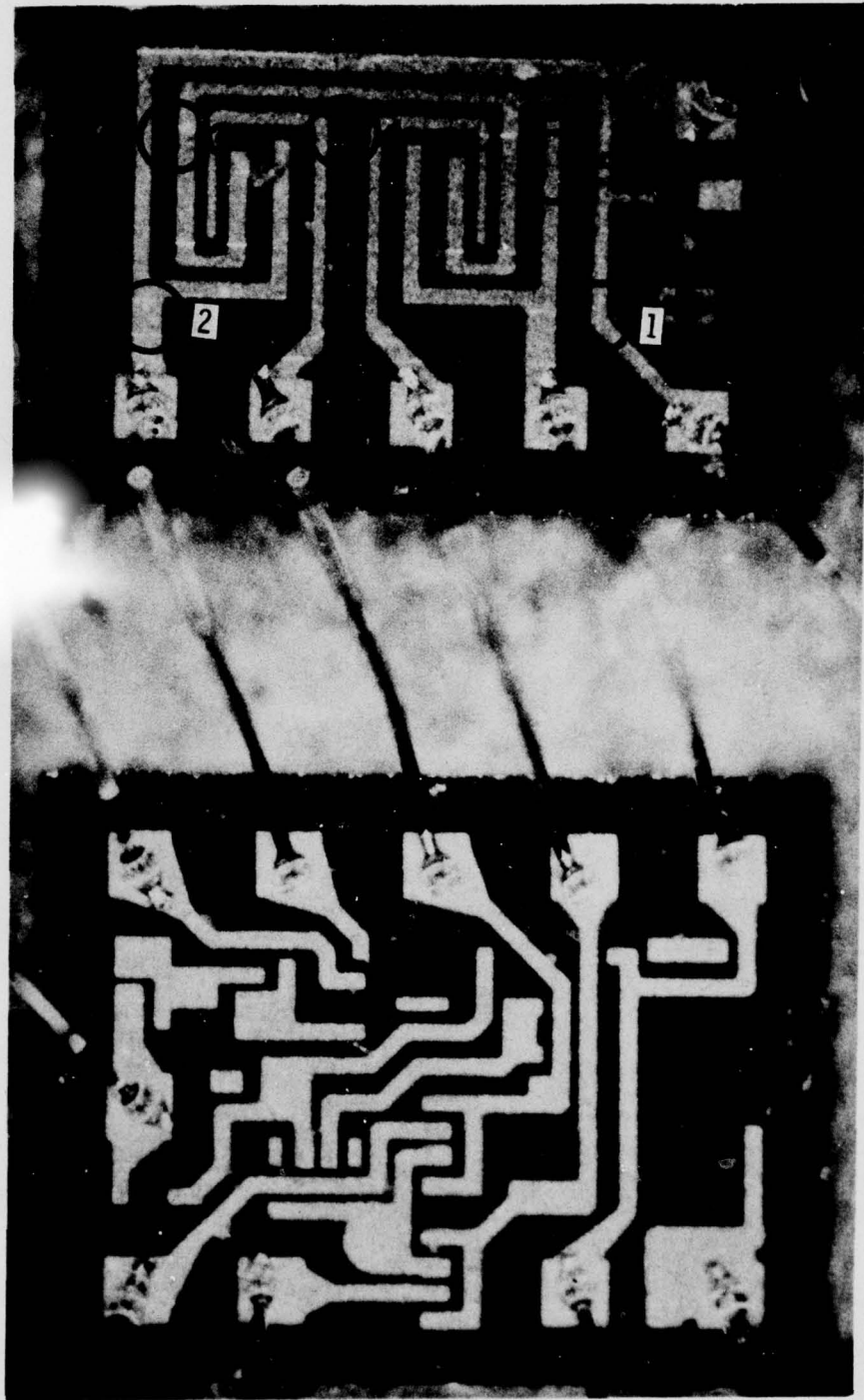
Area #7



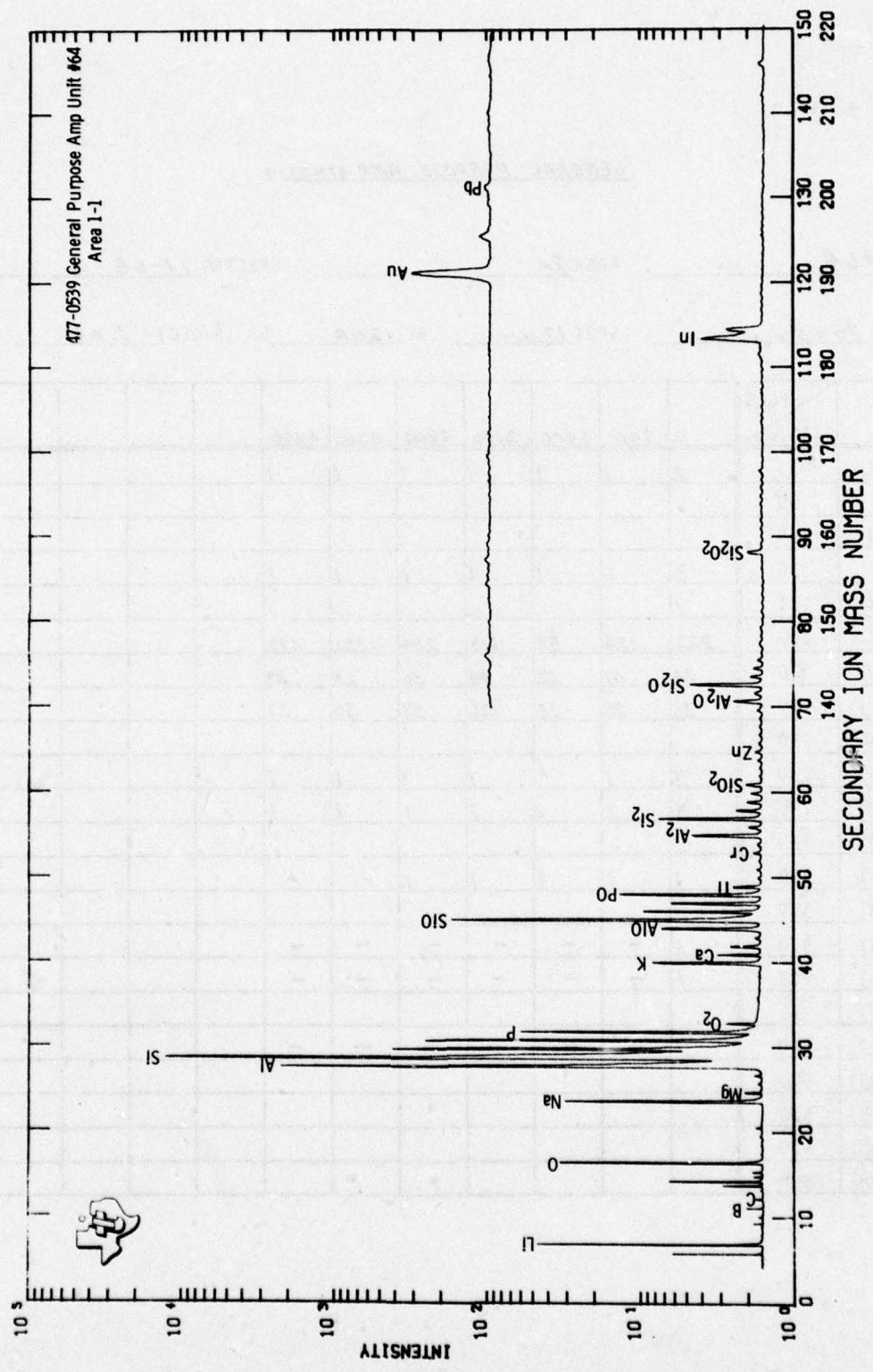
Area #10

**General Purpose Amplifier, Unit #64**

- Area 1: Surface Mass Spectrum-line crater**
- Area 2: Mass Spectra Depth Profile**
- Area 3: False Start**
- Area 4: Mass Spectra Depth Profile**
- Area 5: Mass Spectra Depth Profile**



Set I General Purpose Amplifier Unit #64



GENERAL PURPOSE AMP 477-0539

UNIT #64 . AREA 2 . SPECTRA 74-68 .

RASTER 70 X 56 μm . SPOT 17 μm BC 12NA SR ( $\lambda/\text{SEC}$ ) 1.09 .

ELEM	PLUS START	0	700	1400	2100	2800	3500	4200				
Li (7)	30	2	1	1	1	1	1	1				
B (11)	60											
F (19)	150											
Na (23)	180	3	1	1	1	1	1	1				
Mg (24)	185	1										
Al (27)	205	222	124	89	115	284	322	372				
Si (30)	220	24	47	58	48	50	28	35				
P (31)	230	34	28	25	26	27	30	27				
C1 (35)	250											
K (39)	290	3	1	1	1	1	1	1				
Ca (40)	295	3	1	1	1	1	1	1				
Ti (48)	330											
Cr (52)	350	1	1	1	1	1	-	-				
Ni (58)	380											
Cu (63)	400	1	-	-	-	-	-	-				
Zn (64)	403	1	-	-	-	-	-	-				
Ga (69)	425											
Mo (98)	540	1	-	-	-	-	-	-				
Ag (107)	570											
Sn (118)	610											
Ba (138)	670											
Pb (208)	858											

GENERAL PURPOSE AMP 477-0539

UNIT #64 AREA 4 SPECTRA 271-274

RASTER  $75 \times 65 \mu\text{m}$ . SPOT  $13 \mu\text{m}$  BC 5NA SR (Å/SEC) .36.

ELEM	PLUS START				
		0	685	1369	2117
Li (7)	30				
B (11)	60				
F (19)	150				
Na (23)	180	3	1	1	1
Mg (24)	185				
Al (27)	205	3990	3990	3890	3990
Si (30)	220	11	11	11	11
P (31)	230	28	28	27	24
Cl (35)	250				
K (39)	290	1	1	1	1
Ca (40)	295				
Ti (48)	330				
Cr (52)	350				
Ni (58)	380				
Cu (63)	400				
Zn (64)	403				
Ga (69)	425				
Mo (98)	540				
Ag (107)	570				
Sn (118)	610				
Ba (138)	670				
Pb (208)	858				

GENERAL PURPOSE AMP 477-0539

UNIT #64 . AREA 5 . SPECTRA 275 - 285 .

RASTER 75 X 65 mm . SPOT 13 μm BC 5NA SR ( $\text{\AA}/\text{SEC}$ ) .36 .

ELEM	START	PLUS										
		0	685	1379	2063	2759	3444	4137	4810	5497	6180	6972
Li (7)	30											
B (11)	60	3	2	2	2	2	2	2	2	2	1	1
F (19)	150											
Na (23)	180	2	1	1	1	1	1	1	1	-	-	-
Mg (24)	185											
Al (27)	205	3718	3809	3809	3809	5990	4390	4990	5390	5989	6500	6735
Si (30)	220	12	12	12	12	12	11	11	11	10	9.6	9
P (31)	230	26	29	25	25	20	22	20	18	18	16	14
Cl (35)	250											
K (39)	290	1	-	-	-	-	-	-	-	-	-	-
Ca (40)	295	1	1	1	1	1	1	1	1	-	-	-
Ti (48)	330											
Cr (52)	350											
Ni (58)	380											
Cu (63)	400											
Zn (64)	403											
Ga (69)	425											
Mo (98)	540											
Ag (107)	570											
Sn (118)	610											
Ba (138)	670											
Pb (208)	858											

GENERAL PURPOSE AMP 477-0539

UNIT #64 . AREA 5 . SPECTRA 286 - 291 .

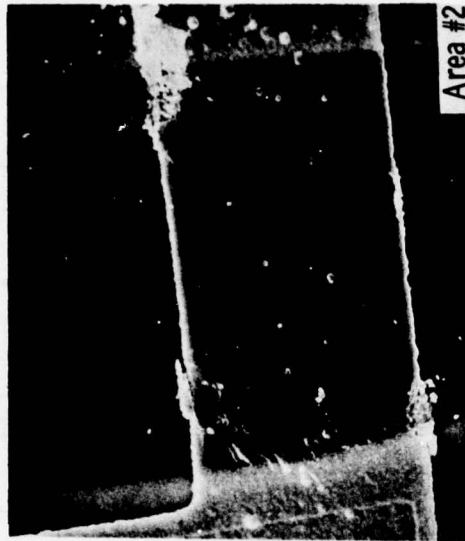
RASTER 75 X 65 mm . SPOT 13 μm BC 5NA SR (Å/SEC) .36 .

ELEM	START	PLUS					
		7788	8470	9169	9851	10535	11817
Li (7)	30						
B (11)	60	1	1	1	1	1	1
F (19)	150						
Na (23)	180	-	-	-	-	-	-
Mg (24)	185						
Al (27)	205	7238	7554	7423	8365	8319	8192
Si (30)	220	9	8.4	8.8	8.4	8.2	8.8
P (31)	230	13	11	10	8	8	8
Cl (35)	250						
K (39)	290	-	-	-	-	-	-
Ca (40)	295	-	-	-	-	-	-
Ti (48)	330						
Cr (52)	350						
Ni (58)	380						
Cu (63)	400						
Zn (64)	403						
Ga (69)	425						
Mo (98)	540						
Ag (107)	570						
Sn (118)	610						
Ba (138)	670						
Pb (208)	858						

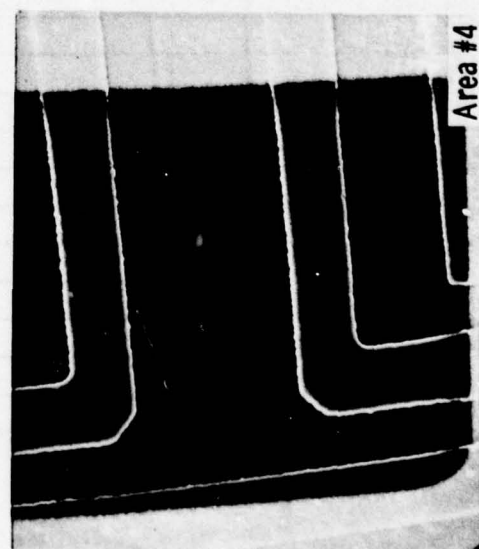
477-0539 General Purpose Amp  
Unit #64



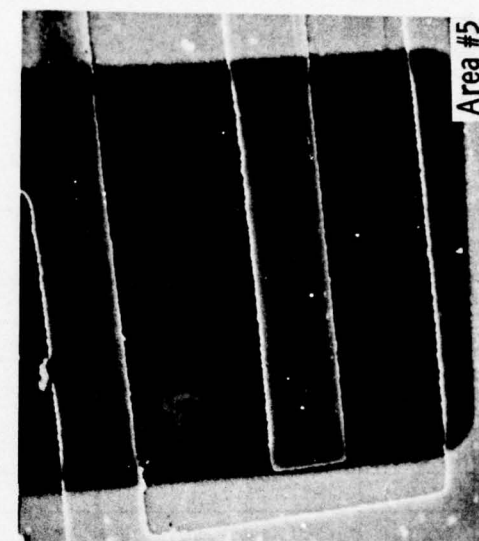
Area #1



Area #2



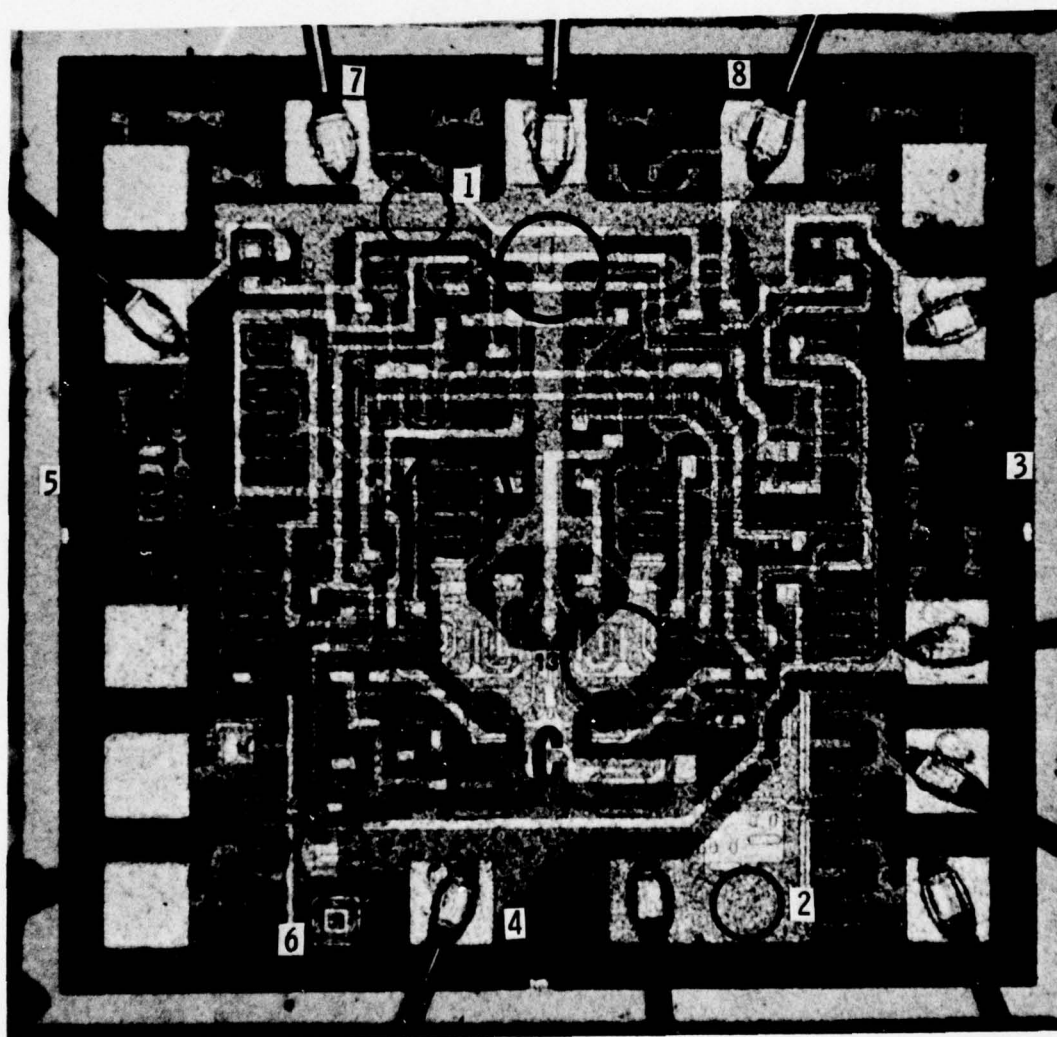
Area #4



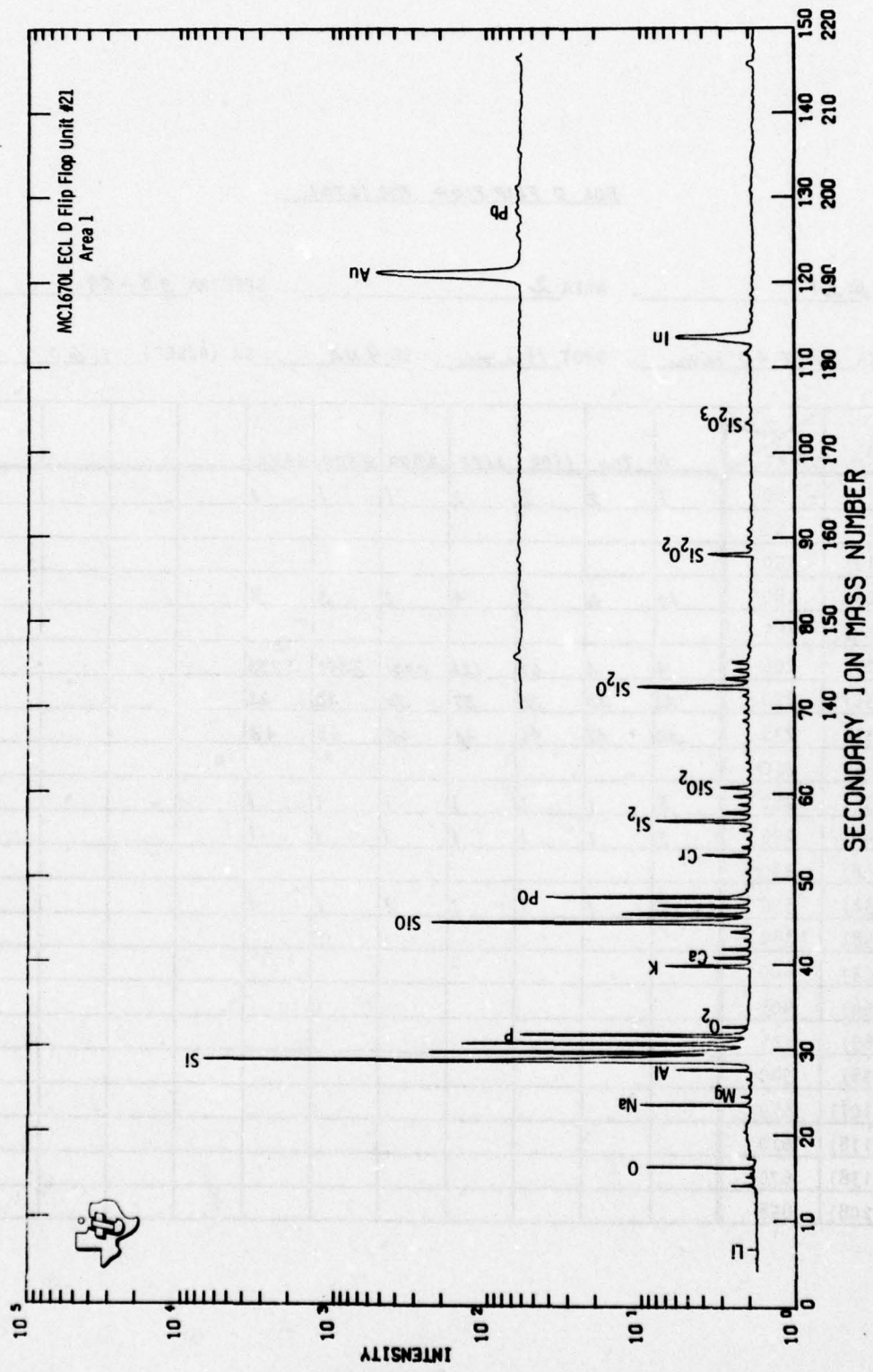
Area #5

ECL D Flip Flop, Unit #21

- Area 1: Surface Mass Spectrum
- Area 2: Mass Spectra Depth Profile
- Area 3: P Peak Count Depth Profile
- Area 4: Mass Spectra Depth Profile
- Area 5: False Start
- Area 6: False Start
- Area 7: False Start
- Area 8: False Start
- Area 9: Ar Sputter Time to Both Aluminum-Oxide Interfaces
- Area 10: Interface Analysis, Glassivation-Insulator Oxide Layers
- Area 11: Interface Analysis, Glassivation-Insulator Oxide Layers
- Area 12: Interface Analysis, Glassivation-Second Level Metal
- Area 13: False Start



Set 1 ECL D Flip Flop Unit #21



ECI = FLIP FLOP MC 1670L

UNIT #21 . AR. . SPECTRA 55-49 .

RASTER 50 X 40 μm . SPOT 1μm BC 9NA SR (Å/SEC) 1.60 .

ELEM	START	PLUS						
		0	700	1400	2100	2800	3500	4200
Li (7)	30	7	2	2	2	1	1	1
B (11)	60							
F (19)	150							
Na (23)	180	10	6	5	4	2	3	3
Mg (24)	185							
Al (27)	205	4	4	67	122	1031	2541	3233
Si (30)	220	22	35	25	37	30	23	22
P (31)	230	52	47	46	44	45	45	48
C1 (35)	250							
K (39)	290	3	1	1	1	1	1	1
Ca (40)	295	2	1	1	1	1	1	1
Ti (48)	330							
Cr (52)	350	2	1	1	1	1	1	1
Ni (58)	380							
Cu (63)	400							
Zn (64)	403							
Ga (69)	425							
Mo (98)	540							
Ag (107)	570							
Sn (118)	610							
Ba (138)	670							
Pb (208)	858							

ECL 0 FLIP FLOP MC 1670L

UNIT #21 . AREA 4 . SPECTRA 66-57 .

RASTER 50 X 40  $\mu\text{ms}$  . SPOT 16  $\mu\text{ms}$  BC 9NA SR (A/SEC) 1.60 .

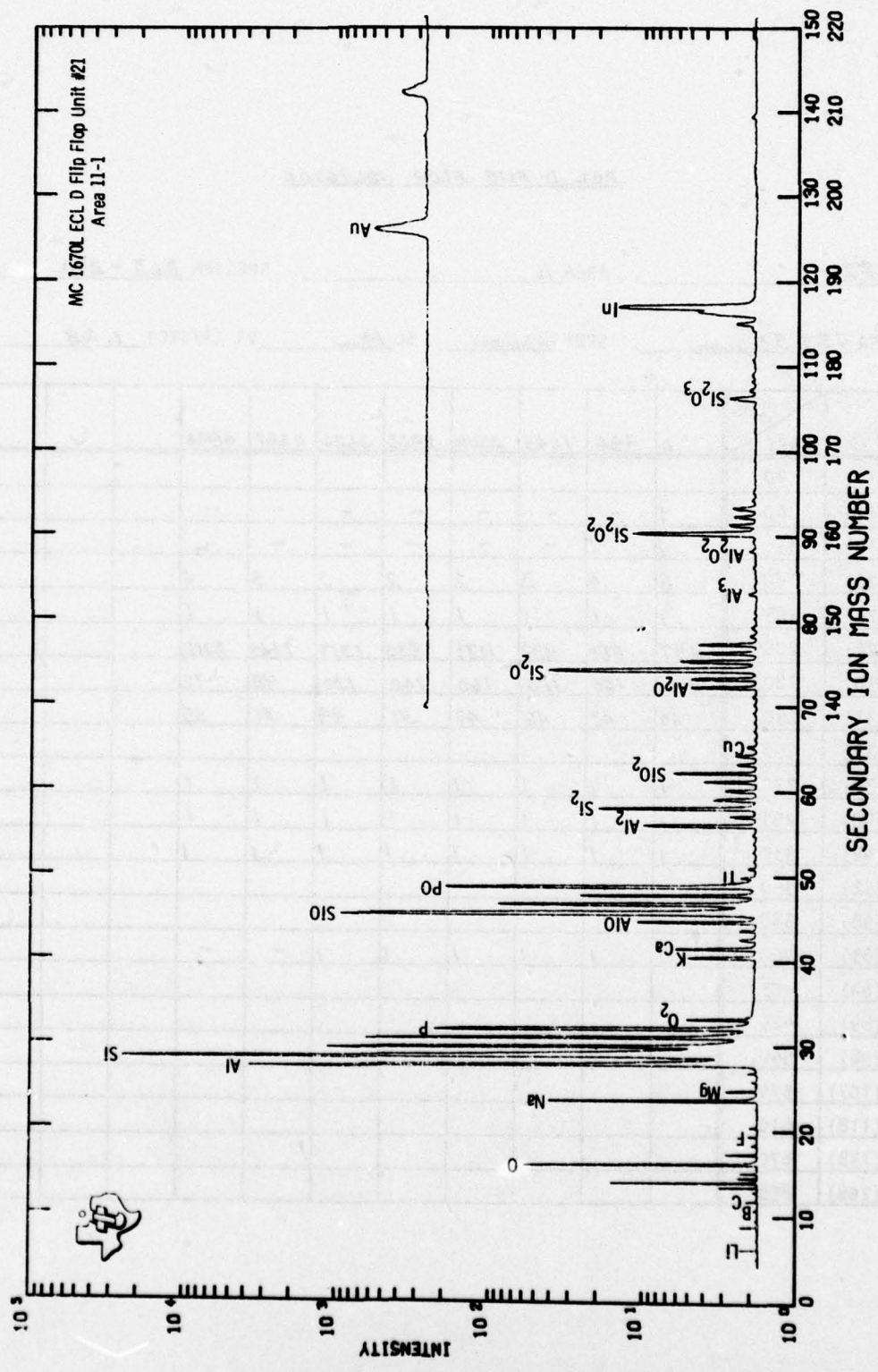
ELEM	PLUS START										
		0	700	1400	2100	2800	3500	4200	4900	5600	6300
Li (7)	30	1	4	2	1	1	2	1	1	1	1
B (11)	60										
F (19)	150										
Na (23)	180	10	8	4	5	5	5	4	4	4	3
Mg (24)	185										
Al (27)	205	4	1	1	2	5	6	5	5	5	4
Si (30)	220	36	60	90	66	54	42	80	65	62	60
P (31)	230	49	44	29	37	43	44	44	48	48	53
C1 (35)	250										
K (39)	290	7	2	1	1	1	1	1	1	1	1
Ca (40)	295	2	1	1	1	1	1	1	1	1	1
Ti (48)	330										
Cr (52)	350	3	1	1	1	1	1	1	1	1	1
Ni (58)	380										
Cu (63)	400										
Zn (64)	403	1	1	-	-	-	-	-	-	-	-
Ga (69)	425										
Mo (98)	540										
Ag (107)	570										
Sn (118)	610	1	1	-	-	-	-	-	-	-	-
Ba (138)	670										
Pb (208)	858										

ECL D FLIP FLOP MC1670L

UNIT #21 . AREA 10 . SPECTRA 251 - 254 .

RASTER 7.3 X 5.3  $\mu\text{m}$  . SPOT 16  $\mu\text{m}$  BC 14 NA SR (Å/SEC) 1.28 .

ELEM	PLUS START				
		0	910	1592	2269
Li (7)	30				
B (11)	60				
F (19)	150	/	-	-	-
Na (23)	180	4	1	1	1
Mg (24)	185	/	1	-	-
Al (27)	205	323	1051	1222	1576
Si (30)	220	78	58	50	39
P (31)	230	45	51	49	58
Cl (35)	250				
K (39)	290	/	1	1	1
Ca (40)	295	/	1	1	1
Ti (48)	330				
Cr (52)	350				
Ni (58)	380				
Cu (63)	400				
Zn (64)	403				
Ga (69)	425				
Mo (98)	540				
Ag (107)	570				
Sn (118)	610				
Ba (138)	670				
Pb (208)	858				



ECL 0 FLIP FLOP MC1670L

UNIT #21 . AREA 11 . SPECTRA 263 - 270 .

RASTER 7.3 X 5.3 mm . SPOT 16 μm BC 14 μ SR (A/SEC) 1.28 .

ELEM	PLUS START								
		0	984	1645	2309	2966	3626	4287	4894
Li (7)	30								
B (11)	60	1	-	-	-	-	-	-	-
F (19)	150	1	1	-	-	-	-	-	-
Na (23)	180	8	4	3	2	2	2	3	4
Mg (24)	185	1	1	1	1	1	1	1	1
Al (27)	205	497	880	939	1131	935	1317	1545	2111
Si (30)	220	200	160	150	160	140	130	98	72
P (31)	230	40	43	46	47	51	49	51	55
Cl (35)	250								
K (39)	290	1	1	1	1	1	1	1	1
Ca (40)	295	1	1	1	1	1	1	1	1
Ti (48)	330	1	1	1	1	1	1	1	1
Cr (52)	350								
Ni (58)	380								
Cu (63)	400	1	1	1	1	1	1	-	-
Zn (64)	403								
Ga (69)	425								
Mo (98)	540								
Ag (107)	570								
Sn (118)	610								
Ba (138)	670								
Pb (208)	858								

ECL 0 FLIP FLOP MC1670L

UNIT #21 . AREA 13 . SPECTRA 255 - 258 .

RASTER 73 X 53 μm . SPOT 16 μm BC 14 NA SR ( $\text{\AA}/\text{SEC}$ ) 1.28 .

ELEM	START	PLUS			
		0	878	1603	2320
Li (7)	30				
B (11)	60				
F (19)	150				
Na (23)	180	3	2	2	1
Mg (24)	185				
Al (27)	205	1996	3177	4837	7614
Si (30)	220	28	23	20	22
P (31)	230	44	45	53	52
Cl (35)	250				
K (39)	290	1	1	1	1
Ca (40)	295	1	1	1	1
Ti (48)	330				
Cr (52)	350				
Ni (58)	380				
Cu (63)	400				
Zn (64)	403				
Ga (69)	425				
Mo (98)	540				
Ag (107)	570				
Sn (118)	610				
Ba (138)	670				
Pb (208)	858				

ECL O FLIP FLOP MC1670L

UNIT #21 . AREA 12 . SPECTRA 259 - 262 .

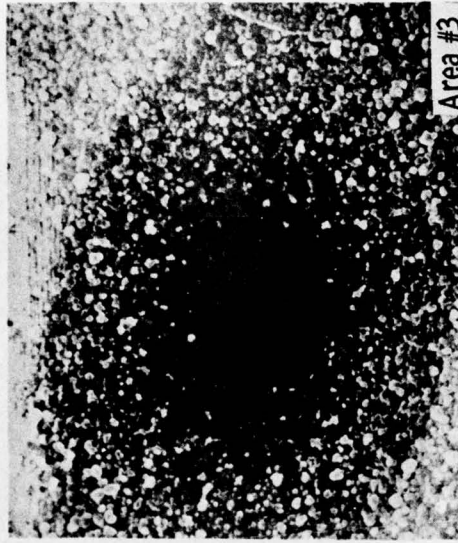
RASTER 73 X 53  $\mu\text{m}$  . SPOT 16  $\mu\text{m}$  BC 14 NA SR ( $\text{\AA}/\text{SEC}$ ) 1.28 .

ELEM	PLUS START				
		0	905	1585	2263
Li (7)	30				
B (11)	60				
F (19)	150				
Na (23)	180	2	1	1	1
Mg (24)	185				
Al (27)	205	2556	2913	2995	2723
Si (30)	220	26	25	23	23
P (31)	230	56	63	60	68
C1 (35)	250				
K (39)	290	1	1	1	1
Ca (40)	295	1	-	-	-
Ti (48)	330				
Cr (52)	350				
Ni (58)	380				
Cu (63)	400				
Zn (64)	403				
Ga (69)	425				
Mo (98)	540				
Aq (107)	570				
Sn (118)	610				
Ba (138)	670				
Pb (208)	858				

MC1670L ECL D Flip Flop Unit #21



Area #2



Area #3

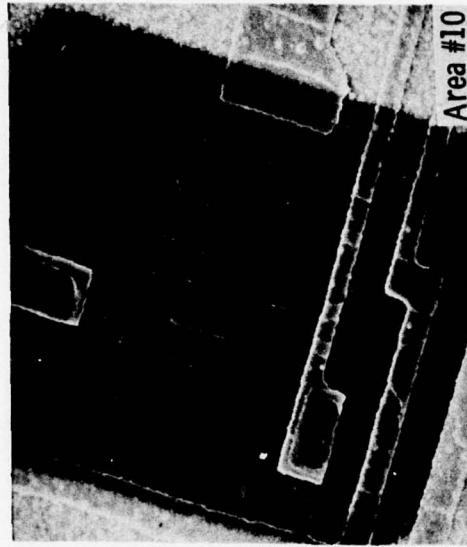


Area #4

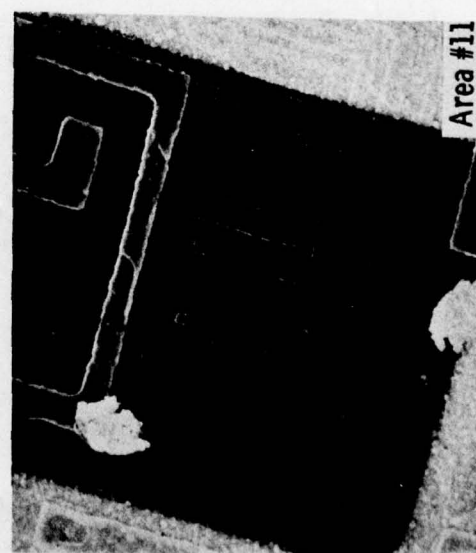
MC1670L ECL D Flip Flop Unit #21



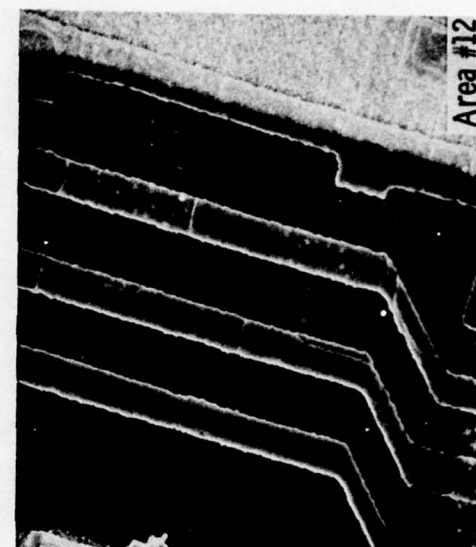
Area #9



Area #10



Area #11

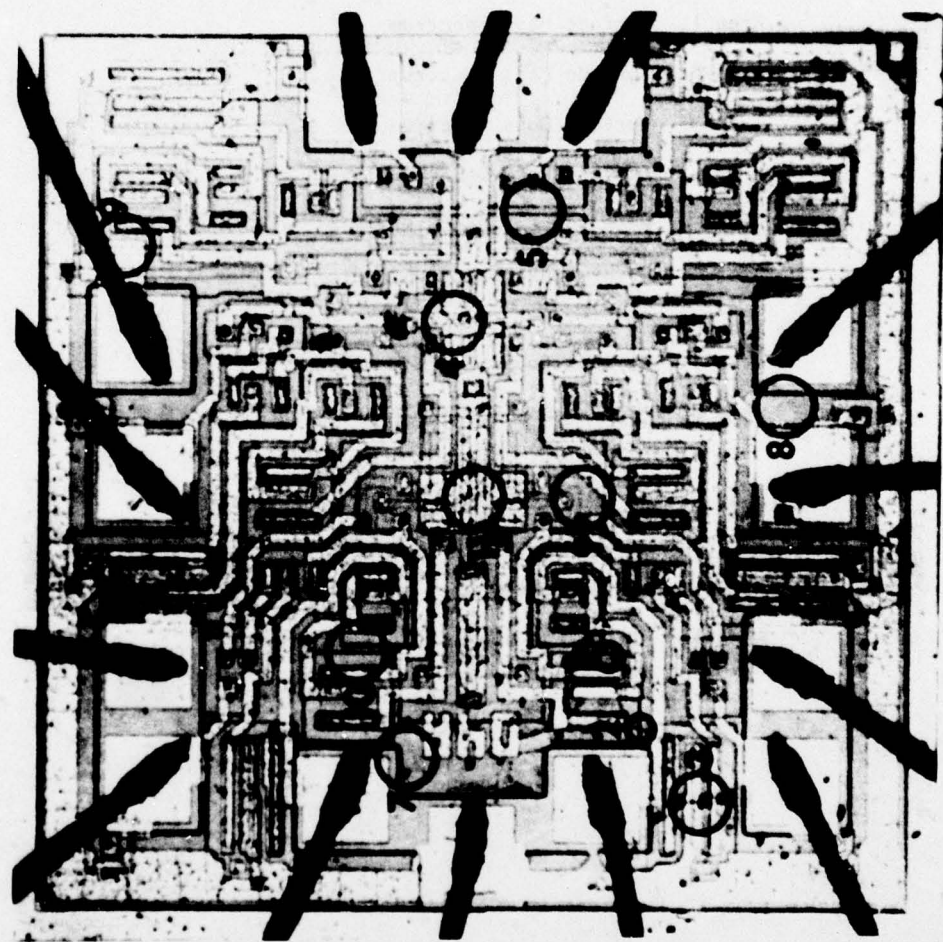


Area #12

**Hex Inverter, Unit #94**

- Area 1: Surface Mass Spectrum**
- Area 2: Surface Mass Spectrum**
- Area 3: Surface Mass Spectrum**
- Area 4: Mass Spectra Depth Profile**
- Area 5: Mass Spectra Depth Profile**
- Area 6: Cr-Ni Peak Count Depth Profile (not included)**
- Area 7: Pb Peak Count Depth Profile**
- Area 8: Pb Peak Count Depth Profile (not included)**
- Area 9: Ar Sputter Time Through Glassivation**
- Area 10: Interface Analysis, Glassivation-Oxide Layers**
- Area 11: Interface Analysis, Glassivation-Aluminum Layers**

Set 1 Hex Inverter Unit #94

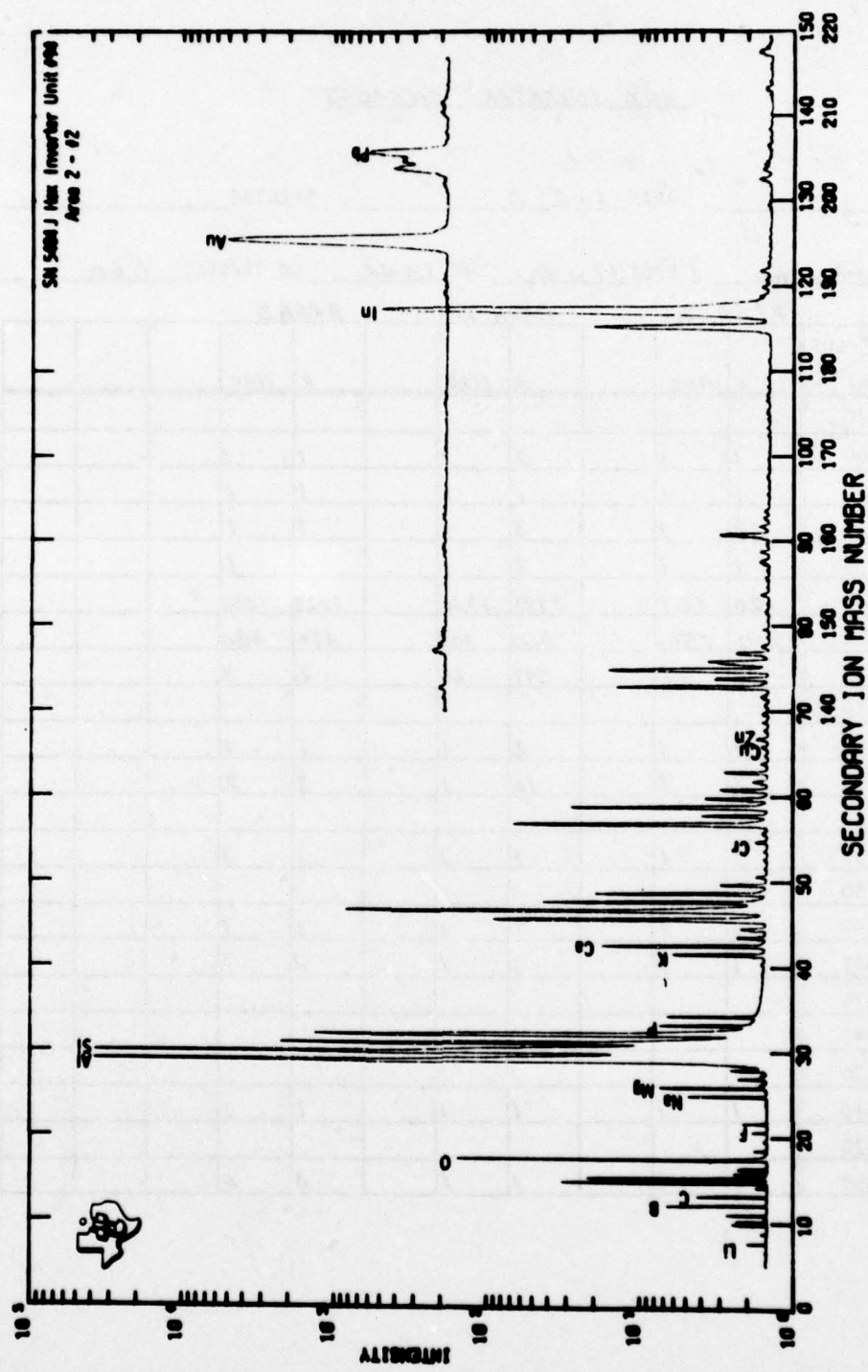


HEX INVERTER SN5404J

UNIT #94 . AREA 1-2-3 . SPECTRA \_\_\_\_\_.

RASTER 60x48 mm . SPOT 17 μm BC 13 NA SR ( $\text{\AA}/\text{SEC}$ ) 1.60 .

ELEM	PLUS START	AREA 1		AREA 2		AREA 3	
		0	1100	0	1100	0	1100
Li (7)	30						
B (11)	60	1	1	2	1	1	1
F (19)	150	1	1	1	1	1	1
Na (23)	180	2	1	3	1	1	1
Mg (24)	185	1	1	2	1	1	1
Al (27)	205	120	167	3281	1216	1023	1085
Si (30)	220	500	550	260	700	470	480
P (31)	230	26	34	247	64	2	3
C1 (35)	250						
K (39)	290	1	1	2	1	1	1
Ca (40)	295	2	1	10	1	3	2
Ti (48)	330						
Cr (52)	350	1	1	1	1	1	1
Ni (58)	380						
Cu (63)	400	1	1	1	1	1	1
Zn (64)	403	1	1	1	1	1	1
Ga (69)	425						
Mo (98)	540						
Ag (107)	570						
Sn (118)	610	1	1	1	1	1	1
Ba (138)	670						
Pb (208)	858	1	1	1	1	4	4



HEX INVERTER SN-5404J

UNIT #94 . AREA 4 . SPECTRA 124 - 134 .

RASTER 70 X 56 mm . SPOT 17 μm BC 13 NA SR (Å/SEC) 1.18 .

ELEM	PLUS START	0	900	1800	2700	3600	4727	5066	7017	8142	9241	10483
Li (7)	30											
B (11)	60	/	/	/	/	/	/	/	/	/	/	/
F (19)	150	/	/	-	-	-	-	-	-	-	-	-
Na (23)	180	/	/	/	/	/	/	/	/	/	/	/
Mg (24)	185	/	/	/	/	/	/	/	/	/	/	/
Al (27)	205	53	50	62	80	91	124	185	267	343	462	570
Si (30)	220	580	560	640	700	820	850	650	750	700	680	650
P (31)	230											
Cl (35)	250											
K (39)	290	/	/	/	/	/	/	/	/	/	/	/
Ca (40)	295	2	/	/	/	/	/	/	/	/	/	/
Ti (48)	330	/	/	/	/	/	/	-	-	-	-	/
Cr (52)	350	/	/	/	/	/	/	/	/	/	/	/
Ni (58)	380											
Cu (63)	400	/	/	/	-	-	-	-	/	/	/	/
Zn (64)	403	/	/	/	/	/	/	/	/	/	/	/
Ga (69)	425											
Mo (98)	540											
Ag (107)	570											
Sn (118)	610	/	/	/	/	/	/	/	/	/	/	/
Ba (138)	670											
Pb (208)	858	/	/	/	/	/	/	/	/	/	/	/

HEX INVERTER SN5404J

UNIT #94 . AREA 5 . SPECTRA 136 - 143 .

RASTER 70 X 56 mm . SPOT 17 mm BC 13 NA SR (1/SEC) 1.18 .

ELEM	PLUS START	0	1125	2245	3362	4486	5619	6744	7868				
Li (7)	30												
B (11)	60	/	/	/	/	/	/	/	/				
F (19)	150	/	/		/	/	-	-	/				
Na (23)	180	/	/	/	/	/	/	/	/				
Mg (24)	185	/	/	/	/	/	/	/	/				
Al (27)	205	/	4	3	5	15	100	250	360				
Si (30)	220	480	760	850	1000	1200	1600	800	750				
P (31)	230												
Cl (35)	250												
K (39)	290	/	/	/	/	/	/	/	/				
Ca (40)	295	3	/	/	/	/	/	/	/				
Ti (48)	330	/	/	/	/	/	/	/	/				
Cr (52)	350	/	/	/	/	/	/	/	/				
Ni (58)	380												
Cu (63)	400	/	/	/	/	/	/	/	/	-			
Zn (64)	403	/	/	/	/	/	/	/	/	-			
Ga (69)	425												
Mo (98)	540												
Ag (107)	570												
Sn (118)	610	/	/	/	/	/	/	/	/	-			
Ba (138)	670												
Pb (208)	858	/	/	/	/	/	/	/	/				

HEX INVERTER SN5404J

UNIT #94 . AREA 10 . SPECTRA 687-690 .

RASTER 70 X 55  $\mu\text{m}$  . SPOT 21  $\mu\text{m}$  BC 11NA SR ( $\text{\AA}/\text{SEC}$ ) 1.01 .

ELEM	PLUS START	0	1054	1738	2428						
Li (7)	30										
B (11)	60	/	/	/	/						
F (19)	150										
Na (23)	180	/	/	/	/						
Mg (24)	185	/									
Al (27)	205	43	54	72	97						
Si (30)	220	110	84	72	66						
P (31)	230	/	/	-	-						
Cl (35)	250										
K (39)	290	/	/	/	/						
Ca (40)	295	/	/	/	/						
Ti (48)	330										
Cr (52)	350										
Ni (58)	380										
Cu (63)	400										
Zn (64)	403										
Ga (69)	425										
Mo (98)	540										
Ag (107)	570										
Sn (118)	610										
Ba (138)	670										
Pb (208)	858										

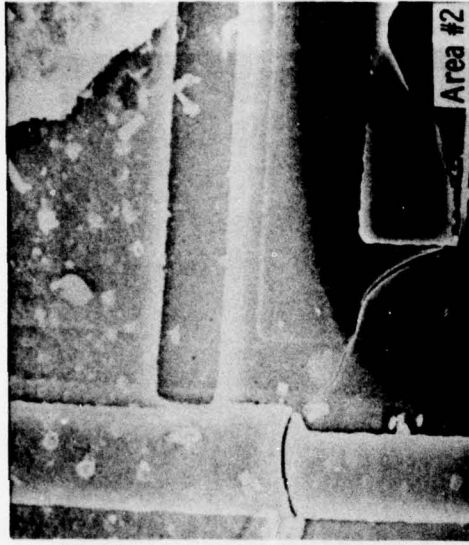
HEY INVERTER SN5404T

UNIT #94 . AREA 11 . SPECTRA 682-686

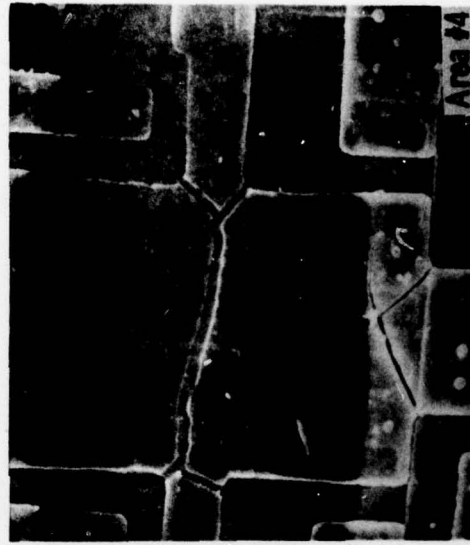
RASTER 44 X 28  $\mu m$ . SPOT 9  $\mu m$  BC 6NA SR ( $\text{\AA}/\text{SEC}$ ) 1.73.

ELEM	START	PLUS				
		0	887	1757	2620	3470
Li (7)	30					
B (11)	60	1	1	1	1	1
F (19)	150					
Na (23)	180	1	1	1	1	1
Mg (24)	185	1	1	—	—	—
Al (27)	205	319	259	122	180	160
Si (30)	220	76	70	56	56	48
P (31)	230	1	1	1	1	1
Cl (35)	250					
K (39)	290	1	1	1	1	1
Ca (40)	295	1	1	1	—	—
Ti (48)	330					
Cr (52)	350					
Ni (58)	380					
Cu (63)	400	1	—	—	—	—
Zn (64)	403					
Ga (69)	425					
Mo (98)	540					
Ag (107)	570					
Sn (118)	610					
Ba (138)	670					
Pb (208)	858					

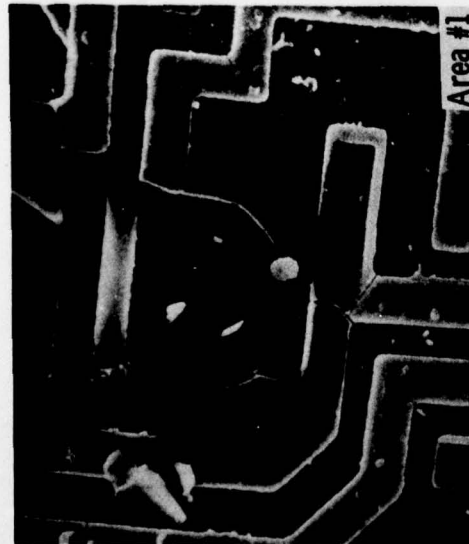
SN5404J Hex Inverter Unit #94



Area #2



Area #4

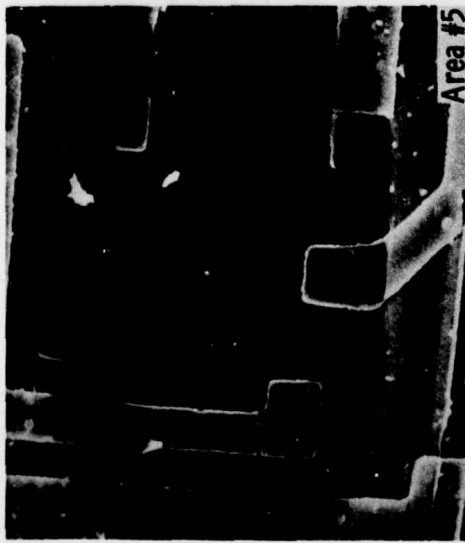


Area #1



Area #3

**SN5404J Hex Inverter Unit #94**



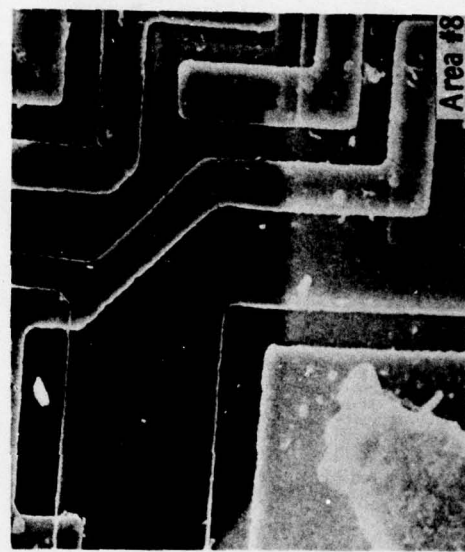
**Area #5**



**Area #6**



**Area #7**



**Area #8**

**MISSION**  
of  
*Rome Air Development Center*

RADC plans and conducts research, exploratory and advanced development programs in command, control, and communications (C<sup>3</sup>) activities, and in the C<sup>3</sup> areas of information sciences and intelligence. The principal technical mission areas are communications, electromagnetic guidance and control, surveillance of ground and aerospace objects, intelligence data collection and handling, information system technology, ionospheric propagation, solid state sciences, microwave physics and electronic reliability, maintainability and compatibility.

